Departamento de Farmacología y Terapéutica
Facultad de Medicina
Universidad Autónoma de Madrid

COX-2 derived prostanoids, reactive oxygen species and GRK2 underlie the functional, structural and mechanical vascular alterations in hypertension

DOCTORAL THESIS

Mª Soledad Avendaño Herrador

2013

Departamento de Farmacología y Terapéutica
Facultad de Medicina
Universidad Autónoma de Madrid

Dra. Mercedes Salaices Sánchez, Catedrática del Departamento de Farmacología y Terapéutica de la Facultad de Medicina de la Universidad Autónoma de Madrid,

Dra. Ana María Briones Alonso, investigadora "Ramón y Cajal" del Departamento de Farmacología y Terapéutica de la Facultad de Medicina de la Universidad Autónoma de Madrid,

CERTIFICAN, que Doña Mª Soledad Avendaño Herrador ha realizado bajo su dirección el presente trabajo: "***COX-2 derived prostanoids, reactive oxygen species and GRK2 underlie the functional, structural and mechanical vascular alterations in hypertension***", como Tesis para alcanzar el grado de Doctor por la Universidad Autónoma de Madrid.

Para que conste a efectos oportunos, expiden y firman la presente en Madrid a 12 de Noviembre de 2013.

Dra. Mercedes Salaices Sánchez	Dra. Ana María Briones Alonso
Catedrática de Farmacología	Investigadora "Ramón y Cajal"

This Thesis has been performed at Departamento de Farmacología y Terapéutica in the Universidad Autónoma de Madrid (UAM) and Instituto de Investigación Sanitaria Hospital la Paz (IdiPAZ). It has been funded by Ministerio de Economía y Competitividad (SAF 2009-07201; SAF 2012-36400), Instituto de Salud Carlos III (Red RECAVA, RD06/0014/0011; RIC RD12/0042/0024) and Fundación Mutua Madrileña. Mª Soledad Avendaño Herrador has been fellow FPU-MEC of Ministerio de Educación (AP-2007-00130).

Lo que sabemos es una gota de agua; lo que ignoramos es el océano.

Isaac Newton

La felicidad suprema en la vida es tener la convicción de que nos aman por lo que somos, o mejor dicho, a pesar de lo que somos.

Víctor Hugo

A mi gran amor, Jose y
a mis padres, Conchi y Pepe

Agradecimientos/Acknowledgements

Después de tantos años de duro trabajo y esfuerzo, en los que parecía que nunca llegaría el día de presentar la tesis, me parece increíble verme aquí escribiendo los agradecimientos.

Para mí la tesis no ha sido tan sólo el trabajo experimental, sino un cambio transcendental a nivel personal y profesional en mi vida; considero que no sólo ha conseguido aportarme conocimientos sobre mi área de trabajo, sino que también me ha enriquecido como persona. Todo ello se lo debo a las muchas y grandes personas que me han acompañado en este viaje. Esta tesis está compuesta de pedacitos de todos mis compañeros de viaje, todos y cada uno de ellos especiales para mí. Por ello tengo que abrirles hoy mi corazón, a todos ellos, y expresarle mi más sincero agradecimiento.

En primer lugar le agradezco a la Dra. Ana Mª Briones, que iniciara esta fabulosa experiencia y a la Dra. Mercedes Salaices que decidiera continuarla. De ambas admiro su buen saber hacer en las cosas, su paciencia infinita conmigo, su compresión, su ayuda, su experiencia y la seguridad que tienen en sí mismas. Ojalá haya conseguido llevarme un poco de todo lo que ellas me han aportado. ¡Muchas gracias!

En segundo lugar me gustaría agradecérselo a la Dra. Sonia Martínez, que ha sido el 50% o más de esta tesis, tanto a nivel experimental como personal. A la Dra. Laura Caracuel, que al igual que Sonia, es una amiga y gran persona, con una paciencia infinita. Sin ellas no hubiera sido lo mismo, han sabido contribuir a mi felicidad en estos años. Muchas gracias guapas, por vuestra paciencia y amistad.

Esta tesis no hubiera sido posible, sin lugar a dudas, sin la ayuda de cada uno de mis compañeros de laboratorio, por eso merecen mi más sincero agradecimiento, la Dra. Ana García, la Dra. María Galán, la Dra. Rosa Aras, la Dra. Amada Beltrán, la Dra.

Marta Miguel, Laura García, Olha y Andrea. Todas ellas en etapas diferentes de la tesis, me han brindado siempre su apoyo, su amistad, comprensión y ha sabido ayudarme a desestresarme cuando lo necesitaba. Echaré de menos nuestras interesantes charlas a la hora de la comida, nuestras elucubraciones sobre los fenómenos paranormales de los servicios y nuestras divertidas teorías. Muchas gracias chicas por haberme regalado un sinfín de buenos momentos.

A mi compañera de Fisiología de la UAM, Esther y a mis compañeros de la URJC, la Dra. Mª Jesús Alonso, la Dra. Raquel Hernanz, la Dra. Mª Teresa Barrús, la Dra. Ángela Martín, el Dr. Vicente Pérez y a Roberto. Muchas gracias por vuestro apoyo, ayuda, compresión y palabras de ánimo cuando lo necesitaba.

A mis compis del IIB, sin ellos la primera etapa de mi tesis en Madrid no hubiera sido la misma. Muchas gracias chicos por tanta ayuda y tantos favores como me hacéis siempre.

Al Dr. Dalton Vasallo y a mis compañeras de trabajo brasileñas Fernanda, Lorena, Maylla, Bruna y Priscilla, que han endulzado con su sonrisa, amistad, apoyo y comprensión muchos momentos de esta etapa. ¡Gracias chicas!

Agradezco el haber colaborado con Elisa Lucas y los Drs. Federico Mayor Jr., Cristina Murga y Miguel Ángel Iñiguez del CBM, la Dra. Victoria Cachofeiro de la Universidad Complutense de Madrid, el Dr. Juan Miguel Redondo del CNIC y los Drs. Gloria Balfagón y Javier Blanco del Dpto. de Fisiología, sin cuyas aportaciones no habría podido realizar una parte importante de esta tesis. ¡Millones de gracias!

Agradezco también a la Dras. Silvia Arribas y Mª Carmen González el haberme dejado utilizar el miógrafo de presión en su laboratorio del Dpto. de Fisiología en la fase inicial de esta tesis. ¡Gracias!

Je veux remercier à le Dr Frédéric JAISSER me permettre de faire mon séjour dans son laboratoire à Paris (France), l'amabilité et la cordialité avec laquelle j'ai été traité pendant mon séjour dans son laboratoire. Je veux également remercier à votre équipe et Maud, tout ce que vous avez fait pour moi, depuis m'aider avec la langue, jusqu´à me prêter leur compréhension et leur soutien. ¡Merci beaucoup à tous!

Quiero agradecérselo también a mis compis de la Casa de España en París, por su amistad y compañía, que hicieron que me sintiera menos sola en tierra extraña. ¡Gracias!

Agradezco al Dr. Jesús Frías Iniesta, exdirector del Departamento de Farmacología y Terapéutica y al Dr. Carlos Sánchez Ferrer, actual Director del Departamento de Farmacología y Terapéutica, permitirme realizar mi trabajo en el Departamento. Asimismo, agradezco al resto de profesores del Departamento el haberme prestado su ayuda y algunos de sus equipos durante estos años.

Quiero también agradecer a la Dra. Mª del Carmen Fernández Criado, Directora del Animalario de la Facultad de Medicina su ayuda en la gestión de los animales y a los chicos de animalario el cuidado y mantenimiento de los mismos así como las risas y charlas a primera hora del día.

A las chicas del confocal, por su infinita paciencia conmigo en el microscopio confocal.

A Yolanda, la chica del criostato, por su ayuda, paciencia, las risas y sus amenas charlas. ¡Gracias Yoli!

Al Dr. Raúl Jiménez Pérez, un amigo del alma, que me ha ayudado siempre que lo he necesitado. Gracias por ser como eres, un luchador entusiasta al que me gustaría parecerme y que no sólo ha contribuido a mi felicidad y a bajar mis niveles de estrés, sino que también me ha regalado un sinfín de buenos momentos. Muchas gracias guapo, sabes que sin tí nada hubiera sido lo mismo.

A mis compañeras de piso "Ana Linares" y "Ana Madrid" por su apoyo, compresión, ánimo y por ayudarme a desestresarme, sois las mejores. Muchas gracias, chicas.

Quiero mencionar también a todos mis amigos ajenos al laboratorio y a mi experiencia madrileña: Patri, Isa, Cande, Angie, Juan, David…. con los que he compartido mis vivencias. Gracias por estar ahí y escucharme.

A mi José, por ser único, por hacerme reír cuando quiero llorar, por hacerme crecer como persona cada día, por apoyarme, por cuidarme, por transformar mis defectos en virtudes y por amarme, millones gracias amor. Te quiero por lo que has hecho de mí y por cómo me haces sentir.

A mi familia política, los padres de Jose, sus hermanos y cuñados, por preocuparse, apoyarme e involucrase en mis preocupaciones. Muchas gracias!

A mi querido tío Manuel, que siempre creyó en mí y sé que se sentiría orgulloso hoy de mí. ¡Gracias tito, por todo lo que me has regalado en la vida!

En último lugar, aunque desde luego no menos importante, también quiero agradecer especialmente, a toda mi familia su constante apoyo. A mis padres, Conchi y Pepe, a mi hermana Inma, mi hermano José y mis cuñados, por preocuparse por mí en los momentos difíciles, por darme su cariño, su comprensión, su entera disposición y ser incondicionales conmigo. Sin ellos no estaría aquí. Agradezco a mis sobrinitos, Ainhoa

y Óscar Jesús que son un amor y una alegría, el que contribuyan con sus risas y juegos a a que me olvide de las preocupaciones.

Ojalá pudiera escribir un libro enorme de todo lo vivido y sentido durante esta etapa, que ha sido mucho y muy intenso. Pero como no puedo, sólo me queda volver a daros las gracias a todos por haberme hecho madurar, mejorar profesionalmente y por hacerme crecer cada día como persona. Esta tesis, como mi vida, se ha compuesto de muchos momentos y experiencias positivas, en los que estáis presentes todos vosotros. Así es que de nuevo…..¡MUCHAS GRACIAS!!!

Index

Abbreviations

AA : arachidonic acid

AC : Adenylyl cyclase

ACE : Angiotensin converting enzyme

ACEI : ACE inhibitor

ADMA : Asymmetric dimethylarginine

AMPK : Adenosine 5'-monophosphate-activated protein kinase

Ang I : Angiotensin I

Ang II : Angiotensin II

AP-1 : Activating protein-1

ARBs : Angiotensin II type I receptor blockers

AT1 receptor : Angiotensin II type 1 receptor

AT2 receptor : Angiotensin II type 2 receptor

BH_4 : Tetrahydrobiopterin

cAMP : Cyclic adenine 3', 5'- monophosphate

Cav-1 : Caveolin-1

cGMP : Cyclic guanosine monophosphate

COX : Cyclooxygenase

COX-1 : Cyclooxygenase 1

COX-2 : Cyclooxygenase 2

cPGES : Cytosolic prostaglandin E_2 synthase

Cu/Zn-SOD : Copper/Zinc superoxide dismutase

DAG : Diacylglycerol

DOCA : Deoxycorticosterone acetate

DP : PGD_2 receptor

ECs : Endothelial cells

EC-SOD : Extracellular superoxide dismutase

EDHF : Endothelium derived hyperpolarizing factor

EGFR : Epidermal growth factor receptor

EMC : Extracellular matrix

eNOS : Endothelial nitric oxide synthase

EP : PGE_2 receptor

ER : Endoplasmic reticulum

ERK : Extracellular signal-regulated kinase

ET-1 : Endothelin-1

FAK: Focal adhesion kinase

FP : $PGF_{2\alpha}$ receptor

GC : Guanylate cyclase

GPCRs : G protein-coupled receptors

GPX : Glutathione peroxidase

GR : Glutathione reductase

GRK2 : G protein-coupled receptor kinase 2

GRKs : G protein-coupled receptor kinases

GRXo : Glutaredoxin (oxidized)

GRXr : Glutaredoxin (reduced)

GSHr : Glutathione (reduced)

GSSG : Glutathione (oxidized)

H_2O_2 : Hydrogen peroxide

$HO^{\cdot}$: Hydroxyl radicals

HSP90 : Heat shock protein 90

11βHSD2 : 11β-Hydroxysteroid dehydrogenase 2

IP : PGI_2 receptor

IP3 : Inositol trisphosphate

JNK : c-Jun N-terminal kinase

JAK2: Janus kinase 2

Ki-Ras2A : Kirsten-Ras 2A

LDL : Low density lipoprotein

MAPK : Mitogen activated protein kinases

Mito-ETC : Mitochondrial electron transport chain

MLC : Myosin light chain

MLCK : Myosin light chain kinase

MLCP : Myosin light chain phosphatase

MMPs : Matrix metalloproteinases

Mn-SOD : Manganese superoxide dismutase

mPGES : Microsomal prostaglandin E_2 synthase

MR : Mineralocorticoid receptor

NADPH : Nicotinamide adenine dinucleotide phosphate (reduced)

NF-κB : Nuclear factor kappa B

NO : Nitric oxide

NOS : Nitric oxide synthase

$O_2^{-\cdot}$: Superoxide anion

$ONOO^-$: Peroxynitrite

PAI-1 : Plasminogen activator inhibitor type 1

PG : Prostaglandin

PGE_2 : Prostaglandin E_2

PGES : PGE_2 synthase

$PGF_{2\alpha}$: Prostaglandin $F_{2\alpha}$

PGG_2: Prostaglandin G_2

PGH_2 : Prostaglandin H_2

PGI_2 : Prostacyclin

PGIS : Prostacyclin synthase

PI3K : Phosphoinositol-3 kinase

PIP2 : Phosphatidylinositol 4,5-bisphosphate

PKA : Protein kinase A

PKC : Protein kinase C

PLA_2 : Phospholipase A_2

PLC : Phospholipase C

PLD : Phospholipase D

PP1 : Protein phosphatase 1

RAAS : Renin-angiotensin-aldosterone system

RAS: Renin-angiotensin system

ROCK : Rho-associated protein kinase

ROS : Reactive oxygen species

SHR : Spontaneously hypertensive rats

SMCs : Smooth muscle cells

SOD : Superoxide dismutase

SR : Sarcoplasmic reticulum

TP : TXA_2 receptor

TRX : Thioredoxin

TRXo : Thioredoxin (oxidized)

TRXr : Thioredoxin (reduced)

TXA_2 : Thromboxane A_2

VSMCs : Vascular smooth muscle cells

WKY : Wistar Kyoto rat

Abstract

The Renin-Angiotesin-Aldosterone System (RAAS) is responsible of the functional and structural alterations of the vasculature associated to hypertension. RAAS activation induces vascular inflammation characterized by marked upregulation of enzymes such as cyclooxygenase 2 (COX-2) and increased reactive oxygen species (ROS) production that might modulate nitric oxide (NO) bioavailability. In addition, G protein-coupled receptor kinases 2 (GRK2) are involved in the desensitization of G protein coupled receptors (GPCR) such as Angiotensin II (Ang II) type 1 receptors (AT1) and in the regulation of NO production.

The main aim of this Thesis was to investigate the role of oxidative stress from NADPH Oxidase and mitochondria, COX-2 derived prostanoids and GRK2 in the vascular functional and structural abnormalities observed in hypertension. In line with this general aim, the Thesis was divided into four specific aims:

1. Knowing the pivotal role of aldosterone in the regulation of vascular tone and in hypertension development, in the first article we analyzed the effect of three weeks aldosterone treatment on noradrenaline-induced vasoconstriction in mesenteric resistance vessels from normotensive (WKY) and spontaneously hypertensive (SHR) rats. We also studied the role of endothelium-derived mediators, such as COX-2-derived prostanoids, NO and ROS in the aldosterone effect. In vessels with endothelium, the contractile responses to noradrenaline were similar in both strains irrespective of the presence or the absence of aldosterone. However, aldosterone treatment diminished the protective effect of the endothelium on noradrenaline contraction. This was probably due to decreased NO availability produced by increased ROS production. In addition, aldosterone increased the participation of COX-2-derived products and TP receptor in the noradrenaline responses. Importantly, the effect of aldosterone on NO, ROS and

prostanonoids was greater in SHR compared to WKY. In conclusion, long-term treatment of rats with aldosterone despite of not affecting noradrenaline contraction, alters the role of endothelium on these responses being this effect more pronounced in SHR than in WKY. Aldosterone treatment alters the release of COX-2-derived prostanoids, NO and ROS that might participate on the above mentioned endothelial modulation.

2. Previous articles of our group and others demonstrated that ROS and COX-2-derived products are involved in vascular responses in hypertension. We next questioned whether a reciprocal relationship between ROS producing enzymes (NADPH Oxidase and mitochondria) and COX-2 might modulate vascular functional responses of conductance and resistance arteries in hypertension. For this purpose, we used two different models of hypertension, Ang II infused mice and SHR rats. Animals were treated with the antioxidant and NADPH Oxidase inhibitor apocynin, the mitochondrial-targeted superoxide dismutase (SOD) 2 mimetic mito-TEMPO, the SOD analogue tempol, or the COX-2 inhibitor celecoxib. Antioxidant treatments diminished the increased vascular COX-2 expression, prostanoids production and the participation of COX-derived contractile prostanoids and TP receptor in phenylephrine responses observed in arteries from both hypertensive models. On the other hand, celecoxib treatment normalized the increased ROS production, NADPH Oxidase expression and activity, SOD2 expression and the participation of ROS in vascular responses in both hypertensive models. Importantly, apocynin, mito-TEMPO, and celecoxib treatments reduced high blood pressure and increased the diminished NO production and the modulation of phenylephrine responses by NO in the Ang II model. Our results demonstrate that the excess of ROS from NADPH Oxidase and/or mitochondria and the

increased vascular COX-2/TP receptor axis act in concert to induce vascular dysfunction and hypertension.

3. Alterations in the structure and mechanical properties of the arteries are important contributors to high blood pressure. Prostanoids from COX-2, microsomal prostaglandin E synthase (mPGES)-1 and prostaglandin E_2 receptors (EP) contribute to vascular remodeling in different cardiovascular pathologies but its role in hypertension is not known. We explored the contribution of the COX-2/mPGES-1/EP1 receptor axis in vascular remodeling and function in conductance and resistance arteries from Ang II infused mice and SHR. Both hypertensive models were treated with celecoxib and the Ang II infused mice were also treated with the EP1 receptor antagonist SC19220. In addition, we used COX-2 deficient ($COX\text{-}2^{-/-}$) mice infused or not with Ang II. Pharmacological blockade of COX-2 did not improve the altered structural parameters (lumen diameter and wall:lumen ratio) observed in arteries from hypertensive animals. However, celecoxib treatment and COX-2 deficiency normalized the increased vascular stiffness and the diminished wall distensibility observed in mesenteric resistance arteries from both hypertension models. These effects were probably due to decreased fibrosis since diminished collagen deposition, improved elastin structure and decreased conective tissue growth factor, tenascin-C and plasminogen activator inhibitor-1 gene expression were observed after COX-2 inhibition. In hypertensive animals vascular mPGES-1 gene was increased which was normalized by celecoxib treatment. The inhibition of EP_1 receptor did not modify the structural parameters. Nevertheless, it normalized the alterations in vascular stiffness, wall distensibility, collagen levels and altered elastin structure observed in Ang II infused mice. COX-2 deficiency and SC19220 treatment diminished the increased vasoconstrictor responses to phenylphrine and the endothelial dysfunction induced by Ang II. These results suggest that the COX-

2/mPGES-1/EP_1 axis modulates extracellular matrix deposition, mechanical properties and vascular function in hypertension.

4. GRK2 is the most abundant GRK in vessels and it plays a determinant role in the control of systemic vascular responses by regulating not only GPCR, such as AT1, but also the AKt-eNOS pathway. Levels or activity of GRK2 are increased in different tissues from animal models of hypertension or in patients and correlate with high blood pressure in humans. In the last article we investigated if GRK2 is involved in the functional, structural and mechanical vascular alterations associated to hypertension. Given the lack of selective inhibitors for GRK2, we investigated the effects elicited by GRK2 inhibition in vascular responses using global adult hemizygous GRK2 mice ($GRK2^{+/-}$). Partial GRK2 deficiency increased the vasodilator responses to acetylcholine and isoproterenol in mesenteric resistance arteries and aorta although no differences in vascular structure and mechanics or in resting blood pressure were observed when compared to wild type (WT) mice. After Ang II infusion, $GRK2^{+/-}$ mice were partially protected against hypertension and showed improved vascular structure (wall:lumen ratio) and mechanical properties (vascular stiffness) when compared to WT littermates. In addition, Ang II infusion increased GRK2 levels and vasoconstrictor responses to phenylephrine in WT but not in GRK2+/- vessels and decreased vasodilator responses to acetylcholine and vascular pAkt and eNOS levels more in WT than in GRK2+/-. Vascular NO production and the modulation of vasoconstrictor responses by endothelial-derived NO were greater in GRK2+/- mice infused with Ang II. Our results describe an important role for GRK2 in systemic hypertension and further establish that an inhibition of GRK2 could be a beneficial treatment for this condition.

In conclusion, the results shown in this Thesis demonstrate that COX-2-derived prostanoids, ROS and GRK2 acting alone or in reciprocal relationship, are key

components involved in the functional, structural and mechanical alterations observed hypertension both in conductance and resistance arteries. Whether pharmacological blockade of these targets might have beneficial effects in hypertension associated vascular damage in humans warrants future investigations.

Introduction

Hypertension is one of the most common chronic diseases affecting more than 1 billion people worldwide. Its importance lies on the fact that it is a major risk factor for cardiovascular diseases such as coronary heart disease, heart failure, stroke and hypertensive nephropathy, all major sources of morbidity and mortality. The etiology of elevated blood pressure cannot be determined in the vast majority of individual with "essential" hypertension. Thus, choices of antihypertensive therapy are typically empirical and are based on board epidemiological categories such as age, race and the presence of coexisting disorders such as diabetes or heart disease. Despite of the high prevalence of hypertension and increasing public awareness of this disorder, control rates of hypertension remain unsatisfactory and a substantial proportion of hypertensive patients under treatment do not achieve the target levels of blood pressure recommended by the current guidelines (57,155). Thus, the knowledge of the underlying mechanisms responsible of these alterations remains a priority for both basic and clinical researchers in the field.

Hypertension is a multifactorial disease resulting from genetic, pathophysiological and environmental factors. During the last years, it has been demonstrated that low-grade inflammation plays an important role in the pathophysiology of hypertension and its associated vascular injury (218). Increased circulating levels of inflammatory molecules are associated to hypertension in both patients and animal models (218). In addition, increased expression of inflammatory enzymes such as the inducible isoform of cyclooxygenase 2 (COX-2) (118) and increased production of reactive oxygen species (ROS) (75,118,169,274) have been described in hypertension. Importantly, these mediators seem to contribute to the functional and structural vascular alterations observed in this pathology. The mechanisms underlying this inflammatory state in the vascular wall may involve mechanisms dependent on high blood pressure and

proinflammatory effects induced by different humoral factors such as components of the renin-angiotensin-aldosterone system (RAAS).

Different receptors and signaling molecules in the vasculature are involved in hypertension development and/or maintenance by affecting vessels function and structure in a deleterious manner. The G protein-coupled receptor (GPCR) family is of outmost importance. G protein-coupled receptor kinases (GRKs) is a family of serine/threonine kinases that initiate receptor uncoupling from the G protein, and thus induce signal termination (203). The GRK2 subtype which is one of the most highly expressed in vessels, plays a determinant role in the control of systemic vascular responses (35,197). GRK2 is involved in the desensitization of GPCR (203) and seems to be involved in the regulation of nitric oxide (NO) production in hypertension (152).

This thesis attempts to unravel the role of oxidative stress, prostanoids and GRK2 in vascular dysfunction and remodeling in hypertension. This Introduction will explore previous evidences indicating that ROS, COX-derived products and GRK2 might participate in the vascular functional, structural and mechanical alterations observed in this pathology.

1. STRUCTURE OF THE VASCULAR WALL

Arteries are anatomically and functionally organized in three layers; intima, media and adventitia (Figure 1) and are composed of different cell types embedded in the extracellular matrix (ECM). The different layers of the vascular wall exert their own influence on both the vasomotor control and the vascular structure, being the final effect the result of the interrelated participation of the three layers.

1.1. LAYERS OF THE VASCULAR WALL

1.1.1. Tunica Intima

The tunica intima delimits the vessel wall towards the lumen of the vessel and comprises the endothelium, consisting of a simple layer of epithelium, and its corresponding basal lamina of connective tissue. The tunica intima is separated from the tunica media by the internal elastic lamina which is located above the connective tissue (Figure 1).

The endothelium is not only a mechanical barrier but also acts as receptor and transmitter of signals between blood and other components of the vascular wall. Endothelial cells (ECs) have exocrine, paracrine and autocrine functions, and they are involved in the regulation of vascular tone, vasculogenesis and angiogenesis, blood coagulation, fibrinolysis, and inflammation (165). ECs are sensitive to hemodynamic changes such as pressure or shear stress forces and to circulating chemical messengers. They respond to these signals by secreting different growth factors and vasoactive substances, including vasodilator factors such as NO and prostaglandin (PG) I_2 or prostacyclin (PGI_2) which also inhibit platelet aggregation (90), and endothelium derived hyperpolarizing factor (EDHF) (211). Main vasoconstrictor factors released

from the endothelium are endothelin-1 (ET-1), ROS and vasoconstrictor prostanoids such as thromboxane A_2 (TXA_2) and PGE_2 (90,240).

1.1.2. Tunica Media

The tunica media is formed by a layer of circumferentially arranged vascular smooth muscle cells (VSMCs) and variable amounts of extracellular matrix (EMC). The tunica media is sepaated from the tunica adventitia by a second layer of elastic fibers, the external elastic lamina, which is located above the VSMCs (Figure 1). VSMCs can release a variety of vasoconstrictor and vasodilator substances including prostanoids and ROS, among others (146). The tunica media respond to the action of different vasoactive factors and hemodynamic forces by contracting or dilating the vessels thus being essential in the control of vascular tone.

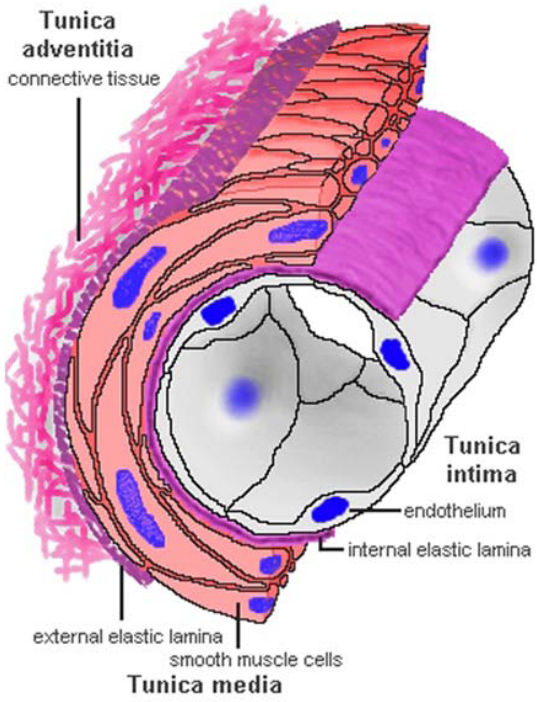

Figure 1. *General structure of the artery wall. Taken from http://www.lab.anhb.uwa.edu.au/mb140/corepages/vascular/vascular.htm*

1.1.3. Tunica Adventitia

The tunica adventitia is mainly composed of connective tissue, fibroblasts, immune cells and perivascular adipose tissue. Depending on the vessel type, a number of small arteries termed *vasa vasorum* can be found to facilitate blood irrigation to the vessel wall. Adventitia also receives the neuronal axons that innervate the muscular tissue (202). In the last years it has become evident that the adventitia is not only a mechanical support for the vessel but also has an active role in the regulation of vascular tone and structure (231) by releasing different factors such as free fatty acids, adipokines (192), adipose-derived relaxing factor (153), ROS (114,201) and COX-2 derived prostanoids (5,24).

1.2. EXTRACELLULAR MATRIX

A major component of the vessel wall is the ECM which is produced by endothelial, smooth muscle and adventitial cells. The ECM is a complex heterogeneous tissue comprising among others collagens, elastin, glycoproteins, and proteoglycans (39). This matrix not only provides structural support to vessels but it is also involved in the mechanical properties and vascular function (39,261). In this sense, the ECM can release a repertoire of insoluble ligands that induce cell signaling to control proliferation, migration, differentiation and survival (39). The main components of the ECM are the following.

- **Collagen** is a very stiff protein which has the physiological role to limit vessel distension (39). The polypeptide precursor of the collagen molecules, procollagen, is secreted to the extracellular compartment where it transforms in tropocollagen. After enzymatic modification, the mature collagen monomers aggregate and become cross-linked to form collagen fibers. Collagen types I and III are the major fibrillar collagens

detectable in vessels although other collagen types such as IV, V and VI are also expressed (261). The distribution of collagens I and III vary depending on the specific region of the vascular tree being examined. Thus, in the ascending aorta, collagens colocalize in the media and adventitia whereas in muscular arteries, type I is distributed mainly in the media and less so in the adventitia, whereas type III is localized predominantly in the adventitia (261).

- **Elastin** is the major protein that imparts the property of elasticity to blood vessels. Elastin functions as a cross-linked polymer as part of an elastic fiber, and its assembly outside the cell requires an association with numerous other extracellular proteins such as microfibrils (14,39,261). Elastin represents 90% of the elastic fibers. The precursor of elastin, tropoelastin, is a highly hydrophobic protein, which is soluble in salt solution. However, elastin is an insoluble protein as a result of cross-linking process between lysine residues. This cross-linking process confers to elastin its elasticity, essential in large arteries which distend during systole and recoil during diastole (261). Elastic fibers are found throughout the vessel wall and, in the medial layer of conduit arteries, they are arranged in concentric fenestrated elastic lamellae. Each elastic lamella alternates and it is physically connected with a concentric ring of VSMCs forming the lamellar unit. In the small arteries, elastin is generally disposed in a fenestrated and compact internal elastic lamina as well as in a smooth fibrous external elastic lamina (14).

Although collagen and elastin are the major contributors to the visco-elastic characteristics of the vascular wall, a number of additional ECM components affect both the compliance characteristics and vasoregulatory abilities of blood vessels.

- **Fibronectin** is a multi-domain ECM protein that interacts with multiple integrins, heparan sulfate proteoglycans, collagens, and fibrins to mediate cellular behaviors (193). The content of fibronectin in blood vessels is important not only because it modifies the mean stress and elastic modulus of the wall (175), but also because it has been suggested that fibronectin is closely associated with the capacity of arteriolar VSMCs to detect and react to mechanical forces via integrin receptors (175). In addition, fibronectin controls the deposition, organization, and stability of other matrix molecules including collagen I, collagen III and thrombospondin-1 and modulates leukocyte infiltration, expression of adhesion molecules, cell proliferation, and VSMCs phenotypic modulation, all factors involved in vascular remodeling (53).

- **Integrins** are transmembrane proteins that mediate attachment of the cell to the ECM and have a role in signal transduction from the ECM to the cell (95). Integrins represent the largest family of cell surface receptors. It has been suggested that changes in integrin profile are important for processes leading to more chronic structural rearrangement of the vascular wall and ECM material (175).

- **Matrix metalloproteinases (MMPs)** are a family of endopeptidases which require a zinc ion at their active site for proteolityc activity (49). They are mainly responsible for the degradation and reorganization of ECM that can lead to physiological or pathological processes. Thus, in normal physiological vascular remodeling, MMP activity is tightly controlled at different levels. However, factors that promotes vessel remodeling upregulate MMP activities. Loss of control of MMP activity could result in degradation of ECM, enabling VSMCs to migrate and proliferate and inflammatory cells to infiltrate the arterial wall (28,39). Thus, partial degradation of the ECM surrounding VSMCs is likely a necessary step for allowing repositioning of cells during remodeling (175).

- **Plasminogen/plasminogen activator system.** Plasmin can degrade ECM directly or indirectly via MMP activation (28). Therefore altered plasmin activity of expression can have high impact on vascular fibrosis. Plasmin is released as a zymogen called plasminogen. The activity of this system is tightly controlled by plasminogen activator inhibitor type 1 which functions as the principal inhibitor of tissue plasminogen activator.

- **Tenascins** are ECM glycoproteins. Tenascin C is mainly found in vessels and it was the first member of a family of four structurally similar proteins identified including tenascin R, W and X (102). Tenancin C has diverse functions including weakening of cell adhesion, up-regulation of the expression and activity of MMP, modulation of inflammatory responses, promotion of myofibroblasts recruitment and enhancement of fibrosis (124).

2. FACTORS REGULATING VASCULAR TONE AND STRUCTURE

Vascular tone and structure are regulated by the equilibrium between vasodilator-antiproliferative- antifibrotic factors and vasoconstrictor- proliferative- profibrotic factors, which are released in large part, by the ECs and VSMCs in response to mechanical or chemical stimuli. The imbalance between these substances leads to the endothelial dysfunction and/or the vascular remodeling observed in cardiovascular diseases. Some of the factors most widely involved in vascular alterations are NO, ROS and prostanoids which are tightly regulated by the RAAS. In addition, GRK2 has been suggested as regulator of vessels function and structure. We will describe here these factors and in the next section we will focus on their role in the vascular alterations observed in hypertension.

2.1. NITRIC OXIDE

NO is the main mediator of endothelium-dependent relaxation. It is a gaseous free radical, very diffusible and with a short half-life. The production of NO is catalyzed by nitric oxide synthase (NOS), which convert the amino acid L-arginine to L-citrulline and NO (99,168) (Figure 2). NOS isoforms are members of a family of cytochrome P450–like reductases linked to a nicotinamide adenine dinucleotide phosphate (NADPH) oxidase enzyme (99). There are three isoforms of NOS that differ in their expression and activity. Endothelial NOS (eNOS) or NOS3 (mainly expressed in ECs) and neuronal NOS or NOS1 (mainly expressed in neurons) are constitutively expressed and its activity depends on Ca^{2+}-calmodulin. The inducible NOS or NOS2 is an inducible isoform initially described in macrophages and also described later in ECs and VSMCs during or after stimulation with several inflammatory agents such as bacterial lipopolysacharide, some proinflammatory interleukins, TNF-α, etc (164,180) and its

activity is independent of calmodulin (11). NO production is also modulated by asymmetric dimethylarginine (ADMA), an endogenous inhibitor of NOS and by its cofactor tetrahydrobiopterin (BH_4) (135,138). After NO production, this diffuses to the underlying VSMCs where it activates soluble guanylate cyclase, causing an increase in cGMP and smooth muscle relaxation by decreasing intracellular calcium (Figure 2).

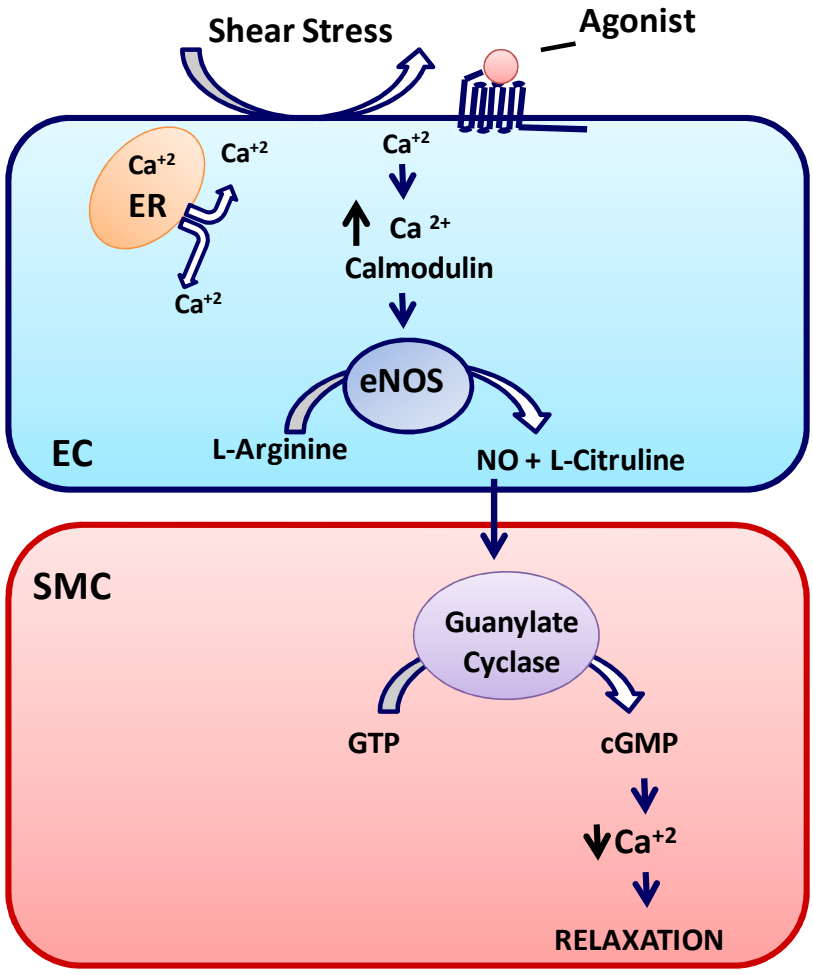

Figure 2. Nitric oxide biosynthesis and action in blood vessels. *Biosynthesis of the key endogenous vasodilator NO is mainly performed in endothelial cells (EC) by endothelial nitric oxide synthase (eNOS). This is triggered by agonists or by shear stress that induce an increase of intracellular free calcium concentration. The amino acid L-Arginine is converted by eNOS into NO with L-Citrulline as a byproduct. NO diffuses into adjacent smooth muscle cells (SMC) where it activates its effector enzyme Guanylate Cyclase, that converts GTP into the second messenger cGMP, which leads to a decrease in intracellular calcium inducing relaxation of SMC.*

eNOS is located in specialized invaginations of plasma membrane called caveolae that are rich in caveolin-1 (Cav-1) (Figure 3) and other specialized proteins such as heat shock protein 90 (HSP90). Association with Cav-1 maintains low basal eNOS activity while the interaction of eNOS with HSP90 augments stimulated eNOS activity. There are several pathways by which eNOS activity can be increased. Activation of specific GPCR with agonists such as acetylcholine or bradykinin can rapidly activate eNOS by calcium-calmodulin dependent displacement of eNOS from Cav-1. eNOS can also be stimulated by phosphorylation of its activating Ser-1177 site by multiple kinases including Akt, cAMP activated protein kinase (AMPK) and cAMP-dependent protein kinase A (PKA). Activation of Akt by phosphoinositide-3-kinase (PI3K) mediates eNOS activation and this is promoted by shear stress, vascular endothelial growth factor, estrogens and insulin. Akt activity can also be stimulated by PKA both directly and through PI3K. PKA is the main downstream pathway for many GPCR, and in addition to activate eNOS through the phospohorylation of Ser-1177, it can also stimulate eNOS through protein phosphatase 1 (PP1)-mediated dephosphorylation of the inhibitory Thr-495 site (Figure 3). However, protein kinase C (PKC) inhibits eNOS activity through phosphorylation of Thr-495 site. This process is mediated by diacylglycerol (DAG) formed by phospholipase C (PLC) that activate PKC. This complex eNOS regulation and interconnections between regulatory pathways of various endothelial and extra-endothelial functions is critical for adequate NO production (135,138).

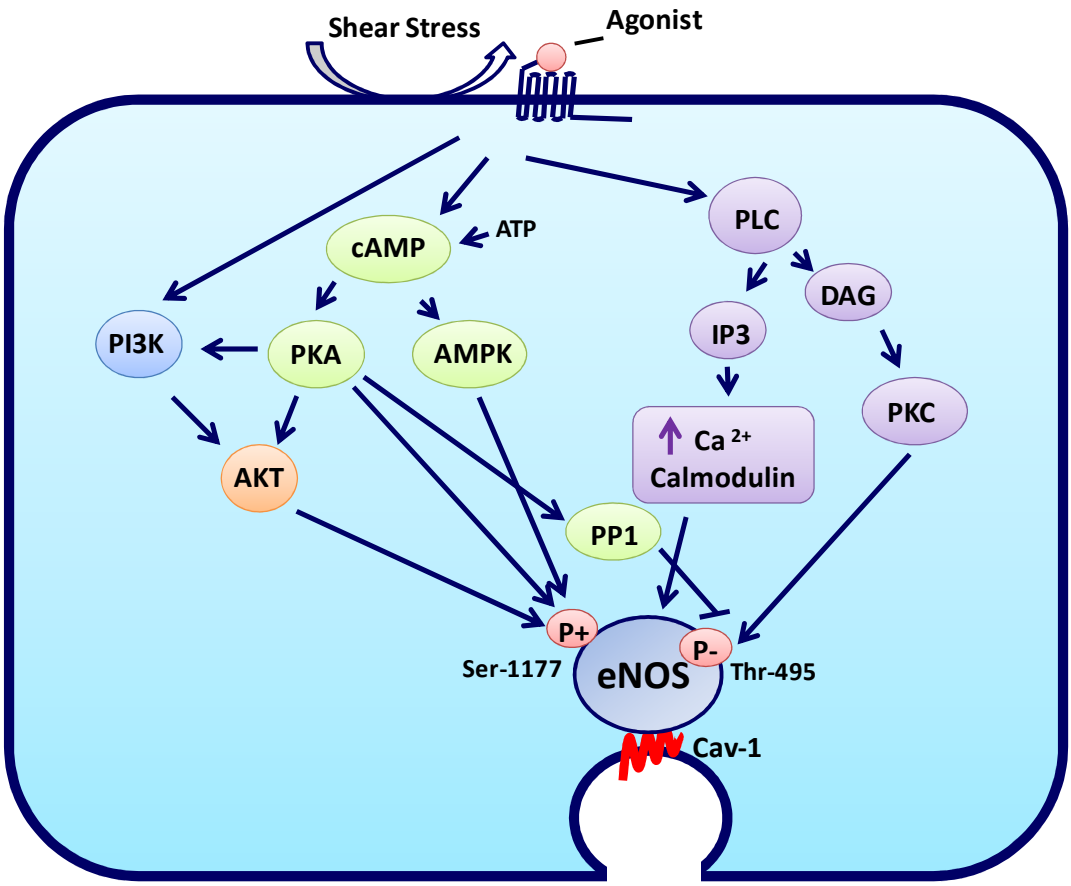

Figure 3. Regulation of endothelial nitric oxide synthase activation. *Endothelial nitric oxide synthase (eNOS) can be activated by calcium calmodulin (Ca^{2+} Calmodulin) mediated displacement of caveolin-1 (Cav-1) and by phosphorylation of its activating Ser-1177 site by multiple kinases including cAMP-activated protein kinase (AMPK), protein kinase A (PKA), and Akt that can be stimulated by phosphoinositol-3 kinase (PI3K). PKA stimulate eNOS through protein phosphatase 1 (PP1) mediated dephosphorylation of the inhibitory Thr-495 site. In contrast, protein kinase C (PKC) inhibits eNOS activity through phosphorylation of Thr-495 site. Diacylglycerol (DAG) formed by phospholipase C (PLC) is the main physiological PKC activator. These pathways are activated by mechanical shear stress or by activation of G-protein coupled receptors by various ligands. Adapted from Koska (138).*

2.2. REACTIVE OXYGEN SPECIES

ROS are reactive derivatives of the oxygen metabolism with superoxide anion ($O_2^{\cdot-}$), hydrogen peroxide (H_2O_2) and peroxynitrite ($ONOO^-$) being of major importance. There is an apparent paradox between the roles of ROS as essential biomolecules in the regulation of many cellular functions and as toxic by-products of metabolism that may

be related at least in part, to differences in the concentrations of ROS produced. Thus, at low intracellular concentrations, ROS have a key role in the physiological regulation of vascular tone, cell growth, adhesion, differentiation, senescence and apoptosis. However, excessive ROS levels may be associated with the development of several cardiovascular diseases (169,250).

$O_2^{-\cdot}$ is highly reactive, has a short half-life and is unable to diffuse across biological membranes except possibly via ion channels (250). $O_2^{-\cdot}$ can dismute to H_2O_2, both spontaneously and enzymatically via any of the three isoforms of the superoxide dismutase (SOD): cytosolic Cu/Zn-SOD or SOD1, mitochondrial Mn-SOD or SOD2 and extracellular EC-SOD or SOD3 (Figure 4). H_2O_2 is more stable than $O_2^{-\cdot}$ and crosses membranes through some members of the aquaporin family (4). H_2O_2 is quickly metabolized to water and oxygen by several enzymatic systems such as glutathione peroxidase, catalase and the thioredoxin (TRX) system, which includes TRX, TRX reductase and TRX peroxidase (peroxiredoxin) (77) (Figure 4). In the presence of transition metals (such as Fe^{2+}) H_2O_2 can be converted to hydroxyl radicals ($HO^{\cdot}$), which are highly reactive and can cause damage to lipids, proteins and DNA. In addition, NO which has a very short half-life, can react with $O_2^{-\cdot}$ to form $ONOO^-$ that is capable of modifying the structure and function of proteins. There are other several non-enzymatic antioxidant systems like ascorbate and tocopherols (250). ROS bioavailability is tightly regulated to maintain healthy levels by a delicate equilibrium between generation and metabolism, so alterations in any of the above mentioned systems might lead to pathological ROS levels.

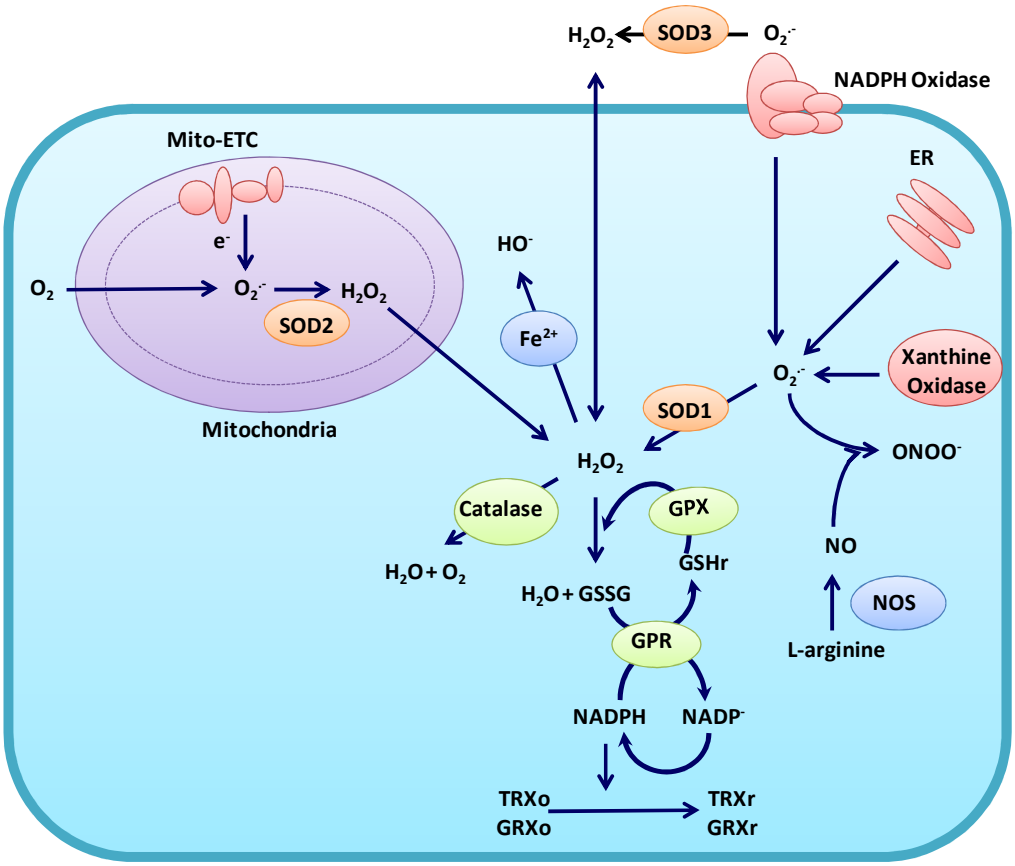

Figure 4. Reactive oxygen species formation and metabolism. *Major sources of ROS generation include the mitochondrial electron transport chain (Mito-ETC), endoplasmic reticulum (ER) system, NADPH oxidase and xanthine oxidase. Superoxide anion ($O_2^{\cdot-}$) is the main initial free radical specie which can be converted to other reactive species. In the mitochondria, $O_2^{\cdot-}$ is generated by the capture of electrons escaping from the Mito-ETC by molecular oxygen (O_2). $O_2^{\cdot-}$ can be rapidly converted to hydrogen peroxide (H_2O_2) by superoxide dismutase (SOD), which is converted to H_2O by catalase, glutathione peroxidase (GPX) or the thioredoxin (TRX) systems. In the presence of transition metals (such as Fe^{2+}), H_2O_2 can be converted to hydroxyl radicals ($HO^{\cdot}$) NO has a very short half-life and can react with superoxide to form $ONOO^-$. Glutathione reductase (GPR); glutaredoxin oxidized (GRXo); glutaredoxin reduced (GRXr); glutathione reduced (GSHr); glutathione oxidized (GSSG); thioredoxin oxidized (TRXo); thioredoxin reduced (TRXr). Adapted from Trachootham et al. (251).*

NADPH oxidase is a major source of ROS in different tissues (75,169). In mammals, there are seven family members of NADPH oxidases, Nox1-Nox5, DUOX1-DUOX2 (Figure 5). Nox1, 2, 4, and 5 are expressed in multiple tissues including the vascular wall with specific cellular and subcellular localizations and regulation, whereas Nox3 and the Duoxs are more tissue specific (75). All Noxs are transmembrane proteins that have a core catalytic subunit (Nox) and a number of regulatory subunits that differ

depending on the Nox isoform studied (169) (Figure 5). Nox2, the prototypic phagocyte NADPH oxidase, is activated when the regulatory subunit p47phox is phosphorylated, complexes with p67phox and p40phox and translocates to the cell membrane to interact with p22phox and Nox2 to assemble the active oxidase, which then transfers electrons from the substrate NADPH to O_2 forming $O_2^{-\cdot}$ (169). Besides differences in their structure and their subcellular location, the catalytic subunits differ in the ROS they produce. Nox1, Nox2, Nox3 and Nox5 produce $O_2^{-\cdot}$ while Nox4, DUOX1 and DUOX2 produce H_2O_2 (75) (Figure 5). While Nox4 shows high constitutive activity, other family members may be activated upon stimulation (143).

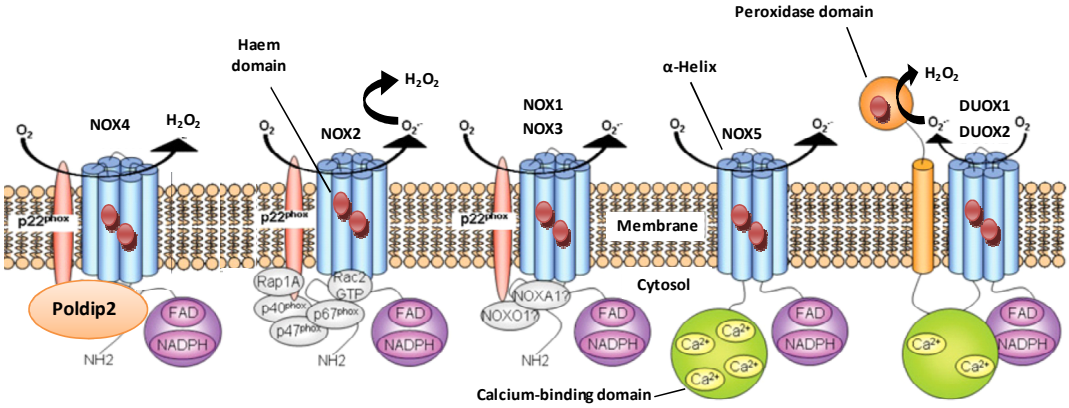

Figure 5. Components of active NADPH oxidase complexes. *Nox1, Nox2, Nox4, and Nox5 are members of the Nox family that are expressed in the cardiovascular system. Nox2 is the classical Nox that was primarily characterized in leukocytes. Nox1, Nox2, and Nox3 function as regulated enzymes involving cytosolic adaptor proteins or "Nox organizers" (p47phox or Noxo1 and p40phox) and "Nox activators" (p67phox or Noxa1) that bind GTP-Rac and affect the flow of electrons. The p22phox component forms a stable heterodimeric complex with Nox core components (Nox1–4), required for post-translation processing or maturation into active oxidases. In Nox1–Nox3 systems, p22phox also promotes plasma membrane targeting of the oxidases and provides a docking site for Nox organizers. However Nox4 only depends on p22phox in order to be active, is constitutively activated, and ROS production is regulated by Poldip2. Nox5 and Duox are calcium-responsive oxidases that contain calcium-binding EF-hands. Nox1, Nox2, Nox3 and Nox5 produce $O_2^{-\cdot}$ while Nox4, DUOX1 and DUOX2 produce H_2O_2. Adapted from Guichard et al. (110) and Montezano and Touyz (169).*

Other sources of ROS in the vascular wall are mitochondria, xantine oxidase, uncoupled eNOS, endoplasmic reticulum, COX, cytochrome P450 and lipoxygenase (Figure 4).

Mitochondria are a major cellular source of ROS. There are several sites in the electron-transport chain where O_2 can be reduced to $O_2^{-\cdot}$ being complex I and III the sites with the greatest capacity. Complex I produces $O_2^{-\cdot}$ in the matrix whereas complex III produces it in either the matrix or the intermembrane space (68,270). Xanthine oxidase, mainly expressed in the endothelium in the vessel wall (145), catalyzes the sequential oxidation of hypoxanthine to xanthine and xanthine to urate and can generate $O_2^{-\cdot}$ and H_2O_2 (141). Endoplasmic reticulum stress is associated with an increase in ROS generation associated to a decrease in the level of antioxidants as consequence of an increase in the threshold of ROS generation (216). Although it was accepted that the main sources of ROS during endoplasmic reticulum stress are endoplasmic reticulum protein oxidation and mitochondria, in the last years the involvement of NADPH oxidase has also been suggested (216). Interestingly this has been associated with several pathologies.

To date, there is a growing body of evidence suggesting that activation of one specific ROS source might lead to the activation of another, providing an explanation for the well-known phenomenon of ROS-induced/ROS production (118). Of particular interest is the interplay between NADPH oxidase and mitochondria. Thus, the activation of NADPH oxidase may increase mitochondrial ROS production and *viceversa*, mitochondrial ROS are able to activate the NADPH oxidase in a number of situations; therefore, mitochondria-targeted antioxidants break the vicious cycle reducing ROS production by both mitochondria and NADPH oxidase (67). Importantly, in this relationship H_2O_2 has a paramount importance (67,69). Another example of this cross-talk between sources of ROS is the fact that ROS from mitochondria and NADPH oxidase influence xanthine oxidase activity and expression (163,227) as well as eNOS uncoupling (227). Self-perpetuating ROS production affects virtually all ROS. Thus,

H_2O_2 activates NADPH oxidase leading to further $O_2^{-\cdot}$ production (4,93). Interestingly, H_2O_2 induces the transition of xanthine dehydrogenase into xanthine oxidase which generates both H_2O_2 and $O_2^{-\cdot}$(163). $ONOO^-$ increases $O_2^{-\cdot}$ generation and decreases NO production by eNOS uncoupling (225). In addition, $ONOO^-$ participates in Ang II-induced mitochondrial H_2O_2 production (74). All together, this suggests that there is a positive feed-forward mechanism whereby ROS may be important for persistent $O_2^{-\cdot}$ production in the vascular wall, particularly in pathological conditions.

It is now evident that ROS are powerful modulators of vascular contraction, dilatation and structural remodeling and participate in vascular alterations in pathological conditions (40,118). The mechanisms responsible of these effects include quenching of vasodilator NO by $O_2^{-\cdot}$, generation of vasoconstrictor lipid peroxidation products, depletion of BH_4, and induction of fibrosis through activation of MMP (40). At intracellular level, ROS induce different processes such as increased intracellular calcium, activation of growth and inflammatory transcription factors and activation of different signaling pathways such as mitogen activated protein kinases (MAPK), protein tyrosine phosphatases, tyrosine kinase, PI3K, and RhoA/ROCK (40).

2.3. PROSTANOIDS

Prostanoids are critical modulators of vascular tone and platelet aggregation in physiological and pathological conditions. Prostanoids are biologically active derivatives of arachidonic acid released from membrane phospholipids by phospholipase A_2. The initial transformation of arachidonic acid to prostanoids involves the production of an unstable intermediate endoperoxide PGG_2 by COX enzymes which also reduce PGG_2 to PGH_2 (Figure 6). COX is located in the membrane of endoplasmic reticulum and/or microsomes. In healthy blood vessels, most prostanoids are produced

by the constitutive isoform COX-1. However, these mediators may also be synthesized by COX-2 that can be induced by inflammatory stimuli and other factors such as Ang II or ET-1 (85,118,204). Additionally, COX-2 is constitutively expressed in pathological conditions in several organs and cell types including the vascular wall (5,85,118,258). After the initial synthesis of the short-lived but biologically active PGH_2, the production of the different prostanoids (the prostaglandins PGE_2, PGD_2, $PGF_{2\alpha}$, PGI_2, and TXA_2) depends on the activity of specific synthases. Particularly interesting is PGE_2 the most abundant prostanoid in the human body. There are three PGE synthases (PGES); one is cytosolic cPGES, and the other two are membrane bound, mPGES-1 and mPGES-2 (Figure 6). Of these three, cPGES and mPGES-2 are constitutive, while mPGES-1 is up-regulated by inflammatory stimuli (91,213).

Prostanoids have different vascular effects depending on the activation of specific receptors (Figure 6). Thus, binding of PGE_2 to four receptor subtypes, namely EP_1-EP_4, has multiple effects at vascular level. EP_1 receptor activates phosphatidylinositol metabolism via G_q, leading to the formation of inositol trisphosphate (IP3) with mobilization of intracellular free calcium which induces vessels contraction. EP_3 receptor can couple via G_i or G_{12} to increase intracellular calcium, inhibition of cAMP generation and activation of the small G protein Rho, leading to vasoconstriction. EP_2 and EP_4 receptors mediate vasodilation through activation of adenylyl cyclase via G_s (204). In addition to modulating vascular function, EP receptors can influence platelet aggregation, monocyte and macrophage migration, VSMCs proliferation and migration, vascular cytokine production or MMP activation (85,186).

PGI_2 which is formed by prostacyclin synthase, binds to the IP receptor to induce vasodilation and inhibit platelet activation by activation of adenylyl cyclase via G_s and

increase intracellular cAMP (204) (Figure 6). Interestingly, in several pathological conditions PGI_2 can also induce vasoconstriction by binding to TP receptors (117,280).

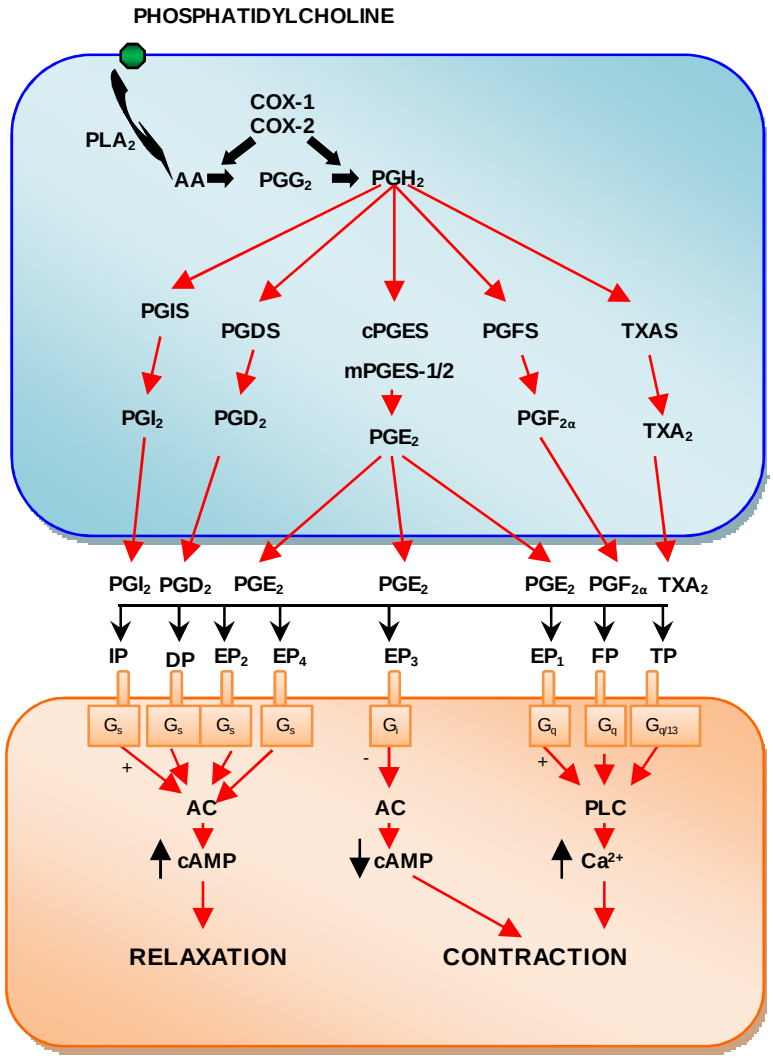

Figure 6. Prostanoids synthesis and signaling. *The COX-1 and COX-2 enzymes catalyze key steps in the biosynthesis of the labile cyclic endoperoxide prostaglandin PGH_2, which is subsequently converted into five structurally related primary prostanoids: the prostaglandins PGE_2, PGD_2, $PGF_{2\alpha}$, PGI_2, and thromboxane A_2 (TXA_2). These prostanoids bind their own receptors EP_{1-4}, DP_{1-2}, FP_2, IP and TP, respectively, which comprise a distinct family of G-protein-coupled receptors. DP1-EP_2-EP_4-IP receptors activate adenylyl cyclase (AC), resulting in the conversion of ATP to cAMP, inducing relaxation. EP_1-FP-TP receptors mediate the mobilization of cytosolic Ca^{2+} through PLC activation, resulting in contraction. EP_3 receptor inhibits the signaling pathway of cAMP, producing contraction.*

TP receptor couples mainly to two types of G-proteins, the G_q and the G_{13} families, resulting in the activation of PLC to induce vasoconstriction (204) (Figure 6). They are involved in platelet aggregation, smooth muscle contraction, expression of adhesion

molecules and adhesion and infiltration of monocytes/macrophages (179). Interestingly, although TXA_2 produced by thromboxane synthase is the preferential physiological ligand for TP receptors, PGH_2 and other prostaglandins, isoprostanes and hydroxyeicosatetraenoic acids can also activate this receptor (84).

2.4. RENIN-ANGIOTENSIN-ALDOSTERONE SYSTEM

The RAAS is one of the most significant and extensively studied hormonal systems in humans. Beginning with the discovery in 1898 by Tigerstedt and Bergman of a factor released from kidneys that controlled blood pressure, the RAAS has expanded into an extensive system of enzymatic cascades, bioactive molecules and multiple receptors.

2.4.1. Angiotensin II

Activation of the renin-angiotensin system (RAS) is originated with the synthesis of renin by the juxtaglomerular cells. In these cells, preprorenin is processed to prorenin and then to active renin, which is secreted into the circulation. Release of renal renin is stimulated by low volume states, high salt content in the distal tubules, renal sympathetic nerve activity and reduced renal perfusion. In the blood, renin, an aspartyl protease, cleaves liver-derived angiotensinogen to form the decapeptide angiotensin I (Ang I). Angiotensin converting enzyme (ACE), primarily found in ECs (especially pulmonary endothelium), hydrolyzes inactive Ang I into the biologically active octapeptide Ang II. In addition of cleaving Ang I, ACE metabolizes the vasodilator compound bradykinin to inactive bradykinin-(1-7). Hence, ACE has a dual role in the vasculature by promoting the production of Ang II, a potent vasoconstrictor while degrading bradykinin, an important vasodilator (Figure 7). In addition to the circulating RAS acting in different organs in an endocrine manner, it is now evident the existence of a local or tissue RAS defined by the synthesis of Ang II from angiotensinogen and enzymes produced locally within tissues (66,181). The local RAS may utilize enzymes

other than renin and ACE for the synthesis of Ang II, such as cathepsins and chymase (139) (Figure 7). This newly synthesized Ang II acts on neighboring cells in an autocrine/paracrine manner. The function and regulation of the tissue RAS is independent of the circulating system (139).

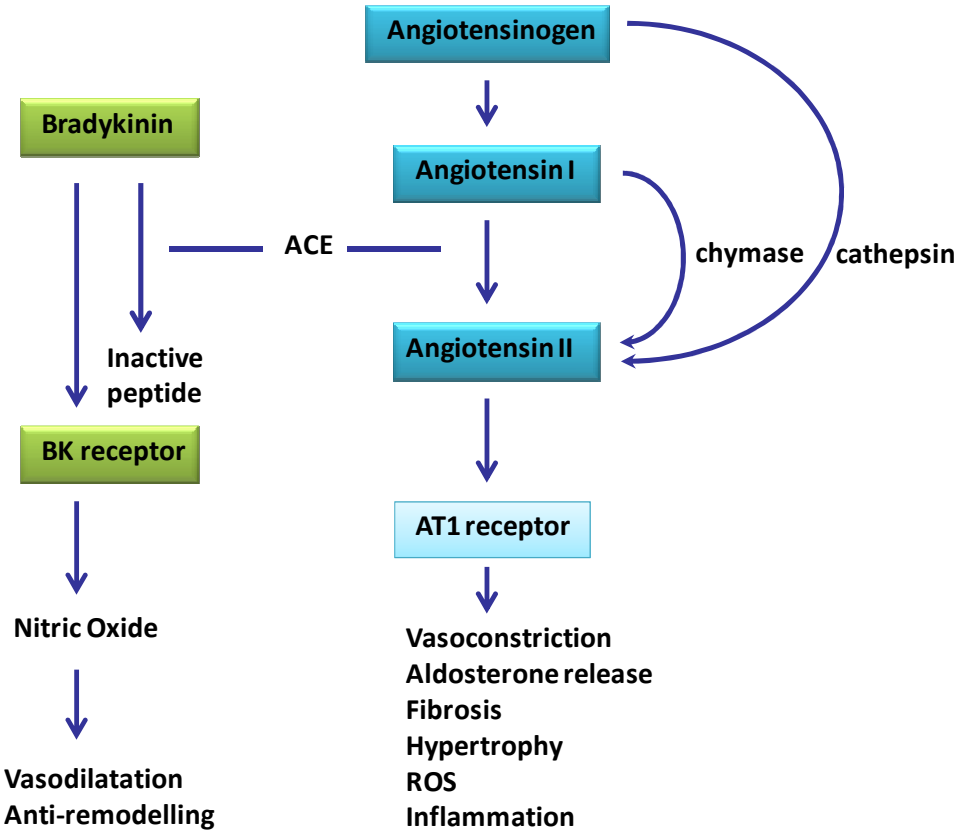

Figure 7. Angiotensin II synthesis. *In the classical renin-angiotensin system (RAS), kidney-derived renin is secreted into the circulation where it cleaves liver-derived angiotensinogen to angiotensin I, which is hydrolyzed to angiotensin II by angiotensin converting enzyme (ACE). ACE also metabolizes bradykinin to inactive metabolites. The local RAS may utilize enzymes other than renin and ACE for the synthesis of angiotensin II such as cathepsins and chymase. Angiotensin II is able to bind to Angiotensin II type 1 receptor (AT1) to trigger different actions such as vasoconstriction, aldosterone release, fibrosis, hypertrophy, induced oxidative stress and inflammation.*

Vascular, cardiac, renal and adrenal effects of Ang II are mediated via two GPCRs, the type 1 (AT1) and the type 2 (AT2) receptors that act, in general, in opposite directions. At vascular level, AT1 and AT2 receptors are located on ECs, VSMCs and adventitial fibroblasts (181). Most of the (patho)physiological effects of Ang II including

vasoconstriction, aldosterone release, thirst, activation of the sympathetic nervous system, cardiac inotropic and chronotropic actions and cardiovascular inflammation, hypertrophy and fibrosis are mediated through AT1 receptors (181) (Figure 7).

Ang II/AT1 receptor couples to small G proteins that activate downstream effectors such as PLC, phospholipase D (PLD) and phospholipase A_2 (PLA_2) and modulates vascular tone (Figure 8). Thus, activation of PLC leads to phosphatidyl inositol hydrolysis, IP3 formation and increase in the intracellular free calcium concentration, which triggers phosphorilation of myosin light chain (MLC) by MLC kinase (MLCK) and contraction. Ang II also induces vessels contraction through the RhoA/Rho kinase pathway, which increases calcium sensibility by inhibiting the myosin light chain phosphatase (MLCP). Similarly, activation of PLD results in the hydrolysis of phosphatidylcholine to phosphatidic acid and choline, which is rapidly converted to DAG, thus allowing a strong activation of PKC inducing contraction and proteins such as NADPH oxidase (247). Moreover, activation of PLA_2 stimulates production of arachidonic acid-derived prostanoids and also the formation of NADPH oxidase-derived ROS, which stimulate contraction (182,249). On the other hand, binding of Ang II to the AT1 receptor induces activation of tyrosine kinases such as c-Src, FAK, PI3K and JAK2, which in turn regulate downstream signaling molecules such as the MEK/MAPK cascade, which regulates and induces NADPH oxidase, cell growth, apoptosis, inflammation and migration (249).

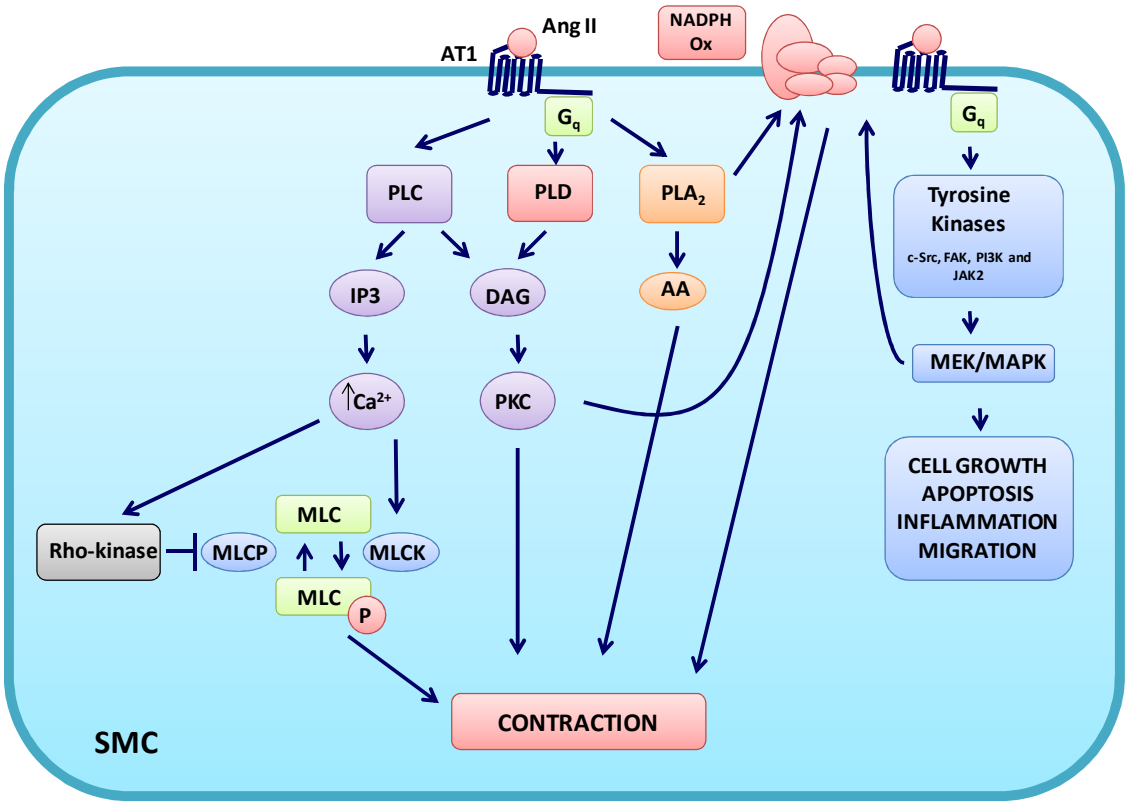

Figure 8. Cell signaling of angiotensin II. *Ang II/AT1 receptor couples to small G proteins that activate downstream effectors such as phospholipase C (PLC), phospholipase D (PLD) and phospholipase A_2 (PLA_2) which stimulate contraction. AT1 receptor activation also induce activation of tyrosine kinases such as c-Src, FAK, PI3K and JAK2, which in turn regulate downstream signaling molecules such as the MEK/MAPK cascade, which regulates and induces NADPH oxidase (NADPH Ox), cell growth, apoptosis, inflammation and migration. Arachidonic acid (AA); diacylglycerol (DAG); inositol trisphosphate (IP3); myosin light chain (MLC); myosin light chain kinase (MLCK); myosin light chain phosphate (MLCP).*

The AT2 receptor shares partial amino acid homology (34 %) to AT1 receptor and is the predominant Ang II receptor in the fetus (181). It is expressed at low levels in the adult vasculature, juxtaglomerular cells, glomeruli and tubules and it elicits effects to counteract those of the AT1 receptor (181). The AT2 receptor mediates actions through protein tyrosine phosphatase activation, NO generation and signaling through sphingolipids to stimulate vasodilation, natriuresis, anti-inflammatory and anti-fibrotic actions and inhibition of cell growth (181).

2.4.2. Aldosterone

Aldosterone production is induced by Ang II, high potassium levels or adrenocorticotropic hormone. It is synthesized from cholesterol mainly in the zona glomerulosa of the adrenal cortex by a series of locus-and orientation-specific enzymatic reactions (195). The major rate-limiting steps for the synthesis of aldosterone are the following. First, cholesterol needs to be transported to the inner mitochondrial membrane by the StAR protein (150,195) and second, conversion of 11-deoxycorticosterone to aldosterone is produced by aldosterone synthase (62).

Aldosterone carries out its effects through the mineralocorticoid receptor (MR) and another type of receptor, the GPCR 30, via genomic and non genomic pathways. The main actions of aldosterone are through its cytoplasmic MR and its specific binding is insured by the coexpression of 11β-HSD2 that metabolizes cortisol or corticosterone in an inactive metabolite, thus preventing the illicit occupation of MR by glucocorticoids (44). Aldosterone induces sodium reabsorption at the level of the distal nephron through its interaction with the MR and activation of the apical epithelial sodium channel (33). MR expression and adosterone actions are not restricted to the kidney but are widely distributed across a range of extrarenal tissues such as the heart, the vessels, adipose tissue, and macrophages (183). Aldosterone induces vessel inflammation and oxidative stress, remodeling and endothelial dysfunction (33). To produce these effects aldosterone diffuses across the cytoplasmic membrane of VSMCs and binds to the MR inducing dimerization and translocation to the nucleus, where the complex binds to the glucocorticoid response element and induces the expression of Sgk-1 (Figure 9). This factor increases Ki-Ras2A, which in turn activates ERK1/2, which is implicated in development of proliferation and fibrosis. On the other hand, nongenomic pathways are MR dependent or independent. Thus, aldosterone in an MR-dependent pathway induces

rapid activation of JNK, p38 and ERK1/2 MAPK through the transactivation of EGFR and c-Src, leading to proliferation and fibrosis processes in the vasculature. Moreover, c-Src induces ROS production which promotes inflammation and oxidative stress and activates Rock and MAPK, which induce migration process. Finally aldosterone, through its interaction with GPR30, activates ERK1/2 nongenomically without intervention of MR (33) (Figure 9).

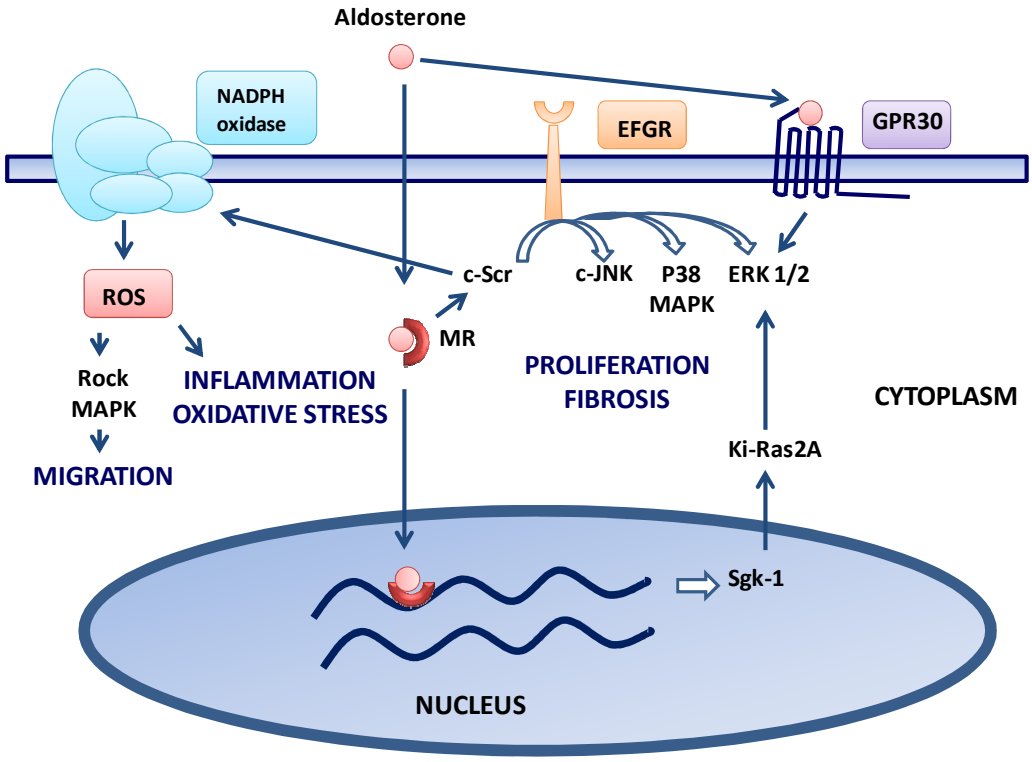

Figure 9. Genomic and nongenomic action of aldosterone. *Aldosterone diffuses across the cytoplasmic membrane of VSMCs, binds to the mineralocorticoid receptor (MR) and translocates to the nucleus. The complex is bound to the glucocorticoid response element and induces the expression of Sgk-1. Sgk-1 increases Ki-Ras2A, which in turn activates ERK1/2 inducing proliferation and fibrosis. Nongenomic pathways are MR dependent or independent. Aldosterone, in an MR-dependent pathway, induces activation of JNK, p38 MAPK, and ERK1/2 through the transactivation of EGFR and c-Src, to induce proliferation and fibrosis processes in the vasculature. c-Src induces reactive oxygen species (ROS) that promotes inflammation and oxidative stress and activates Rho Kinase (Rock) and MAPK inducing migration. Aldosterone, through its interaction with GPR30 can also activate ERK1/2. Adapted from Briet and Schiffrin (33).*

Aldosterone also induces vessels contraction through an increase in the activity of the Na^+-H^+ exchanger through a mechanism involving PLC and IP3 generation through MR-independent pathways (54,267). This results in an immediate increase of intracellular calcium, which it induce myosin light chain phosphorylation and vasoconstriction.

2.5. G PROTEIN-COUPLED RECEPTOR KINASES

GRKs regulate vital processes through the regulation of the expression and function of the seven-transmembrane receptors GPCR, such as Ang II or adrenergic receptors (35,197,209). GPCRs expressed in VSMCs and ECs are responsible for maintaining the balance between contraction and relaxation of vessels and their modulation has been a primary target of therapeutic advances (35). Upon agonist stimulation, GPCRs activate heterotrimeric G proteins which exchange bound GTP for GDP, leading to the dissociation of the G protein into activated G_α and $G_{\beta\gamma}$ subunits (Figures 10 and 11). This dissociation promotes downstream signaling through specific effectors proteins and second messengers (35).

There are four main classes of heterotrimeric G-proteins based on the G_α component. Activation of different G_α subtypes leads to diverse intracellular signaling cascades controlling vascular tone by several mechanisms; (I) $G_{\alpha s}$ induces the activation of adenylyl cyclase resulting in the conversion of ATP to cAMP inducing relaxation; (II) $G_{\alpha q}$ activates PLC which hydrolyzes IP2 into IP3 and DAG, resulting in calcium mobilization and PKC activation inducing contraction; (III) $G_{\alpha i}$ inhibits adenylyl cyclase producing contraction; (IV) $G_{\alpha 12/13}$ and $G_{\alpha q/11}$ activate Rho kinase which inhibits the MLCP, finally activating the MLC and thereby initiating vasoconstriction (21,32,35,185) (Figure 10). The effects derived from the activation of several receptors

at the same time depends on the balance between activated vasodilator and vasoconstrictor responses, which ultimately will be determined by the levels and types of agonists and by vascular bed (Figure 10).

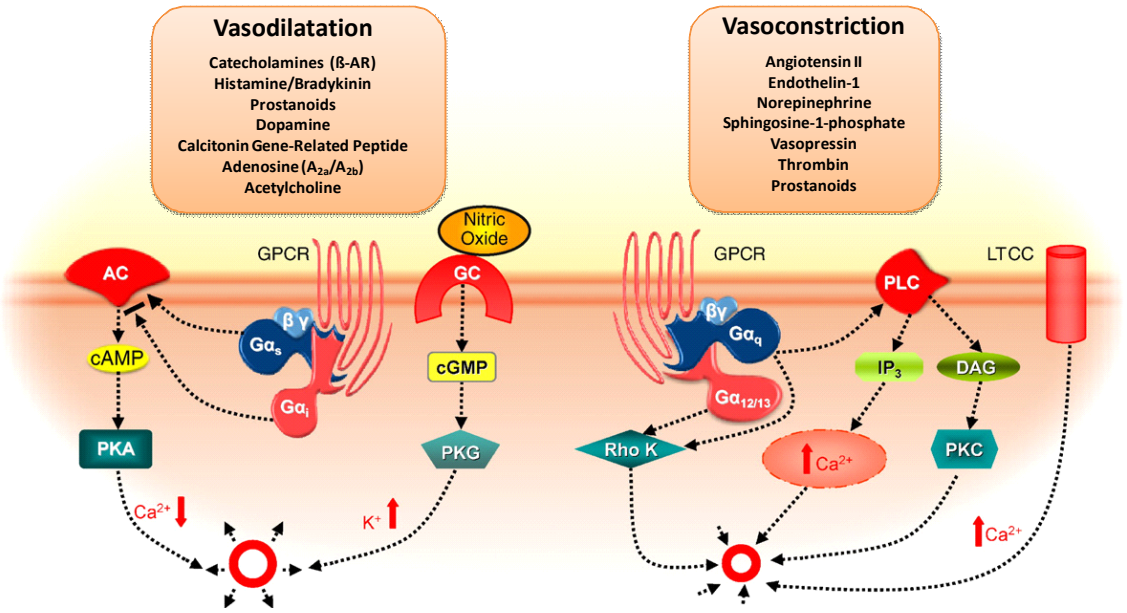

Figure 10. GPCR signaling cascade and its role in vasodilation or vasoconstriction. *Activation of GPCRs via a wide range of agonists leads to activation of adenylyl cyclase (AC) and guanylate cyclase (GC), increases in 2nd messenger concentrations and activation of protein kinase A (PKA) or PKG-mediated vasodilation. Vasoconstrictor agents activate G_q and $G_{12/13}$, which mediates smooth muscle contraction via Protein Kinase C (PKC) or Rho Kinase. Adapted from Brinks and Eckhart (35).*

Agonist binding to GPCR also results in receptor internalization and down-regulation thus attenuating signaling (Figure 11). This is regulated by GRKs, a family of serine/threonine kinases able to phosphorylate the intracellular domains of the receptors, thereby increasing its affinity for the binding of β-arrestin, which further prevents coupling of that receptor to its G_α protein. This process is termed desensitization (23,35,197). Although it has been thought that desensitization of receptors is a mechanism to protect the receptive cell from overstimulation, this process can also be harmful in pathological conditions such as heart failure, where desensitization of the β-adrenergic receptor system marks the decline of ventricular output (35).

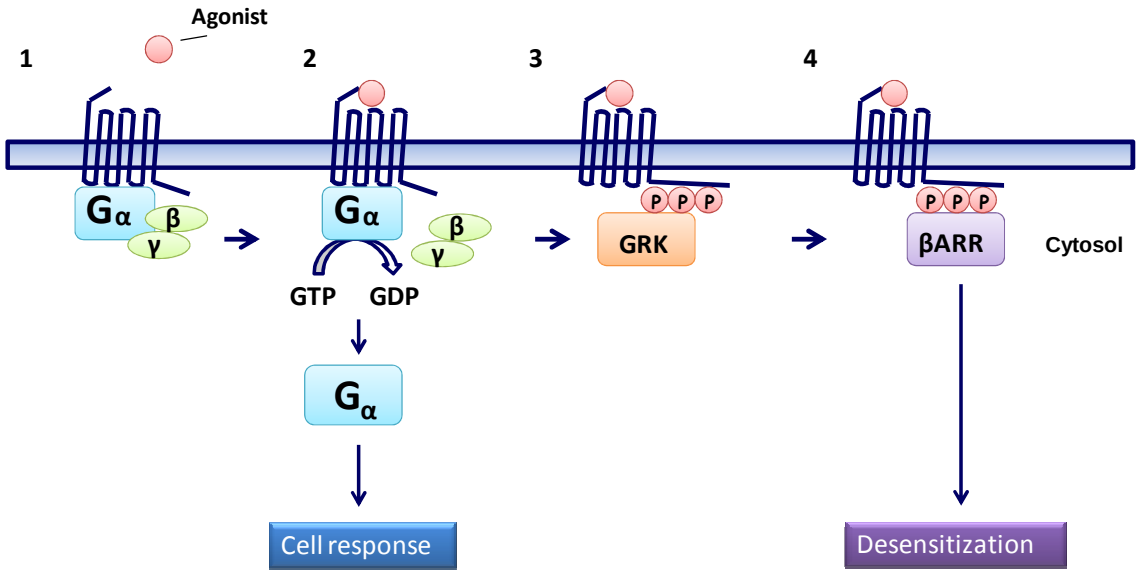

Figure 11. GPCR and GRK signaling. *1-2) Agonist activates the G protein-coupled receptor and induces a conformational change in the receptor that allows that its G_α subunit hydrolyzes the attached GTP to GDP. This exchange triggers the dissociation of the G_α subunit bound to GTP from the $G_{\beta\gamma}$ dimer and the receptor. Then G_α subunit induces the release of the second messengers, which trigger cell response. 3-4) GRK-mediated desensitization and trafficking of GPCRs. Agonist binding to GPCRs not only promotes G-protein activation but makes the receptor a substrate for phosphorylation by GRKs (G protein-coupled receptor kinases). GRK phosphorylation promotes β-arrestin binding which causes G-protein uncoupling.*

GRKs form a family of seven mammalian members (GRK1–GRK7) that share a similar basic structure with a N-terminus that bears an RGS domain, a catalytic and a C-terminal domain (35,197). GRKs can be classified into three subtypes: GRK1 and GRK7 are known as GRK1-like retinal opsin kinases, and are involved in the pathophysiology of deleterious rhodopsin mutations that underlie several inherited retinal disorders (198). GRK2 and GRK3 which are in the GRK2-like subtype enzymes, act on a wide range of GPCRs and were first characterized in studies of the phosphorylation of agonist-occupied β_2-adrenergic receptors. Its importance lies on the fact that they might contribute to diseases such as heart failure (160). Finally, GRK4, GRK5 and GRK6, belong to GRK4-like subfamily, which selectively phosphorylate basic terminal amino acid residues. GRK4 has been found to play an important role in regulating the Dopamine D1 receptor within the renal proximal tubule thus controlling

blood pressure (214). The fact that GRK1/GRK7 are mainly located in the ocular system whereas GRK4 is limited to the proximal tubule of the kidney and testis suggests that these GRKs may be successful therapeutic targets due to their limited distribution and thus low potential for side-effects. However, most of the over 1000 GPCRs of the body seem to be regulated by the four most widely expressed isoforms: GRK2, GRK3, GRK5 and GRK6, and their downstream arrestins.

GRK mRNA levels or activity are regulated in a variety of disease states (197). Vasoconstrictors such as phorbol esters led to enhanced GRK2-promotor activity in a Gαq dependent manner in VSMCs in aorta (199). However, vasodilator stimuli and cytokines inhibit this effect (199). Other investigators found that activation of MAP Kinases (ERK1/2) increased endogenous GRK2 protein levels in primary cardiomyocyte cultures (242). Moreover, in cardiovascular diseases, GRK2 mRNA levels are upregulated (209) in correlation with increased catecholamine levels and β-adrenergic receptor activity (3), which suggests a reciprocal regulation that may explain fundamental alterations of GPCR signaling in many pathophysiological conditions. The role of GRK2 in the context of hypertension will be discussed in next sections of this Introduction.

3. MECHANISMS INVOLVED IN ENDOTHELIAL DYSFUNCTION AND VASCULAR REMODELING IN HYPERTENSION

Hypertension is a major cardiovascular risk factor and it is well established that lowering blood pressure improves cardiovascular prognosis. Hypertension is generally associated to endothelial dysfunction and vascular remodeling and both features play an important role in its pathogenesis (34,97). Particularly important mediators of these vascular alterations in hypertension are RAAS and ET-1 systems which mediate their actions at least in part, by inducing oxidative stress and inflammation which then decrease the bioavailability or the actions of the vasodilator NO and induce ECM deposition. Next section of the Introduction will revise the concepts of endothelial dysfunction and vascular remodeling and the mechanisms involved in these processes, particularly the role of RAAS, NO, ROS and prostanoids.

3.1. ENDOTHELIAL DYSFUNCTION

Endothelial dysfunction is generally defined as the inability of the endothelium to properly maintain vascular homeostasis (138,233,269). This refers to an imbalance between the release of vasodilator and vasoconstrictor endothelium-derived factors (111,138). Endothelial dysfunction occurs when endothelium is absent (89,138). However, in the vast majority of cases, endothelial dysfunction develops less acutely from injurious conditions such as smoking, aging, obesity, insulin resistance, diabetes, lipid disorders, hypertension, inflammatory diseases or infections (138,269). In these situations endothelium may be injured but it is relatively intact. At molecular level, endothelial dysfunction can be promoted by a variety of factors such as oxidative stress products, advanced glycation end products, oxidized LDL particles, lipoprotein

particles, free fatty acids and their metabolites, and inflammation molecules including cytokines or bacterial endotoxin (111,138,269).

One of the most important manifestations of endothelial dysfunction is impaired endothelium dependent relaxation (89) due to impaired NO availability or signaling. However, depending on the vascular bed, other endothelial derived vasodilator factors such as prostaglandins, EDHF or gaseous substances such as H_2S among others, might also be affected (111,138,233,269). It is well known that different vessels from different models of hypertension and from hypertensive patients display diminished endothelium dependent relaxation (42,99,260). However, increases of vasoconstrictor responses or altered modulation of vasoconstrictor responses by endothelium removal or by blockade of the vasodilator NO are also key features of endothelial dysfunction (99). It is important to note that in many pathological situations associated with endothelial dysfunction such as hypertension, the vascular smooth muscle response to NO is in general normal, suggesting that endothelial dysfunction is due to altered NO bioavailability caused mainly by impaired NO synthesis or by enhanced NO inactivation (99,138,269).

In addition to modulate vascular tone, endothelial derived factors modulate platelet aggregation, VSMCs proliferation and migration, monocyte adhesion and expression of adhesion molecules, which exert an important role in pathologies associated to cardiovascular disease (97,210). Therefore, by affecting these parameters, endothelial dysfunction might deeply affect vascular function and structure thus contributing to cardiovascular events.

Increasing evidences demonstrate the association of endothelial dysfunction with markers of vascular damage and with cardiovascular events in patients with essential

hypertension. Thus, it has been described that endothelial dysfunction significantly predicted cardiovascular events independently of traditional cardiovascular risk factors (147). Therefore, a better understanding of the mechanisms responsible of endothelial dysfunction can lead not only to the discovering of novel therapeutic targets but also to the improved and earlier prevention of cardiovascular disease.

3.2. VASCULAR REMODELING

Since 1987, when Glagov reported the surprising finding that atherosclerotic arterial lumen narrowing is not simply the result of enlargement of atherosclerotic lesions (100), a new concept emerged suggesting that the vessel wall can change its structure to maintain the appropriate lumen size to permit normal blood flow. This was termed vascular remodeling (98). This ability of the arteries to adapt its structure in response to physiological and pathological conditions is essential in situations such as pregnancy or aging but also in many arterial diseases. Thus, the inability of vessels to appropriately remodel is considered a form of 'vascular failure' that can lead to pathologic states such as hypertension or atherosclerosis (200).

Remodeling of large conductance arteries is essential in pathologies such as atherosclerosis, aneurisms and restenosis. However, resistance arteries are key elements in the control of blood pressure. In fact, one of the pathologies where remodeling of small arteries is best studied is hypertension and it is now widely accepted that structural abnormalities of microvessels are common alterations associated with chronic hypertension (43,172,174,207,222). The calculation of blood pressure can be approximated by Ohm`s law modified for fluid dynamics (Pressure= flow x resistance) (57). Blood flow depends on cardiac output and blood volume, whereas vascular resistance is mainly determined by the small arteries (diameter < 300 μM) and arterioles

(diameter < 100 μM) (55,207). Vascular resistance can be calculated from the Poiseuille-Hagen formula ($R=(8\eta L)/(\pi.r^4)$), where R is resistance; η is blood viscosity, L is the length of the artery and r is the radius of the artery). Thus, vascular resistance *in vivo* is markedly affected by small changes in the caliber of the vessels. In fact, increased peripheral resistance is a common parameter in essential hypertension which is mainly due to narrowing of the resistance vessels as consequence of functional and/or structural alterations (17,158,176,207,222).

The main feature of hypertensive vascular remodeling is the increased media/lumen ratio, which can occur with or without growth of the vessel wall (i.e. hypertrophic or eutrophic) and with smaller, greater or similar lumen size (inward, outward or compensated) (39,173,207) (Figure 12). Although depending on the vessel type or hypertension model, different types of remodeling and underlying mechanisms can be found, it is generally admitted that changes in hypertensive arteries are the consequence of rearrangement, growth, inflammation and vasoconstriction (176,207,222). We will now discuss the most frequently remodeling processes observed in vessels from hypertensive patients or animal models.

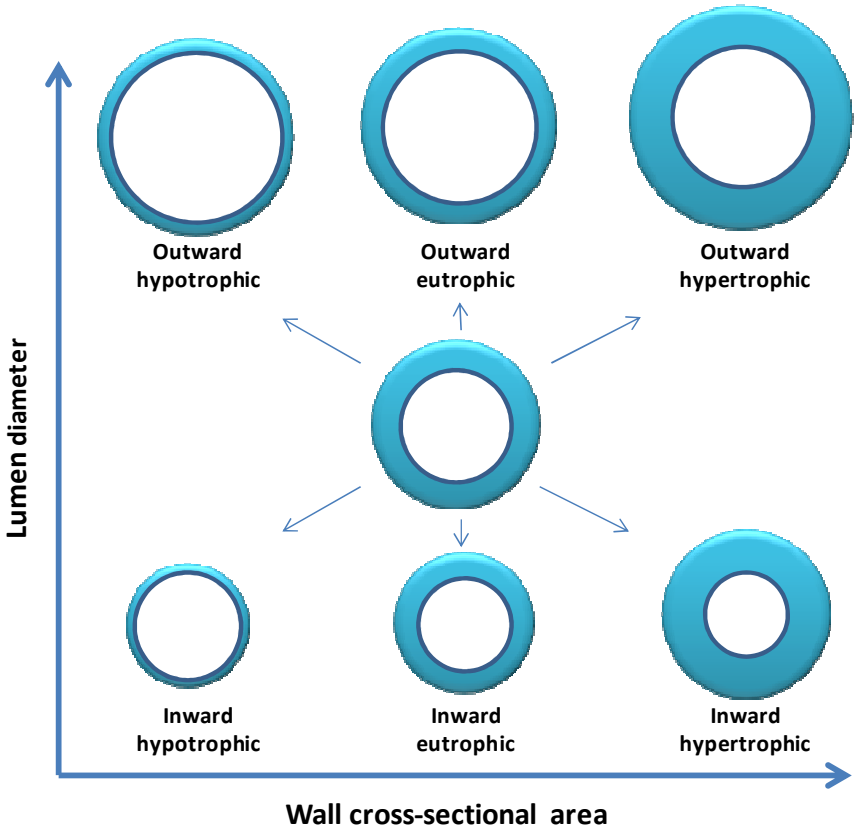

Figure 12. *Patterns of vascular remodeling. Classification refers to changes on the lumen diameter (inward or outward) and vessel cross-sectional area (hypertrophic, hypotrophic or eutrophic). Adapted from Mulvany (173).*

➢ **Eutrophic inward remodeling** is characterized by a decrease in the outer and lumen diameters and an increase in the media thickness and the media/lumen ratio with no change in the wall cross sectional area (173) (Figure 12). It has been suggested that this type of remodeling is due to rearrangement of the same amount of wall material around a smaller vessel lumen (115,207). The mechanisms leading to this type of remodeling are poorly known but some authors suggest that a combination of inward growth and peripheral apoptosis or prolonged vasoconstriction of vascular cells embedded in an expanded ECM can lead to eutrophic remodeling (16,222). Indeed, it has been demonstrated increased collagen and fibronectin deposition as well as increased collagen:elastin ratio which in turn increases vessels stiffness, in small vessels from hypertensive human and rodents (38,125,126,259). Although it is not clear yet

whether the observed changes in ECM deposition are due to altered synthesis or degradation, it seems demonstrated that this altered ECM play a role in the hypertensive disease (14,39). In addition to elastin deficiency, altered spatial organization of elastic fibers might also compromise vascular elasticity. Our group and others have demonstrated in resistance and conduit vessels from spontaneously hypertensive rats (SHR) that more compact elastic lamellae with reduced relative volume of fenestrae are associated with increased vessel stiffness (15,29,36,131). Besides changes in the amount or structure of ECM proteins, others important players that may be participating in the rearrangement of ECM are integrins and transglutaminases enzymes. The later mediates interactions between integrins and ECM (18,106,176).

The role of some mediators involved in vascular remodeling will be more exhaustively discussed in subsequent sections of this Introduction. However, it is important to note that Ang II as well as other inducers of vascular remodeling are vasoactive mediators and that some authors have proposed that maintained constriction is necessary for inducing eutrophic inward remodeling, as mentioned above (16,17,158,159). In fact, early stages of hypertension are thought to be associated with increased presence of vasoconstrictor mediators and thus presumably with increased vascular tone (176). In favor of this hypothesis is the fact that infusion of the vasoconstrictor phenylephrine for 7 days in rats causes pressure-independent inward remodeling of mesenteric small arteries in rats and mice (79,253).

- **Hypertrophic remodeling** is characterized by an increase in the media thickness, media/lumen and cross sectional area associated with a more evident contribution of cell growth (173) (Figure 12). This together with the elastic lamina alterations and the increased deposition of collagen and fibronectin, contribute to increased stiffness. Large arteries undergo outward hypertrophic remodeling and

increased stiffness with aging, and in hypertension there may be an acceleration of this process, leading to enhanced pulse pressure (222). An important factor implicated in hypertrophic remodeling is enhanced ET-1 expression. Thus, mice that overexpressed human preproET-1 in the endothelium exhibited hypertrophic remodeling despite of the unaltered blood pressure (9,10,222).

Although eutrophic remodeling is usually found in small arteries in essential hypertension in humans, in SHR or after Ang II infusion; hypertrophic remodeling has been described in secondary hypertension such as in renovascular hypertension, primary aldosteronism or in pheochromocytoma, in hypertension associated with diabetes mellitus and in acromegaly (222). In mineralocorticoid hypertension in rodents and in salt-sensitive Dahl rats, in both of which the ET system is activated, remodeling of small arteries is also hypertrophic. Thus, when the RAS is even mildly activated (primary hypertension and SHRs), remodeling is usually eutrophic. In salt-dependent hypertension, diabetes mellitus, and malignant hypertension, all conditions in which the ET system is activated, remodeling is hypertrophic (222).

- **Hypotrophic remodeling** is associated with a decrease in the amount of material (i.e diminished cross sectional area) around the vessel wall (173) (Figure 12). This type of remodeling may be related with apoptosis processes and/or rearrangement of the material around the vessel (127). Hypotrophic remodeling has been shown in renal afferent arterioles from SHR (187) and in mesenteric resistance arteries from ouabain-induced hypertensive animals (37). Moreover, patients with autosomal dominant hyperimmunoglobulin E syndrome were found to have a high prevalence of hypotrophic remodeling in carotid arteries with an increased circumferential stress and enhanced susceptibility to dilation and aneurysm formation associated to Ang II and apolipoprotein E (50).

The importance of the vascular structural abnormalities in hypertension lies on the fact that in patients it has been demonstrated that the media to lumen ratio parameter has a prognostic value of cardiovascular events in a high-risk population (162,205). Thus, the presence of structural alterations in the microcirculation may be considered an important link between hypertension and ischemic heart disease, heart failure, cerebral ischemic attacks, and renal failure (207).

Despite the significant advances in the knowledge of the mechanisms responsible of the altered vessel function, structure and mechanical properties in hypertension, this aspect is still a matter of intense research. In the following section, we will describe some of these mechanisms and we will give some insights on how the experimental work performed in this Thesis has contributed to increase this knowledge.

3.3. ROLE OF VASOACTIVE MEDIATORS IN VASCULAR FUNCTION AND STRUCTURE IN HYPERTENSION

As mentioned above, the RAAS, NO, ROS and prostanoids are factors released by vessels that play an important role in regulating the homeostasis of the vessel wall. Other important factor contributing to vessel function and structure is GRK2. In pathological conditions such as hypertension, the levels of these factors are altered and induce changes in endothelial function and/or vascular remodeling processes. This will be revised in the next section.

3.3.1. Renin-Angiotensin-Aldosterone System and Vascular Alterations in Hypertension

It is well known that chronic and/or acute Ang II infusion increases blood pressure (212,262). Ang II may influence blood pressure by inducing catecholamine release in

noradrenergic nerve endings (76,181). Ang II also induces vascular alterations such as increase of vasoconstrictor responses and decrease of endothelial dependent vasodilator responses (212,262). In addition, Ang II influences the architecture and integrity of the vascular wall by modulating cell growth and regulating ECM composition (38,175,222,260). Thus, either *in vitro* or *in vivo*, Ang II induces VSMCs growth or hypertrophy, increases collagen deposition and alters elastin structure (39,140). Signaling by Ang II through AT1 receptors is significantly enhanced in cultured VSMCs from resistance arteries of hypertensive patients (245,246,248) and patients with hypertension have increased vascular responses to exogenous Ang II (191,229). Interestingly, in pathological conditions, AT2 receptor may also stimulate hypertrophy and inflammation (181,266).

Proof of the key role of RAS in the vascular alterations in hypertension is the fact that chronic administration of ACE inhibitors (ACEI) or Ang II receptor blockers (ARBs), lowers blood pressure and improve vascular remodeling and endothelial dysfunction in several hypertensive animal models including the SHR model which is classically associated with hyperactivation of the vascular RAAS (6,64,126,148,181,189,222,228). More importantly, hypertensive patients treated with ACEI, ARBs or with calcium channel blockers but not with atenolol, exhibited significant regression of vascular remodeling of large and small arteries independently of hemodynamic changes (30,34,154,190,219,221). Interestingly, vasodilating β-blockers such as bisoprolol exerted a beneficial effect in vascular remodeling on large arteries thus pointing to the possible role of vasodilation in vascular remodeling (30,190).

With respect to vascular function, ACEI treatment in hypertensive humans improve endothelial function in subcutaneous (206), epicardial (156), peripheral conduit arteries (236) and renal circulation (166), whereas they are ineffective in improving the blunted

response to acetylcholine in the forearm microcirculation (60,137,235). These drugs also selectively improve the vascular response to bradikynin, an effect likely mediated by the hyperpolarizing factor and not by restoring NO availability (235,254). In addition, treatment of hypertensive patients with ARBs restore endothelium-dependent vasodilation to acetylcholine in the subcutaneous microcirculation (220), but not in the forearm circulation (96) and their effect on peripheral conduit arteries is still controversial (97).

As mentioned, aldosterone contributes to the regulation of blood pressure by sustaining a constant extracellular fluid volume via modulation of renal sodium, water reabsorption and potassium excretion mediated by MR (279). However, excessive aldosterone secretion results in hypertension. In fact, among patients with hypertension a higher-than-expected prevalence of primary hyperaldosteronism is noted (195,279). In addition, in individuals with resistant hypertension, aldosterone antagonists are effective tools in lowering blood pressure (279).

Besides its renal effects, aldosterone can contribute to hypertension due to its direct actions on the cardiovascular system (183,195,279). Aldosterone is known to modulate vascular tone by increasing the pressor response to catecholamines, by impairing the vasodilator response to acetylcholine or by upregulating Ang II receptors (19,234,241,265,280). Thus, aldosterone infusion in mice or rats induces a significant decrease in endothelium-dependent relaxation in large (27) and small arteries (134). In addition, part of the effects of Ang II on endothelial function can be attributed to aldosterone. Thus, in Sprague-Dawley rats infused with Ang II, treatment with the MR antagonist spironolactone, partially reversed endothelial dysfunction and abolished Ang II-increased oxidative stress (255). In addition to modulating vascular tone, aldosterone induces vascular fibrosis and hypertrophic remodeling particularly in the presence of

salt (194). In animal models of hypertension such as SHR, vascular fibrosis was prevented by administration of spironolactone independently of blood pressure reduction (25). Furthermore, in Sprague-Dawley rats infused with Ang II, spironolactone reduced systolic blood pressure and blunted the hypertrophic remodeling of small resistance arteries (255).

The mechanisms whereby Ang II and aldosterone participate of endothelial dysfunction and vascular remodeling in hypertension have been an active area of research during the last years. At vascular level, both Ang II and aldosterone induce oxidative stress and inflammation and induce prostanoids synthesis, ROS production and decrease NO availability. The generation of ROS in response to Ang II and/or aldosterone in animal models is usually produced by activation of the NADPH oxidase. In this Thesis, by using Ang II and/or aldosterone infusion we have demonstrated that COX-2-derivatives such as PGE_2 and/or TXA_2 and ROS derived from mitochondria and NADPH Oxidase acting alone or in reciprocal relationship, are key components responsible of the functional, structural and mechanical alterations observed hypertension, both in conductance and resistance arteries (Articles 1, 2 and 3). In the next section, we will revise previous findings describing the relationship between RAAS and inflammation, particularly COX and NADPH Oxidase, and the role of ROS, prostanoids and NO availability in the vascular functional and structural alterations observed in hypertension.

3.3.2. Nitric Oxide and Vascular Alterations in Hypertension

NO plays an important role in regulating systemic vascular resistance, arterial relaxation, and vascular distensibility and plays a major role in maintaining and regulating blood pressure (99). In fact, inhibition of NO with NOS inhibitors increases

blood pressure and induces endothelial dysfunction and arterial stiffness in animal models and in patients (73,99,244,271).

A large body of evidence suggests that hypertension is associated to reduced NO bioavailability. The bioavailability of endothelial NO might be affected at multiple levels including: 1) eNOS mRNA or protein expression, 2) availability of the substrate L-arginine which might compete with ADMA, 3) availability of the cofactors such as BH_4, 4) protein-protein interaction with cav-1 and HSP90, 5) modifications of eNOS activation and 6) reaction of NO with $O_2^{\cdot-}$ to form $ONOO^-$, which might further reduce the bioavailability of BH_4 (122) (Figure 13).

Several evidences have shown that eNOS uncoupling is the underlying cause of endothelial dysfunction in several models and types of hypertension such as deoxycorticosterone acetate (DOCA)-salt hypertension (144), Ang II-induced hypertension (167), essential hypertension in humans (119) and hypertension-induced heart failure (238). eNOS uncoupling has been linked to the decrease of the bioavailability of BH_4 due to its enhanced oxidation (Figure 13). When BH_4 levels are low, eNOS becomes unstable and uncoupled leading to less NO production and more $O_2^{\cdot-}$ generation. The interaction between NO and $O_2^{\cdot-}$ leads to the formation of $ONOO^{-\cdot}$ which, as mentioned, further oxidizes BH_4 (135) (Figure 13). This diminished vascular NO associated to increased ROS production is a major contributor of endothelial dysfunction in hypertension.

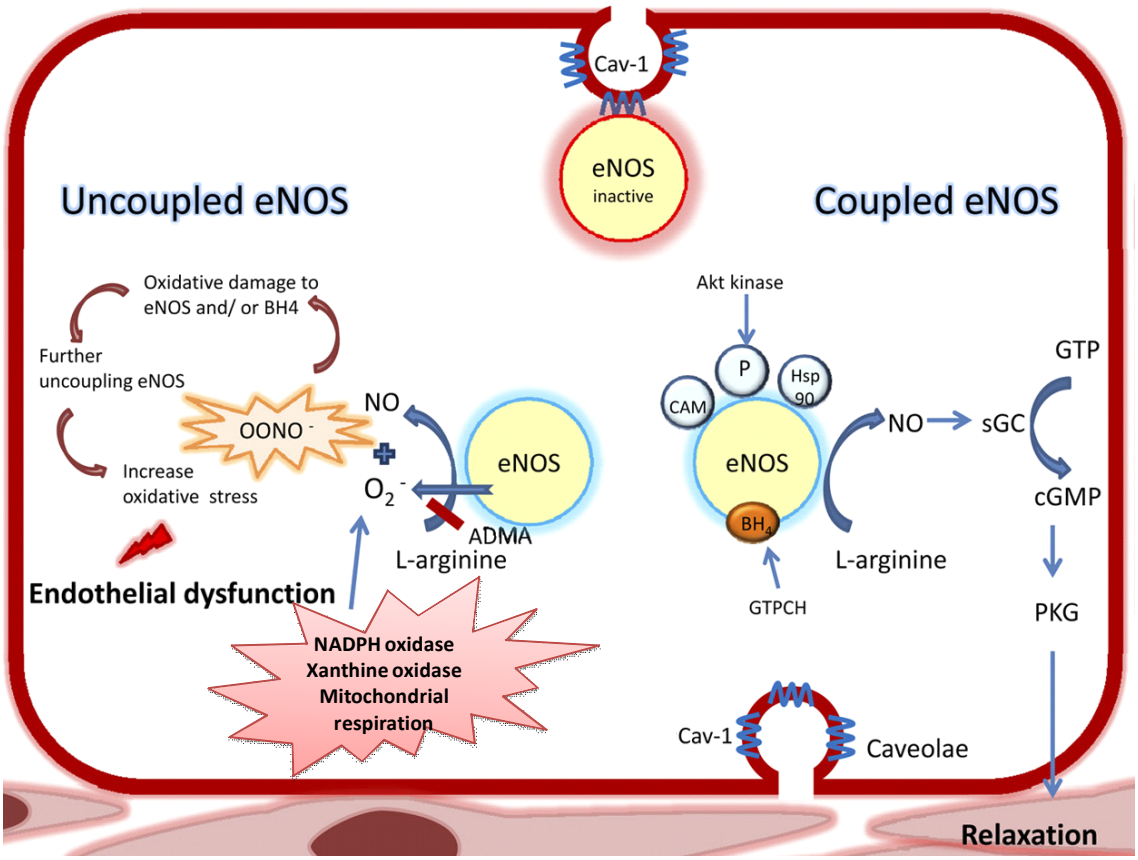

Figure 13. Central role of endothelial NO synthase (eNOS) uncoupling in the pathogenesis of endothelial dysfunction. *eNOS is localized at the plasma membrane caveolae. In endothelial cells (ECs), eNOS is inactive when it is bonded with caveolin 1 (cav-1). When it becomes active, eNOS as a dimmer disassociates from cav-1 and binds with calmodulin (CAM) and heat shock protein 90 (Hsp90). This together with phosphorylation of serine residues (e.g., Ser1177) leads to eNOS activation. Tetrahydrobiopterin (BH_4), an essential cofactor of eNOS, is necessary for optimal eNOS activity. NO plays a major role in relaxation of smooth muscle surrounding arterioles through the cGMP-dependent downstream signaling cascade. Interaction between L-arginine and asymmetric dimethylarginine (ADMA; endogenous competitive inhibitor of NOS) is likely direct competition for eNOS. When availability of L-arginine or BH_4 levels are inadequate, eNOS becomes unstable and uncoupled, leading to subsequently less NO production and more superoxide (O_2^-) generation. Moreover, interaction between NO and O_2^- leads to formation of peroxynitrite ($ONOO^-$), a potent oxidant, which further oxidizes BH_4, resulting in eNOS uncoupling with subsequent endothelial dysfunction in a vicious cycle. Adapted from Kietadisorn et al. (135).*

3.3.3. Oxidative Stress and Vascular Alterations in Hypertension

There is convincing evidence that oxidative stress is critically involved in the pathogenesis of hypertension, although it remains unclear whether increased ROS levels

are a cause or a consequence of high blood pressure (250,256). Elevated vascular and plasma ROS levels and increased contractile responses to H_2O_2 in animal models of hypertension have been described (6,7,38,93,117,250,258). In addition, increased ROS production and reduced antioxidant capacity have been observed in hypertensive patients (142,250).

As mentioned, one of the best-characterized mechanisms whereby oxidative stress alters vascular reactivity is its effect on the NO pathway. Oxidative stress has a role in NOS uncoupling and also cause oxidation of NO to $ONOO^{-\cdot}$ (135,138) affecting multiple cellular enzymes including eNOS itself (22,286). $ONOO^-$ also impairs NO action by altering guanylate cyclase activity in target cells. Furthermore, ROS initiate apoptosis and senescence of ECs through DNA damage (138) and stimulate production of ADMA (138). Excessive oxidative stress has been proposed to be responsible at least in part, for vascular inflammation, remodeling and altered vasoconstrictor and vasodilator responses observed in hypertension (40,118). Thus in previous studies in our laboratory, we observed that different antioxidants such as apocynin and/or SOD decreased vasoconstrictor responses more in arteries from SHR than WKY (7). In addition, we have observed that different antioxidants improve the altered mechanical properties and ECM deposition observed in different models of hypertension such as SHR and Ang II infusion (unpublished data not shown in this Thesis). Other authors have also demonstrated that oxidative is involved in inflammation, impaired endothelium-dependent relaxation and in the alterations in vascular remodeling in hypertension (65,256,257).

Regarding the main source of ROS in hypertension, conflicting results have been published in the literature, possibly due to the fact that ROS sources are closely interconnected (118). It is now evident that NADPH oxidase activity and expression are

increased in hypertension (75,118,169). Administration of NADPH oxidase inhibitors reduces blood pressure and improves the associated structural and functional alterations in animal models (121,256,278). However, the lack of selectivity of some of the compounds used for NADPH oxidases over other enzymes limits their clinical efficacy. Therefore, focus has been shifted to the development of peptide inhibitors of specific NADPH oxidase subunits. Thus, gp91ds-tat and PR39 bind to the p47phox subunit limiting NADPH oxidase activity, although due to their peptide nature they cannot be administered orally (223).

Different factors involved in the pathogenesis of hypertension such as Ang II, aldosterone or ET-1 mediate their effects on the vasculature through the production of ROS (34,38,256). Ang II induces ROS production which, as mentioned above, are involved in the impaired endothelium-dependent relaxation, in the alterations of contractile responses, and in the vascular remodeling in hypertension (38,93,226,256,260). The activity and expression of NADPH Oxidase, the main source of ROS at vascular level, is induced by Ang II (31,75,250). Thus, Ang II induces the expression of Nox1 and Nox4 *in vitro* (41,275) and *in vivo* (94,224). Importantly, Nox1 deficient mice showed a lower increase on blood pressure after Ang II infusion (94). In addition, it has been demonstrated that Nox1 contributes to the Ang II-induced ECM increase in the aorta (94) and is implicated in the impaired endothelium-dependent relaxation via eNOS uncoupling (71) suggesting the important role of Nox1 in endothelial dysfunction and vascular remodeling. The role of Nox4 in vascular alterations in hypertension is controversial. Thus, it has been suggested that Nox4 can act as a vasoprotective protein through mechanisms that include H_2O_2 generation, maintenance of NO production, and expression of the antioxidant heme oxygenase-1 (224). In support of this hypothesis, Nox4 deficient mice infused with Ang II showed

increased endothelial dysfunction and impaired vascular structure without changes in blood pressure (224). However, other authors have suggested a role of Nox4 in O_2^- production induced by Ang II (70,161) and in Ang II-induced hypertension (61).

Similarly to Ang II, aldosterone increases ROS production in VSMCs and ECs by induction of the NADPH oxidases expression and activity (33,181). The findings *in vitro* are corroborated by studies *in vivo* where aldosterone induces vascular oxidative stress and hypertension dependently of MR activation (120,123,184). Importantly, aldosterone effects were inhibited by NADPH-oxidase inhibitors (26) and/or SOD mimetic such as tempol (184). Interestingly, in vessels from aldosterone infused rats, oxidative stress might be involved not only in the impaired endothelium-dependent relaxation and in the alterations of contractile responses (19,27) but also in vascular remodeling of the aorta (217).

In the last few years, in addition to NADPH Oxidase, mitochondria has reemerged as another potential source of ROS in hypertension (69). Antioxidant strategies targeting this organelle reduce high blood pressure and/or prevent hypertension development, reduce ROS production and improve endothelial function in several animal models (72,104,216), pointing to a novel approach for treatment of several pathologies in which oxidative stress plays a role. Interestingly, blockade of mitochondrial ROS also prevented Ang II-induced cardiac hypertrophy and fibrosis (63). An important aspect that deserves further consideration is the fact that several authors have proposed an interaction model between mitochondria and NADPH oxidase on the vasculature where Ang II plays a fundamental role (67,74). Thus in VSMCs, the inhibition of NADPH oxidase prevented mitochondrial dysfunction and diminished mitochondrial ROS production stimulated by Ang II (74). On the other hand, mitochondrial ROS blockade diminished Ang II-induced activation of NADPH Oxidase (74).

3.3.4. Prostanoids and Vascular Alterations in Hypertension

Arteries from hypertensive animal models and patients show increased vascular COX-2 expression and activity (1,5,116,258,260) and this is normalized by treatment with an AT1 receptor antagonist (6), supporting a role for Ang II in the increased vascular COX-2 expression. In agreement, Ang II induces COX-2 expression and prostanoid production in different cell types including VSMCs and adventitial fibroblasts (6,24,188). In addition, Ang II infusion to mice or rats induces either COX-2 upregulation (132,273) or downregulation (257) in different vessels. Similarly to Ang II, aldosterone is able to upregulate COX-2 expression in vessels from normotensive and hypertensive rats (27).

It is now accepted that prostanoids play a key role in the vascular alterations associated to hypertension (85). Thus, contractile prostanoids contribute to the impaired endothelium-dependent vasodilator responses or to the increased vasoconstrictor responses observed in vessels from humans or hypertension models such as the SHR or the Ang II or aldosterone infusion probably by counteracting the vasodilator action of NO (1,5,27,85,92,116,151,257,258,260,268,272,280). Interestingly, part of the effect of Ang II on COX-2 expression in the vasculature might be due to aldosterone since selective MR blockade reduced the expression of COX-2 in coronary arteries from Ang II-infused rats (208). All together, these evidences demonstrate that RAAS is a major regulator of COX-2 expression and activity.

The specific prostanoid involved in vascular alterations in hypertension depends on the animal model or vascular bed studied. Thus, PGH_2, $PGF_{2\alpha}$, and TXA_2 have been described to play an important role in endothelial dysfunction in hypertension probably by binding TP receptors (5,85,101). Although prostacyclin is the main vasodilator

prostanoid generated by COX-2, growing evidence have pointed to PGI_2 as an endothelium-derived vasoconstrictor factor that activates TP receptors in hypertension (27,83,101,103,117,280).

In addition to inducing COX-2 expression, Ang II is able to up-regulate COX-2 downstream proteins such as mPGES-1 (56,263). As discussed above, PGE_2 modulates vascular tone through the four receptor subtypes EP1-4 (86,109,186,284). Importantly, PGE_2 has a role in the control of blood pressure since the lack of EP_1 receptor in Ang II infused mice and EP_1 blockade in SHR, diminished acute and chronic high blood pressure (109,284). In this Thesis we demonstrated that the COX-2/EP1 axis is involved in vascular function regulating vasoconstrictor and vasodilator responses in Ang II infused mice (Articles 2 and 3).

Recent studies demonstrate that PGE_2 is also a key mediator of vascular remodeling in different pathological situations. Thus, the COX-2/mPGEs-1/EP axis is associated with vascular remodeling in processes such as neointimal hyperplasia which is a proliferative response associated with inflammatory cells infiltration, VSMCs proliferation and collagen deposition (51,264,283,285). Although mPGES-1 is expressed in different cell types of the vascular wall including VSMCs and adventitial fibroblasts, it has been recently demonstrated that PGE_2 derived from mPGES-1 in macrophages has an important role in development of neointimal hyperplasia (51). Interestingly, the effects of mPGES-1 on vascular remodeling are mediated by Tenascin-C which is implicated in the regulation of VSMCs growth among other processes (264). The COX-2/mPGEs-1 axis is also involved in aortic aneurisms formation (46,113,263). Moreover, in patients it has been demonstrated that a low dose of acetylsalicylic acid attenuates inflammation in the walls of cerebral aneurysms through downregulation of COX-2/mPGES-1 axis (113). This is an important aspect since aneurisms are characterized among other

processes, by localized connective tissue degradation suggesting that prostanoids might also modulate deposition of ECM proteins.

The specific EP receptor responsible of altered vascular structure varies depending on the vascular bed and pathology analyzed. The $EP_{3\alpha/\beta}$ receptor and the cAMP/PKA and PI3K pathways seem to be involved in neointima hyperplasia (285). EP_2 receptor activates the proinflammatory transcription factor NF-κB in cerebral aneurysm (13). EP_4 receptor seems to play an important role in the development of aortic aneurysms both in animal models (47) and in humans (46). Despite the promising data on the role of prostanoids in vascular remodeling, its role in hypertension-induced vascular remodeling and mechanical alterations is less known. Indeed, very few studies have analyzed this pathway. Virdis and colleagues (259) reported that vascular remodeling observed in Ang II-induced hypertension depends on COX-1/TP receptor axis. In agreement, Sparks and colleagues (230) showed that TP receptors in VSMCs play a major role in vascular remodeling in aorta in hypertension induced by Ang II. In this Thesis, we suggest that the COX-2/mPGES-1/EP_1 axis plays a role in vascular remodeling in small arteries in hypertension by modulating ECM and vascular stiffness (Article 3).

The above mentioned aspects might have clinical implications. It is well known that long-lasting treatment of patients with nonsteroidal antiinflammatory drugs produces multisystemic adverse effects and specific COX-2 inhibitors increase the risk of cardiovascular disease and worsen high blood pressure (8,12). Therefore, drugs targeted downstream from COX-2 would represent a therapeutic alternative. However, the role of mPGES-1-derived PGE_2 in hypertension is still controversial (52,87,128,129,130,264) and the impact of future mPGES-1 inhibitors on cardiovascular risk remains unclear. Therefore, the blockade of specific prostanoids

receptor might constitute promising strategies in order to achieve cardiovascular protection.

3.3.5. Reciprocal Relationship Between ROS and Prostanoids in Hypertension

As can be inferred from the above sections of this Introduction, ROS and prostanoids share many stimuli and intracellular signaling pathways. Therefore, it would not be surprising that both mediators would act in concert to induce their biological effects.

- **ROS induces COX pathway.** Different studies have demonstrated that ROS from different sources can affect both the activity and expression of COX isoforms in vessels. H_2O_2 increases COX-2 gene and protein expression in endothelial or VSMCs (133,149,157). Tert-butyl hydroperoxide, a product of lipid peroxidation, induces greater COX-2 expression and COX-2-mediated vasoconstrictor responses in aorta from hypertensive than normotensive rats (92). The elevated intracellular ROS in the endothelium stimulates the expression and the activity of COX-2 to release $PGF_{2\alpha}$ which causes endothelium-dependent contraction and impair endothelium dependent relaxation through TP receptor (243,274). Similarly, the impairment of endothelium-dependent relaxations induced by bone morphogenic protein 4 (which is elevated in hypertensive patients) is mediated by increased NADPH oxidase-derived ROS followed by COX-2 up-regulation (272). Recently, in human cord umbilical vein ECs Camacho and colleagues (45) also demonstrated a relationship between free radical species and COX-2. In agreement with these studies is the fact that specific COX-2 transcription factors such as NF-kB and AP-1 are sensitive to the redox state (136).

Different ROS also modulates COX-1 and COX downstream prostanoid synthases. Thus, the increased ROS production observed in vessels from hypertensive animals also stimulates COX-1 activity and the production of contractile prostanoids (252,257,282).

H_2O_2 induces TXA_2 production in mesenteric resistance arteries which is responsible for H_2O_2-induced contractile responses (93) and Nox1 mediates the upregulation of thromboxane synthase induced by TNF-α (178). In ECs, H_2O_2 increases PGI_2, PGE_2 and TXA_2 production and up-regulates thromboxane synthase expression (133). In addition, $ONOO^-$ causes nitration and inactivation of PGI_2 synthase and activation of COX, finally leading to a compensatory increase of TXA_2 (274,286). Moreover, NADPH oxidase-derived ROS are involved in mPGES-1 expression and PGE_2 production (20).

We have previously mentioned that mitochondria is being considered a novel source of oxidative stress in hypertension. However, whether this is related with COX derived products is unknown. To our knowledge, ours is the first report to demonstrate that mitochondria-derived ROS affects COX-2 expression and activity in hypertension (Article 2).

- **COX induces ROS activation.** ROS can derive directly from COX in part due to its ability to co-oxidize substances such as NADPH (85,239). However, COX-derived products may also function as autocrine stimulators of ROS. To date, several studies have demonstrated a relationship between COX and oxidative stress. Selective COX-2 inhibitors or COX-2 deletion decrease vascular oxidative stress (232,276,277) and improve vascular function in hypertensive patients likely by ROS reduction (260,269). Moreover, it has been reported that this process is involved in the observed changes in blood pressure (105). It is unclear whether this effect is mediated by inhibition of COX-2-associated ROS production or by inhibition of the synthesis of downstream prostanoids that can directly regulate the expression and activity of several sources of ROS. However, in favor of the latter hypothesis is the fact that prostanoids such as TXA_2 upregulate the expression and activity of NADPH oxidase (93,177,178). In addition, other prostanoids such as $PGF_{2\alpha}$ and 8-isoprostane $F_{2\alpha}$ also induce ROS

production together with increased NADPH oxidase expression (177). It is important to note that the role of PGE_2 on oxidative stress is controversial. Thus, PGE_2 is able to induce ROS formation through EP_1 receptor in Ang II-induced hypertension (47,48,196) and mPGES-1 deletion reduces oxidative stress in hypertension (263). However, other authors suggest that mPGES-1-derived PGE_2 protects against hypertension, probably through inhibition of NADPH oxidase-dependent ROS production (129,130). The reasons for these discrepancies are unclear, but differences appear to be in the background of the animals or the hypertension models (81,284).

The above mentioned studies suggest that prostanoids increase oxidative stress at vascular level. However, prostanoids can also modulate vascular oxidative stress status by decreasing ROS. Thus, PGI_2 reduces the increased ROS production induced by the TP agonist U46619, lipopolysacharide and cytokines through inhibition of NADPH oxidase expression or activity (20,177), thus contributing to the protective effects of PGI_2 in the vascular wall. Whether the protective antioxidant role of PGI_2 is lost in cardiovascular diseases or whether increased pro-oxidant prostanoids overcome antioxidant prostanoids in cardiovascular diseases deserve future investigations.

- **Reciprocal relationship between ROS and prostanoids in hypertension.** Due to the importance of both oxidative stress and prostanoids in the vascular wall, the reciprocal regulation of these mediators might have a critical role in several pathologies through a harmful self-perpetuating cascade. To our knowledge only one study has reported this reciprocal relationship. Thus, in human liver cells phorbol 12-myristate 13-acetate initiates a pathway in which Nox1 activation controls COX-2 expression and activity, which in turn induces Nox4 expression by activation of EP_4 receptors (215).

Based on the strong evidences of the relationship between ROS and COX products described at vascular level, we questioned whether this reciprocal relationship might also be taking place in hypertension. One of the studies presented in this Thesis (Article 2) demonstrate that this reciprocal relationship also exist at vascular level and that in fact, it is responsible of hypertension and of hypertension-associated vascular alterations. We believe that this reciprocal relationship may be a promising therapeutic option with potential beneficial effects to reverse the alterations in vascular function associated to hypertension.

3.3.6. GRK2 and Vascular Alterations in Hypertension

In the last few years, several studies have demonstrated that GRK2 might be particularly important in cardiovascular diseases such as hypertension (23,35). However, the mechanisms whereby GRK2 contributes to hypertension are far from being completely understood. The levels and activity of GRK2 are increased in lymphocytes derived from young hypertensive patients as well as in the VSMCs of animal models of hypertension (107,108). Increased GRK2 expression also correlated with decreased activity of adenylyl cyclase downstream isoproterenol-stimulated β-adrenergic receptors (107). In addition, GRK2, but not GRK3 or GRK5 mRNA levels, increase in correlation with systolic blood pressure in humans. In these hypertensive patients, norepinephrine levels were also increased (59). Therefore, a potential mechanism proposed was that greater sympathetic nervous system activation resulted in exaggerated β adrenergic signaling and subsequent GRK2-mediated desensitization of the receptors (35). Elevated GRK2 levels particularly impair vasodilator β adrenergic receptor responses in different tissues and animal models (23,197), and, interestingly, in human patients treated with β-blockers GRK2 levels return to baseline (2). GRK2 also associates with other GPCR such as ET receptors (88). ET-1 levels were increased in hypertensive patients, and this

was associated with increased GRK2 levels (80,170). In addition, inhibition of GRK2 but not GRK3, GRK5, or GRK6 resulted in reduced desensitization of ET-1-induced calcium and IP3 signaling in VSMCs (170).

Initially it was thought that GRK2 could play a protective role since the increase in vascular GRK2 would induce a lower availability of GPCR receptors such as Ang II, and it could represent a mechanism for adaptation against a hypertensive phenotype. However, transgenic mice overexpressing GRK2 in the VSMCs show increased resting blood pressure, vascular thickening and cardiac hypertrophy and exhibited reduced sensitivity to vascular relaxation induced by the β-adrenergic receptor agonist isoproterenol (78). Thus, the preferential desensitization by GRK2 of vasodilator receptor subtypes versus vasoconstrictor ones has been invoked to explain the effect that upregulated GRK2 levels might have in human and murine hypertension (78). However, novel results implicating GRK2 in non GPCR-dependent pathways are forcing the field to redefine GRK2 participation in the regulation of vascular tone. Thus, it has been shown an interaction of GRK2 with Akt that inhibits Akt-dependent activation of NOS thus impairing NO production (152). Thus, increased GRK2 expression may also play a role in hypertension by reducing NO production (82,152) and thereby deactivating one of the main vasodilator pathways in ECs. In agreement, GRK2 knockdown restored NO production and normalized portal pressure (152). In diabetes animal models it has been suggested that there is an endothelial dysfunction produced by GRK2 upregulation, since GRK2 may be inhibiting Akt/eNOS pathway (237,281). Recently, it has been demonstrated that in SHR exercise training downregulated vascular GRK2 expression and activity, which further increased insulin-stimulated vascular Akt/eNOS activation this might having a role to limit the progression of hypertension induced by exercise (281). Another important question is to define the relative importance of endothelial

GRK2 as compared to VSMCs, since GRK2 depletion in VSMCs in mice cannot prevent portal hypertension (58). These evidences indicate that GRK2 might be a good therapeutic target in hypertension.

It has been described that GRK2 overexpression in VSMCs leads to an increased vascular wall thickness in aorta together with narrowed lumen (78). Recent studies have suggested that G_q signaling may be implicated in this process because inhibition of VSMCs G_q signaling normalized blood pressure and vascular wall thickness (112). Interestingly, GRK2 and arrestins expression are essential for agonist-stimulated VSMCs migration, a key process in some of types of vascular remodeling (171). Although these evidences point to a role for GRK2 in vascular remodeling, it was unclear its possible role in vascular remodeling and mechanical alterations in hypertension. In the Article 4 of this Thesis, we demonstrate for the first time, that GRK2 are key effectors of altered vascular structure and mechanical properties in hypertension.

Aims

Inflammatory mechanisms play an important role in the pathophysiology of hypertension. Thus, increased expression and activity of inflammatory enzymes such as COX-2 and mPGES-1 as well as increased production of ROS mainly from NADPH Oxidase, have been described in different tissues from patients or animal models with hypertension. These mediators seem to contribute to the vascular functional, structural and mechanical alterations observed in hypertension although its specific role is not completely understood. The mechanisms underlying this inflammatory state in hypertension seem to be highly dependent on the components of the RAAS. Particularly, Ang II acting through AT1 receptors is involved in the development and maintenance of hypertension by affecting the function and the structure of the vessels. AT1 receptors, as well as other G protein-coupled receptors, are regulated by desensitization processes involving GRK2. Furthermore, GRK2 is upregulated in different tissues in hypertension and novel evidences suggest that this protein has a role in the regulation of NO production, although its role in vascular alterations in hypertension is unknown.

The main aim of this Thesis was to investigate the role of oxidative stress from NADPH Oxidase and mitochondria, COX-2 derived prostanoids and GRK2 in the vascular functional and structural abnormalities observed in hypertension. The Thesis was divided into four specific aims:

1. To analyze the effect of aldosterone on noradrenaline-induced vasoconstriction in mesenteric resistance arteries from normotensive and hypertensive rats and the role of endothelium-derived mediators such as COX-2-derived prostanoids, NO and ROS in the aldosterone effects.

2. To evaluate whether a reciprocal relationship between ROS producing enzymes (NADPH Oxidase and mitochondria) and COX-2-derived prostanoids might modulate vascular functional responses of conductance and resistance arteries in hypertension.

3. To explore the contribution of the COX-2/mPGES-1/EP1 axis in the structural and mechanical vascular alterations associated to hypertension.

4. To examine the role of GRK2 in Ang II-induced hypertension and in the associated vascular functional, structural and mechanical alterations.

Article 1: Aldosterone Alters the Participation of Endothelial Factors in Noradrenaline Vasoconstriction Differently in Resistance Arteries from Normotensive and Hypertensive Rats

Xavier FE, Blanco-Rivero J, **Avendaño MS**, Sastre E, Yela R, Velázquez K, Salaíces M, Balfagón G.

Eur J Pharmacol. 654:280-288. 2011.

European Journal of Pharmacology 654 (2011) 280–288

Contents lists available at ScienceDirect

European Journal of Pharmacology

journal homepage: www.elsevier.com/locate/ejphar

Cardiovascular Pharmacology

Aldosterone alters the participation of endothelial factors in noradrenaline vasoconstriction differently in resistance arteries from normotensive and hypertensive rats

Fabiano E. Xavier [c,1], Javier Blanco-Rivero [a,1], María Soledad Avendaño [b], Esther Sastre [a], Rubén Yela [a], Kyra Velázquez [a], Mercedes Salaíces [b], Gloria Balfagón [a,*]

[a] Departamento de Fisiología, Facultad de Medicina, Universidad Autónoma de Madrid, Spain
[b] Departamento de Farmacología y Terapéutica Facultad de Medicina, Universidad Autónoma de Madrid, Spain
[c] Departamento de Fisiologia e Farmacologia, Centro de Ciências Biológicas, Universidade Federal de Pernambuco, Recife, Brazil

ARTICLE INFO

Article history:
Received 6 April 2010
Received in revised form 9 December 2010
Accepted 7 January 2011
Available online 22 January 2011

Keywords:
Aldosterone
Mesenteric resistance artery
Nitric oxide
Superoxide anion
Thromboxane A_2
Prostaglandin I_2

ABSTRACT

This study analyzed the effect of aldosterone (0.05 mg/kg per day, 3 weeks) on vasoconstriction induced by noradrenaline in mesenteric resistance arteries from WKY rats and SHR. Contraction to noradrenaline was measured in mesenteric resistance arteries from untreated and aldosterone-treatedrats from both strains. Participation of nitric oxide (NO), superoxide anions, thromboxane A_2 (TxA_2) and prostacyclin in this response was determined. 6-keto-prostaglandin (PG)F1alpha and thromboxane B_2 (TxB_2) releases were determined by enzyme immunoassay. NO and superoxide anion release were also determined by fluorescence and chemiluminiscence, respectively. Aldosterone did not modify noradrenaline-induced contraction in either strain. In mesenteric resistance arteries from both aldosterone-treated groups, endothelium removal or preincubation with NO synthesis inhibitor L-NAME increased the noradrenaline-induced contraction, while incubation with the superoxide anion scavenger tempol decreased it. Preincubation with either the COX-1/2 or COX-2 inhibitor (indomethacin and NS-398, respectively) decreased the noradrenaline contraction in aldosterone-treated animals, while this response was not modified by COX-1 inhibitor SC-560. TxA_2 synthesis inhibitor (furegrelate), or TxA2 receptor antagonist (SQ 29 548) also decreased the noradrenaline contraction in aldosterone-treated animals. In untreated SHR, but not WKY rats, this response was increased by L-NAME, and reduced by tempol, indomethacin, NS-398 or SQ 29 548. Aldosterone treatment did not modify NO or TxB_2 release, but it did increase superoxide anion and 6-keto-PGF(1alpha) release in mesenteric resistance arteries from both strains. In conclusion, chronic aldosterone treatment reduces smooth muscle contraction to alpha-adrenergic stimuli, producing a new balance in the release of endothelium-derived prostanoids and NO.

1. Introduction

Aldosterone is the main circulating mineralocorticoid in humans, and it is normally produced in response to volume depletion and angiotensin stimulation. It participates in the electrolyte balance and plays an important physiological role in the long-term regulation of Na^+ and K^+ in the distal tubules and collecting ducts of the kidney (Giebisch, 1998; Palmer, 1999; Giebisch and Wang, 2000; Palmer and Frindt, 2000). In addition, aldosterone has been reported to play a major role in the regulation of vascular tone as well as in vascular alterations associated to atherosclerosis, heart failure and some forms of hypertension (Pitt et al., 1999; Schiffrin, 2006).

The endothelium plays a pivotal role in the regulation of vascular tone by regulating the release of both relaxing and contracting factors under basal conditions and after stimulation with contractile agonists. The mechanisms by which aldosterone influences vascular function remain to be elucidated; nevertheless, it has been suggested that aldosterone can quantitatively and qualitatively alter the release of endothelial factors (Blanco-Rivero et al., 2005; Xavier et al., 2008). Several studies have demonstrated that aldosterone stimulates a vascular inflammatory response, and this could induce endothelial dysfunction and fibrosis (Blanco-Rivero et al., 2005; Neves et al., 2005; Xavier et al., 2008). In addition, an aldosterone-mediated increase in the release of various inflammatory agents has been described (Blanco-Rivero et al., 2005; Neves et al., 2005; Sanz-Rosa et al., 2005; Xavier et al., 2008). Recently we have reported that vasoconstrictor prostanoids are involved in the impaired endothelium-

* Corresponding author at: Departamento de Fisiología, Facultad de Medicina, Universidad Autónoma de Madrid, C/Arzobispo Morcillo, 4, 28029 Madrid, Spain. Tel.: +34 91 4975450; fax: +34 91 4975353.
E-mail address: gloria.balfagon@uam.es (G. Balfagón).
[1] Both authors have contributed equally and should be considered the first and second authors.

0014-2999/$ – see front matter © 2011 Published by Elsevier B.V.
doi:10.1016/j.ejphar.2011.01.007

dependent vasodilation to acetylcholine induced by aldosterone in conductance and resistance vessels from normotensive and hypertensive rats (Blanco-Rivero et al., 2005; Xavier et al., 2008).

The renin–angiotensin–aldosterone system is involved in alterations of vascular function in hypertensive patients and the study of aldosterone effects on vascular contractility in resistance vessels could be especially relevant, particularly as resistance arteries have a major role in the regulation of vascular resistance and in the haemodynamic abnormalities associated with this pathology. The findings described above raise the possibility that aldosterone may induce variations in endothelial function that would promote changes in vascular contraction. Thus, the purpose of this study was to analyze the effect of aldosterone on noradrenaline-induced vasoconstriction in mesenteric resistance vessels from normotensive (WKY) and hypertensive (SHR) rats, and also study the possible role of endothelium-derived products in that putative aldosterone effect.

2. Methods

2.1. Animal housing

Male 6-month-old Wistar Kyoto rats (WKY) and spontaneously hypertensive rats (SHR) weighing 250 to 300 g were obtained from colonies maintained at the animal quarters of the *Facultad de Medicina* of the *Universidad Autónoma de Madrid*. The investigations conform to the *Guide for the Care and Use of Laboratory Animals* published by the US National Institutes of Health (NIHi Publication No. 85-23, revised 1996) and to the directives 609/86 CEE and R.D. 233/88 of the *Ministerio de Agricultura, Pesca y Alimentación* (registration No. EX-021U) of Spain.

Controlled time-release pellets (Innovative Research of America, U.S.A.), containing aldosterone (0.05 mg/kg per day) or a vehicle, were subcutaneously implanted. Animals were divided into four groups: WKY rats, WKY rats plus aldosterone, SHR, and SHR plus aldosterone (Blanco-Rivero et al., 2005; Xavier et al., 2008). Rats were fed *ad libitum* with standard rat chow (Safe A04, Panlab S.L., Spain). At the end of the treatment period (three weeks), systolic blood pressure (BP) was measured in awake rats by a tail-cuff method (Letica, Digital Pressure Meter, LE5000, Barcelona, Spain). Blood samples were collected by cardiac puncture before the animals were sacrificed. After centrifugation for 15 min at 1500 *g*, the serum was transferred to polypropylene tubes and then frozen at −80 °C.

2.2. Aldosterone, cortisol and noradrenaline levels

Serum levels of aldosterone, cortisol and noradrenaline were analyzed using aldosterone EIA kit, Cortisol EIA Kit (Cayman Chemical, Ann Arbor, Michigan, USA), and noradrenaline research EIA (Labor Diagnostica Nord. Gmbh & Co., Kg: Nordhorn, Germany) respectively. The assays were performed following the manufacturer's instructions. Results were expressed as pg/ml (for aldosterone and cortisol) or ng/ml (for noradrenaline).

2.3. Vessel preparation

After death by CO_2 inhalation, the mesenteric vascular bed was removed and placed in cold (4 °C) Henseleit solution (KHS; in mmol/l: 115 NaCl, 2.5 $CaCl_2$, 4.6 KCl, 1.2 KH_2PO_4, 1.2, $MgSO_4 \cdot 7H_2O$, 25 $NaHCO_3$, 11.1 glucose, and 0.03 EDTA).

For *ex vivo* reactivity experiments the third order branch of the mesenteric arcade (untreated: SHR 262 ± 5.1, n = 8, *vs.* WKY: 301 ± 4.8 μm diameter, n = 10, $P<0.05$; aldosterone-treated: SHR 254 ± 7.0, n = 7, *vs.* WKY: 318 ± 5.4 μm diameter, n = 9, $P<0.05$) was dissected from the mesenteric bed, cleaned of connective tissue and cut in segments of approximately 2 mm in length. Two tungsten wires (40 μm diameter) were introduced through the lumen of the segments and mounted in a small vessel dual chamber myograph (Danish Myo Technology A/S, Aarhus, Denmark) to measure isometric tension according to the method described by Mulvany and Halpern (1977). After a 30 min equilibration period in oxygenated KHS at 37 °C and pH = 7.4, segments were stretched to their optimal lumen diameter for active tension development. This was determined based on the internal circumference-wall tension ratio of the segments by setting their internal circumference, L_0, to 90% of what the vessels would have if they were exposed to a passive tension equivalent to that produced by a transmural pressure of 100 mm Hg (Mulvany and Halpern, 1977).

2.4. Experimental protocols

After a 45 minute-equilibration period, each arterial segment was exposed twice to KCl (120 mmol/l) to assess its maximum contractility. Thirty minutes later, rings were contracted with a concentration of noradrenaline that induced approximately 50% of the KCl contraction, and then acetylcholine (1 μmol/l) was added to assess the integrity of the endothelium. After 60 min, cumulative concentration–response curves for noradrenaline (10 nmol/l–0.1 mmol/l) were generated.

The effect of the nonselective NO synthase inhibitor N-nitro-L-arginine methyl ester (L-NAME, 0.1 mmol/l), as well as that of the superoxide dismutase mimetic 4-hydroxy-2,2,6,6-tetramethylpiperidinoxyl (tempol, 0.1 μmol/l) on concentration–response curves for noradrenaline were investigated.

The possible role of cyclooxygenase-arachidonic acid metabolites in noradrenaline-induced contraction was investigated in segments pre-incubated with either indomethacin (a cyclooxygenase inhibitor, 10 μmol/l), 5-(4-chlorophenyl)-1-(4-methoxyphenyl)-3-trifluoromethyl pyrazole (SC-560, a COX-1 inhibitor, 1 μmol/l) or N-(2-cyclohexyloxy-4-nitrophenyl) methansulfonamide (NS-398, a COX-2 inhibitor, 10 μmol/l), furegrelate (a thromboxane synthase inhibitor, 10 μmol/l) or [1*S*-[1*a*,2*a*(*Z*),3*a*,4*a*]]-7-[3-[[2-(phenylamino) carbonyl]hydrazino]methyl]-7-oxabicyclo [2.2.1] hept-2-yl-5-heptanoic acid (SQ 29 548, a thromboxane A_2 receptor (TP) antagonist, 1 μmol/l).

All drugs were added 30 min before performing the concentration–response curve to noradrenaline.

2.5. NO release

In order to study the effect of aldosterone on noradrenaline-induced nitric oxide (NO) release, the second, third and fourth branches of mesenteric artery from either control or aldosterone-treated WKY rats and SHR were incubated for 60 min in HEPES buffer containing in mmol/l: 119 NaCl, 20 HEPES, 4.6 KCl, 1 $MgSO_4 \cdot 7H_2O$, 0.15 $Na_2HPO_4 \cdot 12H_2O$, 0.4 KH_2PO4, 5 $NaHCO_3$, 1.2 $CaCl_2 \cdot 2H_2O$, and 5.2 glucose, at 37 °C (stabilization period). Afterward, arteries were incubated with the fluorescent probe 4,5-diaminofluorescein (2 μmol/l) for 30 min, and medium was collected to measure basal NO release. Once the organ bath was refilled, noradrenaline was added cumulatively (10 nmol/l–0.1 mmol/l) at 2 min intervals. The medium was collected only at the end of the concentration–response curve to noradrenaline. The fluorescence of the medium was measured at room temperature using a spectrofluorimeter (LS50 Perkin Elmer Instruments, FL WINLAB Software) with excitation wavelength set at 492 nm and emission wavelength at 515 nm. The stimulated NO release was calculated by subtracting the basal NO release from that evoked by noradrenaline. Also, blank measurement samples were collected from the medium without mesenteric segments in order to subtract background emission. Some assays were performed in the presence of L-NAME (0.1 mmol/l). The amount of NO released was expressed as arbitrary units per milligram of tissue.

2.6. Detection of superoxide anions

In order to study the effect of aldosterone on superoxide anion release, the second, third and fourth branches of mesenteric artery from

either control or aldosterone-treated WKY rats and SHR were equilibrated for 30 min in HEPES buffer at 37 °C, transferred to test tubes that contained 1 ml HEPES buffer (pH 7.4) with lucigenin (250 μmol/l) and then kept at 37 °C. The luminometer was set to report arbitrary units of emitted light; repeated measurements were collected for 5 min at 10 s intervals and averaged. 4,5-Dihydroxy-1,3-benzene-disulphonic acid "Tiron" (10 mmol/l), a cell permeant, non-enzymatic scavenger of the superoxide anion, was added to quench the superoxide anion-dependent chemiluminescence. Also, blank measures were collected in the same way without mesenteric segments to subtract background emission.

2.7. Prostanoids production

To measure the release of TxA_2 and prostacyclin, we used a TxB_2 and a 6-keto-$PGF_{1\alpha}$ enzyme immunoassay (EIA) kit (Cayman Chemical, Ann Arbor, Michigan, USA), respectively. The second, third and fourth branches of mesenteric artery were preincubated for 45 min in 200 μl of KHS at 37 °C and continuously gassed with a 95% O_2–5% CO_2 mixture (stabilization period). Afterward, three washout periods of 7 min in a bath of 200 μl of KHS were run before incubation with noradrenaline (10 nmol/l–100 μmol/l). The medium was collected only at the end of the concentration–response curve to noradrenaline. The different assays were performed following the manufacturer's instructions. Results were expressed as pg ml^{-1} mg wet $tissue^{-1}$.

2.8. Collagen I expression

For Western blot analysis of collagen I expression, the second, third and fourth branches of mesenteric resistance arteries from all experimental groups were homogenized in a boiling buffer composed of 1 mmol/l sodium vanadate, 1% sodium dodecyl sulfate (SDS), and 0.01 mol/l pH 7.4 Tris–HCl. Homogenates containing 30 μg protein were electrophoretically separated on a 8.5% SDS-polyacrylamide gel, and then transferred to a polyvinyl difluoride membrane (Bio-Rad Immun-Blot) overnight at 4 °C, 230 mA, using a Bio-Rad Mini Protean III system (Bio-Rad Laboratories, Hercules, CA, USA) containing 25 mmol/l Tris, 190 mM glycine, 20% methanol, and 0.05% SDS. The membrane was blocked for 1 h at room temperature in Tris buffered-saline solution (100 mmol/l, 0.9% w/v NaCl, 0.1% SDS) with 5% powdered fat-free milk before being incubated overnight at 4 °C with mouse monoclonal antibody against collagen I (1:5000, Bionova Científica S.L., Madrid, Spain). After washing, the membrane was incubated with anti-mouse horseradish peroxidase-conjugated immunoglobulin G antibody (1:2000, Amersham International Plc, Little Chalfont, UK). The membrane was thoroughly washed and the immunocomplexes were then detected using an enhanced horseradish peroxidase/luminal chemiluminescence system (ECL Plus, Amersham International Plc) and subjected to autoradiography (Hyperfilm ECL, Amersham International Plc). Signals on the immunoblot were quantified using a computer program (NIH Image V1.56, National Institute of Health, Bethesda, MD, USA). The same membrane was used to determine α-actin expression, and the content of the latter was used to correct protein expression in each sample by means of a monoclonal anti α-actin antibody (1:2000 dilution, Sigma-Aldrich, Madrid, Spain). Rat cornea homogenates were used as a positive control.

2.9. Drugs

Drugs used were noradrenaline hydrochloride, acetylcholine chloride, furegrelate, indomethacin, SC-560, tempol (Sigma; St. Louis, MO, U.S.A.), NS-398 (Calbiochem–Novabiochem GmbH), and SQ 29 548 (ICN Iberica). Stock solutions of drugs were made in distilled water, except for noradrenaline, which was dissolved in a NaCl (0.9%)-ascorbic acid (0.01% wv^{-1}) solution, indomethacin and SQ 29 548, which were dissolved in ethanol, and NS-398, which was dissolved in DMSO. Preincubation with DMSO or ethanol did not modify basal arterial tone. These solutions were kept at −20 °C and appropriate dilutions were made on the day of the experiment.

2.10. Statistical analysis

Noradrenaline contractile response was expressed as a percentage of the maximum response produced by KCl. In order to compare the magnitude of the effects of the different drugs or of endothelium denudation on contractile responses to noradrenaline in segments from all experimental groups, some results were expressed as "differences" of area under the concentration–response curves (dAUC) to noradrenaline in control and experimental situations. AUC were calculated from the individual concentration–response curve plots (GraphPad Prism 5.0 Software, San Diego, CA) and the differences were expressed as a percentage of the difference to AUC of the corresponding control situation.

All values are expressed as means ± S.E.M. of the number of animals used in each experiment. Results were analyzed using one-way or two-way ANOVA for comparison between groups. When ANOVA showed a significant treatment effect, Bonferroni's *post hoc* test was used to compare individual means. Differences were considered statistically significant at $P<0.05$.

3. Results

3.1. Blood pressure

SHR rats presented higher blood pressure levels than WKY rats (SHR: 171 ± 5.0 *vs.* WKY: 118 ± 3.0 mm Hg; $P<0.05$, $N=10$ animals each group) and chronic aldosterone treatment did not modify this parameter in any strain (SHR-aldo: 180 ± 4.0 *vs.* WKY-aldo: 120 ± 8.0 mm Hg, $N=9$ animals each group), as previously reported (Xavier et al., 2008).

3.2. Aldosterone, cortisol and noradrenaline levels

Serum aldosterone levels were higher in untreated SHR than in WKY rats, and increased with aldosterone treatment in both strains (Table 1). Serum cortisol levels were similar in untreated WKY rats and SHR. Aldosterone did not modify cortisol levels in any group of rats (Table 1). The fact that cortisol serum levels remained unaltered indicates that this modification is not associated to changes in aldosterone biosynthesis. Noradrenaline levels were higher in SHR

Table 1
Effect of aldosterone treatment on aldosterone, cortisol and noradrenaline serum levels in WKY rats and SHR.

	WKY control	WKY-aldo	SHR control	SHR-aldo
Aldosterone (pg/ml)	87.82 ± 10.97	234.51 ± 14.86[a]	165.2 ± 1.39[b]	364.2 ± 22.86[a]
Cortisol (pg/ml)	63.49 ± 3.53	63.52 ± 8.51	61.98 ± 8.08	58.94 ± 6.17
Noradrenaline (ng/ml)	22.42 ± 0.89	20.01 ± 2.98	40.44 ± 5.01[b]	41.78 ± 1.57

$N=6$ animals each group.
[a] $P<0.05$ aldosterone *vs.* control release.
[b] $P<0.05$ SHR *vs.* WKY.

rats than in WKY rats, and aldosterone did not modify noradrenaline levels in any group of rats (Table 1).

3.3. Vascular response to KCl and noradrenaline

Contraction to KCl (120 mmol/l) was similar in arteries with endothelium from both untreated and aldosterone-treated WKY rats and SHR (Xavier et al., 2008). In arteries from all experimental groups this response remained unmodified after endothelium removal (results not shown).

Contractile responses to noradrenaline were similar in arteries with endothelium from WKY rats and SHR (Fig. 1) and remained unmodified after aldosterone treatment (Fig. 1). In both aldosterone-treated and untreated WKY rats and SHR, endothelial denudation increased the response to noradrenaline (Fig. 1). In arteries without endothelium the contractile responses produced by noradrenaline were smaller in aldosterone-treated than in untreated WKY rats and SHR (Fig. 1, see dAUC graph in Fig. 1).

To assess the contribution of endothelium-derived NO to the noradrenaline responses, segments were incubated with the NO synthase inhibitor L-NAME. This drug increased the response to noradrenaline in arteries obtained from all experimental groups (Fig. 2). The increase was smaller in aldosterone-treated WKY rats and SHR than in untreated animals (Fig. 2, see dAUC graph in Fig. 2).

In segments from untreated rats, incubation with the superoxide dismutase mimetic, tempol, reduced vasoconstriction to noradrenaline only in segments from SHR (Fig. 2A and C). In both aldosterone-treated WKY rats and SHR pretreatment of mesenteric resistance arteries with tempol reduced the concentration–response curve to noradrenaline, and this reduction was greater in the aldosterone-treated WKY rats and SHR (Fig. 2B and D, see dAUC graph in Fig. 2).

In mesenteric resistance arteries from untreated animals, incubation with either the unspecific COX inhibitor indomethacin or the specific COX-2 inhibitor NS-398 decreased the contractile response to noradrenaline only in hypertensive animals (Fig. 3A and C). In both the aldosterone-treated WKY and SHR groups pretreatment of mesenteric resistance arteries with indomethacin or NS-398 reduced the concentration–response curve to noradrenaline (Fig. 3B and D). The effect of indomethacin and NS-398 was greater in SHR than WKY animals (see dAUC graph in Fig.3). Preincubation with the specific COX-1 inhibitor SC-560 did not alter the vasoconstrictor response to noradrenaline in any experimental group (Fig. 3).

Incubation with the TxA_2 receptor (TP) antagonist SQ 29 548 reduced the contractile response to noradrenaline in segments from the untreated SHR rats but not from the untreated WKY animals (Fig. 4A and B). In segments from both strains treated with aldosterone, SQ 29 548 decreased the noradrenaline vasoconstriction (Fig. 4B and D); however, this effect was greater in SHR than WKY rats (see dAUC graph in Fig. 4).

Preincubation with TxA_2 synthesis inhibitor furegrelate decreased vasoconstriction to noradrenaline in segments from untreated SHR and in segments from both aldosterone-treated groups (Fig. 4). The effect of furegrelate on the aldosterone-treated groups was comparable in both strains. The inhibiting effect of SQ 29 548 was greater than furegrelate only in SHR rats (Fig. 4).

None of the inhibitors used here affected basal arterial tone in untreated or aldosterone-treated groups, whether WKY or SHR animals (results not shown).

3.4. NO release

Both basal and noradrenaline-induced NO releases were higher in arteries from SHR rats than in those from WKY animals. Aldosterone treatment did not modify NO release in either rat strain (Fig. 5A). Preincubation with L-NAME abolished NO release in all experimental groups (results not shown).

3.5. Detection of superoxide anions

Superoxide anion release was higher in SHR than in WKY rats (Fig. 5B). Aldosterone treatment increased superoxide anion levels in both rat strains, but the increase was higher in SHR rats (Fig. 5B).

3.6. Prostanoid production

In mesenteric resistance arteries from all experimental groups, noradrenaline increased the release of both 6-keto-$PGF_{1\alpha}$ and TxB_2 (Fig. 6). Aldosterone increased noradrenaline-induced 6-keto-$PGF_{1\alpha}$

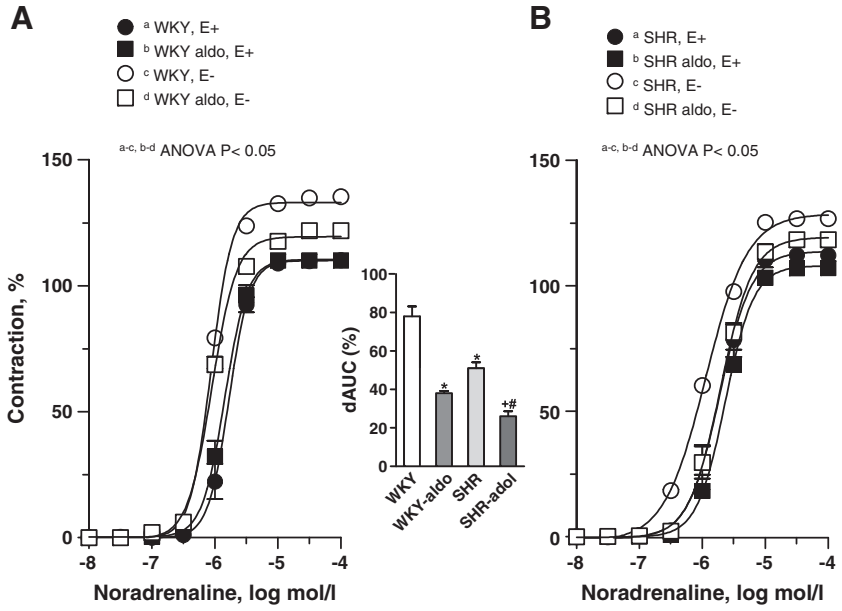

Fig. 1. Effect of chronic treatment with aldosterone (Aldo) on the concentration-dependent contraction to noradrenaline in mesenteric resistance segments from WKY (A) and SHR (B) rats. Results (mean ± S.E.M.) were expressed as a percentage of the initial contraction elicited by KCl. N = 7 animals each curve. Insert graph shows differences in area under the concentration–response curve (dAUC) to noradrenaline in endothelium-intact (E+) and -denuded (E−) arteries. dAUC values (means ± S.E.M.) are expressed as a percentage of the difference in the corresponding AUC for segments with intact endothelium. ANOVA (one way): $^{*}P<0.05$ *vs.* WKY; $^{+}P<0.05$ *vs.* SHR; $^{\#}P<0.05$ *vs.* WKY-aldo.

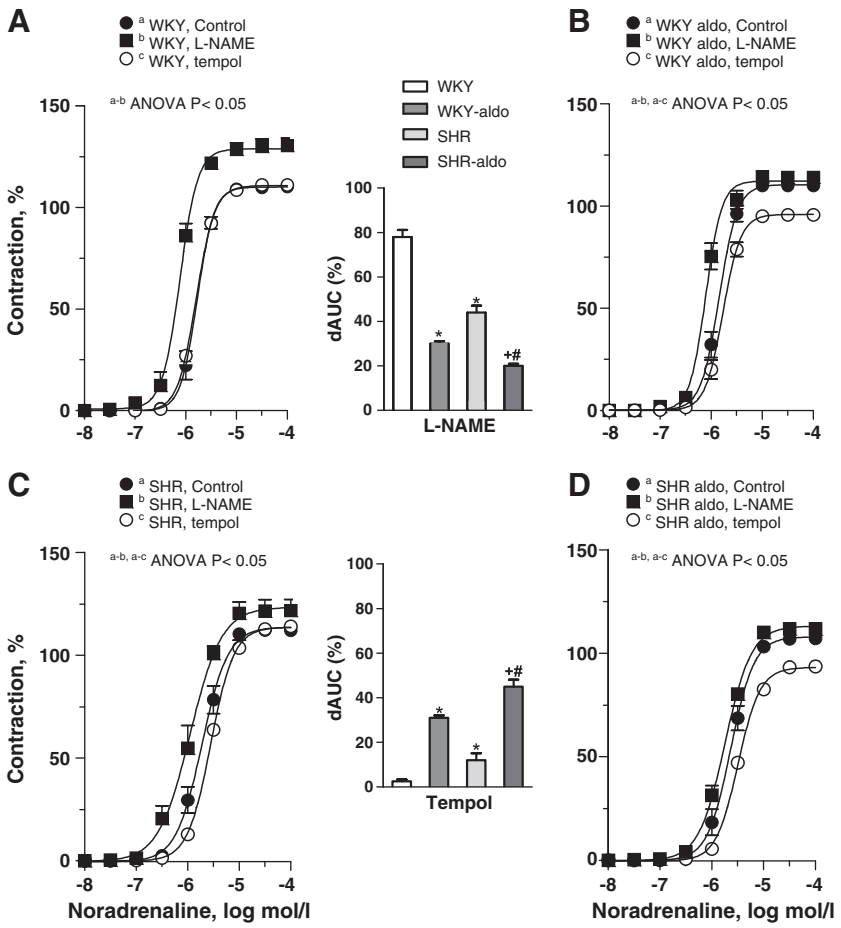

Fig. 2. Effect of L-NAME (0.1 mmol/l) and of tempol (0.1 mmol/l) on the concentration-dependent contraction to noradrenaline in mesenteric resistance segments from untreated and aldosterone-treated WKY and SHR rats. Results (mean ± S.E.M.) are expressed as a percentage of the initial contraction elicited by KCl. N = 7 animals each curve. Insert graph shows differences in area under the concentration–response curve (dAUC) to noradrenaline in the absence (control) or in the presence of either L-NAME or tempol. dAUC values (means ± S.E.M.) are expressed as a percentage in the difference of the corresponding control AUC. ANOVA (one way): $^{*}P<0.05$ *vs.* WKY; $^{+}P<0.05$ *vs.* SHR; $^{\#}P<0.05$ *vs.* WKY-aldo.

levels in mesenteric arteries from both rat strains (Fig. 6). TxB_2 levels were increased by aldosterone in segments from WKY rats, but not from SHR (Fig. 6).

3.7. Collagen I expression

Aldosterone treatment increased collagen I expression in mesenteric resistance arteries from WKY rats and SHR (Fig. 7).

4. Discussion

In physiological and several pathological conditions, including hypertension, aldosterone induces changes in vasomotor responses, which can be associated either to changes in perivascular fibrosis or alterations in the contribution of endothelial mediators in such responses (Duprez et al., 2000; Stier et al., 2002; Funder, 2004; Blanco-Rivero et al., 2005; Sanz-Rosa et al., 2005; Xavier et al., 2008). We observed no changes on BP due to aldosterone treatment. Because an increase in BP associated with aldosterone administration has been reported (Rocha and Funder, 2002; Freel and Connell, 2004), the lack of effect observed in this study could be a consequence of differences in experimental conditions (dose and period treatment).

We have found that aldosterone increases collagen I deposition in mesenteric resistance arteries from both rat strains. However, the concentration-dependent vasoconstriction induced by noradrenaline in mesenteric resistance arteries was not modified by aldosterone in either normotensive or hypertensive rats. In addition, treatment with aldosterone reduced the contractility of vascular smooth muscle to alpha-adrenergic stimulation. This is based on the observation that arteries without endothelium from aldosterone-treated rats (WKY rats and SHR) contracted less to noradrenaline than arteries from untreated rats. This result is surprising, particularly since aldosterone has been described to increase vasoconstrictor responses (Purdy and Weber, 1983; Weber et al., 1983; Schmidt et al., 2003; Michea et al., 2005). The reason for this discrepancy is not known, although it is important to note that most of these earlier studies used conductance arteries and evaluated the acute effects of aldosterone. Additionally, in the present study, aldosterone treatment did not alter noradrenaline serum levels in any strain. This agrees with our previous results in which aldosterone did not modify noradrenaline release from adrenergic nerve endings in superior mesenteric arteries (Balfagón et al., 2004).

Endothelium produces vasoconstrictor mediators involved in the impaired endothelium-dependent vasodilation observed in conductance and resistance vessels from rats treated with aldosterone (Blanco-Rivero et al., 2005; Xavier et al., 2008). These endothelial mediators could also affect vasoconstrictor responses since these responses are also modulated by endothelium. We have previously reported that the altered endothelial vasodilator and vasoconstrictor factors in ouabain-induced hypertension counter-acted any alterations in the vasoconstrictor response to alpha adrenergic stimuli (Xavier et al., 2004; Padilha et al., 2008). Thus, aldosterone treatment could be producing either a reduction in the response of vascular smooth muscle to alpha-adrenergic stimulation or an alteration in the

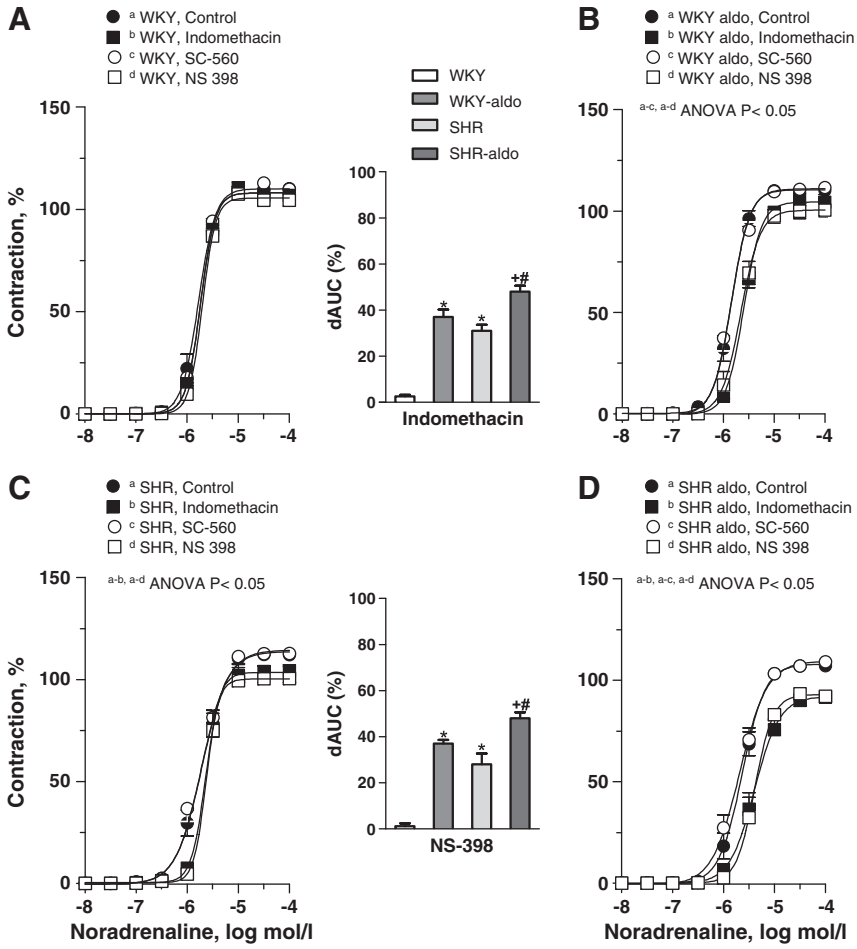

Fig. 3. Effect of indomethacin (10 μmol/l), of SC-560 (1 μmol/l) or of NS-398 (10 μmol/l) on the concentration dependent contraction to noradrenaline in mesenteric resistance segments from untreated and aldosterone-treated WKY and SHR rats. Results (mean ± S.E.M.) are expressed as a percentage of the initial contraction elicited by KCl. N = 7 animals each curve. Insert graph shows differences in area under the concentration–response curve (dAUC) to noradrenaline in the absence (control) or in the presence of either indomethacin or NS-398. dAUC values (means ± SEM) are expressed as a percentage of the difference of the corresponding control AUC. ANOVA (one way): $^{*}P<0.05$ *vs.* WKY; $^{+}P<0.05$ *vs.* SHR; $^{\#}P<0.05$ *vs.* WKY-aldo.

modulation of this vasoconstrictor response through effects on endothelial vasoactive factors.

The next objective was to determine possible quantitative or qualitative differences in the participation of endothelial factors in this contractile response in both aldosterone-treated and non-treated WKY rats and SHR. Both endothelium removal and NO synthase inhibition (L-NAME) increased the vasoconstriction to noradrenaline in rat mesenteric resistance arteries from WKY rats and SHR, and the effect was smaller in vessels from SHR. This suggests a reduction on endothelial and NO modulation in the contractile response to noradrenaline in resistance mesenteric arteries from hypertensive rats, as previously described (Bauersachs, 2004; Alvarez et al., 2005; Miyagawa et al., 2007). Treatment with aldosterone reduced the negative modulation of endothelium and NO in the response to noradrenaline in WKY rats and SHR. This corroborates previous studies showing that aldosterone alters the release of endothelial factors, an effect which involves, among others, a reduction in the release/bioavailability of NO (Nagata et al., 2006; Cachofeiro et al., 2008). Aldosterone did not modify basal or noradrenaline-stimulated NO release in either strain, an observation that does agree with those using functional probes, in which NO modulation is reduced after aldosterone treatment. Previous studies report increased NO bioavailability through the action aldosterone receptor antagonists (Farquharson and Struthers, 2000). An increase in superoxide anion release due to aldosterone treatment (Sanz-Rosa et al., 2005; Virdis et al., 2002), leading to an increased NO metabolism and consequently to a decrease in NO bioavailability has also been reported. We confirmed that aldosterone enhanced superoxide anion release in arteries from both WKY rats and SHR. This increase in superoxide anions can explain the altered NO participation in the noradrenaline-induced contraction observed in arteries from aldosterone treated rats. Thus, we analyzed the functional participation of these superoxide anions in the vasoconstrictor response to noradrenaline. In untreated rats preincubation with the permeable superoxide dismutase mimetic tempol only decreased the response to noradrenaline in SHR, but, when both strains were treated with aldosterone, the tempol preincubation reduced the noradrenaline response in the two strains, but the effect was greater in SHR. Taken together these results indicate that the reduced NO modulation of the contractile response to noradrenaline in aldosterone-treated rats involves a reduction of NO bioavailability caused by an increase in the NO metabolism brought about by a rise in superoxide anion release.

Vasoconstrictor response to adrenergic agonists is also largely mediated by COX-derived vasoconstrictor prostanoids (Tabernero et al., 1999; Xavier et al., 2003; Alvarez et al., 2005). Two COX isoforms have been described, constitutive COX-1, and inducible COX-2, and both of them release prostanoids from the endothelium in this vascular bed (McKee et al., 2003; Xavier et al., 2008). In untreated rats, the non-selective COX inhibitor indomethacin and the COX-2 inhibitor NS-398 reduced the vasoconstrictor response to noradrenaline only in arteries from SHR, as previously described in conductance arteries (Alvarez et al., 2005). Aldosterone increases vascular

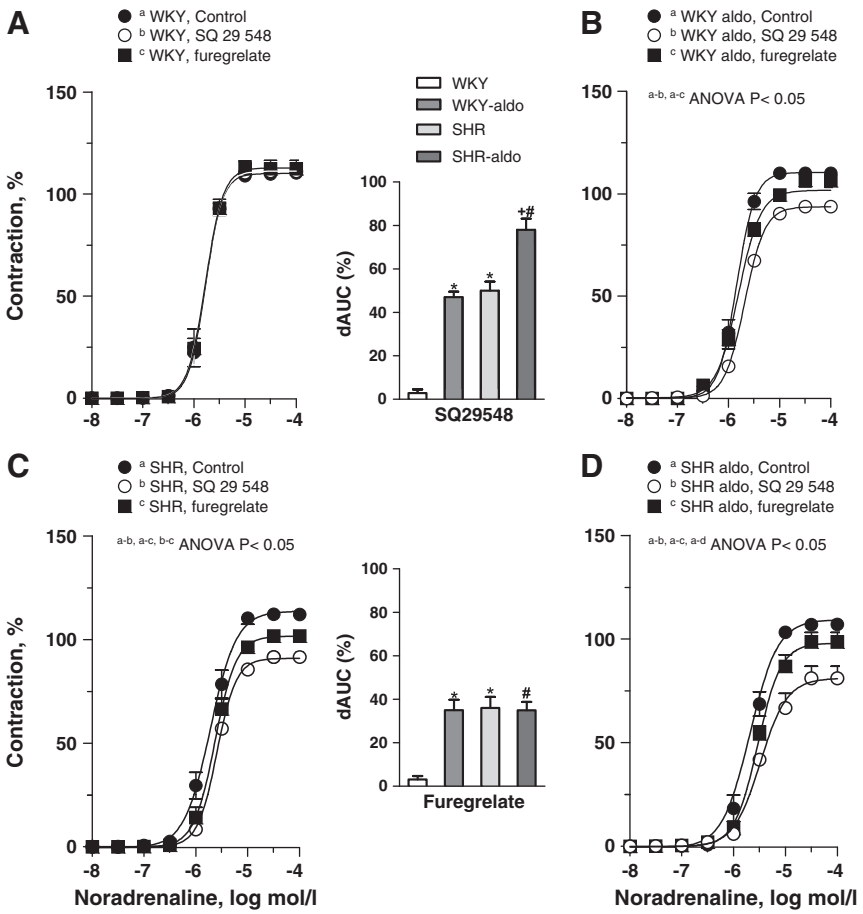

Fig. 4. Effect of furegrelate (10 μmol/l) and of SQ 29 548 (1 μmol/l) on the concentration dependent contraction to noradrenaline in mesenteric resistance segments from untreated and aldosterone-treated WKY rats and SHR. Results (mean ± S.E.M.) are expressed as a percentage of the initial contraction elicited by KCl. N = 7 animals each curve. Insert graph shows differences in area under the concentration–response curve (dAUC) to noradrenaline in the absence (control) or in the presence of either SQ 29 548 or furegrelate. dAUC values (means ± S.E.M.) are expressed as a percentage of the difference of the corresponding control AUC. ANOVA (one way): $^{*}P<0.05$ *vs.* WKY; $^{+}P<0.05$ *vs.* SHR; $^{\#}P<0.05$ *vs.* WKY-aldo.

COX-2 expression and COX-2-derived prostanoids in both WKY rats and SHR (Blanco-Rivero et al., 2005; Xavier et al., 2008). In rats from both strains treated with aldosterone both indomethacin and NS-398 produced a reduction in contractions elicited by noradrenaline. Additionally, the selective COX-1 inhibitor SC-560 did not modify the vasoconstrictor response to noradrenaline in either untreated or aldosterone-treated rats, ruling out the participation of COX-1 derivates in our experimental conditions. These results suggest that aldosterone treatment increases the participation of vasoconstrictor COX-2 derived prostanoids in noradrenaline responses in resistance arteries from both normotensive and hypertensive animals.

Vasoconstrictor prostanoids such as TxA_2 elicit their effect through activation of thromboxane (TP) receptors (Carvalho et al., 1997; Alvarez et al., 2005; Blanco-Rivero et al., 2005; Gluais et al., 2005; Xavier et al., 2008). Thus, we antagonized TP receptor by incubating arteries with SQ 29 548 and inhibited TxA_2 synthase with furegrelate. In untreated rats, SQ 29 548 or furegrelate only modified the noradrenaline response in segments from SHR, indicating the TxA_2 participation in the response to noradrenaline only in hypertension, as previously reported (Carvalho et al., 1997; Suzuki et al., 2000). Preincubation with SQ 29 548 or furegrelate decreased vasoconstrictor response to noradrenaline in both WKY rats and SHR treated with aldosterone. This suggests that the participation of TxA_2 in noradrenaline-induced contractions is increased by aldosterone in both WKY rats and SHR. This effect of aldosterone could be attributed to the increase in vasoconstrictor response induced by TP receptor stimulation (Xavier et al., 2008), but changes in TxA_2 release due to aldosterone treatment cannot be ruled out. In fact, in WKY rats, TxA_2 release was increased by aldosterone, but the release of this prostanoid remained unmodified by aldosterone treatment in SHR.

However, when comparing the effect of SQ 29 548 and furegrelate on the contractile response induced by noradrenaline in arteries from aldosterone-treated rats, it is possible to observe that the SQ 29 548-induced reduction in the noradrenaline response was greater than the furegrelate-induced reduction. This suggests the involvement of another vasoconstrictor prostanoid, in addition to TxA_2, and via the TP receptor, in the response to noradrenaline in arteries from aldosterone-treated animals. The fact that TxA_2 release was not modified by aldosterone treatment in hypertensive rats reinforces the hypothesis of the participation of contractile prostanoids other than TxA_2 in vasoconstriction to noradrenaline in resistance arteries from aldosterone-treated rats. In previous reports, we have demonstrated that prostacyclin has a dose-dependent vasoconstrictor role, mediated by TP and EP1 receptor activation (Blanco-Rivero et al., 2005; Xavier et al., 2008; Xavier et al., 2009). Additionally, we have also reported that the acetylcholine-induced release of prostacyclin was increased in conductance and resistance arteries from aldosterone-treated SHR rats and that this prostanoid is involved on the endothelial dysfunction induced by this mineralocorticoid hormone (Blanco-Rivero et al., 2005; Xavier et al., 2008). Thus, we analyzed possible changes in prostacyclin release in hypertensive rats after aldosterone treatment. In the present study noradrenaline-induced prostacyclin release was increased in arteries from both WKY rats and SHR treated with aldosterone. These results suggest that, in addition

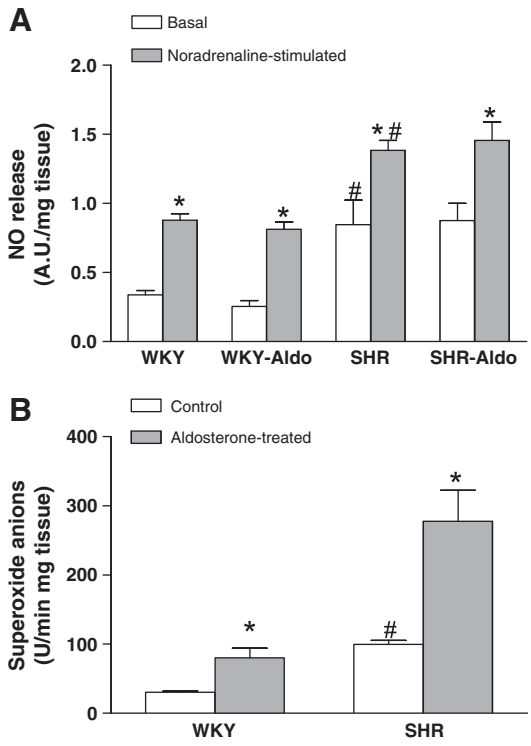

Fig. 5. (A) Effect of aldosterone treatment on basal and NA-induced NO release in mesenteric resistance segments from WKY rats and SHR. Results (mean ± S.E.M.) are expressed as arbitrarial fluorescence units (A.U.)/mg tissue. N = 6 animals each group. *P<0.05 *vs.* basal. #P<0.05 SHR/SHR-aldo *vs.* WKY/WKY-aldo. (B) Effect of aldosterone treatment on superoxide anion release in mesenteric resistance segments from WKY and SHR rats. Results (mean ± S.E.M.) are expressed as chemoluminiscence units (U)/min mg tissue. N = 6 animals each group.*P<0.05 aldosterone *vs.* control release. #P<0.05 SHR *vs.* WKY.

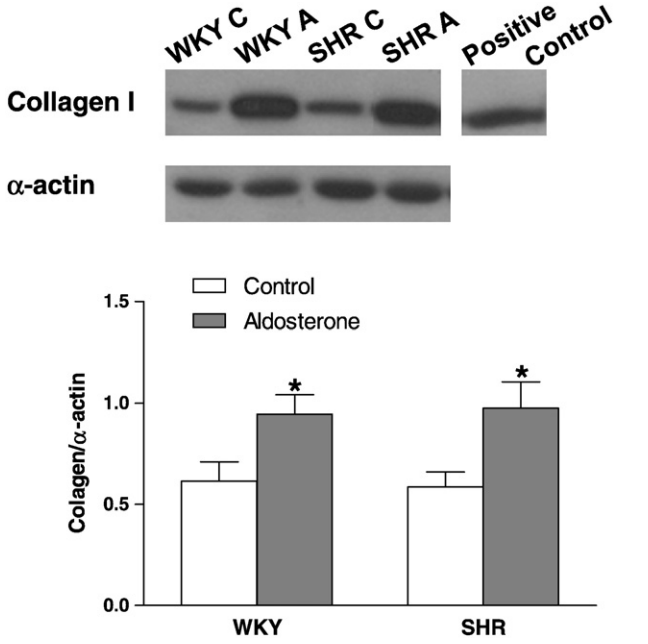

Fig. 7. Western blot for collagen I expression in mesenteric resistance artery segments from control and aldosterone-treated WKY rats and SHR. Figure is representative of preparations from four rats from each group. Lower panel shows densitometric analysis for collagen I expression.

to TxA_2, prostacyclin acting on the TP receptor could contribute to the vasoconstrictor response to noradrenaline in resistance vessels from rats treated with aldosterone.

In conclusion, results presented here in mesenteric resistance arteries suggest that chronic aldosterone treatment reduces the smooth muscle contraction to alpha-adrenergic stimuli; a new balance in the release of endothelium-derived prostanoids and NO is produced as a result in differences in normotensive and hypertensive rats, and these differences prevent changes in the noradrenaline concentration–response curves in arteries with endothelium.

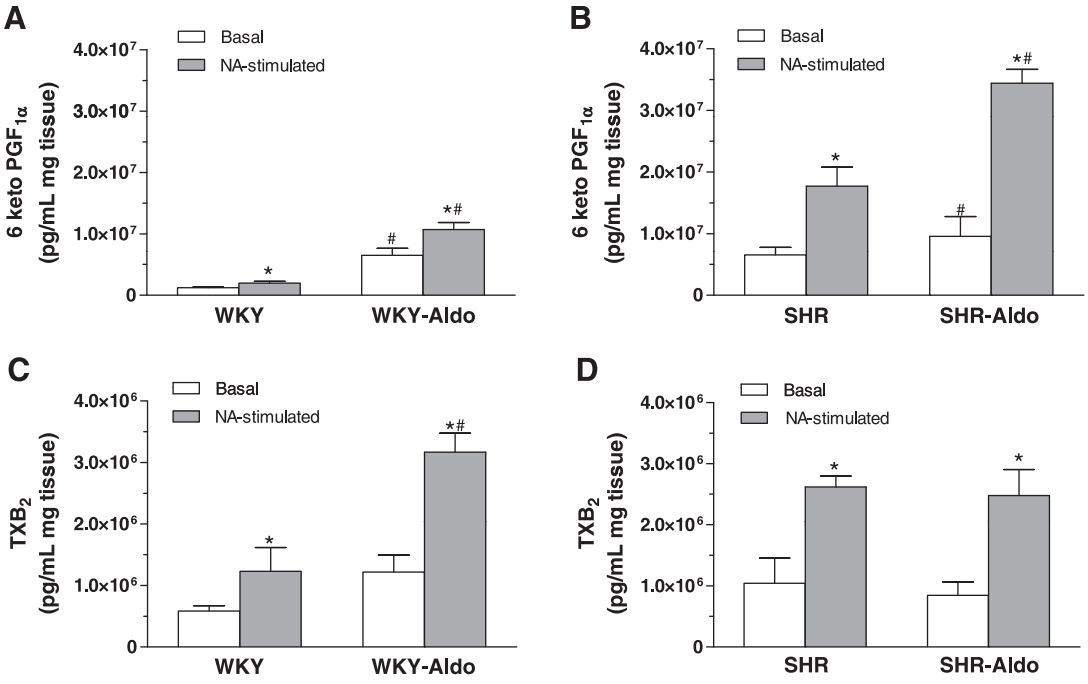

Fig. 6. Basal and noradrenaline-induced 6 keto $PGF_{1\alpha}$ (A, B) TXB_2 (C, D) release in mesenteric resistance artery segments from untreated and aldosterone-treated WKY rats and SHR. Results (mean ± S.E.M.) are expressed as pg prostanoid/mL mg tissue. N = 6 animals each group. *P<0.05 *vs.* basal. #P<0.05 aldosterone *vs.* control release.

Acknowledgements

This work was supported by grants from Ministerio de Ciencia e Innovación (DEP2006-56187-C04-04, SAF2009-10374, SAF2009-07201) and Instituto de Salud Carlos III (Red RECAVA, RD06/0014/0011).

References

Alvarez, Y., Briones, A.M., Balfagon, G., Alonso, M.J., Salaices, M., 2005. Hypertension increases the participation of vasoconstrictor prostanoids from cyclooxygenase-2 in phenylephrine responses. J. Hypertens. 23, 767–777.

Balfagón, G., Márquez-Rodas, I., Alvarez, Y., Alonso, M.J., Cachofeiro, V., Salaices, M., Lahera, V., 2004. Aldosterone modulates neural vasomotor response in hypertension: role of calcitonin gene-related peptide. Regul. Pept. 120 (1–3), 253–260.

Bauersachs, J., 2004. Aldosterone antagonism in heart failure: improvement of cardiac remodelling, endothelial dysfunction and platelet activation. Eur J Clin Invest 34, 649–652.

Blanco-Rivero, J., Cachofeiro, V., Lahera, V., Aras-Lopez, R., Marquez-Rodas, I., Salaices, M., Xavier, F.E., Ferrer, M., Balfagón, G., 2005. Participation of prostacyclin in endothelial dysfunction induced by aldosterone in normotensive and hypertensive rats. Hypertension 46, 107–112.

Cachofeiro, V., Miana, M., de Las Heras, N., Martín-Fernández, B., Ballesteros, S., Fernández-Tresguerres, J., Lahera, V., 2008. Aldosterone and the vascular system. J. Steroid Biochem. Mol. Biol. 109, 331–335.

Carvalho, M.H., Fortes, Z.B., Nigro, D., Oliveira, M.A., Scivoletto, R., 1997. The role of thromboxane A_2 in the altered microvascular reactivity in two-kidney, one-clip hypertension. Endothelium 5, 167–178.

Duprez, D., De Buyzere, M., Rietzschel, E.R., Clement, D.L., 2000. Aldosterone and vascular damage. Curr. Hypertens. Rep. 2, 327–334.

Farquharson, C.A., Struthers, A.D., 2000. Spironolactone increases nitric oxide bioactivity, improves endothelial vasodilator dysfunction, and suppresses vascular angiotensin I/angiotensin II conversion in patients with chronic heart failure. Circulation 101, 594–597.

Freel, E.M., Connell, J.M., 2004. Mechanisms of hypertension: the expanding role of aldosterone. J. Am. Soc. Nephrol. 15, 1993–2001.

Funder, J.W., 2004. Aldosterone, mineralocorticoid receptors and vascular inflammation. Mol. Cell. Endocrinol. 217, 263–269.

Giebisch, G., 1998. Renal potassium transport: mechanisms and regulation. Am. J. Physiol. 274, 817–833.

Giebisch, G., Wang, W., 2000. Renal tubule potassium channels: function, regulation and structure. Acta Physiol. Scand. 170, 153–173.

Gluais, P., Lonchampt, M., Morrow, J.D., Vanhoutte, P.M., Feletou, M., 2005. Acetylcholine-induced endothelium-dependent contractions in the SHR aorta: the Janus face of prostacyclin. Br. J. Pharmacol. 146, 834–845.

McKee, A.P., Van Riper, D.A., Davison, C.A., Singer, H.A., 2003. Gender-dependent modulation of alpha 1-adrenergic responses in rat mesenteric arteries. Am. J. Physiol. Heart Circ. Physiol. 284, 1737–1743.

Michea, L., Delpiano, A.M., Hitschfeld, C., Lobos, L., Lavandero, S., Marusic, E.T., 2005. Eplerenone blocks nongenomic effects of aldosterone on the Na^+/H^+ exchanger, intracellular Ca^{2+} levels, and vasoconstriction in mesenteric resistance vessels. Endocrinology 146, 973–980.

Miyagawa, K., Ohashi, M., Yamashita, S., Kojima, M., Sato, K., Ueda, R., Dohi, Y., 2007. Increased oxidative stress impairs endothelial modulation of contractions in arteries from spontaneously hypertensive rats. J. Hypertens. 25, 415–421.

Mulvany, M.J., Halpern, W., 1977. Contractile properties of small arterial resistance vessels in spontaneously hypertensive and normotensive rats. Circ. Res. 41, 19–26.

Nagata, D., Takahashi, M., Sawai, K., Tagami, T., Usui, T., Shimatsu, A., Hirata, Y., Naruse, M., 2006. Molecular mechanism of the inhibitory effect of aldosterone on endothelial NO synthase activity. Hypertension 48, 165–171.

Neves, M.F., Amiri, F., Virdis, A., Diep, Q.N., Schiffrin, E.L., 2005. Role of aldosterone in angiotensin II-induced cardiac and aortic inflammation, fibrosis, and hypertrophy. Can. J. Physiol. Pharmacol. 83, 999–1006.

Padilha, A.S., Peçanha, F.M., Vassallo, D.V., Alonso, M.J., Salaices, M., 2008. Ouabain treatment changes the role of endothelial factors in rat resistance arteries. Eur. J. Pharmacol. 600 (1–3), 110–116.

Palmer, L.G., 1999. Potassium secretion and the regulation of distal nephron K channels. Am. J. Physiol. 277, 821–825.

Palmer, L.G., Frindt, G., 2000. Aldosterone and potassium secretion by the cortical collecting duct. Kidney Int. 57, 1324–1328.

Pitt, B., Zannad, F., Remme, W.J., Cody, R., Castaigne, A., Perez, A., Palensky, J., Wittes, J., 1999. The effect of spironolactone on morbidity and mortality in patients with severe heart failure, Randomized Aldactone Evaluation Study Investigators. N. Engl. J. Med. 341, 709–717.

Purdy, R.E., Weber, M.A., 1983. Enhancement and prolongation of vascular smooth muscle contraction by aldosterone. Blood Vessels 20, 34–43.

Rocha, R., Funder, J.W., 2002. The pathophysiology of aldosterone in the cardiovascular system. Ann. NY Acad. Sci. 970, 89–100.

Sanz-Rosa, D., Cediel, E., de las Heras, N., Miana, M., Balfagon, G., Lahera, V., Cachofeiro, V., 2005. Participation of aldosterone in the vascular inflammatory response of spontaneously hypertensive rats: role of the NFkappaB/IkappaB system. J. Hypertens. 23, 1167–1172.

Schiffrin, E.L., 2006. Effects of aldosterone on the vasculature. Hypertension 47, 312–318.

Schmidt, B.M., Oehmer, S., Delles, C., Bratke, R., Schneider, M.P., Klingbeil, A., Fleischmann, E.H., Schmieder, R.E., 2003. Rapid nongenomic effects of aldosterone on human forearm vasculature. Hypertension 42, 156–160.

Stier, C.T., Chander, P.N., Rocha, R., 2002. Aldosterone as a mediator in cardiovascular injury. Cardiol. Rev. 10, 97–107.

Suzuki, H., Ikezaki, H., Hong, D., Rubinstein, I., 2000. PGH(2)-TxA(2)-receptor blockade restores vasoreactivity in a new rodent model of genetic hypertension. J. Appl. Physiol. 88, 1983–1988.

Tabernero, A., Giraldo, J., Vila, E., 1999. Modelling the changes due to the endothelium and hypertension in the a-adrenoreceptor-mediated responses of rat aorta. J. Auton. Pharmacol. 19, 219–228.

Virdis, A., Neves, M.F., Amiri, F., Viel, E., Touyz, R.M., Schiffrin, E.L., 2002. Spironolactone improves angiotensin-induced vascular changes and oxidative stress. Hypertension 40, 504–510.

Weber, M.A., Purdy, R.E., Drayer, J.I., 1983. Interactions of mineralocorticoids and pressor agents in vascular smooth muscle. Hypertension 5, 41–46.

Xavier, F.E., Davel, A.P., Rossoni, L.V., Vassallo, D.V., 2003. Time-dependent hyperreactivity to phenylephrine in aorta from untreated diabetic rats: role of prostanoids and calcium mobilization. Vascul Pharmacol 40, 67–76.

Xavier, F.E., Rossoni, L.V., Alonso, M.J., Balfagón, G., Vassallo, D.V., Salaices, M., 2004. Ouabain-induced hypertension alters the participation of endothelial factors in alpha-adrenergic responses differently in rat resistance and conductance mesenteric arteries. Br. J. Pharmacol. 143, 215–225.

Xavier, F.E., Aras-López, R., Arroyo-Villa, I., Campo, L.D., Salaices, M., Rossoni, L.V., Ferrer, M., Balfagón, G., 2008. Aldosterone induces endothelial dysfunction in resistance arteries from normotensive and hypertensive rats by increasing thromboxane A_2 and prostacyclin. Br. J. Pharmacol. 154, 1225–1235.

Xavier, F.E., Blanco-Rivero, J., Ferrer, M., Balfagón, G., 2009. Endothelium modulates vasoconstrictor response to prostaglandin I2 in rat mesenteric resistance arteries: interaction between EP1 and TP receptors. Br. J. Pharmacol. 158 (7), 1787–1795.

Article 2: Reciprocal Relationship Between Reactive Oxygen Species and Cyclooxygenase-2 and Vascular Dysfunction in Hypertension

Martínez-Revelles S*, **Avendaño MS*,** García-Redondo AB, Alvarez Y, Aguado A, Pérez-Girón JV, García-Redondo L, Esteban V, Redondo JM, Alonso MJ, Briones AM, Salaices M.

Antioxid Redox Signal. 18:51-65. 2013

ANTIOXIDANTS & REDOX SIGNALING
Volume 18, Number 1, 2013

DOI: 10.1089/ars.2011.4335

Discoveries

ORIGINAL RESEARCH COMMUNICATION

Reciprocal Relationship Between Reactive Oxygen Species and Cyclooxygenase-2 and Vascular Dysfunction in Hypertension

Sonia Martínez-Revelles,[1,*] María S. Avendaño,[1,*] Ana B. García-Redondo,[1] Yolanda Álvarez,[1] Andrea Aguado,[1] Jose V. Pérez-Girón,[1] Laura García-Redondo,[1] Vanesa Esteban,[2] Juan M. Redondo,[2] María J. Alonso,[3] Ana M. Briones,[1] and Mercedes Salaices[1]

Abstract

Aims: This study evaluates a possible relationship between reactive oxygen species (ROS) and cyclooxygenase (COX)-2-derived products in conductance and resistance arteries from hypertensive animals. Angiotensin II (Ang II)-infused mice or spontaneously hypertensive rats treated with the NAD(P)H Oxidase inhibitor apocynin, the mitochondrion-targeted SOD2 mimetic Mito-TEMPO, the superoxide dismutase analog tempol, or the COX-2 inhibitor Celecoxib were used. ***Results:*** Apocynin, Mito-TEMPO, and Celecoxib treatments prevented Ang II-induced hypertension, the increased vasoconstrictor responses to phenylephrine, and the reduced acetylcholine relaxation. The NOX-2 inhibitor gp91ds-tat, the NOX-1 inhibitor ML171, catalase, and the COX-2 inhibitor NS398 abolished the *ex vivo* effect of Ang II-enhancing phenylephrine responses. Antioxidant treatments diminished the increased vascular COX-2 expression, prostanoid production, and/or participation of COX-derived contractile prostanoids and thromboxane A_2 receptor (TP) in phenylephrine responses, observed in arteries from hypertensive models. The treatment with the COX-2 inhibitor normalized the increased ROS production ($O_2\cdot^-$ and H_2O_2), NAD(P)H Oxidase expression (NOX-1, NOX-4, and p22phox) and activity, MnSOD expression, and the participation of ROS in vascular responses in both hypertensive models. Apocynin and Mito-TEMPO also normalized these parameters of oxidative stress. Apocynin, Mito-TEMPO, and Celecoxib improved the diminished nitric oxide (NO) production and the modulation by NO of phenylephrine responses in the Ang II model. ***Innovation:*** This study provides mechanistic evidence of circuitous relationship between COX-2 products and ROS in hypertension. ***Conclusion:*** The excess of ROS from NAD(P)H Oxidase and/or mitochondria and the increased vascular COX-2/TP receptor axis act in concert to induce vascular dysfunction and hypertension. *Antioxid. Redox Signal.* 18, 51–65.

Introduction

ANGIOTENSIN II (ANG II)-DERIVED reactive oxygen species (ROS) participate, among other effects, in the impaired endothelium-dependent relaxation, in the alterations of contractile responses, and in the vascular remodeling observed in hypertension (7, 17, 26, 33). NAD(P)H Oxidase is one of the main sources of superoxide anion ($O_2\cdot^-$) at vascular level (8, 12). Both NAD(P)H Oxidase activity and NAD(P)H Oxidase subunit expression are increased in hypertension and by Ang II exposure (6, 12, 29), although other systems such as xanthine oxidase also play a role (8). In vascular cells, the NAD(P)H oxidase possesses cytosolic subunits (p47phox, p67phox, or homologs) and membrane-bound subunits (NOX-1/NOX-2/NOX-4/NOX-5 and p22phox), which form a functional enzyme complex upon activation (8, 12, 29). However, conflicting results on the role of each specific NOX isoform in the vascular alterations or in hypertension development are found (8, 12, 29). In addition, during the last few years, mitochondria are recognized as another potential source of ROS in hypertension. The $O_2\cdot^-$ derived from Ang II-activated NAD(P)H Oxidase induces mitochondrial ROS

[1]Department of Pharmacology, School of Medicine, Universidad Autónoma de Madrid, Institute for Health Research of La Paz University Hospital (IdiPAZ), Madrid, Spain.
[2]Department of Vascular Biology and Inflammation, Centro Nacional de Investigaciones Cardiovasculares, Madrid, Spain.
[3]Department of Biochemistry, Physiology and Molecular Genetics, Universidad Rey Juan Carlos, Alcorcón, Spain.
*These two authors contributed equally.

Innovation

It has been accepted that reactive oxygen species (ROS) and cyclooxygenase (COX)-derived prostanoids are important mediators of vascular alterations in hypertension. Our findings demonstrate that a specific feed-forward relationship between ROS and COX-2/TP receptors serves as a pathological link between Angiotensin II, vascular dysfunction, and hypertension. We suggest that by modulating ROS and COX pathways, antioxidants targeting NAD(P)H Oxidase and/or mitochondria or TP receptor antagonists could be promising therapeutic options with potential beneficial effects to reverse the alterations in vascular function associated to hypertension.

production, which further activates NAD(P)H Oxidase, increases cellular $O_2\cdot^-$ production, and modulates vascular responses, thus supporting an important relationship between these two sources of ROS in the vasculature (10, 11).

In addition to ROS, vasoconstrictor prostanoids from the constitutive (cyclooxygenase [COX]-1) or inducible (COX-2) COX are mediators responsible of the endothelial dysfunction in hypertension (13). We and others have previously described increased COX-2 expression and participation of COX-2-derived prostanoids on vasoconstrictor- and endothelium-dependent vasodilator responses of vessels from different models of hypertension and from hypertensive patients (1, 2, 16, 20, 28, 32, 34–36, 38). The increased COX-2 expression and activity found in hypertension were normalized by treatment with an Ang II type 1 receptor antagonist (4), suggesting the participation of Ang II in these effects. In support of this, *in vitro* studies demonstrate that Ang II induces COX-2 expression and prostanoid production in different vascular cell types (4, 5, 15, 24, 36). *In vivo*, Ang II infusion induces vascular COX-1 upregulation (21, 30), and either COX-2 downregulation (30) or upregulation (9, 21, 36) in different vessels has been described.

There seems to be a close, yet not totally understood, interaction or feed-forward mechanisms between ROS and COX-derived products. ROS can activate COX expression and/or activity (14, 17, 22), and antioxidant treatments abolish the role of COX on endothelium-dependent contractile responses (37). Additionally, COX activity is also involved in the generation of ROS in vessels from spontaneously hypertensive rats (SHRs) (18, 27). After Ang II stimulation, both positive and negative unidirectional relationships between ROS and COX-2/COX-1 expression or activity have been found (4, 5, 30, 36). In addition, a mutual relationship between ROS and COX activities has been found in liver cells (25). However, studies addressing this relationship at vascular level and the role of mitochondrial oxidative stress are lacking. The aim of the present study was to evaluate the contribution of ROS derived from NAD(P)H Oxidase and mitochondria on the participation of COX-derived products on vasoconstrictor responses in conductance and resistance arteries from the Ang II-induced hypertensive model. We also evaluated whether COX-2-derived products can modulate ROS production and their effects on vascular function. Our findings demonstrate that there is a circuitous relationship between COX-2 and ROS products in hypertension, which in turn participates in the alterations in vascular function associated to this pathology.

Results

ROS and COX-2 blockade decreases blood pressure and cardiac and vascular hypertrophy in Ang II-infused mice

Systemic infusion of Ang II increased systolic blood pressure (SBP), induced left ventricular hypertrophy, reduced aortic lumen diameter, and increased aortic media thickness (Fig. 1A and Supplementary Fig. S1; Supplementary Data are available online at www.liebertpub.com/ars). The NAD(P)H Oxidase inhibitor apocynin, the mitochondrion-targeted SOD2 mimetic Mito-TEMPO, and the COX-2 inhibitor Celecoxib treatments attenuated the increase in SBP induced by Ang II (Fig. 1A) and improved the reduced lumen diameter (Supplementary Fig. S1B). In addition, both Mito-TEMPO and Celecoxib decreased cardiac hypertrophy and normalized the aortic media thickness (Supplementary Fig. S1A, C). Combined treatment with Celecoxib and Mito-TEMPO reduced, but not normalized, the increased SBP (Fig. 1A) and normalized cardiac hypertrophy induced by Ang II (Supplementary Fig. S1A). Apocynin or Celecoxib treatments did not modify SBP in control mice (control: 98.6 ± 1.1 mm Hg; apocynin: 101.1 ± 1.8 mm Hg; Celecoxib: 99 ± 2.8 mm Hg, $n = 4–7$). These results indicate that ROS and COX-2 inhibitors exert protective effects, preventing development of hypertension and vascular and cardiac hypertrophy.

In a previous study, Dikalova *et al.* (11) demonstrated that Mito-TEMPO decreased established hypertension induced by Ang II. We therefore evaluated the effects of apocynin and Celecoxib when administered 7 days after Ang II infusion; at this time, mice are hypertensive (Supplementary Fig. S2A). Both Celecoxib and apocynin decreased SBP, but not left ventricular hypertrophy (Supplementary Fig. S2A, B). In addition, in a model of established hypertension, Celecoxib, but not the superoxide dismutase (SOD) mimetic tempol or Mito-TEMPO, treatment reduced SBP in SHRs (control: 219.9 ± 7.6 mm Hg; Celecoxib: 184.8 ± 5.5 mm Hg, $p < 0.01$; tempol: 209.7 ± 2.7 mm Hg; Mito-TEMPO: 212.9 ± 5.4 mm Hg, $n = 4–10$). However, neither Celecoxib nor tempol did affect SBP in Wistar Kyoto (WKY) (control: 151.9 ± 3.2 mm Hg; Celecoxib: 148.7 ± 3 mm Hg; tempol: 146.9 ± 2 mm Hg, $n = 4–7$).

ROS and COX-2 blockade improves vasoconstrictor- and endothelium-dependent vasodilator responses

Phenylephrine-induced contractile responses were greater in aortic segments from Ang II-infused than control mice. This increase was abolished by apocynin, Mito-TEMPO, or Celecoxib treatments (Fig. 1B). In control mice, these treatments did not have any effect on phenylephrine responses (data not shown). In *ex vivo* experiments, Ang II (1-μM 1-h incubation) also potentiated phenylephrine responses; this potentiation was reduced by co-incubation with the COX-2 inhibitor NS398 (1 μM), apocynin (0.3 mM), the NOX-2 inhibitor gp91ds-tat (5 μM), the NOX-1 inhibitor ML171 (0.5 μM), or the H_2O_2 detoxificant enzyme catalase (1000 U/ml) (Fig. 1E, F).

The endothelium-dependent vasodilator responses induced by acetylcholine (ACh) were smaller in arteries from Ang II-infused than control mice. Treatments with apocynin, Mito-TEMPO, or Celecoxib improved the impaired ACh relaxation in Ang II-infused (Fig. 1C) mice, but did not have any effect in control mice (data not shown). However, endothelium-

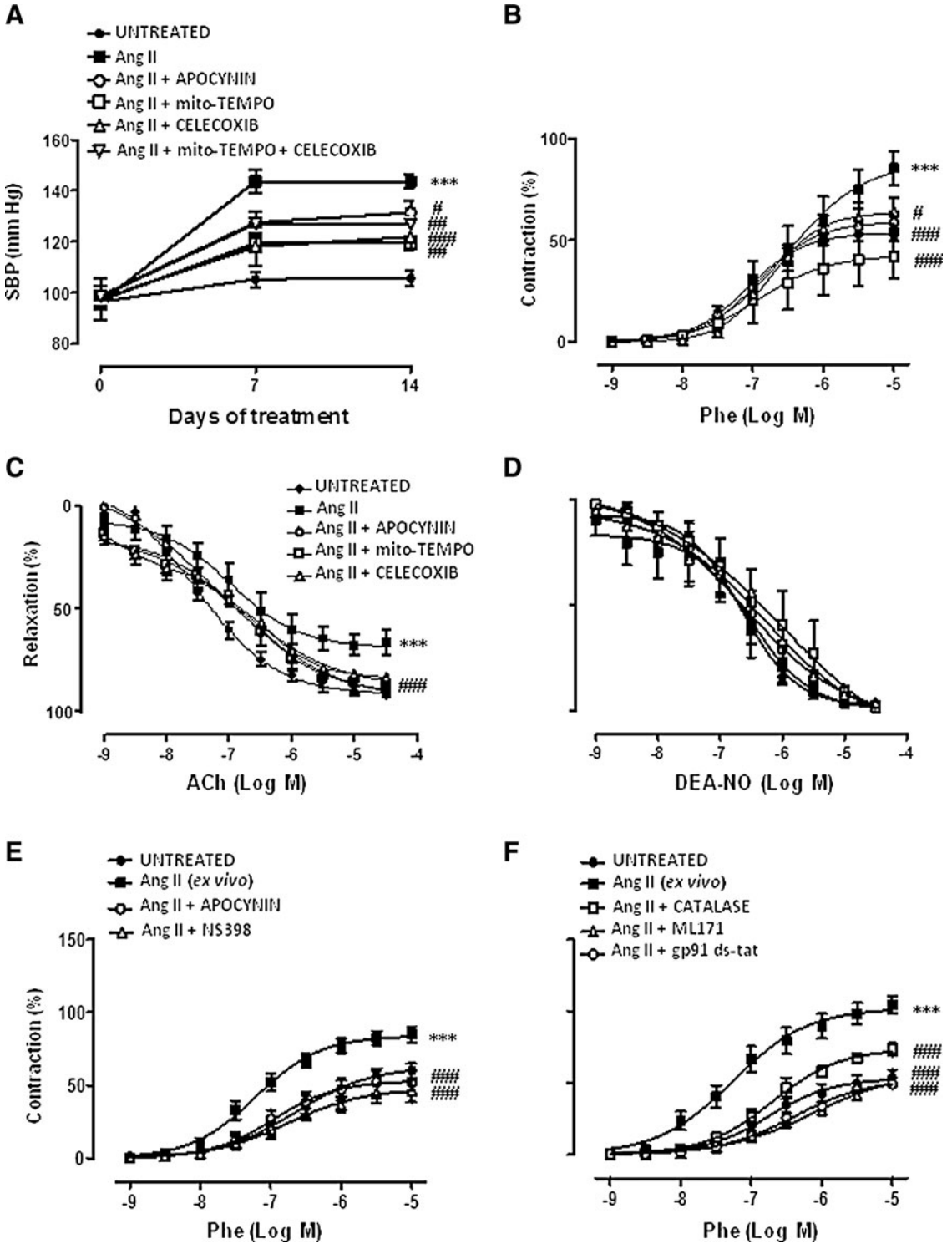

FIG. 1. Antioxidants and COX-2 blockade decrease blood pressure and improve vasoconstrictor and vasodilator responses in Ang II-infused mice. (A) Effect of apocynin, Mito-TEMPO, Celecoxib, and Mito-TEMPO plus Celecoxib treatments on systolic blood pressure (SBP) in Angiotensin II (Ang II)-infused mice. Untreated mice were used as controls. **(B, C, D)** Concentration–response curves to phenylephrine (Phe), acetylcholine (ACh), and diethylamine NONOate (DEA-NO) in aortic segments from mice untreated and treated with Ang II in the absence and the presence of apocynin, Mito-TEMPO, and Celecoxib. **(E, F)** Concentration–response curves to Phe in aortic segments incubated *ex vivo* with Ang II (1 μM, 1 h) alone or in combination with apocynin, NS398, catalase, ML171, or gp91ds-tat. Data represent mean ± SEM. $n = 5$–15. $^{***}p < 0.001$ *versus* untreated; $^{\#}p < 0.05$, $^{\#\#}p < 0.01$, and $^{\#\#\#}p < 0.001$ *versus* Ang II. SEM, standard error of the mean.

independent relaxation to diethylamine NONOate (DEA-NO) was not modified by Ang-II infusion or by apocynin, Mito-TEMPO, or Celecoxib treatments (Fig. 1D). Celecoxib or apocynin had no effects in phenylephrine responses or in ACh relaxation when administered 7 days after Ang II infusion (Supplementary Fig. S2C, D), suggesting that these treatments prevent, but not reverse, these vascular alterations induced by Ang II.

We have previously described that SHR aorta showed increased contractile responses to phenylephrine and impaired ACh-induced relaxation compared to normotensive WKY rats (2, 3). Neither tempol nor Celecoxib treatment affected phenylephrine responses in SHRs (Supplementary Fig. S3B, D). However, Celecoxib, but not tempol, increased ACh relaxation in SHRs (Supplementary Fig. S3A, C), suggesting that COX-2 is involved in endothelial dysfunction in SHRs, as described (32). In WKY rats, Celecoxib or tempol treatments did not modify phenylephrine or ACh responses (data not shown).

ROS and COX-2 blockade improves the participation of nitric oxide on phenylephrine responses

To evaluate whether ROS and COX-2-derived prostanoids might affect the nitric oxide (NO) pathway, we evaluated the effect of the different treatments on the modulation by NO of vasoconstrictor responses, the vascular NO release, and endothelial nitric oxide synthase (eNOS) expression. The NOS inhibitor *N*-nitro-L-arginine methyl ester (L-NAME, 100 μM) enhanced phenylephrine-induced contraction more in aorta from Ang II-infused mice than control (Fig. 2A). Apocynin, Mito-TEMPO, and Celecoxib treatments increased the effect of L-

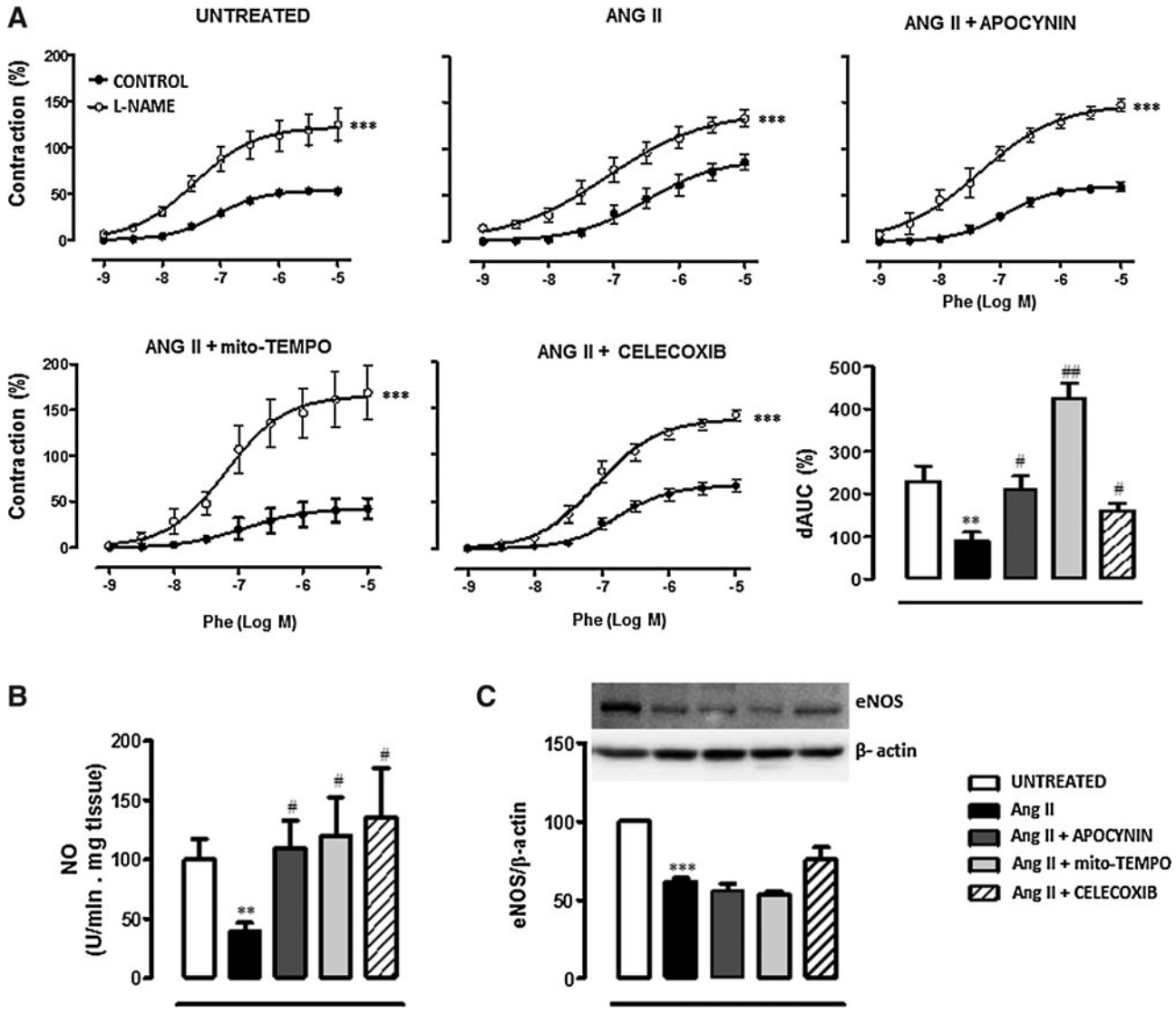

FIG. 2. Antioxidants and COX-2 blockade increase NO production and its participation on vasoconstrictor responses in Ang II-infused mice. (A) Effect of *N*-nitro-L-arginine methyl ester (L-NAME) on the concentration–response curve to phenylephrine (Phe) in aortic segments from mice untreated and treated with Ang II in the absence and the presence of apocynin, Mito-TEMPO, and Celecoxib. Differences of the area under the concentration–response curve (dAUC) to Phe in the presence and the absence of L-NAME are also shown. **(B)** Quantification of nitric oxide (NO) release and **(C)** densitometric analysis and representative blot of endothelial nitric oxide synthase (eNOS) protein expression in aortic segments from mice untreated and treated with Ang II in the absence and the presence of apocynin, Mito-TEMPO, and Celecoxib. Data represent mean ± SEM. $n = 5$–15. $^{**}p < 0.01$ and $^{***}p < 0.001$ *versus* control or *versus* untreated; $^{\#}p < 0.05$ and $^{\#\#}p < 0.01$ *versus* Ang II.

NAME in the vessel from Ang II-infused mice (Fig. 2A). These results suggest decreased NO production and/or bioavailability after Ang II infusion that is restored by antioxidants and COX-2 inhibitors. In agreement, NO release was reduced in aorta from Ang II-infused mice, and apocynin, Mito-TEMPO, and Celecoxib treatments normalized NO levels (Fig. 2B). Ang II also decreased eNOS protein expression in aorta. However, this decrease was not modified by any treatment (Fig. 2C).

COX-2 blockade reduces the increased oxidative stress and its participation on phenylephrine responses

We next evaluated the effects of Ang II infusion in different parameters of vascular oxidative stress, and whether COX-2 blockade might modulate these effects. Figure 3A shows that basal $O_2\cdot^-$ production was greater in the aortic wall from Ang II-infused than control mice. This was particularly evident in adventitia and media layers. In addition, aortic NAD(P)H Oxidase activity and *p22phox*, but not *p47phox*, gene expression were increased in Ang II-infused compared to control mice (Fig. 3B–D). The increased $O_2\cdot^-$ production, NAD(P)H Oxidase activity, and *p22phox* gene expression were normalized by apocynin, Mito-TEMPO, and Celecoxib treatments (Fig. 3A–D). Aortic and plasma malondialdehyde (MDA) levels, a marker of lipid peroxidation, were also greater in Ang II-infused than in control mice (Fig. 3E and Supplementary Fig. S4A). All treatments decreased aortic MDA levels (Fig. 3E). However, the increase in plasma MDA was prevented by apocynin and Celecoxib, but not by Mito-TEMPO treatment (Supplementary Fig. S4A), suggesting a greater role of mitochondria in vascular than plasma oxidative stress.

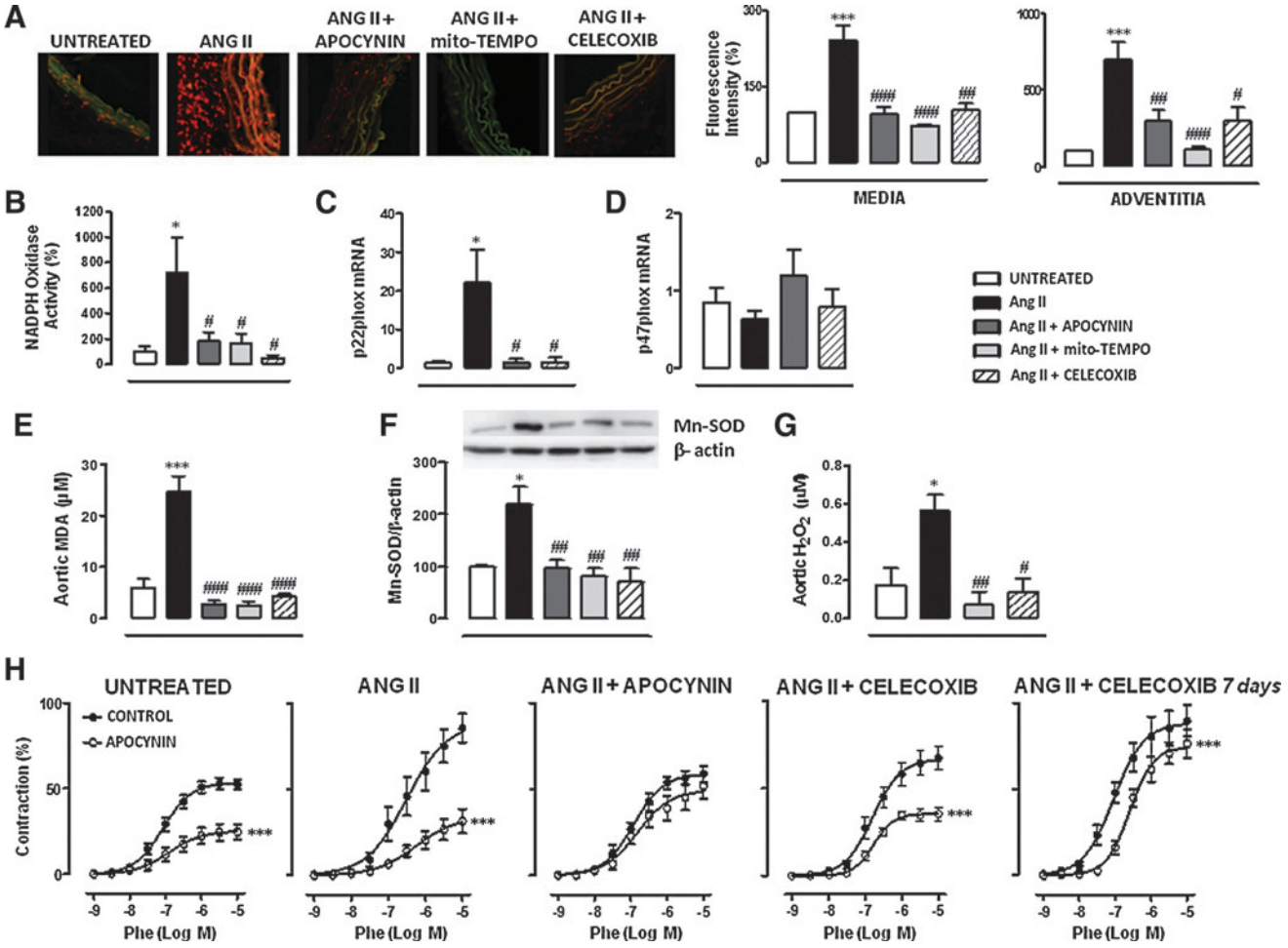

FIG. 3. COX-2 blockade reduces the increased oxidative stress and its participation on vasoconstrictor responses in Ang II-infused mice. (A) Representative fluorescent confocal photomicrographs of vascular superoxide anion ($O_2\cdot^-$) production in aortic segments of mice untreated and treated with Ang II in the absence and the presence of apocynin, Mito-TEMPO, and Celecoxib (to see this illustration in color the reader is referred to the web version of this article at www.liebertpub.com/ars). Image size 238×238 μm. Vascular $O_2\cdot^-$ quantification in the media and in the adventitial layers is also shown. **(B)** Basal NAD(P)H oxidase activity, **(C)** p22phox and **(D)** p47phox mRNA levels, **(E)** aortic malondialdehyde (MDA) levels, **(F)** densitometric analysis, and representative blot of MnSOD protein expression and **(G)** H_2O_2 production in aortic segments from mice untreated and treated with Ang II in the absence and the presence of apocynin, Mito-TEMPO, and Celecoxib. **(H)** Effect of *in vitro* apocynin on the concentration–response curve to phenylephrine (Phe) in aortic segments from untreated mice and mice treated with Ang II, Ang II plus apocynin, Ang II plus Celecoxib, and Ang II plus Celecoxib (administered 7 days after Ang II infusion). Data represent mean ± SEM. $n = 5$–10. $^*p < 0.05$ and $^{***}p < 0.001$ *versus* control or *versus* untreated; $^{\#}p < 0.05$, $^{\#\#}p < 0.01$, and $^{\#\#\#}p < 0.001$ *versus* Ang II. (To see this illustration in color, the reader is referred to the web version of this article at www.liebertpub.com/ars.)

We then evaluated whether alterations in antioxidant mechanisms might be also involved in the Ang II-induced $O_2\cdot^-$ production. Ang II increased MnSOD, but not Cu/Zn- and EC-SOD protein expression, and this was normalized by apocynin, Mito-TEMPO, and Celecoxib treatments (Fig. 3F and Supplementary Fig. S4B, C). Since MnSOD expression is increased by Ang II treatment, we questioned whether the product of SOD activity, H_2O_2, was also modified in our experimental paradigm. As shown in Figure 3G, Ang II increased aortic H_2O_2 production that was normalized by Mito-TEMPO and Celecoxib treatments.

The participation of ROS in vascular contractile responses was evaluated *in vitro* by preincubation of vessels with apocynin (0.3 m*M*). As shown in Figure 3H, apocynin inhibited the phenylephrine-induced contraction more in aorta from Ang II-infused than control mice. As expected, *in vivo* apocynin treatment abolished the *in vitro* effect of this drug on phenylephrine-induced contraction. In addition, Celecoxib treatment decreased the inhibitory effect of apocynin in Ang II-treated mice (Fig. 3H). When Celecoxib was administered 7 days after Ang II infusion, a decrease in the *in vitro* effect of apocynin was also observed (Fig. 3H), suggesting that COX-2 blockade not only prevents but also reverses the increased participation of ROS in vascular responses.

We previously described a greater inhibitory effect of *in vitro* apocynin and SOD on phenylephrine responses in aorta from SHRs than WKY rats (3). SHR treatment with Celecoxib abolished the inhibitory effects of apocynin and SOD (150 U/mL) on phenylephrine responses (Fig. 4A). In addition, Celecoxib treatment normalized the increased

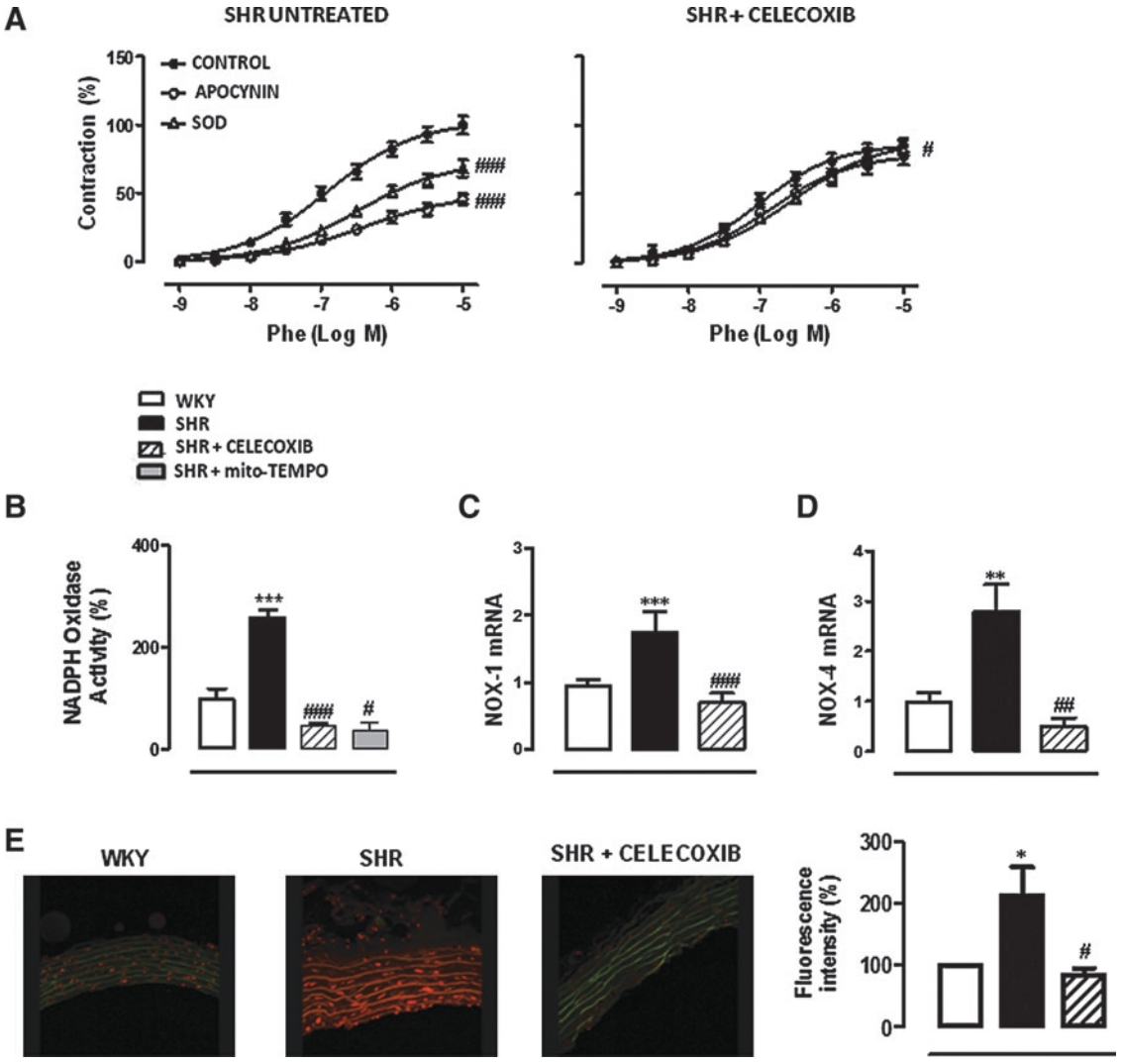

FIG. 4. COX-2 blockade reduces the increased oxidative stress and its participation on vasoconstrictor responses in SHR. **(A)** Effect of apocynin and superoxide dismutase (SOD) on the concentration–response curve to phenylephrine (Phe) in aortic segments from spontaneously hypertensive rats (SHRs) untreated or treated with Celecoxib. **(B)** Basal NAD(P)H Oxidase activity, **(C)** NOX-1, and **(D)** NOX-4 mRNA levels in aortic homogenates from Wistar Kyoto (WKY) rats, SHRs, and SHRs treated with Celecoxib or Mito-TEMPO. **(E)** Representative fluorescent confocal photomicrographs of vascular superoxide anion ($O_2\cdot^-$) production in aortic segments from WKY rats, SHRs, and SHRs treated with Celecoxib (to see this illustration in color the reader is referred to the web version of this article at www.liebertpub.com/ars). Image size 375 × 375 μm. Vascular $O_2\cdot^-$ quantification in the media is also shown. Data represent mean ± SEM. $n = 7$–9. $^*p < 0.05$, $^{**}p < 0.01$, $^{***}p < 0.001$ *versus* WKY rats; $^{\#}p < 0.05$, $^{\#\#}p < 0.01$, and $^{\#\#\#}p < 0.001$ *versus* SHR or *versus* control. (To see this illustration in color, the reader is referred to the web version of this article at www.liebertpub.com/ars.)

NAD(P)H Oxidase activity (Fig. 4B), *NOX-1* and *NOX-4* gene expression (Fig. 4C, D) and $O_2 \cdot^-$ production (Fig. 4E), observed in aorta from SHRs. The increase in NAD(P)H Oxidase activity was also diminished by Mito-TEMPO treatment (Fig. 4B).

ROS blockade decreases COX-2 expression and the participation of prostanoids on phenylephrine responses

We then evaluated the effects of Ang II infusion in COX-2 and COX-1 expression and/or activity (evaluated as vascular function) and whether oxidative stress might be modulating COX expression and/or the participation of COX products in vascular responses. Ang II significantly increased aortic COX-2, but not COX-1, expression that was reversed by apocynin, Mito-TEMPO, and Celecoxib treatments (Figs. 5A, B and 6A). The participation of COX-2-derived prostanoids in phenylephrine responses was evaluated by the incubation of vessels with NS398 (1 μM). This drug inhibited phenylephrine responses in aorta from Ang II-infused, but not in control, mice (Fig. 5C). As expected, Celecoxib treatment abolished the inhibitory effect of NS398. In addition, apocynin and Mito-TEMPO treatments inhibited the effect of NS398 in Ang II-infused mice (Fig. 5C), suggesting that ROS modulate the COX-2 pathway. When apocynin was administered 7 days after Ang II infusion, a decrease in the *in vitro* effect of NS398 was also observed (Fig. 5C), suggesting that ROS blockade not only prevents but also reverses the participation of COX-2-derived prostanoids in vascular responses.

The participation of COX-1-derived prostanoids in phenylephrine responses was evaluated by the incubation with the COX-1 inhibitor SC560 (1 μM). SC560 slightly inhibited the phenylephrine response in control mice. This effect was more pronounced in Ang II-infused mice and was reduced by apocynin, but unaffected by Celecoxib, treatment (Fig. 6B). These results suggest that Ang II also induces COX-1 activity, which is modulated by oxidative stress.

The participation of thromboxane A_2 receptor (TP) and EP_1 receptors on phenylephrine responses was analyzed using the

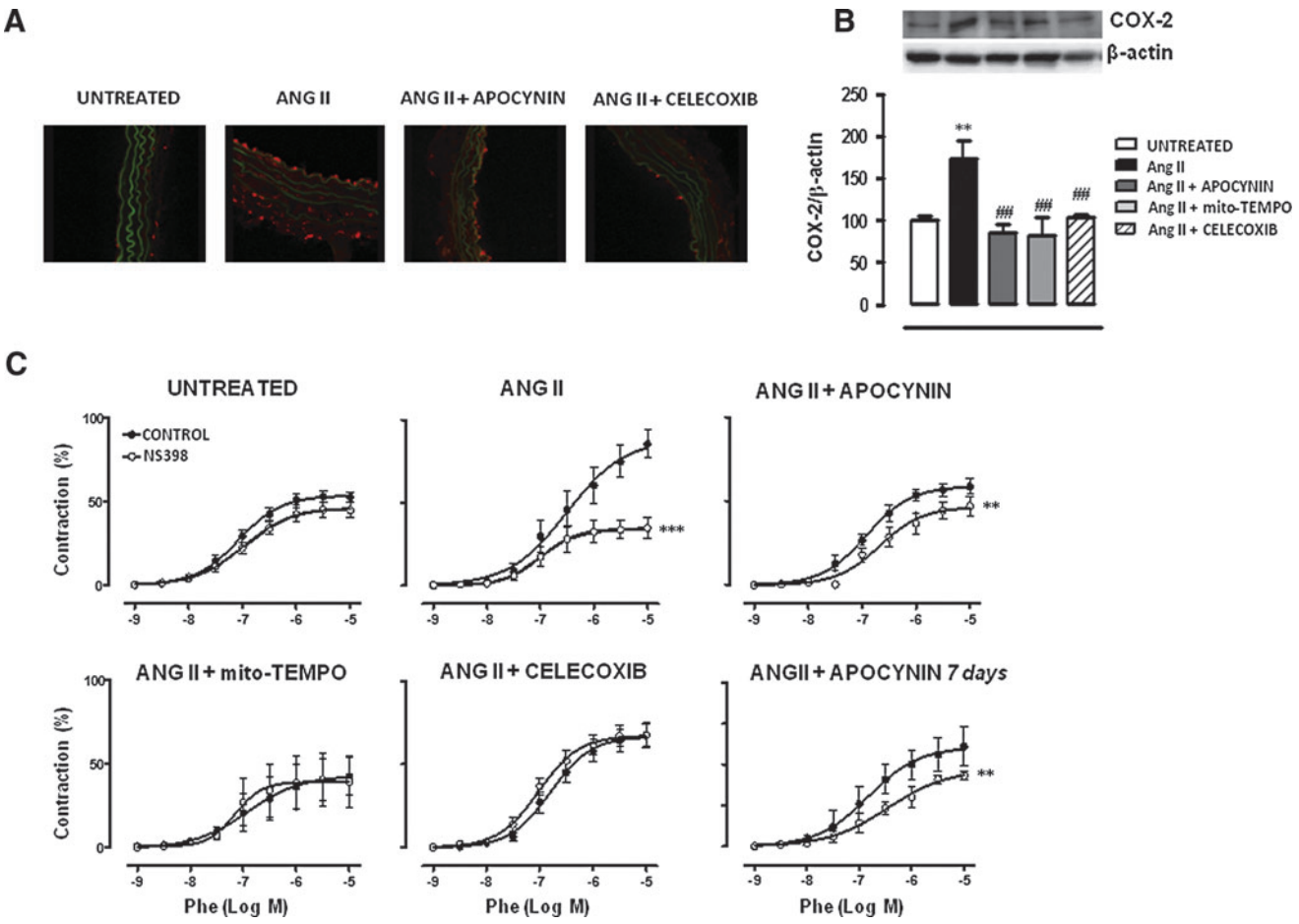

FIG. 5. Antioxidants reduce the increased COX-2 expression and the participation of COX-2-derived prostanoids on vasoconstrictor responses in Ang II-infused mice. (A) Representative fluorescent confocal photomicrographs of cyclooxygenase (COX)-2 immunolocalization in aortic segments of mice untreated and treated with Ang II in the absence and the presence of apocynin and Celecoxib. Image size 238×238 μm (to see this illustration in color the reader is referred to the web version of this article at www.liebertpub.com/ars). **(B)** Densitometric analysis and representative blot of COX-2 protein expression and **(C)** effect of *in vitro* NS398 on the concentration–response curve to phenylephrine (Phe) in aortic segments from mice untreated and treated with Ang II in the absence and the presence of apocynin, Celecoxib, Mito-TEMPO, or apocynin (administered 7 days after Ang II infusion). Data represent mean ± SEM. $n = 5$–10. $^{**}p < 0.01$ and $^{***}p < 0.001$ *versus* control or *versus* untreated; $^{\#\#}p < 0.01$ *versus* Ang II. (To see this illustration in color, the reader is referred to the web version of this article at www.liebertpub.com/ars.)

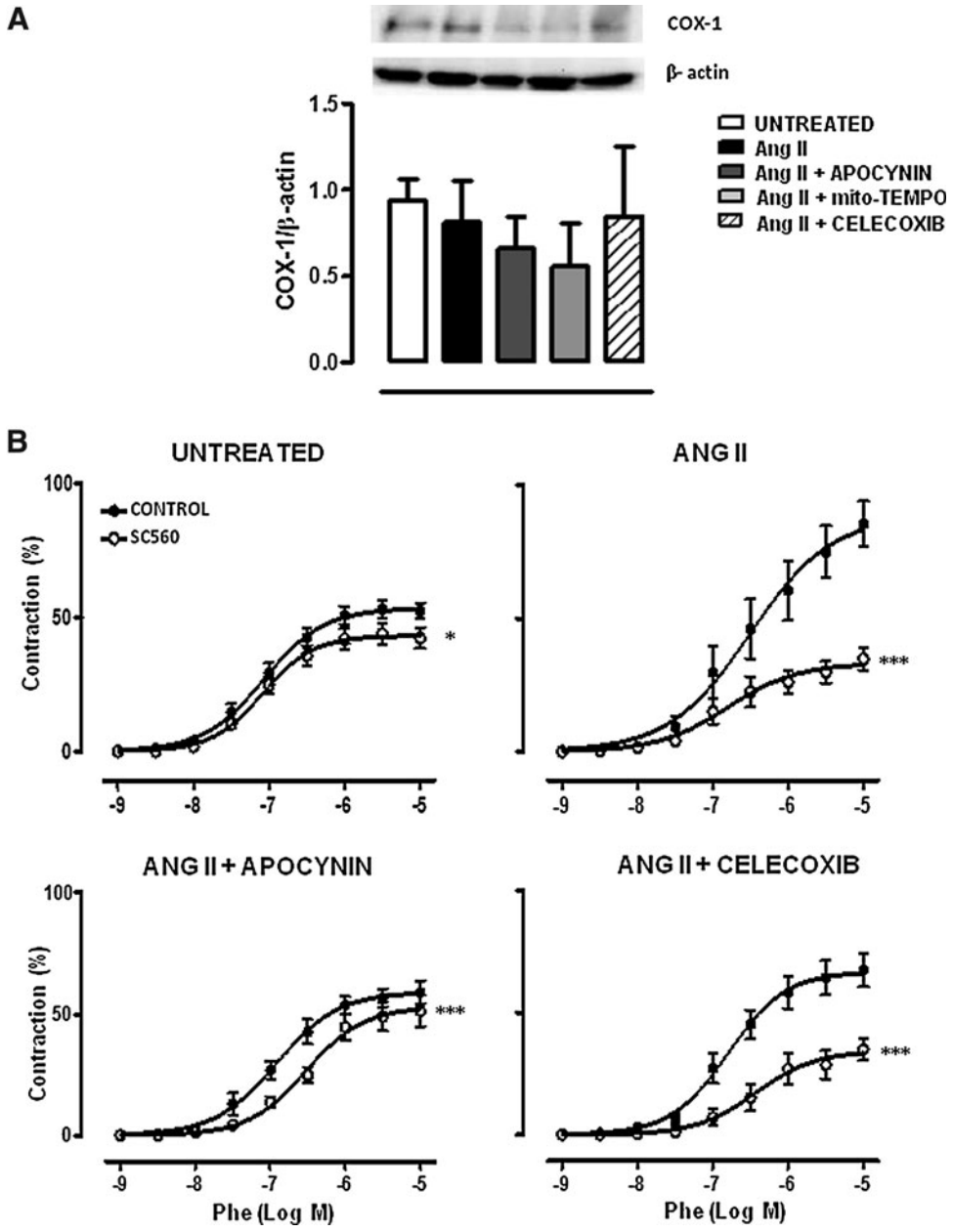

FIG. 6. Antioxidants reduce the increased participation of COX-1-derived prostanoids on vasoconstrictor responses in Ang II-infused mice. (A) Densitometric analysis and representative blot of COX-1 protein expression in aortic segments from mice untreated and treated with Ang II in the absence and the presence of apocynin, Mito-TEMPO, and Celecoxib. **(B)** Effect of SC560 on the concentration–response curve to phenylephrine (Phe) in aortic segments from mice untreated and treated with Ang II in the absence and the presence of apocynin and Celecoxib. Data represent mean ± SEM. $n = 5$–15. $^{*}p < 0.05$ and $^{***}p < 0.001$ *versus* control.

respective selective antagonists of these receptors SQ29548 and SC19220. Neither SQ29548 (1 μM) nor SC19220 (1 μM) did modify phenylephrine responses in aorta from control mice. However, in Ang II-infused mice, both drugs inhibited phenylephrine responses (Fig. 7). This inhibitory effect of SQ29548 was decreased by apocynin and Celecoxib treatments. However, only Celecoxib reduced the inhibitory effect of SC19220 (Fig. 7).

Previously we found that COX-2 expression, 13,14-dihydro-15-keto-$PGF_{2\alpha}$ levels, and the inhibitory effect of NS398 and SQ29548 on phenylephrine responses were greater in aorta from SHRs than WKY rats (2). Now, we confirmed some of these data, and we observed that COX-1 gene and protein expression were also increased (Fig. 8). SHR treatment with tempol decreased the inhibitory effect of NS398 and SQ29548 on phenylephrine responses (Fig. 8A) and normalized the increased 13,14-dihydro-15-keto-$PGF_{2\alpha}$ levels (Fig. 8D). However, tempol treatment did not modify COX-2 protein expression or mRNA levels (Fig. 8B, C). In WKY rats, tempol did not affect COX-2 protein, 13,14-dihydro-15-keto-$PGF_{2\alpha}$ levels (Fig. 8A, D), or mRNA (data not shown). Interestingly, Mito-TEMPO treatment of SHRs diminished the increased COX-2 and COX-1 gene and protein expression (Fig. 8E–H), suggesting that mitochondrial-specific antioxidants might be more effective than general antioxidants in modulating COX expression in the SHR model.

Effect of mitochondrial ROS and COX-2 blockade in resistance arteries from Ang II-infused mice

To further evaluate whether the observed effects in aorta are vascular bed specific and taking into account the importance of resistance arteries in control and maintenance of blood pressure, we performed an additional set of experiments in resistance arteries. We aimed to evaluate the role of ROS, particularly mitochondrial ROS, and COX-2-derived

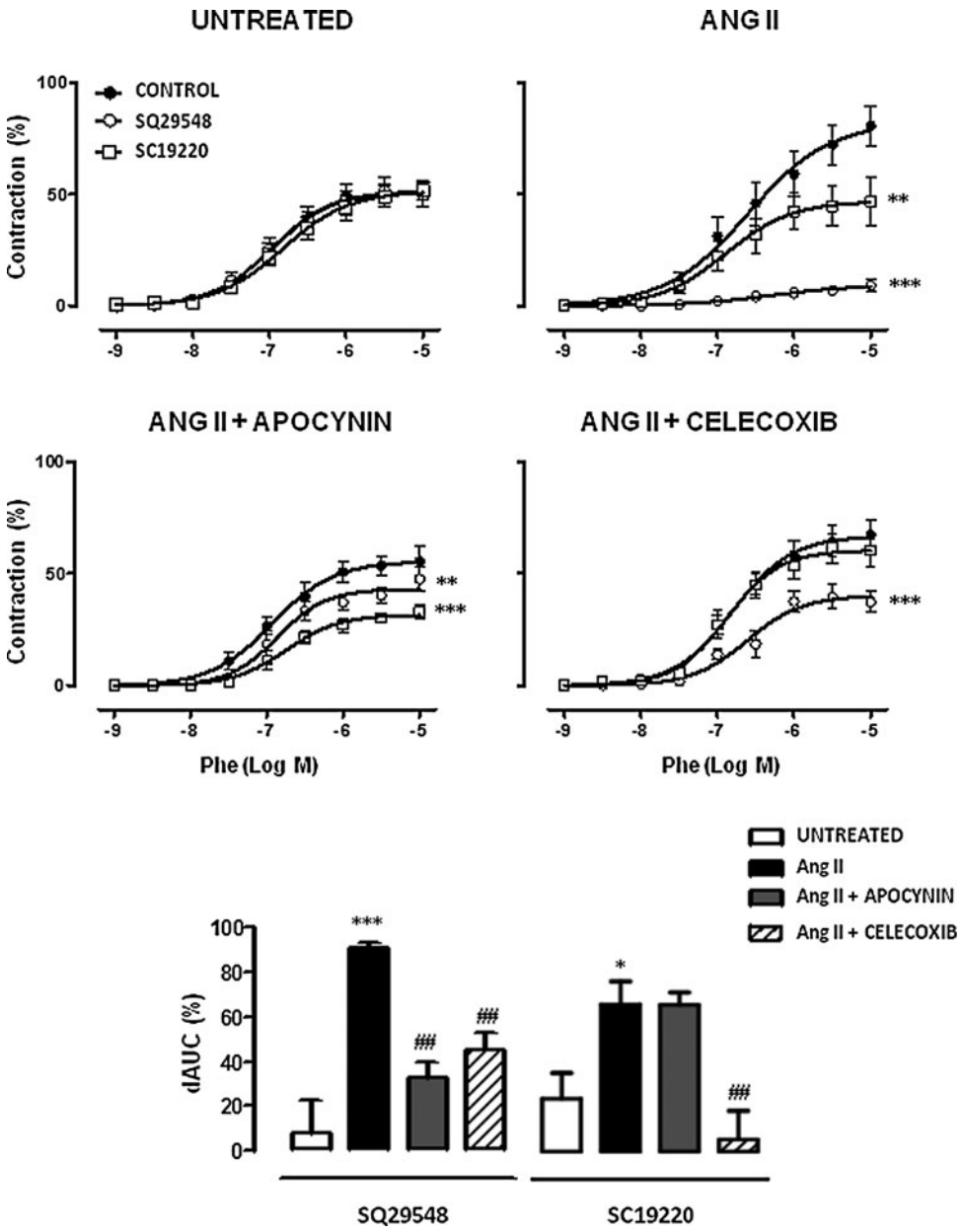

FIG. 7. Antioxidants reduce the participation of vasoconstrictor prostanoids acting on TP receptors on phenylephrine responses in Ang II-infused mice. Effect of SQ29548 and SC19220 on the concentration–response curve to phenylephrine (Phe) in aortic segments from mice untreated and treated with Ang II, Ang II plus apocynin, and Ang II plus Celecoxib. dAUCs are also shown. Data represent mean ± SEM. $n = 5$–15. $^{*}p < 0.05$, $^{**}p < 0.01$, and $^{***}p < 0.001$ *versus* control or *versus* untreated; $^{\#\#}p < 0.01$ *versus* Ang II.

prostanoids in the alterations induced by Ang II in vascular responses and the possible relationship between these two enzymatic pathways. In mesenteric resistance arteries (MRAs), Ang II infusion did not modify phenylephrine contractile responses, but impaired ACh-induced relaxation (Table 1). Mito-TEMPO, but not Celecoxib, treatment inhibited phenylephrine responses. In addition, both Celecoxib and Mito-TEMPO improved ACh-induced relaxation in MRAs from Ang-II infused animals (Table 1).

The NOS inhibitor L-NAME increased the vasoconstrictor response induced by phenylephrine in control, but not in Ang II-infused mice (Supplementary Fig. S5A). Mito-TEMPO and Celecoxib treatments restored the increase in the phenylephrine responses induced by L-NAME in MRA from Ang II-infused mice (Supplementary Fig. S5A).

NS398 inhibited phenylephrine responses only in MRA from Ang II-infused mice, and this inhibition was abolished by Mito-TEMPO (Supplementary Fig. S5B). However, SC560 did not affect phenylephrine responses in any experimental group (data not shown). The incubation of the arteries with SOD inhibited the phenylephrine response only in MRA from Ang II-infused mice, and Celecoxib treatment abolished this effect (Supplementary Fig. S5C). These results suggest that the relationship between ROS and COX-2-derived products might be a general vascular mechanism.

Discussion

The present study provides evidence that demonstrates that ROS and COX-2-derived prostanoids are important mediators of vascular dysfunction and hypertension development. In addition, we demonstrate that there is a crucial vicious circle between ROS and COX-2-derived prostanoids in this pathology. Both NAD(P)H Oxidase and mitochondrion-derived $O_2 \cdot^-$ participate in the increased COX-2 expression and activity. In addition, COX-2

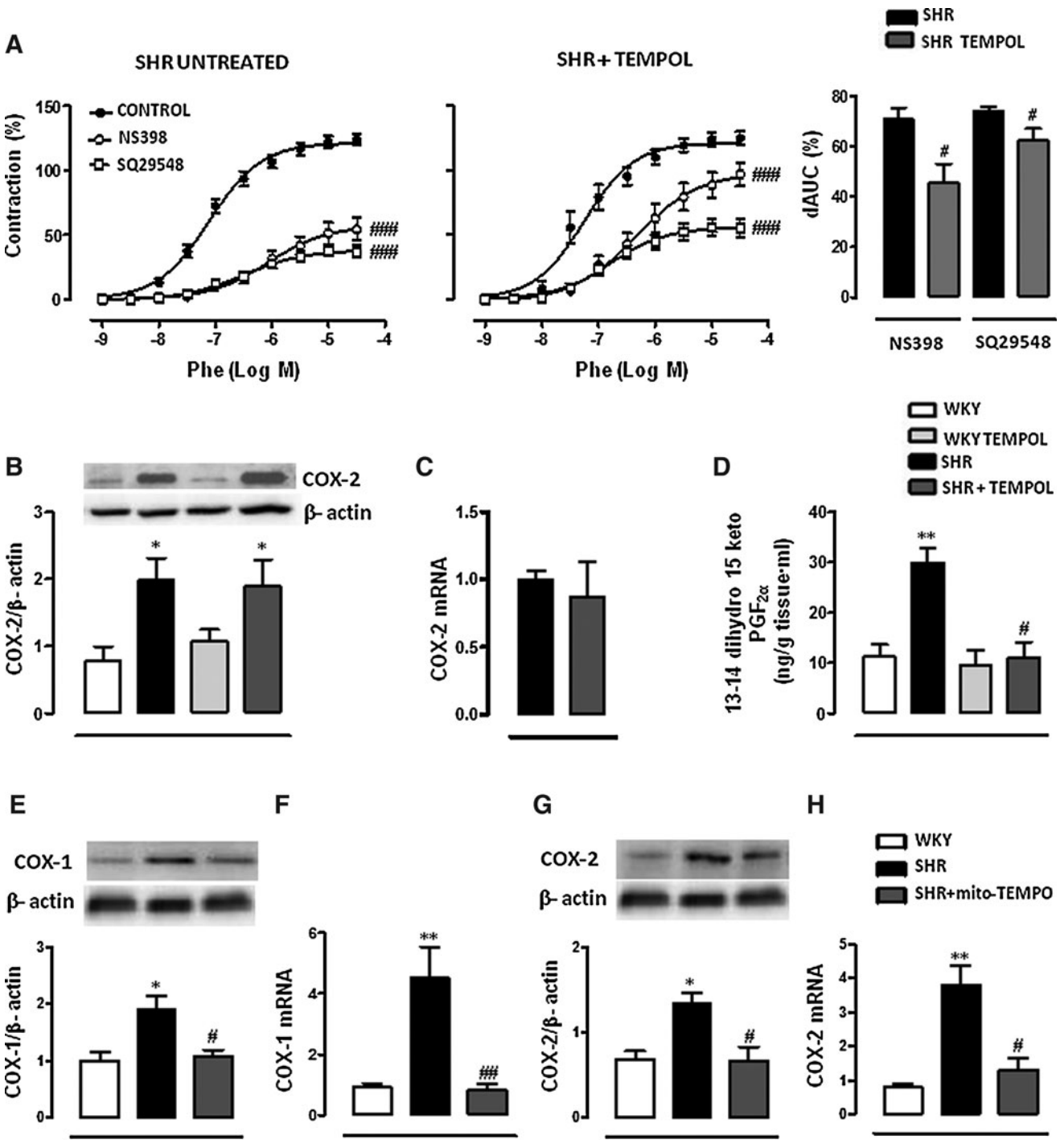

FIG. 8. Antioxidants reduce the increased COX-2 and COX-1 expression and the participation of vasoconstrictor prostanoids acting on TP receptors on phenylephrine responses in SHR. (A) Effect of NS398 and SQ29548 on the concentration–response curve to phenylephrine (Phe) in aortic segments from SHR untreated or treated with tempol. dAUCs are also shown. **(B)** Densitometric analysis and representative blot of COX-2 protein expression in aortic segments from WKY rats and SHRs untreated and treated with tempol. **(C)** COX-2 mRNA expression in rat aorta from SHR untreated or treated with tempol. **(D)** Release of 13,14-dihydro-15-keto-$PGF_{2\alpha}$ to the incubation medium after concentration–response curves to Phe in aortic segments from WKY rats and SHRs untreated or treated with tempol. **(E–H)** Densitometric analysis and representative blots of COX-1 and COX-2 protein expression and mRNA levels in aortic segments from WKY rats and SHRs untreated and treated with Mito-TEMPO. $n = 5–12$. $^{*}p < 0.05$ and $^{**}p < 0.01$ *versus* WKY; $^{\#}p < 0.05$, $^{\#\#}p < 0.01$, and $^{\#\#\#}p < 0.001$ *versus* SHR or *versus* control.

Table 1. pD2 and Maximal Response of Phenylephrine and Acetylcholine in Mesenteric Resistance Arteries from Untreated Mice and Mice Treated with Angiotensin II With or Without Mito-TEMPO, and Celecoxib

	Control	*Ang II*	*Ang II + Mito-TEMPO*	*Ang II + Celecoxib*
Phenylephrine				
pD2	6.19 ± 0.10	6.27 ± 0.06	5.88 ± 0.14[a]	6.12 ± 0.10
Emax	115.8 ± 3.3	118.5 ± 4.8	110.5 ± 17.7	118.1 ± 3.1
Acetylcholine				
pD2	7.70 ± 0.29	6.83 ± 0.23[b]	7.93 ± 0.20[a]	8.13 ± 0.54[a]
Emax	95.8 ± 1.7	86.3 ± 8.1[b]	118.2 ± 14.1[a]	97.72 ± 3.2[a]

[a] $p < 0.05$ *versus* Ang II.
[b] $p < 0.05$ *versus* Control.
Data are expressed as mean ± SEM of 5–15 animals.
pD2, negative logarithm of the concentration that produces a 50% of maximal response; Emax, maximal response; Ang II, Angiotensin II.

derivatives modulate $O_2 \cdot^-$ availability by affecting NAD(P)H Oxidase.

It is well known that Ang II increases vascular NAD(P)H Oxidase activity and $O_2 \cdot^-$ production (6, 12, 29). In addition, mitochondria are becoming as an important source of $O_2 \cdot^-$ in response to Ang II due, in part, to NAD(P)H Oxidase activation (10, 11). It is also evident that Ang II induces COX-2 expression and prostanoid production in vascular cell types such as endothelial cells (36), vascular smooth muscle cells (4, 24), and adventitial fibroblasts (5, 15) as well as in whole vessels (36). Oxidative stress has been also suggested to induce COX activity (13, 17, 30) or upregulate COX-2 expression (4, 14, 16, 38), and this is particularly increased in hypertension (16). In addition, we and other authors have previously demonstrated that COX-derived products induce $O_2 \cdot^-$ production in SHR arteries (18, 27). Recently, a reciprocal regulation of NAD(P)H Oxidase and the COX-2 pathway has been described in liver cells (25). However, to our knowledge, there are no studies demonstrating a circuitous relationship between these two pathways in the vascular wall.

Effects of ROS and COX-2 blockade in blood pressure and vascular function and structure

In the present study, we observed that treatment of Ang II-infused mice with the selective COX-2 inhibitor Celecoxib, the mitochondrion-targeted SOD2 mimetic Mito-TEMPO, and the NAD(P)H Oxidase inhibitor apocynin prevented, in part, hypertension development. In addition, Celecoxib and Mito-TEMPO partially prevented cardiac and vascular hypertrophy, supporting a role of COX-2-derived products and ROS in hypertension and cardiac and vascular remodeling. This is in agreement with previous reports (11, 28, 33), although no modification of blood pressure after COX-2 inhibition has also been found (31). The combination of Mito-TEMPO and Celecoxib did not further decrease blood pressure; however, it normalized the increased cardiac hypertrophy, suggesting that COX-2 and ROS pathways might be interconnected to participate in the development of hypertension, although they might act through different intracellular mechanisms to modulate cardiac hypertrophy. It has been previously described that Mito-TEMPO, but not tempol, decreased established Ang II-induced hypertension (11). We now observed that apocynin and Celecoxib when administered 7 days after Ang II infusion, decreased SBP, but not left ventricular hypertrophy, suggesting that COX-2 or ROS blockade not only prevents but also reverses hypertension development after Ang II infusion. In agreement, Celecoxib decreased blood pressure in the SHRs, although no effect on blood pressure was observed after Mito-TEMPO and tempol treatments. Higher doses, earlier administration, or longer duration of the treatments might be needed to achieve hypotensive effects of antioxidants in the SHR model.

The exposure to Ang II either *in vivo* or *ex vivo* in the organ bath increased phenylephrine responses and impaired ACh relaxation without effect on DEA-NO-induced relaxations in mouse aorta. Other authors have also described endothelial dysfunction after Ang II infusion (21, 30). All chronic treatments abolished the increased phenylephrine-induced contraction and improved ACh responses. In addition, the increased phenylephrine responses after Ang II incubation *ex vivo* were also normalized by apocynin, the specific NOX-2 inhibitor gp91ds-tat, the specific NOX-1 inhibitor ML171 (19), and the COX-2 inhibitor NS398. These results demonstrate that COX-2, mitochondria, and NAD(P)H Oxidase blockade protects the vascular wall against the damaging effects of Ang II. Our results are in agreement with observations made in this and other models of hypertension where it has been described increased participation of ROS from NAD(P)H Oxidase and mitochondrion- (11, 33) and COX-2-derived prostanoids (1, 2, 21, 32, 34, 36, 38) in vasoconstrictor or endothelium-dependent vasodilator responses.

Reciprocal relationship between ROS and COX-2

It is well known that hypertension is associated with increased vascular ROS production from NAD(P)H Oxidase, among other sources, and/or with altered antioxidant defenses (8, 12). In agreement, we observed in aorta from Ang II-infused mice and/or SHRs, increased vascular oxidative stress as demonstrated by increased ROS production ($O_2 \cdot^-$ and H_2O_2), MDA levels, NAD(P)H Oxidase activity, NAD(P)H Oxidase subunit expression (NOX-1, NOX-4 and p22phox), and increased participation of ROS in vasoconstrictor responses, as shown by the greater inhibitory effect of apocynin on phenylephrine responses. In addition, we observed increased MnSOD, but not Cu/Zn- or EC-SOD expression, probably as a compensatory mechanism against the increased mitochondrial $O_2 \cdot^-$ production. This upregulation of MnSOD would explain the increased aortic H_2O_2 production observed after Ang II that might affect vascular function. In fact, catalase incubation abolished the potentiation of phenylephrine responses induced by Ang II.

Prostanoids from COX-1 and COX-2 are also increased in different models of hypertension and are responsible of the endothelial dysfunction observed in this pathology (13). Herein, we observed that arteries from Ang II-infused mice and/or SHRs show increased COX-2 expression and activity and increased participation of COX-2-derived vasoconstrictor prostanoids in contractile responses. Interestingly, COX-1 expression was also increased in SHR aorta, but unaffected in the Ang II-infused mice in spite of the increased participation of COX-1-derived prostanoids in phenylephrine responses observed in this model. Conflicting results on the role of COX-1 or COX-2 in vasodilator and vasoconstrictor responses have been found depending on the hypertension model or the vessel studied (1–4, 13, 21, 28, 30, 36, 38). It has been proposed that TP receptor activation plays a pivotal role in vascular alterations in hypertension (13). Herein, we confirm the essential role of the TP receptor in the phenylephrine responses in the Ang II-infused model and also suggest the involvement of EP_1 receptors in these responses.

In the present study, besides the demonstration of the role of COX-2-derived products and ROS in vascular responses, we uncover a reciprocal relationship between ROS and COX-2-derived products in aorta from Ang II-infused mice and SHRs. This is based on the following findings: first, Celecoxib treatment normalized the increased NAD(P)H Oxidase activity and expression, ROS production, and their participation on vascular responses in both the Ang II-infused mice and SHRs. In addition, Celecoxib normalized the increased MnSOD expression probably as a consequence of the normalized oxidant status. Celecoxib treatment also decreased COX-2 expression probably due to the observed effects of Celecoxib on blocking oxidative stress. Secondly, Mito-TEMPO and/or apocynin normalized the COX-2 upregulation and the increased participation of COX-1- and COX-2-derived prostanoids in vascular responses induced by Ang II infusion. Furthermore, the activation of TP, but not of EP_1, receptors is modulated by oxidative stress. In SHRs, Mito-TEMPO, but not tempol, normalized the increased COX-2 expression, suggesting that specific mitochondrion-targeted antioxidants might be more efficient in modulating COX expression than nonspecific antioxidants. However, tempol was able to diminish the increased $PGF_{2\alpha}$ release and the participation of COX-2-derived prostanoids in vascular responses in SHRs. Interestingly, Mito-TEMPO also decreased COX-1 expression in SHRs. This relationship between ROS and COX-2 is not specific of conductance arteries, since in MRA, a similar ROS-COX modulation was observed. This is based on results demonstrating that Mito-TEMPO and Celecoxib treatments abolished the inhibitory effects of NS398 or SOD on phenylephrine responses, respectively. As described above, several studies have demonstrated a unidirectional relationship between ROS and COX-derived products (4, 13, 14, 16–18, 27, 38). However, to our knowledge, this is the first study that demonstrates that there is a circuitous relationship between these two pathways in the vascular wall and particularly, the essential role of mitochondria in this relationship.

The fact that Celecoxib abolished the inhibitory effect of NS398, but not of the specific COX-1 inhibitor SC560, on phenylephrine responses suggests that the observed effects on the COX-2 blockade pathway are specific. COX-2 blockade

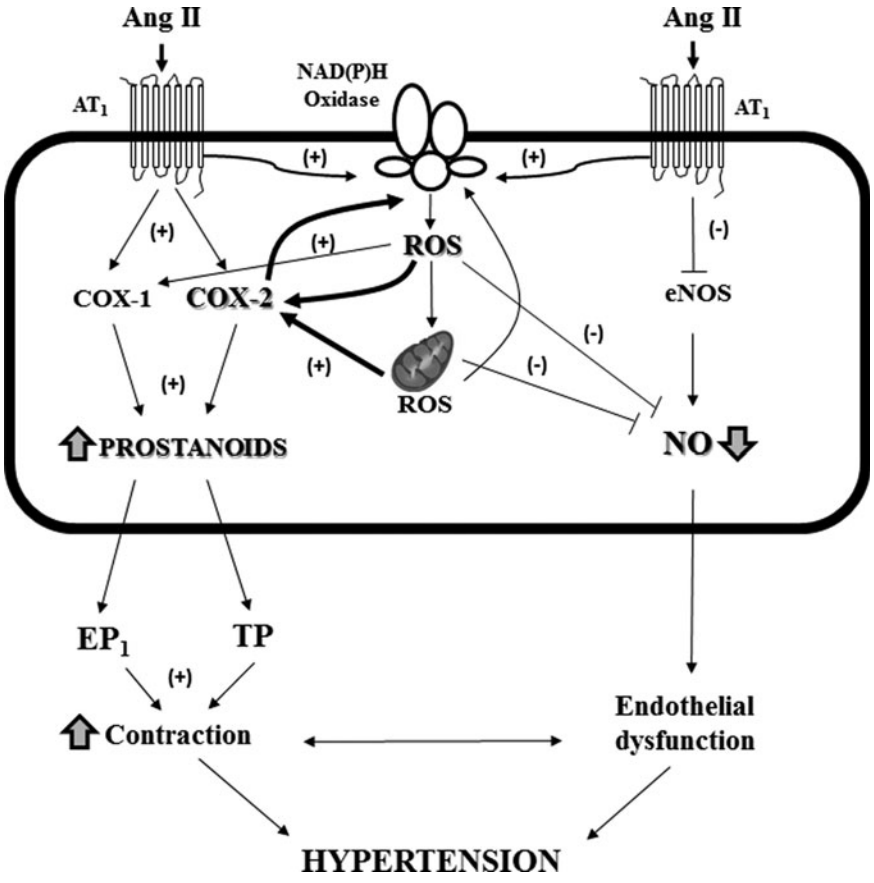

FIG. 9. Scheme demonstrating the relationship between Ang II, reactive oxygen species (ROS), and COX and its putative role in vascular dysfunction in hypertension. In vascular cells such as endothelial and smooth muscle cells, Ang II binds to AT_1 receptors and induces NAD(P)H Oxidase and COX-1/COX-2 activation and ROS and prostanoid production. COX-2-dependent prostanoids activate NAD(P)H Oxidase and ROS activate COX-2, and probably COX-1, in a circuitous relationship. In addition, ROS derived from mitochondria either directly or through NAD(P)H Oxidase activation activate COX-2. These events stimulate prostaglandin E_2 (EP_1) and thromboxane A_2 receptor (TP) activation and increase vascular smooth muscle contraction. Ang II also induces decreased eNOS expression and NO production, which might be further decreased by inactivation by ROS. This, in turn, induces endothelial dysfunction. All together, these vascular alterations participate in hypertension development.

also affects downstream pathways, since the participation of TP and EP_1 receptors in vascular responses is reduced. On the other hand, both apocynin and the mitochondrion-targeted antioxidant Mito-TEMPO normalized NAD(P)H oxidase activity and expression, ROS production, and MnSOD expression. This is in agreement with the recent evidence demonstrating that $O_2\cdot^-$ derived from Ang II-activated NAD(P)H Oxidase induces mitochondrial ROS production, which further activates NAD(P)H Oxidase and increases cellular $O_2\cdot^-$ production (10, 11).

It is well known that prostanoids and ROS can oppose to the vasodilator effects of NO by counteracting its effects or by reducing its bioavailability. Our results in Ang II-infused mice demonstrate that treatment with Celecoxib, Mito-TEMPO, or apocynin normalized the decreased vascular NO production and also restored the impaired modulation induced by NO of phenylephrine responses, the latter found both in conductance and resistance arteries. Interestingly, any of the treatments improved the decreased eNOS expression induced by Ang II, suggesting that alterations in NO availability are responsible of the altered endothelial function. Alternatively, changes in eNOS activity might also explain the observed differences. In fact, some investigators have demonstrated that antioxidants promoted increased proportion of eNOS expressed as a dimer (23).

In conclusion, our results point to the excess of ROS from NAD(P)H Oxidase and/or mitochondria and the increased vascular COX-2/TP receptor axis acting in concert to decrease NO bioavailability in hypertension, thus inducing vascular dysfunction and hypertension development (Fig. 9).

Material and Methods

Animal models

We used C57BL6 mice infused with Ang II (1.44 mg/Kg/day, 2 weeks, subcutaneously by osmotic minipumps; Alza Corp) alone or in combination with (i) the NAD(P)H Oxidase inhibitor apocynin (1.5 m*M* in the drinking water); (ii) the mitochondrion-targeted SOD2 mimetic Mito-TEMPO (0.7 mg/Kg/day i.p.); (iii) the COX-2 inhibitor Celecoxib (25 mg/Kg/day i.p.), and (iv) Mito-TEMPO plus Celecoxib. All treatments started 24 h before Ang II infusion. Control animals without treatments or with Celecoxib or apocynin treatments were also studied. In another set of experiments, mice were treated with Mito-TEMPO or with Celecoxib 7 days after Ang II infusion.

Six-month-old male WKY rats and SHRs were used. SHRs were divided into four groups: (i) control, (ii) treated with the SOD mimetic tempol (1 m*M*, in the drinking water, 18 days), (iii) treated with Mito-TEMPO (0.7 mg/Kg/day i.p., 18 days), and (iv) treated with Celecoxib (25 mg/Kg/day i.p., 3 weeks). Untreated WKY rats or rats treated with tempol or Celecoxib were also used.

In preliminary experiments, we observed that vehicles did not affect SBP or vascular function neither in the Ang II-infused mice nor in the SHRs (data not shown).

Blood pressure was measured by tail-cuff pletysmography. All experimental procedures were approved by the Animal Care and Use Committee of our Institution, according to the guidelines for ethical care of experimental animals of the European Community. The study was conducted in accordance with the National Institutes of Health (NIH) Guide for the Care and Use of Laboratory Animals (NIH Publication No. 85-23, revised 1996) and the current Spanish and European laws (RD 223/88 MAPA and 609/86).

For blood samples acquisition, left ventricular hypertrophy determination, and tissue preparation, please see the Online supplement.

Histological analysis

Aortas were fixed with 4% paraformaldehyde and embedded in a Tissue Tek OCT medium. Sections from fixed aortas were stained with hematoxylin and eosin.

Reactivity experiments

Reactivity of mouse aorta and first-order branches of the mesenteric artery or rat aorta was studied in a wire myograph or by isometric tension recording, respectively, as described (4, 17).

NO release

NO release was measured with the fluorescent probe DAF-2.

Measurement of $O_2\cdot^-$ production

The oxidative fluorescent dye dihydroethidium (DHE) was used to evaluate production of $O_2\cdot^-$ *in situ*, as described (7).

Measurement of H_2O_2

H_2O_2 measurements in aortic segments were performed using the horseradish peroxidase-linked Amplex Red fluorescence assay.

NAD(P)H Oxidase activity

The lucigenin-enhanced chemiluminescence assay was used to determine the NAD(P)H Oxidase activity in total protein aortic homogenates.

Western blot

Aortic homogenates were electrophoretically separated on 7.5% SDS– polyacrylamide gel electrophoresis, as described (4). Western immunoblot was performed with antibodies for eNOS, COX-2, COX-1, MnSOD, Cu/Zn-SOD, and EC-SOD.

Immunofluorescence

COX-2 was localized in frozen transverse sections by immunofluorescence, as described (2).

Measurement of MDA production

Plasma and aortic MDA levels were measured by a modified thiobarbituric acid assay.

Reverse transcription-polymerase chain reaction assay

COX-2, COX-1, β_2-microglobulin, NOX-1, NOX-4, p22phox, p47phox, and cyclophilin mRNA levels were determined in aortic homogenates. Total RNA was obtained by using TRIzol. Quantitative polymerase chain reaction was performed using TaqMan Gene Expression Assays or the fluorescent dye SyBRGreen.

Measurement of prostaglandin $F_{2\alpha}$ production

The levels of the metabolite of $PGF_{2\alpha}$ 13,14-dihydro-15-keto-$PGF_{2\alpha}$ were determined using an enzyme immunoassay commercial kit.

Data analysis and statistics

All data are expressed as mean values ± standard error of the mean, and *n* represents the number of animals. Results were analyzed by using an unpaired Student's *t*-test or a one-way or two-way analysis of variance followed by Bonferroni's *post hoc* test. A $p < 0.05$ was considered significant.

The detailed methods are included in the Supplementary Materials and Methods section.

Acknowledgments

This study was supported by Ministerio de Ciencia e Innovación (SAF2009-07201 and Red RECAVA, RD06/0014/0011, and RD06/0014/0005), Sociedad Española de Farmacología-Almirall Prodesfarma, and Fundación Mutua Madrileña. AMB is supported through the Ramón y Cajal program (RYC-2010-06473), and SM-R by a fellowship from the Alianza Cuatro Universidades.

We thank the Animal Care Facility of the Faculty of Medicine (UAM) for their help with the animals.

Author Disclosure Statement

The authors declare no competing financial interests

References

1. Adeagbo AS, Zhang X, Patel D, Joshua IG, Wang Y, Sun X, Igbo IN, and Oriowo MA. Cyclo-oxygenase-2, endothelium and aortic reactivity during deoxycorticosterone acetate salt-induced hypertension. *J Hypertens* 23: 1025–1036, 2005.
2. Álvarez Y, Briones AM, Balfagón G, Alonso MJ, and Salaices M. Hypertension increases the participation of vasoconstrictor prostanoids from cyclooxygenase-2 in phenylephrine responses. *J Hypertens* 23: 767–777, 2005.
3. Alvarez Y, Briones AM, Hernanz R, Pérez-Girón JV, Alonso MJ, and Salaices M. Role of NADPH oxidase and iNOS in vasoconstrictor responses of vessels from hypertensive and normotensive rats. *Br J Pharmacol* 153: 926–935, 2008.
4. Álvarez Y, Pérez-Girón JV, Hernanz R, Briones AM, García-Redondo A, Beltrán A, Alonso MJ, and Salaices M. Losartan reduces the increased participation of cyclooxygenase-2-derived products in vascular responses of hypertensive rats. *J Pharmacol Exp Ther* 321: 381–388, 2007.
5. Beltrán AE, Briones AM, García-Redondo AB, Rodríguez C, Miguel M, Alvarez Y, Alonso MJ, Martínez-González J, and Salaices M. p38 MAPK contributes to angiotensin II-induced COX-2 expression in aortic fibroblasts from normotensive and hypertensive rats. *J Hypertens* 27: 142–154, 2009.
6. Brandes RP, Weissmann N, and Schröder K. NADPH oxidases in cardiovascular disease. *Free Radic Biol Med* 49: 687–706, 2010.
7. Briones AM, Rodríguez-Criado N, Hernanz R, García-Redondo AB, Rodrigues-Díez RR, Alonso MJ, Egido J, Ruiz-Ortega M, and Salaices M. Atorvastatin prevents angiotensin II-induced vascular remodeling and oxidative stress. *Hypertension* 54: 142–149, 2009.
8. Briones AM and Touyz RM. Oxidative stress and hypertension: current concepts. *Curr Hypertens Rep* 12: 135–142, 2010.
9. Chia E, Kagota S, Wijekoon EP, and McGuire JJ. Protection of protease-activated receptor 2 mediated vasodilatation against angiotensin II-induced vascular dysfunction in mice. *BMC Pharmacol* 11: 10, 2011.
10. Dikalov SI and Nazarewicz RR. Angiotensin II-induced production of mitochondrial ROS: Potential mechanisms and relevance for cardiovascular disease. *Antioxid Redox Signal* 2012 [Epub ahead of print]; DOI: 10.1089/ars.2012.4604.
11. Dikalova AE, Bikineyeva AT, Budzyn K, Nazarewicz RR, McCann L, Lewis W, Harrison DG, and Dikalov SI. Therapeutic targeting of mitochondrial superoxide in hypertension. *Circ Res* 107: 106–116, 2010.
12. Drummond GR, Selemidis S, Griendling KK, and Sobey CG. Combating oxidative stress in vascular disease: NADPH oxidases as therapeutic targets. *Nat Rev Drug Discov* 10: 453–471, 2011.
13. Félétou M, Huang Y, and Vanhoutte PM. Endothelium-mediated control of vascular tone: COX-1 and COX-2 products. *Br J Pharmacol* 164: 894–912, 2011.
14. Feng L, Xia Y, Garcia GE, Hwang D, and Wilson CB. Involvement of reactive oxygen intermediates in cyclooxygenase-2 expression induced by interleukin-1, tumor necrosis factor-alpha, and lipopolysaccharide. *J Clin Invest* 95:1669–1675, 1995.
15. Galán M, Miguel M, Beltrán AE, Rodríguez C, García-Redondo AB, Rodríguez-Calvo R, Alonso MJ, Martínez-González J, and Salaices M. Angiotensin II differentially modulates cyclooxygenase-2, microsomal prostaglandin E2 synthase-1 and prostaglandin I2 synthase expression in adventitial fibroblasts exposed to inflammatory stimuli. *J Hypertens* 29: 529–536, 2011.
16. Garcia-Cohen EC, Marin J, Diez-Picazo LD, Baena AB, Salaices M, and Rodriguez-Martinez MA. Oxidative stress induced by tert-butyl hydroperoxide causes vasoconstriction in the aorta from hypertensive and aged rats: role of cyclooxygenase-2 isoform. *J Pharmacol Exp Ther* 293: 75–81, 2000.
17. García-Redondo AB, Briones AM, Avendaño MS, Hernanz R, Alonso MJ, and Salaices M. Losartan and tempol treatments normalize the increased response to hydrogen peroxide in resistance arteries from hypertensive rats. *J Hypertens* 27: 1814–1822, 2009.
18. García-Redondo AB, Briones AM, Beltrán AE, Alonso MJ, Simonsen U, and Salaices M. Hypertension increases contractile responses to hydrogen peroxide in resistance arteries through increased thromboxane A2, Ca2+, and superoxide anion levels. *J Pharmacol Exp Ther* 328: 19–27, 2009.
19. Gianni D, Taulet N, Zhang H, DerMardirossian C, Kister J, Martinez L, Roush WR, Brown SJ, Bokoch GM, and Rosen H. A novel and specific NADPH oxidase-1 (Nox1) small-molecule inhibitor blocks the formation of functional invadopodia in human colon cancer cells. *ACS Chem Biol* 5: 981–993, 2010.
20. Hernanz R, Briones AM, Alonso MJ, Vila E, and Salaices M. Hypertension alters role of iNOS, COX-2, and oxidative stress in bradykinin relaxation impairment after LPS in rat cerebral arteries. *Am J Physiol Heart Circ Physiol* 287: H225–H234, 2004.
21. Kane MO, Etienne-Selloum N, Madeira SV, Sarr M, Walter A, Dal-Ros S, Schott C, Chataigneau T, and Schini-Kerth VB. Endothelium-derived contracting factors mediate the Ang II-induced endothelial dysfunction in the rat aorta: preventive effect of red wine polyphenols. *Pflugers Arch* 459: 671–679, 2010.

22. Kiritoshi S, Nishikawa T, Sonoda K, Kukidome D, Senokuchi T, Matsuo T, Matsumura T, Tokunaga H, Brownlee M, and Araki E. Reactive oxygen species from mitochondria induce cyclooxygenase-2 gene expression in human mesangial cells: potential role in diabetic nephropathy. *Diabetes* 52: 2570–2577, 2003.
23. Leo CH and Hart JL, Woodman OL. 3′,4′-Dihydroxyflavonol reduces superoxide and improves nitric oxide function in diabetic rat mesenteric arteries. *PLoS One* 6: e20813, 2011.
24. Ohnaka K, Numaguchi K, Yamakawa T, and Inagami T. Induction of cyclooxygenase-2 by angiotensin II in cultured rat vascular smooth muscle cells. *Hypertension* 35: 68–75, 2000.
25. Sancho P, Martín-Sanz P, and Fabregat I. Reciprocal regulation of NADPH oxidases and the cyclooxygenase-2 pathway. *Free Radic Biol Med* 51: 1789–98, 2011.
26. Schulz E, Gori T, and Münzel T. Oxidative stress and endothelial dysfunction in hypertension. *Hypertens Res* 34: 665–673, 2011.
27. Tang EH, Leung FP, Huang Y, Feletou M, So KF, Man RY, and Vanhoutte PM. Calcium and reactive oxygen species increase in endothelial cells in response to releasers of endothelium-derived contracting factor. *Br J Pharmacol* 151: 15–23, 2007.
28. Tian XY, Wong WT, Leung FP, Zhang Y, Wang YX, Lee HK, Ng CF, Chen ZY, Yao X, Au CL, Lau CW, Vanhoutte PM, Cooke JP, and Huang Y. Oxidative stress-dependent cyclooxygenase-2-derived prostaglandin f(2α) impairs endothelial function in renovascular hypertensive rats. *Antioxid Redox Signal* 16: 363–373, 2012.
29. Touyz RM, Briones AM, Sedeek M, Burger D, and Montezano AC. NOX isoforms and reactive oxygen species in vascular health. *Mol Interv* 11: 27–35, 2011.
30. Virdis A, Colucci R, Fornai M, Duranti E, Giannarelli C, Bernardini N, Segnani C, Ippolito C, Antonioli L, Blandizzi C, Taddei S, Salvetti A, and Del Tacca M. Cyclooxygenase-1 is involved in endothelial dysfunction of mesenteric small arteries from angiotensin II-infused mice. *Hypertension* 49: 679–686, 2007.
31. Virdis A, Colucci R, Neves MF, Rugani I, Aydinoglu F, Fornai M, Ippolito C, Antonioli L, Duranti E, Solini A, Bernardini N, Blandizzi C, and Taddei S. Resistance artery mechanics and composition in angiotensin II-infused mice: effects of cyclooxygenase-1 inhibition. *Eur Heart J* 2011 [Epub ahead of print]; Doi: 10.1093/eurheartj/ehr138.
32. Virdis A, Colucci R, Versari D, Ghisu N, Fornai M, Antonioli L, Duranti E, Daghini E, Giannarelli C, Blandizzi C, Taddei S, and Del Tacca M. Atorvastatin prevents endothelial dysfunction in mesenteric arteries from spontaneously hypertensive rats: role of cyclooxygenase 2-derived contracting prostanoids. *Hypertension* 53: 1008–1016, 2009.
33. Virdis A, Neves MF, Amiri F, Touyz RM, and Schiffrin EL. Role of NAD(P)H oxidase on vascular alterations in angiotensin II-infused mice. *J Hypertens* 22: 535–542, 2004.
34. Wenceslau CF, Davel AP, Xavier FE, and Rossoni LV. Long-term ouabain treatment impairs vascular function in resistance arteries. *J Vasc Res* 48: 316–326, 2011.
35. Widlansky ME, Price DT, Gokce N, Eberhardt RT, Duffy SJ, Holbrook M, Maxwell C, Palmisano J, Keaney JF Jr, Morrow JD, and Vita JA. Short- and long-term COX-2 inhibition reverses endothelial dysfunction in patients with hypertension. *Hypertension* 42: 310–315, 2003.
36. Wong SL, Lau CW, Wong WT, Xu A, Au CL, Ng CF, Ng SS, Gollasch M, Yao X, and Huang Y. Pivotal role of protein kinase Cdelta in angiotensin II-induced endothelial cyclooxygenase-2 expression: a link to vascular inflammation. *Arterioscler Thromb Vasc Biol* 31: 1169–1976, 2011.
37. Wong SL, Wong WT, Tian XY, Lau CW, and Huang Y. Prostaglandins in action indispensable roles of cyclooxygenase-1 and −2 in endothelium-dependent contractions. *Adv Pharmacol* 60: 61–83, 2010.
38. Wong WT, Tian XY, Chen Y, Leung FP, Liu L, Lee HK, Ng CF, Xu A, Yao X, Vanhoutte PM, Tipoe GL, and Huang Y. Bone morphogenic protein-4 impairs endothelial function through oxidative stress-dependent cyclooxygenase-2 upregulation: implications on hypertension. *Circ Res* 107: 984–991, 2010.

Address correspondence to:
Prof. Mercedes Salaices
Department of Pharmacology
School of Medicine
Universidad Autónoma de Madrid
Arzobispo Morcillo 4
28029 Madrid
Spain

E-mail: mercedes.salaices@uam.es

Dr. Ana María Briones
Department of Pharmacology
School of Medicine
Universidad Autónoma de Madrid
Arzobispo Morcillo 4
28029 Madrid
Spain

E-mail: ana.briones@uam.es

Date of first submission to ARS Central, October 13, 2011; date of final revised submission, May 17, 2012; date of acceptance, June 6, 2012.

Abbreviations Used

ACh = acetylcholine
Ang II = Angiotensin II
COX = cyclooxygenase
dAUC = differences of the area under the concentration–response curve
DEA-NO = diethylamine NONOate
DHE = dihydroethidium
eNOS = endothelial nitric oxide synthase
L-NAME = *N*-nitro-L-arginine methyl ester
MRA = mesenteric resistance arteries
ROS = reactive oxygen species
SBP = systolic blood pressure
SHR = spontaneously hypertensive rats
SOD = superoxide dismutase
WKY = Wistar Kyoto

Supplementary Data

Supplementary Materials and Methods

Blood samples and left ventricular hypertrophy determination

Blood samples were collected in eppendorfs containing anticoagulant (sodium heparin 5%; Hospira) and placed in ice. Blood samples were centrifuged at 1500 *g* for 15 min at 4°C. The obtained plasma was frozen at −20°C and kept at −80°C until used to determine malondialdehyde (MDA).

Hearts were removed for assessing left ventricular hypertrophy. For this, the ratio between the left ventricular dry weight and the length of the tibia was calculated.

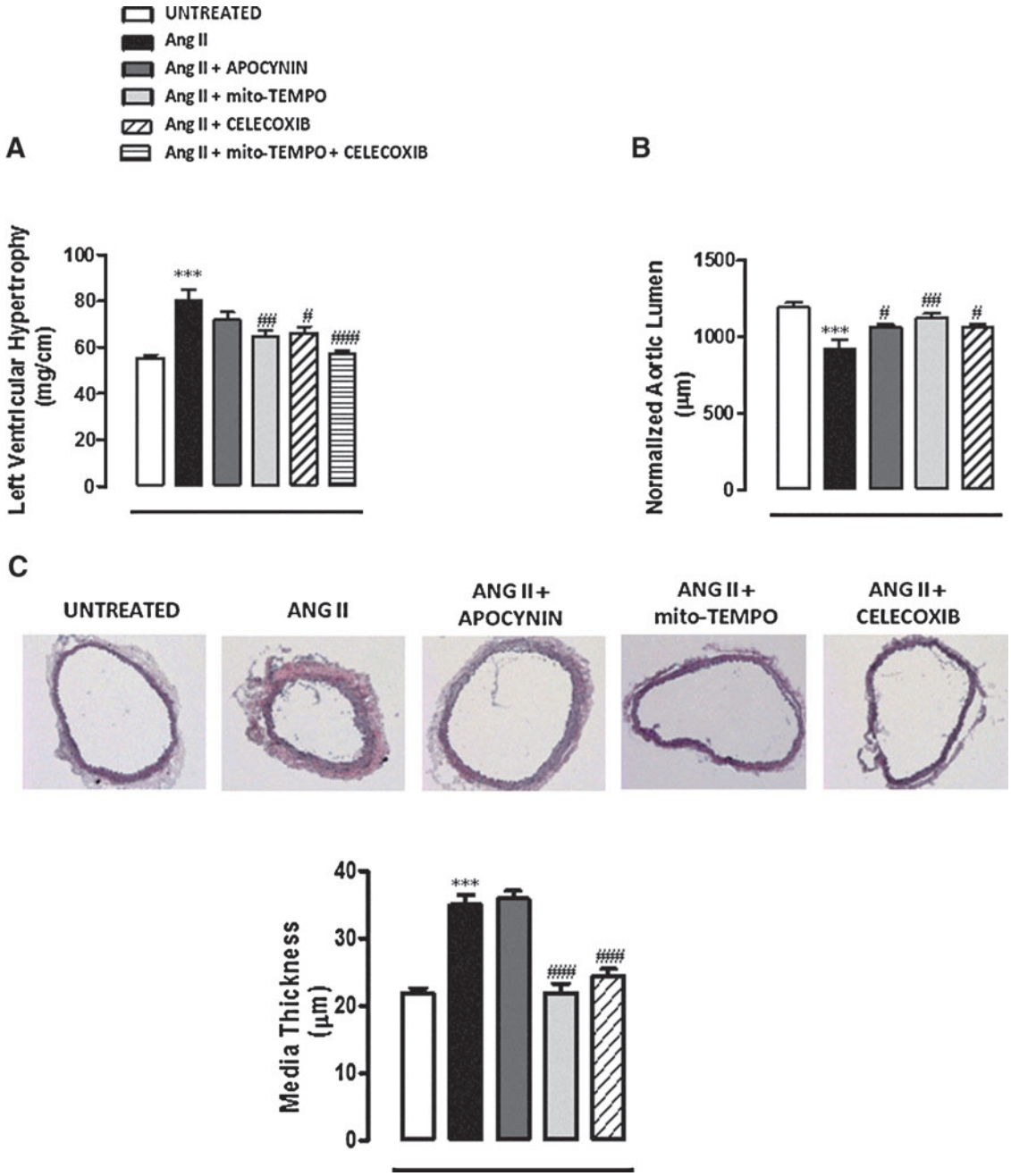

SUPPLEMENTARY FIG. S1. Antioxidants and COX-2 blockade improve cardiac and vascular hypertrophy in Ang II-infused mice. Effect of apocynin, Mito-TEMPO, Celecoxib, and Mito-TEMPO plus Celecoxib treatments on left ventricular hypertrophy **(A)**, aortic lumen diameter **(B)**, and media thickness **(C)** in Angiotensin II (Ang II)-infused mice. Untreated mice were used as controls. Image size 722 × 541 μm (to see this illustration in color, the reader is referred to the web version of this article at www.liebertpub.com/ars). Data represent mean ± SEM. $n = 5$–15. $^{***}p < 0.001$ *versus* untreated; $^{\#}p < 0.05$, $^{\#\#}p < 0.01$, $^{\#\#\#}p < 0.001$ *versus* Ang II. SEM, standard error of the mean.

Tissue preparation

Mice or rats were euthanized by CO_2, and the mesenteric vascular bed and aorta were removed and placed in cold (4°C) Krebs-Henseleit solution (KHS) (115 m*M* NaCl, 25 m*M* $NaHCO_3$, 4.7 m*M* KCl, 1.2 m*M* $MgSO_4.7H_2O$, 2.5 m*M* $CaCl_2$, 1.2 m*M* KH_2PO_4, 11.1 m*M* glucose, and 0.01 m*M* Na_2EDTA) bubbled with a 95% O_2–5% CO_2 mixture.

Aortic segments [for histological studies, vascular reactivity, superoxide anion ($O_2\cdot^-$) and H_2O_2 production, NAD(P)H Oxidase activity, MDA levels, immunofluorescence studies, Western blot studies, reverse transcription-polymerase chain reaction (RT-PCR), and nitric oxide (NO) and prostanoid release] and first-order branches of the mesenteric artery (for vascular reactivity) were dissected free of fat and connective tissue and maintained in KHS. Segments used for $O_2\cdot^-$ production were placed in KHS containing 30% sucrose for 20 min, transferred to a cryomold (Bayer Química Farmacéutica) containing a Tissue Tek OCT-embedding medium (Sakura Finetek Europe), and then immediately frozen in liquid nitrogen for storage at −70° C until $O_2\cdot^-$ measurement. For immunofluorescence and for histology studies, arterial segments were fixed with 4% phosphate-buffered paraformaldehyde (pH = 7.4) for 1 h and washed in three changes of phosphate-buffered saline solution (PBS, pH = 7.4). After washing, arterial segments were placed in PBS containing 30% sucrose for 20 min, transferred to a cryomold containing the Tissue Tek OCT-embedding medium, and frozen in liquid nitrogen. Tissues were kept at −70°C until the day of the experiments. Other segments were immediately frozen in liquid nitrogen and kept at −70°C until the day of the protein or gene expression studies, MDA and H_2O_2 production, or for measurement of NAD(P)H Oxidase activity.

Histological analysis

Aortas were fixed with 4% paraformaldehyde and embedded in a Tissue Tek OCT medium as described above. About 10-μm cross sections from fixed aortas were stained with hematoxylin and eosin. All images were acquired at room temperature using a microscope (DM2500; Leica) with 10× objective. Media thickness was measured with Metamorph Image Analysis Software (Universal Imaging, Molecular Devices).

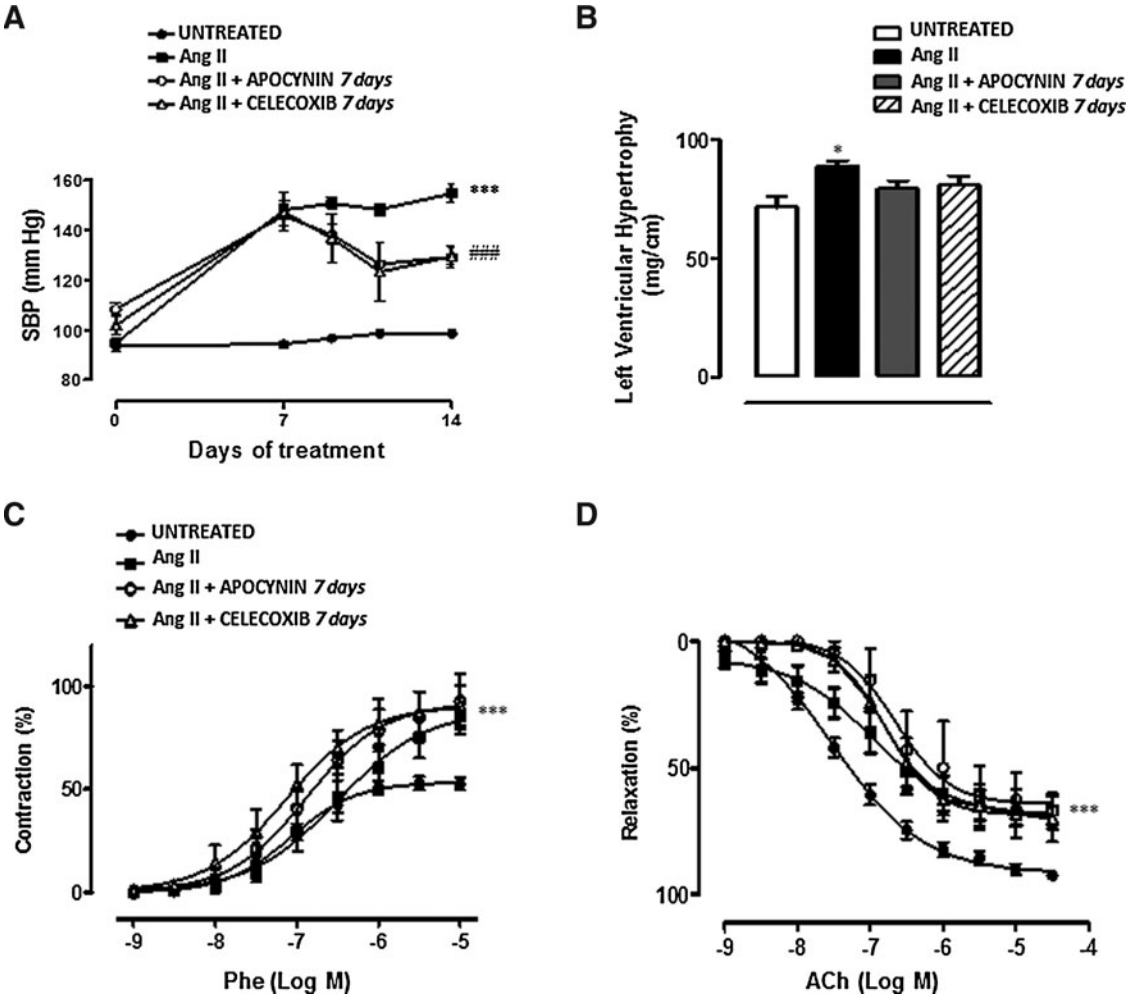

SUPPLEMENTARY FIG. S2. Antioxidants and COX-2 blockade decrease established hypertension and cardiac hypertrophy in Ang II-infused mice. Effects of apocynin or Celecoxib administered 7 days after Ang II infusion on systolic blood pressure (SBP) **(A)**, left ventricular hypertrophy **(B)**, and concentration–response curves to phenylephrine (Phe) **(C)** or acetylcholine (ACh) **(D)** in Ang II-infused mice. Data represent mean ± SEM. $n = 5$–6. $^{*}p < 0.05$ and $^{***}p < 0.001$ *versus* untreated; $^{\#\#\#}p < 0.001$ *versus* Ang II.

Reactivity experiments

Reactivity of mouse aorta and first-order branches of the mesenteric artery or rat aorta was studied in a wire myograph or by isometric tension recording, respectively, as previously described (2, 4). After a 30-min equilibration period in oxygenated KHS, arterial segments were stretched to their optimal lumen diameter for active tension development. Contractility of segments was then tested by an initial exposure to a high-K^+ solution (K^+-KHS, 120 or 75 m*M* for mice and rats, respectively). The presence of endothelium was determined by the ability of 10 μM acetylcholine (ACh) to relax arteries precontracted with phenylephrine at ~50% K^+-KHS contraction. Afterward, concentration–response curves to ACh, phenylephrine, and diethylamine NONOate (DEA-NO) were performed. The effects of *N*-nitro-L-arginine methyl ester (L-NAME), NS398, SC560, SQ29548, SC19220, apocynin, and SOD were analyzed by their addition 30 min before the phenylephrine concentration–response curves. A single concentration-dependent curve was performed in each segment. In another set of experiments, mouse aortic segments were preincubated *in vitro* with Angiotensin II (Ang II) (1 h) in the absence or presence of apocynin, gp91ds-tat, ML171, catalase, or NS398 before the phenylephrine concentration–response curves. These drugs were added 30 min before Ang II.

Vasoconstrictor responses were expressed as a percentage of the tone generated by K^+-KHS. Vasodilator responses were expressed as a percentage of the previous tone generated by phenylephrine. To compare the effect of the different inhibitors on the phenylephrine responses in segments from the different experimental groups, some results were expressed as differences of the area under the concentration–response curves (dAUCs) in control and experimental situations. AUCs were calculated from the individual concentration–response curve plots; the differences were expressed as a percentage of the AUC of the corresponding control situation.

NO release

After an equilibration period of 60 min in an HEPES buffer (in m*M*: NaCl 119; HEPES 20; $CaCl_2$ 1.2; KCl 4.6; $MgSO_4$ 1; KH_2PO_4 0.4; $NaHCO_3$ 5; glucose 5.5; Na_2HPO_4 0.15; pH 7.4) at 37°C, aortic segments were incubated with the fluorescent probe 4,5-diaminofluorescein (DAF-2; 2 μM) for 45 min. Then, the medium was collected to measure basal NO release. Afterward, these segments were incubated with phenylephrine (1 μM, 1 min) and ACh (10 μM, 1 min). Thereafter, the medium was collected to measure agonist-induced NO release. The fluorescence of the medium was measured at room temperature using a spectrofluorimeter (FLUOstar OPTIMA BMG Labtech) with an excitation wavelength set at 492 nm and emission wavelength at 515 nm. To avoid variations in fluorescence among the different days, all experimental conditions were measured each day.

The induced NO release was calculated by subtracting basal NO release from that evoked by ACh. Also, blank samples were collected in the same way than from the segment-free medium to correct for background emission. The amount of NO released was expressed as arbitrary units·mg^{-1} tissue. Samples from nontreated animals were

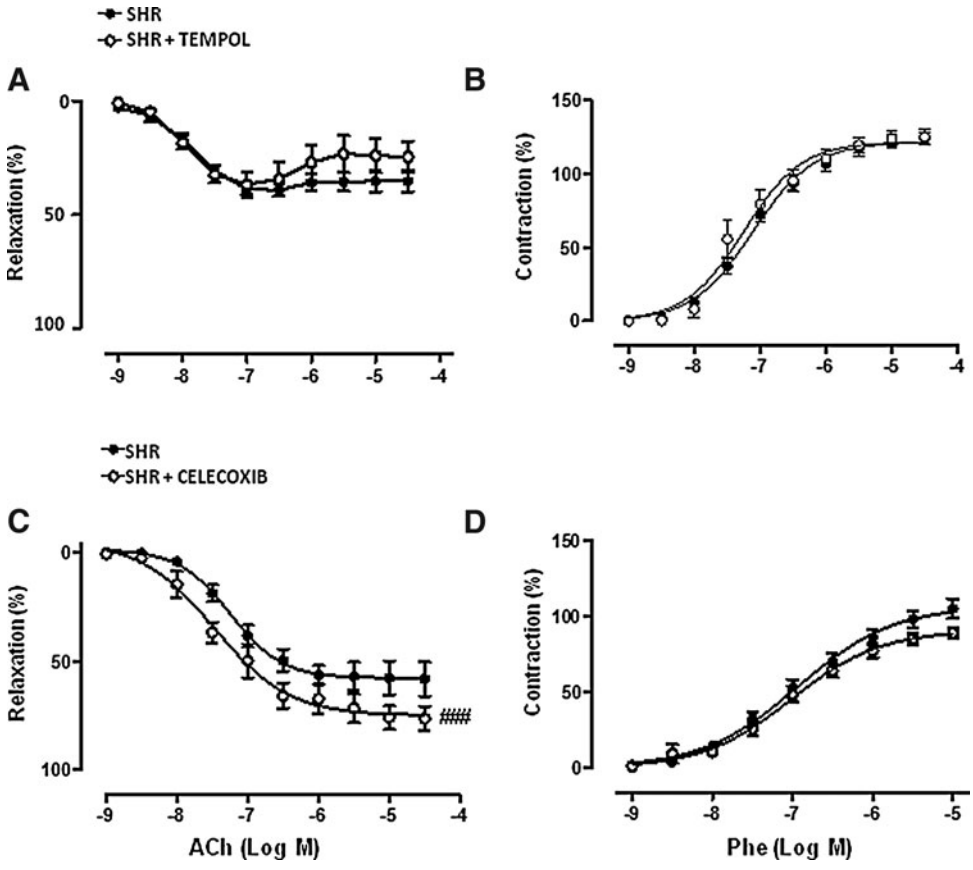

SUPPLEMENTARY FIG. S3. Effect of antioxidants and COX-2 blockade on vasoconstrictor and vasodilator responses in SHR. Concentration–response curves to ACh **(A, C)** and phenylephrine (Phe) **(B, D)** in aortic segments from spontaneously hypertensive rats (SHR) untreated or treated with tempol or Celecoxib. Data represent mean ± SEM. $n = 5$–10. $^{###}p < 0.001$ *versus* SHR untreated.

used as controls, and variations of NO release were calculated as the amount relative to controls.

Measurement of $O_2\cdot^-$ production

The oxidative fluorescent dye dihydroethidium (DHE) was used to evaluate production of $O_2\cdot^-$ *in situ*, as previously described (3). Briefly, serial aortic sections were equilibrated in a Krebs-HEPES buffer (in m*M*: NaCl 130, KCl 5.6, $CaCl_2$ 2, $MgCl_2$ 0.24, HEPES 8.3, glucose 11, pH 7.4). Then, a fresh buffer containing DHE (2 μM, 30 min, 37 °C) was added and then viewed by a fluorescent laser-scanning confocal microscope (Leica TCS SP2; ×63) (Ex561 and Em610 nm), using the same imaging settings in each case. As a negative control of the staining, parallel sections were preincubated with tempol (100 μM). In these conditions, no staining was observed in the vascular wall. $O_2\cdot^-$ production was quantitatively analyzed with MetaMorph Image Analysis Software. Four areas per ring were sampled for each experimental condition. The integrated optical densities in the target region were calculated.

Measurement of H_2O_2

H_2O_2 measurements in aortic segments were made using the horseradish peroxidase-linked Amplex Red fluorescence assay. Briefly, Amplex Red (100 μM) and horseradish peroxidase type II (0.2 U/ml) were added to the aortic homogenates. Fluorescence readings were made in triplicate in a 96-well plate at Ex/Em = 530/580 nm using 50-μl samples of media. H_2O_2 concentration was calculated using a standard curve and normalized to cellular protein as measured by the Lowry assay.

NAD(P)H Oxidase activity

The lucigenin-enhanced chemiluminescence assay was used to determine the NAD(P)H Oxidase activity in total protein aortic homogenates. Tissues were homogenized in a lysis buffer (in m*M*: KH_2PO_4 50, ethylene glycol tetraacetic acid 1, sucrose 150, pH 7.4). The reaction was started by the addition of NAD(P)H (0.1 m*M*) to the suspension containing sample, lucigenin (5 μM), and assay phosphate buffer. The luminescence was measured in a plate luminometer (Auto-Lumat LB 953, Berthold). Buffer blank was subtracted from each reading. Activity was expressed as relative light units/mg protein. Samples from nontreated animals were used as controls, and variations of NAD(P)H Oxidase activity were calculated as the amount relative to controls.

Western blot

Aortic segments were homogenized in an ice-cold Tris–EDTA buffer as described (2). Homogenates (30 μg protein per lane) and prestained molecular SDS-PAGE standards (Bio-Rad Laboratories) were electrophoretically separated on a 7.5% SDS– polyacrylamide gel electrophoresis and transferred to polyvinylidene difluoride membranes overnight. Western immunoblot was performed with a monoclonal antibody for eNOS (1:1000; Transduction Laboratories), a polyclonal antibody for cyclooxygenase (COX)-2 (1:200; Santa Cruz Biotechnology, Inc.) and COX-1 (1:200; Alexis Biochemicals), and a polyclonal antibody for MnSOD (0.025 μg/ml; StressGen Bioreagent Corp.), Cu/Zn-SOD (1:10,000; Nventa Biopharmaceuticals), and EC-SOD (1:5000; StressGen Bioreagent Corp.). After washing, membranes were

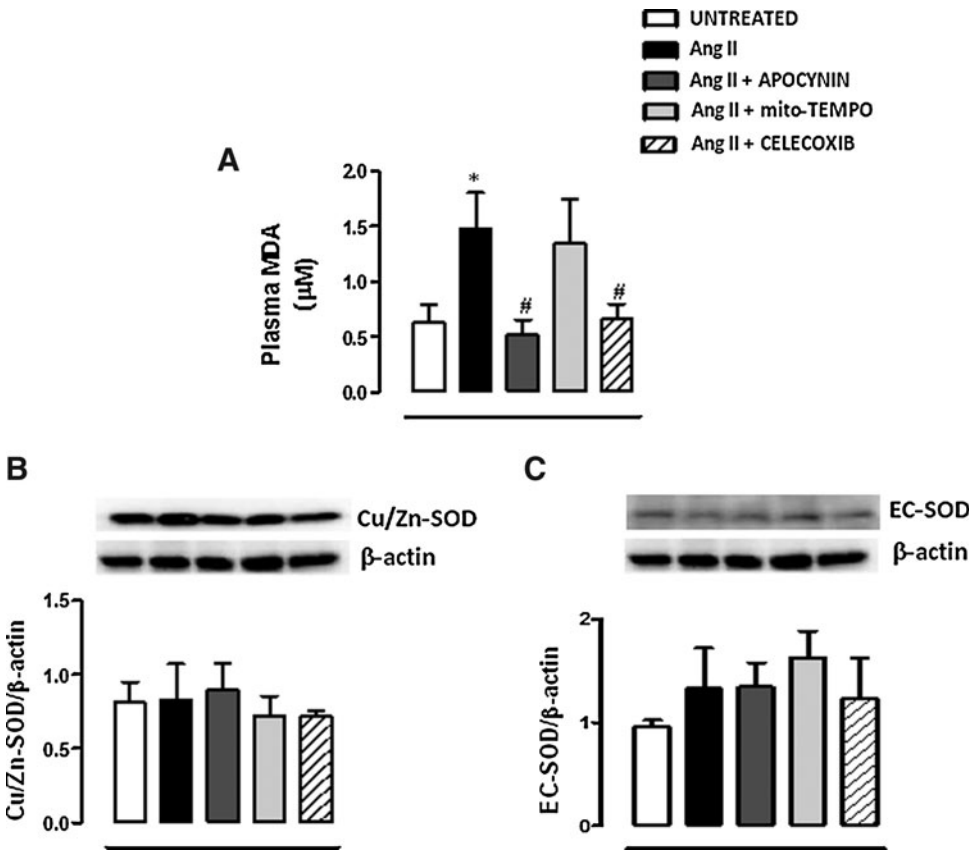

SUPPLEMENTARY FIG. S4. Effect of antioxidants and COX-2 blockade on plasma MDA and vascular expression of Cu/Zn-SOD and EC-SOD in Ang II-infused mice. (A) Plasma malondialdehyde (MDA) levels and **(B, C)** densitometric analysis and representative blot of Cu/Zn-SOD and EC-SOD protein expression in aortic segments from mice untreated and treated with Ang II in the absence and the presence of apocynin, Mito-TEMPO, and Celecoxib. Data represent mean ± SEM. $n = 5$–7. $^*p < 0.05$ *versus* untreated; $^{\#}p < 0.05$ *versus* Ang II.

incubated with peroxidase-conjugated secondary antibodies (anti-mouse, anti-goat, or anti-rabbit IgG, 1:2000; Transduction Laboratories). Immunocomplexes were detected using an enhanced horseradish peroxidase/luminol chemiluminescence system (Luminata™ Forte; Millipore Corporation). Signals on the immunoblot were quantified using National Institutes of Health ImageJ software. The same membrane was used to determine β-actin expression, using a monoclonal antibody anti-β-actin (1:100,000, Sigma-Aldrich) as a gel-loading control. Data are expressed as the ratio between signals on the immunoblot corresponding to eNOS, COX-2, MnSOD, Cu/Zn-SOD, EC-SOD, and β-actin and calculated as a percentage of control animals.

Immunofluorescence

COX-2 was immunolocalized as described (1). Briefly, frozen transverse sections (14 μm) were cut on to gelatin-coated slides and air-dried for at least 60 min. After blockade, sections were incubated with a polyclonal antibody against COX-2 (1:100, Santa Cruz Biotechnology, Inc.) in PBS containing 2% bovine serum albumin for 1 h at 37°C in a humidified chamber. After washing, rings were incubated with the secondary antibody, a donkey anti-goat (COX-2, 1:200) IgG conjugated to Cy™3 (Jackson Immunoresearch Laboratories, Inc.), for 1 h at 37°C in a humid box. After washing, immunofluorescent signals were viewed using an inverted Leica TCS SP2 confocal laser-scanning microscope with oil immersion lens (x63). Cy™3-labeled antibody was visualized by excitation at 561 nm and detection at 600–700 nm. The specificity of the immunostaining was evaluated by omission of the primary antibody and processed as above. Under these conditions, no staining was observed in the vessel wall.

Measurement of MDA production

Plasma and aortic MDA levels were measured by a modified thiobarbituric acid assay. Samples were mixed with 20% trichloroacetic acid in 0.6 *M* HCl (1:1, v/v), and the tubes were kept in ice for 20 min to precipitate plasma components to avoid possible interference. Samples were centrifuged at 1500 *g* for 15 min before adding 120 m*M* thiobarbituric acid in

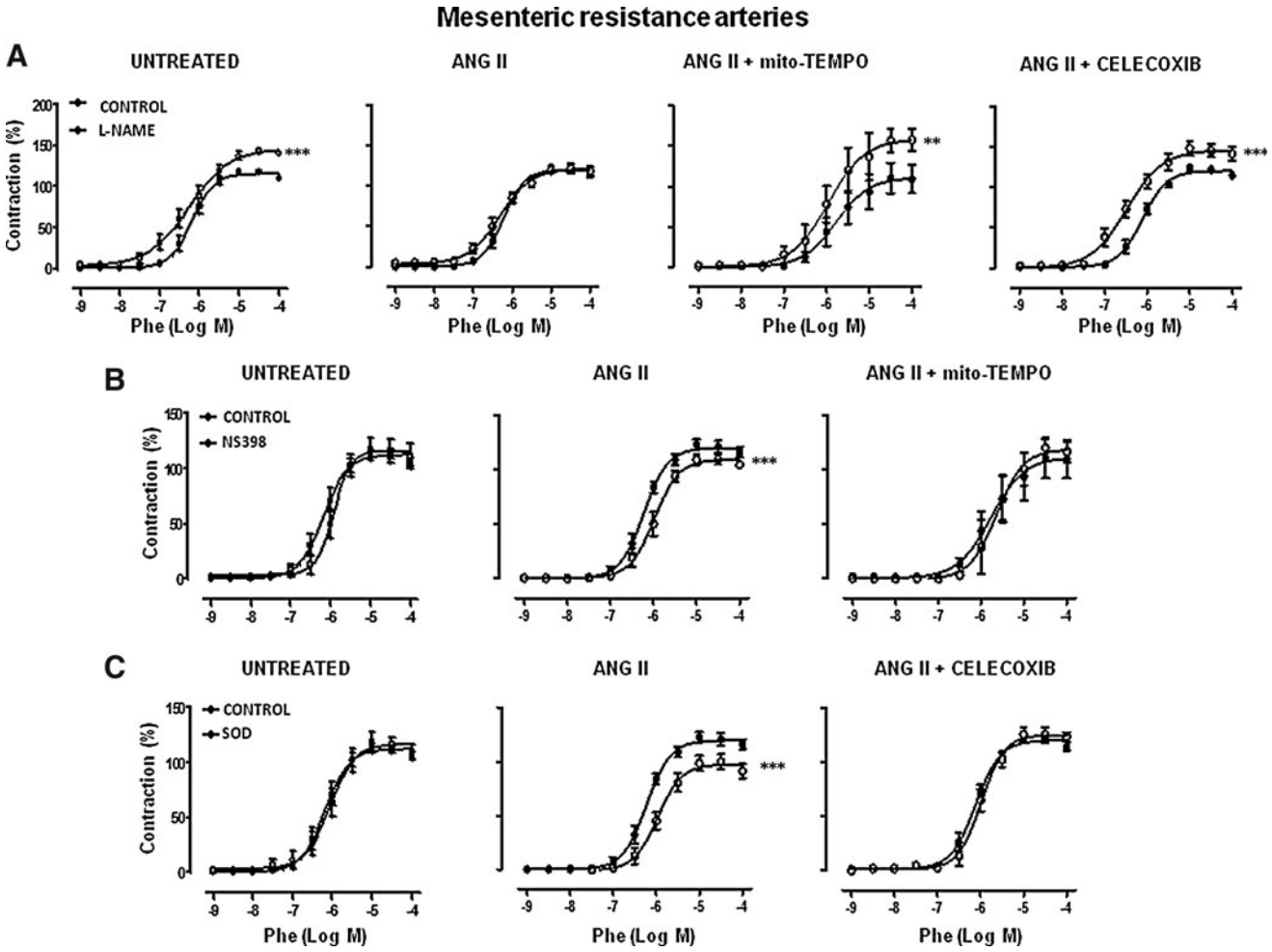

SUPPLEMENTARY FIG. S5. Effect of antioxidants and COX-2 blockade on vasoconstrictor responses in resistance arteries from Ang II-infused mice. (A) Effect of *N*-nitro-L-arginine methyl ester (L-NAME) on the concentration–response curve to phenylephrine (Phe) in mesenteric resistance arteries from mice untreated and treated with Ang II, Ang II plus Mito-TEMPO, and Ang II plus Celecoxib. Effect of NS398 **(B)** and superoxide dismutase (SOD) **(C)** on the concentration–response curve to Phe in mesenteric resistance arteries from mice untreated and treated with Ang II and Ang II plus Mito-TEMPO **(B)** or Ang II plus Celecoxib **(C)**. Data represent mean ± SEM. $n = 5$–10. $^{**}p < 0.01$ and $^{***}p < 0.001$ *versus* control.

260 m*M* Tris, pH 7, to the supernatant in a proportion of 1:5 (v/v). Then, the mixture was boiled at 97°C for 30 min. Spectrophotometric measurements at 535 nm were made at 20°C.

RT-PCR assay

COX-1, COX-2, NOX-1, NOX-4, p22phox, p47phox, β_2-microglobulin, and cyclophilin mRNA levels were determined in mouse or rat aortic homogenates. Total RNA was obtained by using TRIzol (Invitrogen Life Technologies). A total of 1 μg of DNAse I-treated RNA was reverse-transcribed into cDNA using TaqMan® Reverse Transcription Reagents in a final volume of 10 μL. Quantitative polymerase chain reaction (qPCR) for COX-2 was performed using TaqMan Gene Expression Assays (COX-2: Rn00568225_m1; β_2-microglobulin: Rn00560865_m1; Applied Biosystems) as previously described (2). qPCR for COX-1 NOX-1, NOX-4, p22phox, and p47phox was performed using the fluorescent dye SyBR-Green (iTaq FAST SyBR Green Supermix with ROX; Bio-Rad). As normalizing internal controls, we amplified cyclophilin and β_2-microglobulin as housekeeping genes. All qPCRs were performed in duplicate. Primers sequences are COX-1 (FW: CAACCTACAACACAG CACAT; RV: CCTTCTCAGCAG CAATCG), NOX-1 (FW: CGGCAGAAGGTCGTGATTA; RV: TGGAGCAGAGGTCA GAGT), NOX-4 (FW: GCCTCCATC AAGCCAAGA; RV: CCAGTCATCCAGTAGAGTGTT), cyclophilin (FW: GGAG ATGGCACAGGAGGAA; RV: ATAG TGCTTCAGCTTGAA GTTCTCAT), p22phox (FW: ATCTGT CTGCTGGAGTAT; RV: CGTAGTAATTCCTGGTGAG), p47phox (FW: CCCAA CTACGCAGGTGAACC; RV: AGCC GGTGATATCCCCT TTC), and β_2-microglobulin and (FW: ACCCTGGTCTTTC TGGTGCTT; RV: TAGCAGTTCAGTAT GTTCGGCTT). Quantification was performed on 7500 Fast (Applied Biosystems). PCR cycles proceeded as follows: initial denaturation for 30 s at 95°C, followed by 40 cycles at 95°C for 5 s, 60°C for 30 s. At the end of the PCR, a melting curve analysis was performed to show the specificity of the product detected. To calculate the relative index of gene expression, we employed the $2^{-\Delta\Delta Ct}$ method using untreated samples as calibrator (5).

Measurement of prostaglandin $F_{2\alpha}$ production

The levels of the metabolite of $PGF_{2\alpha}$ 13,14-dihydro-15-keto-$PGF_{2\alpha}$ were determined in the incubation medium after completion of the phenylephrine concentration–response curves using an enzyme immunoassay commercial kit (Cayman Chemical). The medium was frozen in liquid nitrogen, kept at −70°C until analysis, and processed, following the manufacturer's instructions.

Drugs and solutions

Drugs used were ACh chloride, DEA-NO, 4,5-diaminofluorescein, DHE, *N*-nitro-L-arginine methyl ester, phenylephrine hydrochloride, superoxide dismutase, tempol, SC19220, apocynin, catalase, ML171 (Sigma-Aldrich), NS398 (Calbiochem), Mito-TEMPO (Santa Cruz Biotechnology), SQ29548 (ICN Iberica), and gp91ds-tat (Anaspec). Celecoxib and SC560 were generously provided by Pfizer, Inc., and Laboratorios Menarini, respectively. DHE was obtained from Invitrogen. SC560 and SQ29548 were dissolved in ethanol. NS398 and SC19220 were dissolved in DMSO. ML171 was dissolved in 75% ethanol. Celecoxib was dissolved in 0.5% carboxymethylcellulose and 0.025% Tween20 in water. Further dilutions were in distilled water.

Supplementary References

1. Álvarez Y, Briones AM, Balfagón G, Alonso MJ, and Salaices M. Hypertension increases the participation of vasoconstrictor prostanoids from cyclooxygenase-2 in phenylephrine responses. *J Hypertens* 23: 767–777, 2005.
2. Álvarez Y, Pérez-Girón JV, Hernanz R, Briones AM, García-Redondo A, Beltrán A, Alonso MJ, and Salaices M. Losartan reduces the increased participation of cyclooxygenase-2-derived products in vascular responses of hypertensive rats. *J Pharmacol Exp Ther* 321: 381–388, 2007.
3. Briones AM, Rodríguez-Criado N, Hernanz R, García-Redondo AB, Rodrigues-Díez RR, Alonso MJ, Egido J, Ruiz-Ortega M, and Salaices M. Atorvastatin prevents angiotensin II-induced vascular remodeling and oxidative stress. *Hypertension* 54: 142–149, 2009.
4. García-Redondo AB, Briones AM, Avendaño MS, Hernanz R, Alonso MJ, and Salaices M. Losartan and tempol treatments normalize the increased response to hydrogen peroxide in resistance arteries from hypertensive rats. *J Hypertens* 27: 1814–1822, 2009.
5. Livak KJ and Schmittgen TD. Analysis of relative gene expression data using real-time quantitative PCR and the 2(-Delta Delta C(T)) Method. *Methods* 25: 402–408, 2001.

Article 3: Role of COX-2/mPGES-1/EP_1 Axis on Vascular Remodeling in Hypertension

Avendaño MS*, Martínez-Revelles S*, Simões MR, Aguado A, Aras-López R, Íñiguez MA, Cachofeiro MV, Vassallo DV, Salaices M, Briones AB

To be submitted to *Hypertension*.

ROLE OF COX-2/mPGES-1/EP_1 AXIS ON VASCULAR REMODELING IN HYPERTENSION

Avendaño MS*[1], Martínez-Revelles S*[1], Simões MR[1,4], Aguado A[1], Aras-López R[1], Íñiguez MA[2], Cachofeiro MV[3], Vassallo DV[4], Salaices M[1&], Briones AB[1&]

[*]These authors contributed equally

[&]Corresponding authors

[1]Departmento de Farmacología, Facultad de Medicina, Universidad Autónoma de Madrid, Instituto de Investigación Hospital Universitario La Paz (IdiPAZ), 28029, Madrid, Spain; [2]Departamento de Biología Molecular and Centro de Biología Molecular "Severo Ochoa", Universidad Autónoma de Madrid and CSIC, Spain [3]Departamento de Fisiología, Facultad de Medicina, Universidad Complutense, 28040, Madrid, Spain. [4]Department of Physiological Sciences, Federal University of Espirito Santo, Vitoria, ES, Brazil

Corresponding authors:

Mercedes Salaices: mercedes.salaices@uam.es

Ana M. Briones: ana.briones@uam.es

Department of Pharmacology. Faculty of Medicine

Universidad Autónoma de Madrid

Arzobispo Morcillo 4, 28029 Madrid, Spain

Phone: 34914975399. Fax: 34914975380

Short title: COX-2/mPGES-1/EP1 axis in vascular remodeling in hypertension

Abstract

Prostanoids from cyclooxygenase (COX)-2 and microsomal prostaglandin E synthase (mPGES)-1 and prostaglandin E_2 receptors (EP) contribute to vascular remodeling in different cardiovascular pathologies but its role in hypertension is less known. Spontaneously hypertensive rats (SHR) and Angiotensin II (AngII) infused mice were treated with the COX-2 inhibitor celecoxib or with the EP1 receptor antagonist SC19220. COX-2 deficient mice infused or not with AngII were also used. Function and structure of conductance and resistance arteries was evaluated. Celecoxib treatment did not modify the altered structural parameters (lumen diameter and wall:lumen ratio) observed in mesenteric resistance arteries from SHR or AngII-infused animals but restored structural changes in aorta from AngII-infused mice. Celecoxib treatment and COX-2 deficiency improved the increased vascular stiffness and the diminished wall distensibility observed in mesenteric resistance arteries from SHR and AngII-infused mice. This was accompanied with decreased vascular fibrosis since diminished collagen deposition, normalization of altered elastin structure and decreased connective tissue growth factor, tenascin-C and plasminogen activator inhibitor-1 gene expression were observed after COX-2 inhibition. Hypertensive animals showed increased vascular mPGES-1 expression that was normalized by celecoxib. SC19220 treatment did not modify vessel structure but normalized the alterations in vascular stiffness, wall distensibility, collagen deposition and elastin structure after AngII infusion. COX-2 deficiency and SC19220 treatment also diminished the increased vasoconstrictor responses and the endothelial dysfunction induced by AngII. These results suggest that the COX-2/mPGES-1/EP_1 axis modulates ECM deposition, mechanical properties and vascular function in hypertension.

Keywords: COX-2, mPGES-1, EP1, stiffness, extracellular matrix, vascular function

Introduction

Hypertension is characterized by the development of functional and structural alterations of the vasculature such as increased vasoconstrictor responses, endothelial dysfunction and increased wall to lumen ratio with increased or unaltered wall tissue amount (Levy *et al*. 2008; Mulvany 2008; Rizzoni and Agabiti-Rosei. 2012; Schiffrin. 2012). The mechanisms responsible of the altered vessel structure, also termed vascular remodeling, are a matter of intense debate and both the increase in blood pressure and the prolonged vasoconstriction have been proposed as main stimulus responsible for inward remodeling (Prewitt *et al*. 2002; Bakker *et al*. 2004; Martinez-Lemus *et al*. 2011; Rizzoni and Agabiti-Rosei. 2012). The cellular processes underlying these events are alterations in cell growth, migration, differentiation, and increased extracellular matrix (ECM) deposition (Mulvany 2008; Levy *et al*. 2008; Briones *et al*. 2010; Rizzoni and Agabiti-Rosei. 2012 ; Anwar *al*. 2012) and in fact, these modifications besides of changing the structure of the vessels, modify the mechanical properties of the arteries increasing vessel stiffness which further contribute to inward remodeling (Prewitt *et al*. 2002; Briones *et al*. 2009; Briones *et al*. 2010; Rizzoni and Agabiti-Rosei. 2012; Schiffrin 2012).

It is well known that Angiotensin II (AngII) influences the architecture and integrity of the vascular wall by modulating cell growth and regulating ECM composition (Schiffrin *et al*. 2004; Mulvany 2008; Briones *et al*. 2009). In addition, Ang II is strongly associated with vascular inflammation characterized by marked upregulation of inflammatory proteins such as cyclooxygenase-2 (COX-2). Thus, i*n vitro* and *in vivo* studies have demonstrated that Ang II induces COX-2 expression and prostanoids production in different vascular cell types and vascular beds (Álvarez *et al*. 2007; Beltrán *et al*. 2009; Jaimes *et al*. 2010; Kane *et al*. 2010; Wong *et al*. 2011; Chia *et al*. 2011; Mukherjee *et al*. 2012; Martínez-Revelles *et al*. 2013). In addition, COX-2 is upregulated in different vascular beds from spontaneously hypertensive

rats (SHR) (Álvarez *et al.* 2007; Bagnost *et al.* 2010; Hernanz *et al.* 2012; Martínez-Revelles *et al.* 2013) in an Ang II-dependent manner (Álvarez *et al*., 2007).

Besides COX-2, Ang II up-regulates COX-2 downstream proteins such as the inducible isoform of prostaglandin E synthase (PGES), microsomal PGES-1 (mPGEs-1) (Wang *et al.* 2008). The COX-2/mPGES-1 axis generates PGE_2 which plays diverse roles in the vasculature. Specifically, PGE_2 modulates vascular tone through the four receptor subtypes namely EP1-4 (Foudi *et al.* 2012; Kida *et al.* 2013). In addition, recent studies demonstrate that COX-2/mPGES-1/EP is a key mediator of vascular remodeling in different pathological situations such as atherosclerosis, aneurysms and restenosis (Cipollone *et al.* 2004; Yang et al., 2004; Wang *et al.* 2008, 2011; Cao *et al.* 2012; King *et al.* 2006; Gitlin *et al.* 2007; Zhang et al. 2013; Chen et al., 2013) although its role in vascular remodeling in hypertension is unknown. Importantly, these effects of PGE_2 on vascular function and structure might have a role in the control of blood pressure since the lack of EP_1 receptor blunts acute pressure response to Ang II and reduces chronic Ang II-dependent hypertension (Guan *et al.* 2007).

The aim of the present study was to evaluate the contribution of the COX-2/mPGES-1/EP1 axis in vascular function and remodeling in hypertension. We combined pharmacological treatments and genetically modified animal models to demonstrate that in hypertension, PGE_2 derived from COX-2 and mPGES-1 acts on EP1 receptors to damage vascular function and to increase vessel stiffness by facilitating the deposition of different ECM proteins. These effects are responsible, at least in part, of the high blood pressure.

Material and Methods

Animal models

The following groups of C57BL6 male mice were used: 1) infused with Ang II (1.44 mg/Kg/day, 2 weeks, subcutaneously by osmotic minipumps, Alza Corp., CA, USA); 2) infused with Ang II and the COX-2 inhibitor, celecoxib (25 mg/Kg/day i.p.) and 3) infused with Ang II and the EP_1 inhibitor, SC19220 (10 mg/Kg/day i.p.). All treatments started 24 h before Ang II-infusion. Control animals without treatments were also studied. In another set of experiments, mice were treated with celecoxib 7 days after Ang II infusion.

COX-2-wild-type ($COX\text{-}2^{+/+}$) and COX-2-deficient ($COX\text{-}2^{-/-}$) mice of a hybrid C57BL6×129SV genetic background were obtained from The Jackson Laboratories (B6;129S-Ptgs2tm1Jed/J strain). $COX\text{-}2^{-/-}$ and $COX\text{-}2^{+/+}$ matched controls were produced by crossing the COX-2 heterozygous mutant line. Alzet micro-osmotic pumps were implanted subcutaneously in groups of three month old male mice of the indicated genotypes to deliver 1.44 mg/kg/day Ang II (Sigma-Aldrich) or saline for 4 weeks.

Six-month old male WKY and SHR were also used. SHR rats were divided into two groups: 1) control, 2) treated with celecoxib (25 mg/Kg/day i.p., 3 weeks). In preliminary experiments, we observed that celecoxib treatment did not affect systolic blood pressure or vascular structure and mechanical properties in C56BL6 control mice or in WKY (data not shown).

Blood pressure was measured by tail-cuff pletysmography. All experimental procedures were approved by the Animal Care and Use Committee of our Institution, according to the guidelines for ethical care of experimental animals of the European Community. The study was conducted in accordance with the National Institutes of Health (NIH) Guide for the Care

and Use of Laboratory Animals (NIH Publication No. 85-23, revised 1996) and the current Spanish and European laws (RD 223/88 MAPA and 609/86).

Tissue preparation

Animals were euthanized by CO_2 and aorta and first and third-order branches of the mesenteric artery were dissected free of fat and connective tissue and maintained in cold (4°C) Krebs-Henseleit solution (KHS) (115 mmol/L NaCl, 25 mmol/L$NaHCO_3$, 4.7 mmol/L KCl, 1.2 mmol/L $MgSO_4.7H_2O$, 2.5 mmol/L $CaCl_2$, 1.2 mmol/L KH_2PO_4, 11.1 mmol/L glucose, and 0.01 mmol/L Na_2EDTA) bubbled with a 95% O_2-5% CO_2 mixture. The analysis of vascular structure and function were made on the same day. For immunofluorescence and histology studies arterial segments were fixed with 4% phosphate buffered paraformaldehyde (pH=7.4) for 1 h and washed in three changes of phosphate buffered saline solution (PBS, pH=7.4). After washing, arterial segments were placed in PBS containing 30% sucrose for 20 min, transferred to a cryomold containing Tissue Tek OCT embedding medium and frozen in liquid nitrogen. Tissues were kept at –70ºC until the day of the experiments. Other segments were immediately frozen in liquid nitrogen and kept at –70ºC until the day of the gene expression studies.

Pressure myography

The structural and mechanical properties of mesenteric resistance arteries (MRA) were studied with a pressure myograph (Danish Myo Tech, Model P100, J.P. Trading I/S, Aarhus, Denmark). Vessels were placed on two glass microcannulae and secured with surgical nylon suture. After any small branches were tied off, vessel length was adjusted so that the vessel walls were parallel without stretch. Intraluminal pressure was then raised to 120 mmHg in mice and 140 mmHg in rats, and the artery was unbuckled by adjusting the cannulae. The segment was then set to a pressure of 45 mmHg in mice and 70 mmHg in rats, and allowed to

equilibrate for 60 min at 37°C in calcium-free KHS ($0Ca^{2+;}$ omitting calcium and adding 1 mM EGTA) intravascular and extravascular perfused, gassed with a mixture of 95% O_2 and 5% CO_2. Intraluminal pressure was reduced to 3 mmHg. A pressure-diameter curve was obtained by increasing intraluminal pressure in 20 mmHg steps from 3 to 120 mmHg in mice and from 3 to 140 mmHg in rats. Internal and external diameters were continuously measured under passive conditions (D_{i0Ca}, D_{e0Ca}) for 3 min at each intraluminal pressure. The final value used was the mean of the measurements taken during the last 30 s when the measurements reached a steady state. Finally, the artery was set to 45 mmHg in mice and 70 mmHg in rats in $0Ca^{2+}$-KHS and then pressure-fixed with 4% paraformaldehyde (PFA; in 0.2 M phosphate buffer, pH 7.2–7.4) at 37°C for 60 min and kept in 4% PFA at 4°C for confocal microscopy studies.

Calculation of passive structural and mechanical parameters

From internal and external diameter measurements in passive conditions the following structural and mechanical parameters were calculated:

$$\text{Wall thickness (WT)} = (D_{e0Ca} - D_{i0Ca})/2$$

$$\text{Cross-sectional area (CSA)} = (\pi/4) \times (D_{e0Ca}^{2} - D_{i0Ca}^{2})$$

$$\text{Wall:lumen} = (D_{e0Ca} - D_{i0Ca})/2D_{i0Ca}$$

Incremental distensibility represents the percentage of change in the arterial internal diameter for each mmHg change in intraluminal pressure and was calculated according to the formula:

$$\text{Incremental distensibility} = \Delta D_{i0Ca}/(D_{i0Ca} \times \Delta P) \times 100.$$

Circumferential wall strain (ε) = $(D_{i0Ca} - D_{00Ca})/D_{00Ca}$, where D_{00Ca} is the internal diameter at 3 mmHg and D_{i0Ca} is the observed internal diameter for a given intravascular pressure both measured in $0Ca^{2+}$ medium.

Circumferential wall stress (σ) = $(P \times D_{i0Ca})/(2WT)$, where P is the intraluminal pressure (1 mmHg = 1.334×10^3 dynes·cm^{-2}) and WT is wall thickness at each intraluminal pressure in $0Ca^{2+}$-KHS.

Arterial stiffness independent of geometry is determined by the Young's elastic modulus (E =stress/strain). The stress-strain relationship is non-linear; therefore, it is more appropriate to obtain a tangential or incremental elastic modulus (E_{inc}) by determining the slope of the stress-strain curve ($E_{inc} = \delta\sigma/\delta\varepsilon$). Einc was obtained by fitting the stress-strain data from each animal to an exponential curve using the equation: $\sigma = \sigma_{orig} e^{\beta\varepsilon}$, where σ_{orig} is the stress at the original diameter (diameter at 3 mmHg). Taking derivatives on the equation presented earlier, we see that $E_{inc} = \beta\sigma$. For a given σ-value, E_{inc} is directly proportional to β. An increase in β implies an increase in E_{inc}, which means an increase in stiffness.

Confocal microscopy study of nuclei distribution

Pressure-fixed intact arteries were incubated with the nuclear dye Hoechst 33342 (0.01 mg·mL^{-1}) for 15 min. After being washed, the arteries were mounted on slides with a well made of silicon spacers to avoid artery deformation. They were viewed using a Leica TCS SP2 confocal system fitted with an inverted microscope and argon and helium-neon laser sources with oil immersion lens (×63, zoom 2) (Ex 351–364 nm and Em 400–500 nm). At least two serial optical sections (stacks of images) of 0.5 µm thick serial optical slices were taken from the adventitia to the lumen in different regions along the artery length. Thereafter, individual projections of the vessel were reconstructed with Metamorph image analysis software (Universal Imaging, Molecular Devices Corp., Downingtown, PA,USA) and used

for quantification. The nuclei numbers were measured in Z-axis as previously described (Arribas *et al*; 1997) with minor modifications.

To allow comparison among the different groups, the following calculations were performed on segments 1 mm long: artery volume (in mm^3) (volume = wall CSA (mm^2) × 1 mm); total number of adventitial and smooth muscle cells (cell n = *n* of nuclei per stack × *n* of stacks per artery volume); total number of endothelial cells (EC) was calculated per luminal surface of 1-mm-long artery; luminal surface area =2πdiameter/2.

Organization of internal elastic lamina

The elastin organization within the internal elastic lamina was studied in segments of small mesenteric arteries, using fluorescence confocal microscopy based on the autofluorescent properties of elastin (excitation wavelength 488 nm and emission wavelength 500–560 nm) as previously described (Briones *et al*; 2003). Briefly, the experiments were performed in intact pressure-fixed segments with a Leica TCS SP2 confocal system. Serial optical sections from the adventitia to the lumen (z step = 0.5 μm) were captured with a X63 oil objective (Zoom 4 in mice, and Zoom 2 in rats), using the 488 nm line of the confocal microscope. A minimum of two stacks of images of different regions was captured in each arterial segment. Quantitative analysis of the internal elastic lamina was performed with Metamorph Image Analysis Software, as previously described (Briones *et al*., 2003). From each stack of serial images, individual projections of the internal elastic lamina were reconstructed, and total fenestrae number and fenestra area were measured.

Collagen determination

Mesenteric arteries and hearts were fixed in 4% sodium-buffered formaldehyde and embedded in Tissue Tek OCT medium as described above. Tissues were cut into 5 μm

sections using a cryostat. Collagen was quantified in Picro-sirius red-stained sections [0.1% (wt/vol) Sirius red 3FB in saturated aqueous picric acid] for 30 min with gentle agitation]. Three-four sections for each animal were analyzed with a 40X objective lens under microscopy transmitted light (Leica DM 2000) using an Image System Analysis (Leica; LAS). The area of collagen in the media layer was identified after excluding perivascular fibrosis of the vessel as the ratio of collagen deposition to the total media area.

Histological analysis

Aortas were fixed with 4% paraformaldehyde and embedded in Tissue Tek OCT medium. 14-µm cross sections from fixed aortas were stained with hematoxylin-eosin. All images were acquired at room temperature using a microscope (DM2000; Leica) with 10× objective. Morphometric determinations of the lumen and vessel areas were performed by using Metamorph image analysis software. All microscopic images of the sections were traced for the calculations of the areas. To determine the luminal area, the cross-sectional area enclosed by the internal elastic lamina was corrected to a circle by applying the form factor $l^2/4\pi$ to the measurement of the internal elastic lamina, where l is the length of the lamina. Vessel area was determined by the cross-sectional area enclosed by the external elastic lamina corrected to a circle, applying the same form factor ($l^2/4\pi$) to the measurement of the external elastic lamina. The media area was calculated as the difference between the corrected vessel and luminal areas. Internal and external diameters were calculated from luminal and vessel areas, respectively. This method avoids miscalculations of areas caused by eventual collapse of the immersion-fixed arteries.

RT-PCR assay

Connective tissue growth factor (CTGF), plasminogen activator inhibitor-1 (PAI-1), tenascin C, vimentin, mPGEs-1 and cyclophilin mRNA levels were determined in rat aortic

homogenates. mPGEs-1 and β_2-microglobulin mRNA levels were analyzed in mice aortic homogenates. Total RNA was obtained by using TRIzol (Invitrogen Life Technologies, Philadelphia, PA, USA). A total of 1 μg of DNAse I treated RNA was reverse-transcribed into cDNA using TaqMan® Reverse Transcription Reagents in a final volume of 10 μl. qPCR for CTGF, PAI-1 and vimentin were performed using Taqman Gene Expression Assays (CTGF: Rn00573960_m1; PAI-1: Rn00578319_m1; vimentin: Rn00579738_ml in rats, Applied Biosystems, Foster City, CA, USA). qPCR for Tn-C and mPGEs-1 in rats, and mPGEs-1 in mice, were performed using the fluorescent dye SyBRGreen (iTaq FAST SyBRGreen Supermix with ROX, Bio-Rad, USA). As normalizing internal controls we amplified cyclophilin in rats and β_2-microglobulin in mice, as housekeeping genes. All qPCRs were performed in duplicate. Primers sequences are: Tn-C in rat (FW: ACCTCTCTGGAATTGCTCCCA; RW: CATCTGAAACTAGAAGGTTGTC), mPGES-1 in rat (FW: AGGAGTGACCCAGATGTG; RW: ATGTATCCAGGCGATGAGA), cyclophilin in rat (FW: GGAGATGGCACAGGAGGAA; RW: ATAGTGCTTCAGCTTGAAGTTCTCAT), mPGES-1 in mouse (FW: AGGATGCGCTGAAACGTGGAG; RW: CCGAGGAAGAGGAAAGGATAG) and β_2-microglobulin in mouse ((FW: ACCCTGGTCTTTCTGGTGCTT; RW: TAGCAGTTCAGTATGTTCGGCTT). Quantification was performed on a 7500 Fast (Applied Biosystems). PCR cycles proceeded as follows: initial denaturation for 30 s at 95°C, followed by 40 cycles at 95°C for 5 s, 60°C for 30 s. At the end of the PCR, a melting curve analysis was performed to show the specificity of the product detected. To calculate the relative index of gene expression, we employed the $2^{-\Delta\Delta Ct}$ method using untreated samples as calibrator.

Immunofluorescence

Immunolocalization for mPGES-1 was performed in aortic sections. Briefly, frozen transverse sections (14 µm) were cut on to gelatin-coated slides and air-dried for at least 60 min. After blockade, sections were incubated with a polyclonal antibody against mPGES-1 (1:100, Cayman) in PBS containing 2% BSA for 1 h at 37ºC in a humidified chamber. After washing, rings were incubated with the secondary antibody, an anti-rabbit IgG conjugated to Cy^{TM}3 (1:200) (Jackson Immunoresearch Laboratories, Inc., West Grove, PA, USA) for 1 h at 37ºC in a humid box. After washing, immunofluorescent signals were viewed using an inverted Leica TCS SP2 confocal laser scanning microscope with oil immersion lens (x40). Cy^{TM}3 labelled antibody was visualized by excitation at 561 nm and detection at 600-700 nm. The specificity of the immunostaining was evaluated by omission of the primary antibody and processed as above. Under these conditions, no staining was observed in the vessel wall.

Reactivity Experiments

Reactivity of mouse aorta and first-order branches of the mesenteric artery was studied in a wire myograph. After a 30-min equilibration period in oxygenated Krebs Henseleit solution (KHS), arterial segments were stretched to their optimal lumen diameter for active tension development. Contractility of segments was then tested by an initial exposure to a high-K^+ solution (K^+-KHS, 120 mmol/L). The presence of endothelium was determined by the ability of 10 µmol/L ACh to relax arteries precontracted with phenylephrine at approximately 50% K^+-KHS contraction. Afterwards, concentration-response curves to acetylcholine, phenylephrine and DEA-NO were performed. The effect of SC19220 was analyzed by its addition 30 min before the phenylephrine concentration-response curves. A single concentration-dependent curve was performed in each segment.

Vasoconstrictor responses were expressed as a percentage of the tone generated by K^+-KHS. Vasodilator responses were expressed as a percentage of the previous tone generated by phenylephrine.

Data Analysis and Statistics

All data are expressed as mean values ± SEM and *n* represents the number of animals. Results were analyzed by using unpaired Student's *t*-test or one-way or two-way ANOVA followed by Bonferroni's *post hoc* test. A $p<0.05$ was considered significant.

Results

Role of COX-2 derived prostanoids in vascular remodeling and mechanical alterations in hypertension

As described previously (Martínez-Revelles *et al.*, 2013), Ang II-infused mice showed increased systolic blood pressure (SBP) that was partially prevented by celecoxib treatment (Table 1).

In mesenteric resistance arteries (MRA), lumen and vessel diameters from Ang II-infused mice were reduced when compared with controls (Figures 1A and 1B). Wall thickness (data not shown) and wall:lumen ratio (Figure 1C) were increased and cross-sectional area was unaffected (data not shown) by Ang II administration. In aorta, vessel diameter, media thickness, media:lumen ratio and cross-sectional area were increased in Ang II-infused mice compared with controls whereas lumen diameter was unaffected (Figure S1). Celecoxib treatment did not modify the effects of Ang II in structural parameters in MRA (Figure 1), but restored all the structural parameters in aorta (Figure S1). Ang II decreased the number of smooth muscle and endothelial cells but did not affect adventitial cells number (Figures 1D,

1E and 1F). Celecoxib treatment restored the altered smooth muscle and endothelial cells number (Figures 1D-F).

Vessel from Ang II-infused mice showed reduced incremental distensibility (Figure 2A) and increased vessel stiffness, as shown by the leftward shift of the stress-strain relationship (Figure 2B) and the larger value of β (β untreated control: 4.17±0.10; Ang II: 6.40±0.35; $P<0.05$). Celecoxib treatment abolished these effects of Ang II (Figure 2A and 2B). Thus, β value was smaller in arteries from Ang II plus Celecoxib than in vessels from Ang II-infused mice (β Ang II plus Celecoxib: 4.52±0.15; $P<0.05$ vs Ang II).

We next evaluated the ECM proteins, elastin and collagen. As shown in Figure 2, the mean fenestrae area and the total number of fenestrae were reduced in MRA from Ang II-infused mice (Fig 2C). Celecoxib treatment abolished the differences found in the total number of fenestrae but not in the size of the fenestrae (Figure 2C). Ang II increased collagen content in MRA and celecoxib treatment reduced this effect (Figure 2D). Similar effects were observed in coronary arteries (figure S2A).

To further confirm the role of COX-2 derived prostanoids in the altered vascular mechanics in hypertension, WT ($COX\text{-}2^{+/+}$) and COX-2 knockout mice ($COX\text{-}2^{-/-}$) were infused with Ang II. As shown in Table 1, SBP was similar in untreated $COX\text{-}2^{+/+}$ and $COX\text{-}2^{-/-}$ mice. Ang II infusion increased SBP in both groups (Table 1). At the end of the treatment, SBP was slightly greater in $COX\text{-}2^{-/-}$ compared to $COX\text{-}2^{+/+}$ mice (Table 1). As shown in Figure S2B, left ventricular hypertrophy was greater in untreated $COX\text{-}2^{-/-}$ compared to $COX\text{-}2^{+/+}$. $COX\text{-}2^{+/+}$ Ang II-infused mice exhibited an augmented left ventricular hypertrophy with respect to their untreated mice. However, when $COX\text{-}2^{-/-}$ mice were infused with Ang II, there was no difference in left ventricular hypertrophy between both groups (Figure 2SB). Compared to $COX\text{-}2^{+/+}$ animals, vessels from $COX\text{-}2^{-/-}$ mice showed smaller incremental distensibility at

low pressures (data not shown) and increased stiffness (Figure 3B, β COX-$2^{+/+}$: 4.28±0.07; β COX-$2^{-/-}$: 4.93±0.15, P<0.05). Ang II infusion decreased incremental distensibility in COX-$2^{+/+}$ but not in COX-$2^{-/-}$ mice (Figures 3A). In addition, Ang II increased vascular stiffness in COX-$2^{+/+}$ mice (COX-$2^{+/+}$ plus Ang II: 5.07±0.15; *P*<0.05 vs COX-$2^{+/+}$) but not in COX-$2^{-/-}$ (COX-$2^{-/-}$ plus Ang II: 5.14±0.19) (Figure 3B). Fenestrae area was similar (Figure 3C) and fenestrae number was smaller (Figure 3D) in COX-$2^{-/-}$ compared to COX-$2^{+/+}$ mice. Ang II infusion reduced the fenestrae area in COX-$2^{+/+}$ mice but not in COX-$2^{-/-}$ mice (Figure 3C). In addition, Ang II decreased fenestrae number in COX-$2^{+/+}$ but increased it in COX-$2^{-/-}$ mice (Figure 3C). Thus, fenestrae number was greater in Ang II infused COX-$2^{-/-}$ mice than COX-$2^{+/+}$ (Figure 3C). There were no differences in collagen deposition in MRA from COX-$2^{-/-}$ compared to COX-$2^{+/+}$ mice (Figure 3D). Ang II increased collagen deposition in the media of the COX-$2^{+/+}$ animals but not in the COX-$2^{-/-}$ mice (Figure 3D).

All together these findings suggest that COX-2 blockade prevents, at least in part, Ang II-induced vascular remodeling and mechanical alterations by affecting ECM proteins such as collagen and elastin.

We next aimed to elucidate whether COX-2 blockade might reverse vascular remodeling and/or mechanical alterations in established hypertension. Thus, we analyzed the effects of celecoxib when administered 7 days after the beginning of Ang II infusion as well as its effects in SHR, a model of established hypertension. As previously reported (Martínez-Revelles, *et al.* 2013), celecoxib treatment decreased SBP of Ang II-infused mice (Table 1). This celecoxib treatment did not affect the decreased lumen and vessel diameters (data not shown), the increased wall thickness (data not shown) or the increased wall:lumen ratio (Figure 4A) but normalized the decreased incremental distensibility and the augmented stiffness observed after Ang II infusion (Figures 4B and 4C) (β Untreated: 3.77±0.13; Ang II: 6.26±0.54; *P*<0.05; Ang II+Celecoxib: 4.07±0.31; *P*<0.05). Additionally, this celecoxib

treatment did not restore the decreased fenestrae area but normalized the decreased fenestrae number and the increased collagen deposition induced by Ang II (Figures D and E).

As expected, MRA from SHR showed decreased lumen and vessel diameters (Figures 5A and 5B), increased wall thickness (data not shown), and increased wall:lumen ratio (Figure 5C) when compared with WKY. As previously reported (Martínez-Revelles, *et al.* 2013), celecoxib treatment decreased SBP of SHR (Table 1). However, celecoxib treatment did not modify these structural parameters (Figure 5A-C). Vessel from SHR also showed reduced incremental distensibility (Figure 6A) and increased stiffness (Figure 6B) (β WKY: 4.77±0.14; SHR: 6.40±0.17; $P<0.05$) compared to WKY. Celecoxib treatment slightly improved the diminished incremental distensibility (Figure 6A) and the increased vessel stiffness when compared with untreated SHR (Figure 6B, β SHR plus Celecoxib: 5.57±0.20; $P<0.05$). The mean fenestrae area and the total number of fenestrae were diminished in SHR compared to WKY and celecoxib treatment abolished these differences (Figure 6C). Collagen deposition was greater in MRA from SHR compared to WKY and celecoxib treatment normalized this effect (Figure 6D). We then evaluated other profibrotic genes in the SHR model. As shown in Figure 7, aortic Tenascin-C, CTGF and PAI-1 gene expression were increased in SHR compared with WKY and celecoxib treatment normalized this expression (Figures 7A-C). Similar results were observed for the fibroblasts marker vimentin (Figure 7D).

All together, these data demonstrate that COX-2 has a role in extracellular matrix deposition in hypertension that in turns determines vascular stiffness.

Role of mPGEs-1 and EP_1 receptor in vascular remodeling in hypertension

We next explored the role of mPGES-1 and EP1 receptors in the vascular alterations induced by hypertension. As shown in Figure 8A, mPGES-1 was highly expressed in the media layer

of the Ang II infused mice. In addition, Ang II-infused mice exhibited larger aortic mPGES-1 gene expression that control mice and celecoxib treatment normalized this increase (Fig 8B). Interestingly, SHR aorta also showed increased mPGES-1 expression compared to WKY and celecoxib treatment decreased this expression (Figure 8C).

The treatment with the EP1 inhibitor SC19220 prevented the increased SBP induced by Ang II infusion (Table 1) but it did not modify the altered structure neither in MRA (data not shown) nor in aorta (Figure 9A and Figure S1). However, SC19220 treatment improved the diminished incremental distensibility and the increased stiffness induced by Ang II (β untreated: 3.77±0.13; Ang II: 6.26±0.54; $P<0.05$; Ang II plus SC19220: 4.42±0.14; $P<0.05$) (Figures 9B and 9C). Moreover, the diminished fenestrae area and number (Figure 9D) and the increased collagen content (Figure 9E) were significantly improved by SC19220 treatment.

These results indicate that PGE_2 probably derived from the COX-2/mPGEs-1 axis in response to Ang II acts on EP_1 to induce changes in vascular stiffness and collagen and elastin deposition.

Role of COX-2/EP$_1$ receptor in the altered vascular function in Ang II-induced hypertension

We have previously described that COX-2 inhibition with celecoxib improves vascular dysfunction induced by Ang II (Martínez-Revelles *et al.,* 2013). Herein, we aim to evaluate whether the beneficial effect induced by pharmacological COX-2 blockade would be also observed in COX-$2^{-/-}$ mice. Ang II infusion to COX-$2^{+/+}$ mice increased vasoconstrictor responses to phenylephrine both in MRA and aorta and diminished the vasodilator response to acetylcholine only in aorta (Figure S3). COX-2 deficiency prevented these effects (Figure

S3). Endothelium-independent relaxation to diethylamine NONOate (DEA-NO) was similar in all groups (data not shown).

In our previous study, we demonstrated that SC19920 when added *in vitro* to the organ bath decreased the Ang II-induced increase in phenylephrine responses in aorta and this effect was dependent on COX-2 (Martínez-Revelles *et al.*, 2013). This was confirmed in the present study in MRA since *in vitro* SC19220 administration decreased the vasoconstrictor response induced by phenylephrine in Ang II-infused mice but not in control mice (Figure S4A). In addition, celecoxib treatment abolished this effect (Figure S4A). When administered *in vivo*, SC19220 not only improved the increased vascular contractile responses induced by Ang II, but also abolished the Ang II-dependent endothelial dysfunction (Figure S4B and S4C). Endothelium-independent relaxation to diethylamine NONOate (DEA-NO) was not modified by Ang II infusion or by SC19220 treatment (Figure S4D).

These results indicate that PGE_2 derived from COX-2 in response to Ang II acts on EP_1 to induce increased contractile responses and endothelial dysfunction.

Discussion

The major novel finding of this study is that the COX-2/mPGES-1/EP_1 axis contribute to the mechanical alterations associated to hypertension by modulating ECM deposition. In addition, we demonstrate that this pathway is responsible of the increased vasoconstrictor and the diminished vasodilator responses that might contribute to vascular remodeling and hypertension development.

Ang II is involved in the genesis and progression of hypertension by inducing accumulation of ECM proteins such as collagen and by altering elastin structure. This determines altered vascular dimensions and mechanical properties (Rupérez *et al.* 2007; Briones *et al.* 2009; Virdis *et al.* 2012). COX-2 expression and prostanoids production are induced by Ang II in

different vessels and vascular cell types (Álvarez *et al.* 2007; Beltrán *et al.* 2009; Wong *et al*., 2010; Martínez-Revelles *et al.* 2013) and is highly expressed in vessels from hypertensive patients or animals models (Álvarez *et al.* 2007; Tian *et al.* 2012; Martínez-Revelles *et al.* 2013, Virdis *et al*., 2013) where it participates of vascular dysfunction. Our results demonstrate that COX-2 derived prostanoids are responsible of mechanical vascular alterations in hypertension by modulating ECM deposition. This is based on the fact that in two different models of hypertension, COX-2 blockade with celecoxib reduced the increased vascular stiffness, the diminished vascular distensibility, the increased collagen deposition and the altered elastin structure observed in resistance arteries. In this line of evidence, COX-$2^{-/-}$ mice were resistant to Ang II-induced vascular stiffness and ECM alterations. Our results are in agreement with previous data demonstrating that COX-2 derived products participate in the increased collagen levels observed in different tissues such as the infarcted (LaPointe *et al.* 2004) or the diabetic (Kellogg *et al*., 2009) heart. To our knowledge, only one study (Virdis *et al*. 2012) has demonstrated a relationship between COX derived prostanoids and mechanical alterations in hypertension being the COX-1 isoform responsible of such alterations. We do not have a clear explanation to this discrepancy. However, neither the dose of Ang II nor the COX-2 inhibitor, were the same that those used in the present study. An interesting data arising from our study is the fact that in the absence of Ang II, COX-$2^{-/-}$ mice show increased vascular stiffness and altered elastin structure suggesting that COX-2 derived prostanoids are beneficial in basal conditions and that only after an inflammatory challenge as induced by Ang II, COX-2 shifts beneficial prostanoids production to damaging prostanoids production.

Besides of changing collagen and elastin, we demonstrate that prostanoids from COX-2 modulate other profibrotic and proliferative factors in the hypertensive vasculature. Thus, increased expression of CTGF, PAI-1 and tenascin-C gene levels were observed in aorta from

SHR and this was normalized by celecoxib treatment. CTGF is a potent profibrotic and growth factor associated with increased levels of collagen synthesis that is modulated by prostanoids in renal cells (Chen *et al.* 2013). PAI-1, a major effector and downstream target of TGF-β is affected by COX-2 derived prostanoids in the kidney of a model of hypertension and diabetes (Cheng *et al.* 2002). Tenascin-C regulates cell proliferation and migration and matrix organization during tissue remodelling and seems to be modulated by COX-2 and mPGES-1 derived prostanoids (Wang *et al*., 2011, Chen *et al*., 2013). The increase of vimentin expression observed in SHR suggests a higher proportion of fibroblasts that might further contribute to the increased ECM deposition in this strain. This was restored by celecoxib treatment suggesting that COX-2 prostanoids can modulate fibroblast recruitment. In agreement, reduced cell invasion and fibroblast proliferation in infarcted tissue of rats treated with rofecoxib was observed (Scheuren *et al*., 2002).

A role for COX-2 have also been demonstrated in vascular remodeling in other pathological situations such as atherosclerosis, aneurysm and restenosis (Cipollone *et al.* 2004; Yang *et al*., 2004; Wang *et al.* 2008; King *et al.* 2006; Gitlin *et al.* 2007; Zhang *et al*. 2013).We did not observe improved vascular structure (wall:lumen or diameters) in Ang II-infused or in SHR MRA. However, we found improved vascular structure in aorta after COX-2 blockade. It is plausible that the different vascular beds might undergo different remodeling processes probably in response to differences in intravascular pressure (Prewitt *et al*. 2002). In agreement, we observed that Ang II induces hypertrophic remodeling in aorta but eutrophic remodeling is observed in MRA. Similar differences among vessels types are found in the SHR, being hypertrophic remodeling observed in aorta (Sanz-Rosa *et al*., 2005) and eutrophic remodeling observed in MRA (present results, Briones *et al*., 2003).

Similarly to COX-2, increased mPGES-1 expression or PGE_2 levels have been involved in pathological vascular remodeling processes such as atherosclerosis, restenosis and aneurisms

(Cipollone *et al.* 2004; Gómez-Hernández *et al*., 2006; Wang *et al.* 2008; Cipollone *et al*. 2008; Wang *et al*., 2011; Zhang *et al*., 2013). Ang II can enhance PGE_2 generation as a consequence of mPGES-1 induction (Cipollone *et al.* 2004; Wang *et al.* 2008). This would be consistent with the hypothesis that mPGES-1 and COX-2 could be coregulated, and that stimulated PGE_2 synthesis may depend on upregulation of both enzymes (Cipollone *et al.* 2008). Accordingly, we observed an increase in the vascular levels of mPGES-1, both in Ang II infused mice and in SHR, that was abolished by celecoxib treatment indicating that COX-2 derived products are able to regulate mPGES-1 levels. In agreement, the induction of mPGES-1 in macrophages seem to be regulated through a positive feedback loop dependent on PGE_2 binding to EP4 (Khan *et al*., 2012).

PGE_2 via EP receptor subtypes has important actions in the cardiovascular system by controlling vascular tone and cell adhesion (Foudi *et al.* 2012). Patients with carotid atherosclerosis depict an overexpression of EPs in the vulnerable region of plaques (Gómez-Hernández *et al.* 2006). Recently, a role for EP3 receptor has been demonstrated in neointima hyperplasia (Zhang *et al*., 2013). Regarding ECM synthesis, EP4 receptor activation increases fibrosis in the kidney (Mohamed et al., 2013). Herein, we report for the first time that the EP_1 receptor blocker SC19220 normalized the altered mechanical properties, collagen deposition and altered elastin structure induced by Ang II infusion in MRA. Nevertheless, SC19220 did not modify structural parameters, neither in MRAs nor aorta from Ang II infused mice probably reflecting the already described role of thromboxane receptors (TP) in these alterations (Virdis *et al*., 2012; Sparks *et al*., 2013). All together, these results suggest that different prostanoids acting on different receptor subtypes might have varying roles in vascular remodeling in hypertension being the COX-2/mPGES-1/EP1 axis a key factor in vascular mechanical alterations in Ang II induced hypertension.

It is now evident that vascular remodeling in hypertension is a complex process influenced by a variety of processes including hemodynamic, humoral, immune or vasoactive factors among others (Schiffrin 2012, Prewitt *et al.* 2002; Rizzoni and Agabiti-Rosei. 2012). In this and in our previous study (Martínez-Revelles *et al.* 2013), we observed that the treatment of Ang II infused mice or SHR with celecoxib or with SC19220, prevented or decreased in part, high blood pressure, which is in agreement with previous reports (Guan *et al.* 2007; Tian *et al.* 2012). This suggests that decreased blood pressure might be responsible at least in part, of the improved vascular mechanics. Alternatively, improved vascular mechanics can contribute to decrease blood pressure in hypertension. However, COX-$2^{-/-}$ mice were not protected against Ang II induced hypertension probably reflecting the contribution of other organs or systems or differences attributable to genetic backgrounds (Yang *et al.* 2004). It has also been postulated that vascular remodeling in hypertension would be reflection of prolonged exposition of the vessels to vasoconstrictors (Prewitt *et al.* 2002; Bakker *et al.* 2004; Martinez-Lemus *et al.*, 2011; Rizzoni and Agabiti-Rosei. 2012). Vasoconstrictor prostanoids from COX-2 are increased in different models or patients with hypertension (Widlansky *et al.*, 2003; Álvarez *et al.* 2007; Virdis *et al.*, 2009; Wong *et al.*, 2011; Tian *et al.*, 2012; Martínez-Revelles *et al.* 2013; Virdis *et al.*, 2013) and are involved in the endothelial dysfunction observed in this pathology (Widlansky *et al.*, 2003; Virdis *et al.*, 2009; Tian *et al.*, 2012; Martínez-Revelles *et al.* 2013). Herein we confirmed our hypothesis that Ang II induces COX-2-dependent contractile prostanoids production that impairs vascular function (Martínez Revelles *et al.*, 2013). Thus, COX-$2^{-/-}$ mice were protected from the deleterious effect of AngII in vascular contraction and relaxation. In addition, we demonstrate a key role for EP1 in these vascular functional alterations since treatment of the mice with EP1 antagonist also restored the increased vasoconstriction and the diminished vasodilation induced by Ang II. In

agreement, EP_1 receptor is involved in an increase in SBP and in vasoconstrictor response by Ang II (Guan *et al.* 2007).

In conclusion, our results suggest that the COX-2/mPGES-1/EP_1 axis is involved in the development of vascular remodeling in hypertension acting through changes in ECM deposition that might be influenced by the increased systolic blood pressure and vasoconstrictor responses.

Perspectives

Hypertension is an inflammatory disease, characterized by the development of functional and structural alterations in the vasculature. Prostanoids play an important role in the regulation of blood pressure and have been involved in vascular remodeling in other pathological situations such as atherosclerosis, aneurysm and restenosis. Our results provide novel evidences suggesting the implication of COX-2/mPGES in hypertension and the role of COX-2/EP_1 in vascular remodeling in hypertension. Thus we propose that the control of EP_1 receptor has a potential utility as therapeutic target.

Acknowledgements

The authors thank the Animal Care Facility of the Faculty of Medicine of UAM.

Sources of Funding

Ministerio de Economía y Competitividad (SAF2009-07201, SAF2011-23800), Instituto de Salud Carlos III (RD06/0014/0011, RD12/0042/0024), UAM-Grupo Santander, Fundación Mutua Madrileña and the Ramón y Cajal program (AMB, RYC-2010-06473).

Conflicts of Interest/Disclosure

None

References

Álvarez Y, Pérez-Girón JV, Hernanz R, Briones AM, García-Redondo A, Beltrán A, Alonso MJ, Salaices M. Losartan reduces the increased participation of cyclooxygenase-2-derived products in vascular responses of hypertensive rats. J *Pharmacol Exp Ther.* 321(1):381-8. 2007.

Álvarez Y, Briones AM, Hernanz R, Pérez-Girón JV, Alonso MJ, and Salaices M. Role of NADPH oxidase and iNOS in vasoconstrictor responses of vessels from hypertensive and normotensive rats. Br J Pharmacol 153: 926–935. 2008.

Anwar MA, Shalhoub J, Lim CS, Gohel MS, Davies AH. The effect of pressure-induced mechanical stretch on vascular wall differential gene expression. *J Vasc Res.* 49(6):463-78. 2012.

Arribas SM, González C, Graham D, Dominiczak AF, McGrath JC. Cellular changes induced by chronic nitric oxide inhibition in intact rat basilar arteries revealed by confocal microscopy. *J Hypertens.*15(12 Pt 2):1685-93. 1997.

Bagnost T, Ma L, da Silva RF, Rezakhaniha R, Houdayer C, Stergiopulos N, André C, Guillaume Y, Berthelot A, Demougeot C. Cardiovascular effects of arginase inhibition in spontaneously hypertensive rats with fully developed hypertension. *Cardiovasc Res.* 87(3):569-77. 2010.

Bakker EN, Buus CL, VanBavel E, Mulvany MJ. Activation of resistance arteries with endothelin-1: from vasoconstriction to functional adaptation and remodeling. *J Vasc Res.* 41(2):174-82. 2004.

Beltrán AE, Briones AM, García-Redondo AB, Rodríguez C, Miguel M, Alvarez Y, Alonso MJ, Martínez-González J, Salaices M. p38 MAPK contributes to angiotensin II-induced COX-2 expression in aortic fibroblasts from normotensive and hypertensive rats. *J Hypertens.* 27(1):142-54. 2009.

Briet M, Schiffrin EL. Treatment of arterial remodeling in essential hypertension. *Curr Hypertens Rep*. 2013 Feb;15(1):3-9.

Briones AM, González JM, Somoza B, Giraldo J, Daly CJ, Vila E, González MC, McGrath JC, Arribas SM. Role of elastin in spontaneously hypertensive rat small mesenteric artery remodelling. *J Physiol*. 552(Pt 1):185-95. 2003.

Briones AM, Rodríguez-Criado N, Hernanz R, García-Redondo AB, Rodrigues-Díez RR, Alonso MJ, Egido J, Ruiz-Ortega M, Salaices M. Atorvastatin prevents angiotensin II-induced vascular remodeling and oxidative stress. *Hypertension.* 54(1):142-9. 2009.

Briones AM, Arribas SM, Salaices M. Role of extracellular matrix in vascular remodeling of hypertension. *Curr Opin Nephrol Hypertens.* 19(2):187-94. 2010.

Cao RY, St Amand T, Li X, Yoon SH, Wang CP, Song H, Maruyama T, Brown PM, Zelt DT, Funk CD. Prostaglandin receptor EP4 in abdominal aortic aneurysms. *Am J Pathol.*181(1):313-21. 2012.

Cipollone F, Fazia M, Iezzi A, Pini B, Cuccurullo C, Zucchelli M, de Cesare D, Ucchino S, Spigonardo F, De Luca M, Muraro R, Bei R, Bucci M, Cuccurullo F, Mezzetti A. Blockade of the angiotensin II type 1 receptor stabilizes atherosclerotic plaques in humans by inhibiting prostaglandin E2-dependent matrix metalloproteinase activity. *Circulation.* 109(12):1482-8. 2004.

Cipollone F, Cicolini G, Bucci M. Cyclooxygenase and prostaglandin synthases in atherosclerosis: recent insights and future perspectives. *Pharmacol Ther.* 118(2):161-80. 2008.

Cheng HF, Wang CJ, Moeckel GW, Zhang MZ, McKanna JA, Harris RC. Cyclooxygenase-2 inhibitor blocks expression of mediators of renal injury in a model of diabetes and hypertension. *Kidney Int.* 62(3):929-39. 2002.

Chen L, Yang G, Xu X, Grant G, Lawson JA, Bohlooly-Y M, FitzGerald GA. Cell selective cardiovascular biology of microsomal prostaglandin E synthase-1. *Circulation.* 127(2):233-43. 2013.

Chia E, Kagota S, Wijekoon EP, McGuire JJ. Protection of protease-activated receptor 2 mediated vasodilatation against angiotensin II-induced vascular dysfunction in mice. *BMC Pharmacol.* 11:10. 2011.

Foudi N, Gomez I, Benyahia C, Longrois D, Norel X. Prostaglandin E2 receptor subtypes in human blood and vascular cells. *Eur J Pharmacol.*695(1-3):1-6. 2012.

Gitlin JM, Trivedi DB, Langenbach R, Loftin CD. Genetic deficiency of cyclooxygenase-2 attenuates abdominal aortic aneurysm formation in mice. *Cardiovasc Res.* 73(1):227-36. 2007.

Guan Y, Zhang Y, Wu J, Qi Z, Yang G, Dou D, Gao Y, Chen L, Zhang X, Davis LS, Wei M, Fan X, Carmosino M, Hao C, Imig JD, Breyer RM, Breyer MD. Antihypertensive effects of selective prostaglandin E2 receptor subtype 1 targeting. *J Clin Invest.* 117(9):2496-505. 2007.

Gómez-Hernández A, Martín-Ventura JL, Sánchez-Galán E, Vidal C, Ortego M, Blanco-Colio LM, Ortega L, Tuñón J, Egido J. Overexpression of COX-2, Prostaglandin E synthase-1 and prostaglandin E receptors in blood mononuclear cells and plaque of patients with carotid atherosclerosis: regulation by nuclear factor-kappaB. *Atherosclerosis.* 187(1):139-49. 2006.

Hernanz R, Martín Á, Pérez-Girón JV, Palacios R, Briones AM, Miguel M, Salaices M, Alonso MJ. Pioglitazone treatment increases COX-2-derived prostacyclin production and reduces oxidative stress in hypertensive rats: role in vascular function. *Br J Pharmacol*. 166(4):1303-19. 2012.

Jaimes EA, Hua P, Tian RX, Raij L. Human glomerular endothelium: interplay among glucose, free fatty acids, angiotensin II, and oxidative stress. *Am J Physiol Renal Physiol.* 298(1):F125-32. 2010.

Kane MO, Etienne-Selloum N, Madeira SV, Sarr M, Walter A, Dal-Ros S, Schott C, Chataigneau T, Schini-Kerth VB. Endothelium-derived contracting factors mediate the Ang II-induced endothelial dysfunction in the rat aorta: preventive effect of red wine polyphenols. *Pflugers Arch.* 459(5):671-9. 2010.

Kellogg AP, Converso K, Wiggin T, Stevens M, Pop-Busui R. Effects of cyclooxygenase-2 gene inactivation on cardiac autonomic and left ventricular function in experimental diabetes. *Am J Physiol Heart Circ Physiol*. 296(2):H453-61. 2009.

Kida T, Sawada K, Kobayashi K, Hori M, Ozaki H, Murata T. Diverse effects of prostaglandin E2 on vascular contractility. *Heart Vessels.* 2013. [Epub ahead of print]

King VL, Trivedi DB, Gitlin JM, Loftin CD. Selective cyclooxygenase-2 inhibition with celecoxib decreases angiotensin II-induced abdominal aortic aneurysm formation in mice. *Arterioscler Thromb Vasc Biol.* 26(5):1137-43. 2006.

Khan KM, Kothari P, Du B, Dannenberg AJ, Falcone DJ. Matrix metalloproteinase-dependent microsomal prostaglandin E synthase-1 expression in macrophages: role of TNF-? and the EP4 prostanoid receptor. *J Immunol.* 188(4):1970-80. 2012.

LaPointe MC, Mendez M, Leung A, Tao Z, Yang XP. Inhibition of cyclooxygenase-2 improves cardiac function after myocardial infarction in the mouse. *Am J Physiol Heart Circ Physiol.* 286(4):H1416-24. 2004.

Levy BI, Schiffrin EL, Mourad JJ, Agostini D, Vicaut E, Safar ME, Struijker-Boudier HA. Impaired tissue perfusion: a pathology common to hypertension, obesity, and diabetes mellitus. *Circulation.* 118(9):968-76. 2008.

Martinez-Lemus LA, Zhao G, Galiñanes EL, Boone M. Inward remodeling of resistance arteries requires reactive oxygen species-dependent activation of matrix metalloproteinases. *Am J Physiol Heart Circ Physiol*. 300(6):H2005-15. 2011.

Martínez-Revelles S*, Avendaño MS*, García-Redondo AB, Alvarez Y, Aguado A, Pérez-Girón JV, García-Redondo L, Esteban V, Redondo JM, Alonso MJ, Briones AM, Salaices M. Reciprocal relationship between reactive oxygen species and cyclooxygenase-2 and vascular dysfunction in hypertension. *Antioxid Redox Signal.* 18(1):51-65. 2013.

Mohamed R, Jayakumar C, Ramesh G. Chronic administration of EP4-selective agonist exacerbates albuminuria and fibrosis of the kidney in streptozotocin-induced diabetic mice through IL-6. *Lab Invest.* 93(8):933-45. 2013

Mukherjee K, Gitlin JM, Loftin CD. Effectiveness of cyclooxygenase-2 inhibition in limiting abdominal aortic aneurysm progression in mice correlates with a differentiated smooth muscle cell phenotype. J Cardiovasc Pharmacol. 60(6):520-9. 2012.

Mulvany MJ. Small artery remodelling in hypertension: causes, consequences and therapeutic implications. *Med Biol Eng Comput*. 46(5):461-7. 2008.

Prewitt RL, Rice DC, Dobrian AD. Adaptation of resistance arteries to increases in pressure. *Microcirculation.* 9(4):295-304. 2002.

Rizzoni D, Agabiti-Rosei E. Structural abnormalities of small resistance arteries in essential hypertension. *Intern Emerg Med.* 7(3):205-12. 2012.

Rupérez M, Rodrigues-Díez R, Blanco-Colio LM, Sánchez-López E, Rodríguez-Vita J, Esteban V, Carvajal G, Plaza JJ, Egido J, Ruiz-Ortega M. HMG-CoA reductase inhibitors decrease angiotensin II-induced vascular fibrosis: role of RhoA/ROCK and MAPK pathways. *Hypertension.* 50(2):377-83. 2007.

Sanz-Rosa D, Oubiña MP, Cediel E, De las Heras N, Aragoncillo P, Balfagón G, Cachofeiro V, Lahera V. Eplerenone reduces oxidative stress and enhances eNOS in SHR: vascular functional and structural consequences. *Antioxid Redox Signal.* 7(9-10):1294-301. 2005.

Scheuren N, Jacobs M, Ertl G, Schorb W. Cyclooxygenase-2 in myocardium stimulation by angiotensin-II in cultured cardiac fibroblasts and role at acute myocardial infarction. *J Mol Cell Cardiol.* 34(1):29-37. 2002.

Schiffrin EL, Touyz RM. From bedside to bench to bedside: role of renin-angiotensin-aldosterone system in remodeling of resistance arteries in hypertension. *Am J Physiol Heart Circ Physiol*. 287(2):H435-46. 2004.

Schiffrin EL. Vascular remodeling in hypertension: mechanisms and treatment. *Hypertension*. 2012.

Sparks MA, Makhanova NA, Griffiths RC, Snouwaert JN, Koller BH, Coffman TM. Thromboxane receptors in smooth muscle promote hypertension, vascular remodeling, and sudden death. *Hypertension.* 61(1):166-73. 2013.

Tian XY, Wong WT, Leung FP, Zhang Y, Wang YX, Lee HK, Ng CF, Chen ZY, Yao X, Au CL, Lau CW, Vanhoutte PM, Cooke JP, Huang Y. Oxidative stress-dependent cyclooxygenase-2-derived prostaglandin f(2α) impairs endothelial function in renovascular hypertensive rats. *Antioxid Redox Signal.* 15;16(4):363-73. 2012.

Virdis A, Colucci R, Versari D, Ghisu N, Fornai M, Antonioli L, Duranti E, Daghini E, Giannarelli C, Blandizzi C, Taddei S, and Del Tacca M. Atorvastatin prevents endothelial dysfunction in mesenteric arteries from spontaneously hypertensive rats: role of cyclooxygenase 2-derived contracting prostanoids. Hypertension 53: 1008–1016, 2009.

Virdis A, Colucci R, Neves MF, Rugani I, Aydinoglu F, Fornai M, Ippolito C, Antonioli L, Duranti E, Solini A, Bernardini N, Blandizzi C, Taddei S. Resistance artery mechanics and composition in angiotensin II-infused mice: effects of cyclooxygenase-1 inhibition. *Eur Heart J.* 33(17):2225-34. 2012.

Virdis A, Bacca A, Colucci R, Duranti E, Fornai M, Materazzi G, Ippolito C, Bernardini N, Blandizzi C, Bernini G, Taddei S. Endothelial dysfunction in small arteries of essential

hypertensive patients: role of cyclooxygenase-2 in oxidative stress generation. *Hypertension.* 62(2):337-44. 2013.

Wang M, Lee E, Song W, Ricciotti E, Rader DJ, Lawson JA, Puré E, FitzGerald GA. Microsomal prostaglandin E synthase-1 deletion suppresses oxidative stress and angiotensin II-induced abdominal aortic aneurysm formation. *Circulation.* 117(10):1302-9. 2008.

Wang M, Ihida-Stansbury K, Kothapalli D, Tamby MC, Yu Z, Chen L, Grant G, Cheng Y, Lawson JA, Assoian RK, Jones PL, Fitzgerald GA. Microsomal prostaglandin e2 synthase-1 modulates the response to vascular injury. *Circulation.* 123(6):631-9. 2011.

Widlansky ME, Price DT, Gokce N, Eberhardt RT, Duffy SJ, Holbrook M, Maxwell C, Palmisano J, Keaney JF Jr, Morrow JD, and Vita JA. Short- and long-term COX-2 inhibition reverses endothelial dysfunction in patients with hypertension. *Hypertension.* 42: 310–315, 2003.

Wong SL, Wong WT, Tian XY, Lau CW, and Huang Y. Prostaglandins in action indispensable roles of cyclooxygenase-1 and - 2 in endothelium-dependent contractions. *Adv Pharmacol.* 60: 61–83, 2010.

Wong SL, Lau CW, Wong WT, Xu A, Au CL, Ng CF, Ng SS, Gollasch M, Yao X, Huang Y. Pivotal role of protein kinase Cdelta in angiotensin II-induced endothelial cyclooxygenase-2 expression: a link to vascular inflammation. *Arterioscler Thromb Vasc Biol.* 31(5):1169-76. 2011.

Wong SL, Lau CW, Wong WT, Xu A, Au CL, Ng CF, Ng SS, Gollasch M, Yao X, and Huang Y. Pivotal role of protein kinase Cdelta in angiotensin II-induced endothelial

cyclooxygenase-2 expression: a link to vascular inflammation. *Arterioscler Thromb Vasc Biol.* 31: 1169–1976, 2011.

Yang HM, Kim HS, Park KW, You HJ, Jeon SI, Youn SW, Kim SH, Oh BH, Lee MM, Park YB, Walsh K. Celecoxib, a cyclooxygenase-2 inhibitor, reduces neointimal hyperplasia through inhibition of Akt signaling. *Circulation.* 110(3):301-8. 2004.

Zhang J, Zou F, Tang J, Zhang Q, Gong Y, Wang Q, Shen Y, Xiong L, Breyer RM, Lazarus M, Funk CD, Yu Y. Cyclooxygenase-2-Derived Prostaglandin E2 Promotes Injury-Induced Vascular Neointimal Hyperplasia Through the E-prostanoid 3 Receptor. Circ Res. 113(2):104-14. 2013.

Figure Legends

Figure 1. Lumen and vessel diameter (A,B), wall to lumen ratio (C), total number of adventitial cells (AC) (D), smooth muscle cells (SMC) (E) and endothelial cells (EC) (F) in mesenteric resistance arteries from mice untreated or treated with Angiotensin II (Ang II) or Ang II plus celecoxib. Data represent mean±SEM. n=5-23. *P<0.05, **P<0.01 and ***P<0.001 vs untreated, #P<0.05 and ##P<0.01 vs Ang II.

Figure 2. Incremental distensibility (A) and stress-strain relationships (B) in mesenteric resistance arteries (MRA) from mice untreated or treated with Angiotensin II (Ang II) or Ang II plus celecoxib. C) Representative confocal projections and quantification of fenestra area and total number of fenestra of the internal elastic lamina of MRA from mice untreated or treated with Ang II or Ang II plus celecoxib. Projections were obtained from serial optical sections captured with a fluorescence confocal microscope (×63 objective, zoom ×4); image size: 59.5x59.5 μm. (D) Representative images and quantitative analysis of collagen content in the media layer from transversal sections of MRAs from mice untreated or treated with Ang II or Ang II plus celecoxib. Images were captured with a light microscope (×40 objective); image size: 310.9x233.1 μm. Data represent mean±SEM. n=7-23. *P<0.05 and ***P<0.001 vs untreated, #P<0.05 and ###P<0.001 vs Ang II. Statistical symbols in the stress-strain curves represent differences between the slopes of the curves (β parameter) which are shown in the main text.

Figure 3. Incremental distensibility (A) and stress-strain relationships (B) in mesenteric resistance arteries (MRA) from untreated and Angiotensin II (Ang II)-treated COX-$2^{+/+}$ and COX-$2^{-/-}$ mice. C) Representative confocal projections and quantification of fenestra area and total number of fenestra of the internal elastic lamina of MRA from untreated and AngII-infused COX-$2^{+/+}$ and COX-$2^{-/-}$ mice. Projections were obtained from serial optical sections

captured with a fluorescence confocal microscope (×63, zoom ×4); image size: 59.5x59.5 μm. (D) Representative images and quantitative analysis of collagen content in the media layer from transversal sections of MRAs from from untreated and Ang II-treated COX-$2^{+/+}$ and COX-$2^{-/-}$ mice. Images were captured with a light microscope (×40 objective); image size: 310.9x233.1 μm. Data represent mean±SEM. n=6-9. *P<0.05, **P<0.01 and ***P<0.001 vs untreated, #P<0.05 and ###P<0.001 vs COX-$2^{+/+}$ or vs COX-$2^{+/+}$ Ang II. Statistical symbols in the stress-strain curves represent differences between the slopes of the curves (β parameter) which are shown in the main text.

Figure 4. Wall to lumen ratio (A), incremental distensibility (B) and stress-strain relationships (C) in mesenteric resistance arteries (MRA) from mice untreated or treated with Angiotensin II (Ang II) or Ang II plus celecoxib (administered 7 days after Ang II infusion). (D) Representative confocal projections and quantification of fenestra area and total number of fenestra of the internal elastic lamina of MRA from mice untreated or treated with Ang II or Ang II plus celecoxib. Projections were obtained from serial optical sections captured with a fluorescence confocal microscope (×63 objective, zoom ×4); image size: 59.5x59.5 μm. (E) Representative images and quantitative analysis of collagen content in the media layer from transversal sections of MRAs from mice untreated or treated with Ang II or Ang II plus celecoxib. Images were captured with a light microscope (×40 objective); image size: 310.9x233.1 μm. Data represent mean±SEM. n=5-7. *P<0.05 and ***P<0.001 vs untreated, #P<0.05 and ###P<0.001 vs Ang II. Statistical symbols in the stress-strain curves represent differences between the slopes of the curves (β parameter) which are shown in the main text.

Figure 5. Lumen and vessel diameter (A, B) and wall to lumen ratio (C) intraluminal pressure in mesenteric resistance arteries from WKY, SHR, and SHR treated with celecoxib. Data represent mean±SEM. n=12-14. ***P<0.001 vs WKY.

Figure 6. Incremental distensibility (A) and stress-strain relationships (B) in mesenteric resistance arteries (MRA) from WKY, SHR, and SHR treated with celecoxib. (C) Representative confocal projections and quantification of fenestra area and total number of fenestra of the internal elastic lamina of MRA from WKY, SHR, and SHR treated with celecoxib. Projections were obtained from serial optical sections captured with a fluorescence confocal microscope (×63 objective, zoom ×2); image size: 119×119μm. (D) Representative images and quantitative analysis of collagen content in the media layer from transversal sections of MRAs from WKY, SHR, and SHR treated with celecoxib. Images were captured with a light microscope (×40 objective); image size: 310.9x233.1 μm. Data represent mean±SEM. n=5-14. *P<0.05, **P<0.01 and ***P<0.001 vs WKY, #P<0.05 and ##P<0.01 vs SHR. Statistical symbols in the stress-strain curves represent differences between the slopes of the curves (β parameter) which are shown in the main text.

Figure 7. Tenascin-C (A), CTGF (B), PAI-1 (C) and Vimentin (D) mRNA levels in aortic homogenates from WKY, SHR, and SHR treated with celecoxib. Data represent mean±SEM. n=5-12. *P<0.05, **P<0.01 and ***P<0.001 vs WKY, #P<0.05 and ##P<0.01 vs SHR.

Figure 8. Representative fluorescent confocal photomicrographs of mPGES-1 immunolocalization (A) in aortic segments from mice untreated or treated with Angiotensin II (Ang II) or Ang II plus celecoxib. Image size 238x238 μm. (B) mRNA levels of mPGES-1 in aortic homogenates from mice untreated or treated with Ang II or Ang II plus celecoxib or WKY, SHR, and SHR treated with celecoxib. Data represent mean±SEM. n=5-11. *P<0.05 and ***P<0.001 vs control or vs WKY, ##P<0.01 and ##P<0.001 vs Ang II or vs SHR.

Figure 9. Wall to lumen ratio (A), incremental distensibility (B) and stress-strain relationships (C) in mesenteric resistance arteries (MRA) from mice untreated or treated with Ang II or Ang II plus SC19220. (D) Representative confocal projections and quantification of fenestra area and total number of fenestra of the internal elastic lamina of MRA from mice untreated or treated with Ang II or Ang II plus SC19220. Projections were obtained from serial optical sections captured with a fluorescence confocal microscope (×63 objective, zoom ×4); image size: 59.5x59.5 μm. (E) Representative images and quantitative analysis of collagen content in the media layer from transversal sections of MRAs from mice untreated or treated with Ang II or Ang II plus SC19220. Images were captured with a light microscope (×40 objective); image size: 310.9x233.1 μm. Data represent mean±SEM. n=5-7. *P<0.05 and ***P<0.001 vs untreated, #P<0.05, ###P<0.01 and ###P<0.001 vs Ang II. Statistical symbols in the stress-strain curves represent differences between the slopes of the curves (β parameter) which are shown in the main text.

Figure S1. Lumen and vessel diameter (A, B), media thickness (C), media/lumen ratio (D) and cross-sectional-area (CSA) (E) in aorta from untreated or treated with Angiotensin II (Ang II), Ang II plus celecoxib or Ang II plus SC19220. Representative photographs of hematoxylin-eoxin aortic sections are shown. Data represent mean±SEM. n=7-8. *P<0.05, **P<0.01 and ***P<0.001 vs untreated animals. #P<0.05 vs Ang II.

Figure S2. (A) Representative images and quantitative analysis of perivascular collagen content from transversal sections of coronary artery and (B) left ventricular hypertrophy from mice untreated or treated with Angiotensin II (Ang II) or Ang II plus celecoxib. Images were captured with a light microscope (×40 objective); image size: 310.9x233.1 μm. Data represent mean±SEM. n=5-6. ***P<0.001 vs untreated, #P<0.05 vs Ang II.

Figure S3. A Concentration–response curves to phenylephrine (Phe) (A,B) and acetylcholine (ACh) (C) in mesenteric resistance arteries (MRA) and aorta from untreated and Ang II-treated COX-$2^{+/+}$ and COX-$2^{-/-}$ mice. Data represent mean±SEM. n=4-9. ***P<0.001 vs untreated.

Figure S4. (A) Effect of SC19220 (administered *in vitro* to the organ bath) on the concentration–response curve to phenylephrine (Phe) in mesenteric resistance arteries from untreated, Angiotensin II (Ang II) and Ang II plus celecoxib-treated mice. (B,C,D) Concentration–response curves to phenylephrine (Phe), acetylcholine (ACh), and diethylamine NONOate (DEA-NO) in aortic segments from mice untreated or treated with Ang II or Ang II plus SC19220. Data represent mean±SEM. n=5-10. ***P<0.001 vs control or vs untreated, ###P<0.001 vs Ang II.

Table 1. Systolic blood pressure (mm Hg) in different groups of rats and Angiotensin II (Ang II)-infused mice untreated and treated with celecoxib or SC19220.

	Untreated	**Ang II**	**Celecoxib treatment**	**Celecoxib treatment** (7 days)	**SC19220 treatment**
C57BL6	101.8±2.5	144±3.9*	123,1±4,5*#	129.9±3.2*#	118.7±3.2*#
COX-2$^{+/+}$	100.6±2	163±3.5*			
COX-2$^{-/-}$	103.2±1.9	177.7±4.6*#			
WKY	162.2±6.8		149,6±3,1		
SHR	235.4±3.1#		208.1±6.3*#		

Data are expressed as mean±SEM. n=5-9. *P<0.05 vs untreated. #P<0.05 vs Ang II, vs WKY or vs COX-2$^{+/+}$.

Figure 1

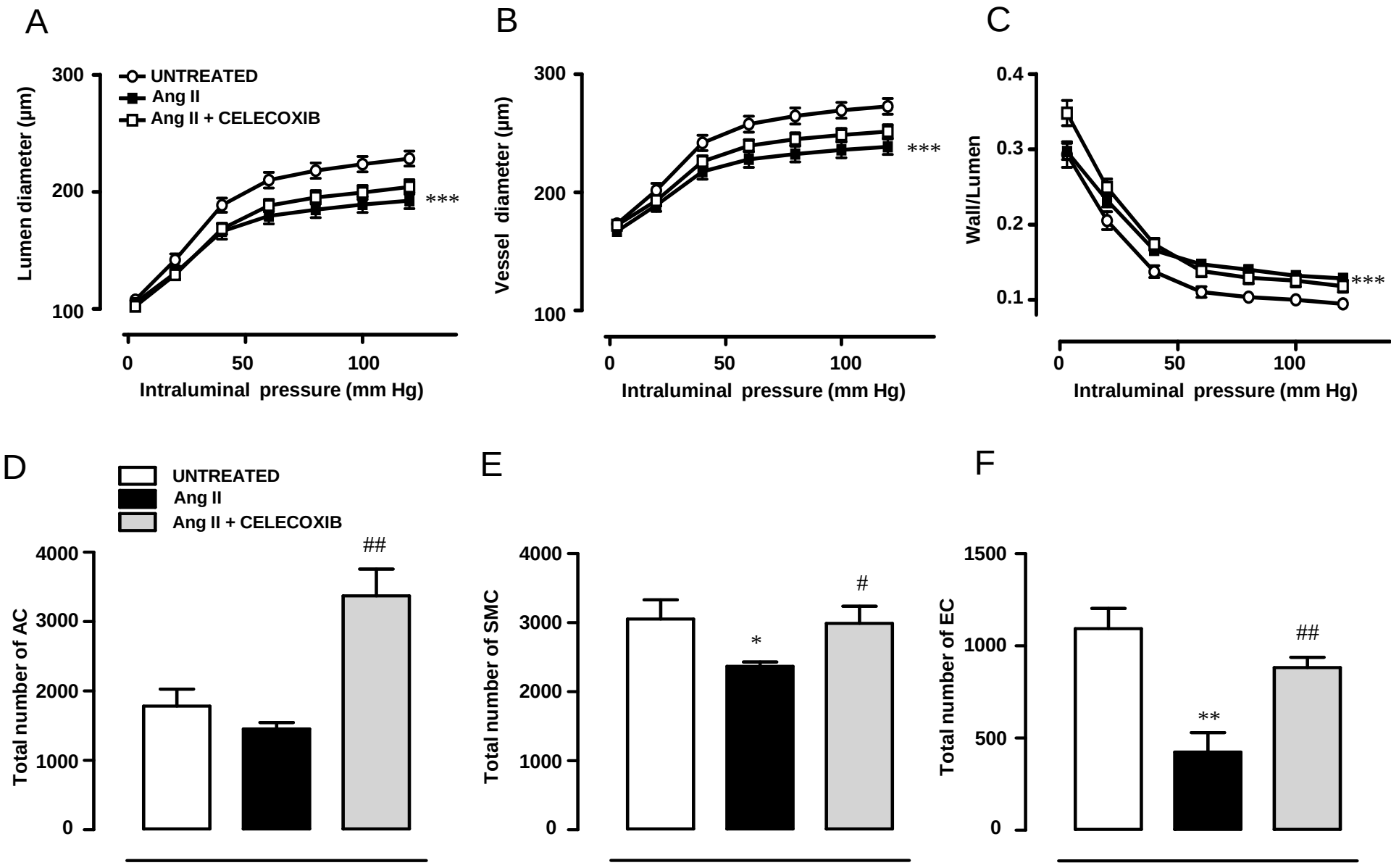
A
B
C
UNTREATED
Ang II
Ang II + CELECOXIB
Lumen diameter (µm)
Vessel diameter (µm)
Wall/Lumen
Intraluminal pressure (mm Hg)
***
D
E
F
Total number of AC
Total number of SMC
Total number of EC
##
*
#
**

Figure 2

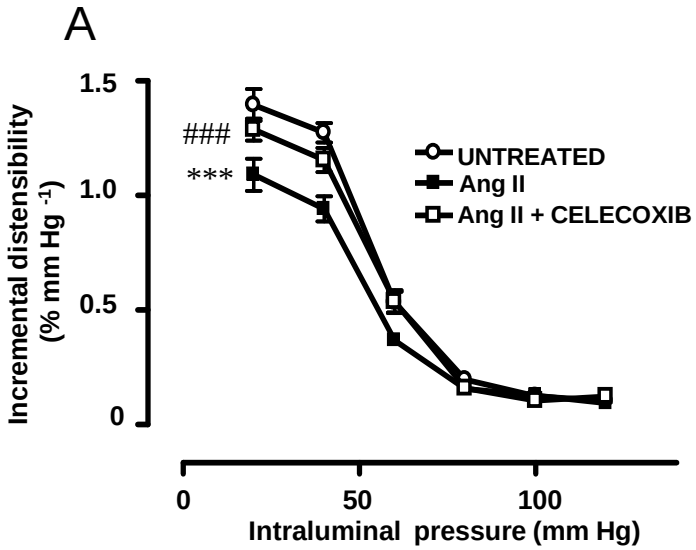
A
Incremental distensibility (% mm Hg -1)
1.5
1.0
0.5
0
###
***
UNTREATED
Ang II
Ang II + CELECOXIB
0
50
100
Intraluminal pressure (mm Hg)

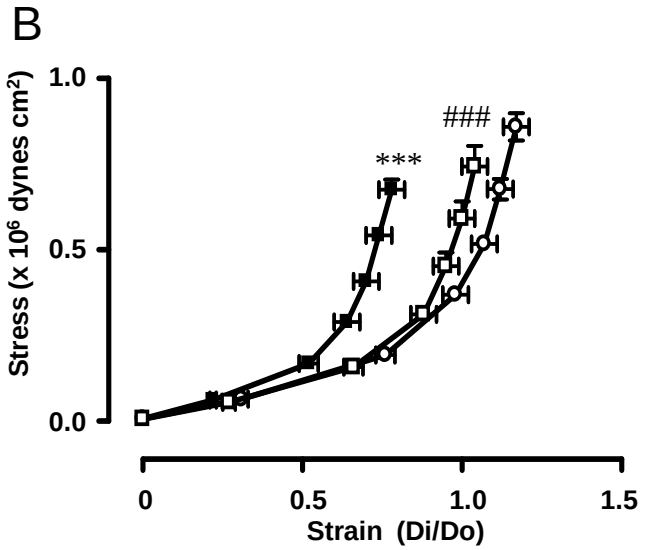
B
Stress (x 10⁶ dynes cm²)
1.0
0.5
0.0
***
###
0
0.5
1.0
1.5
Strain (Di/Do)

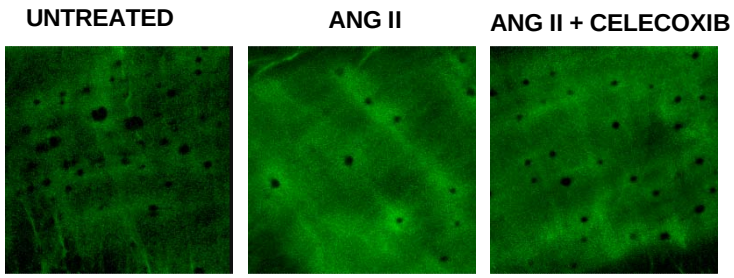
UNTREATED
ANG II
ANG II + CELECOXIB

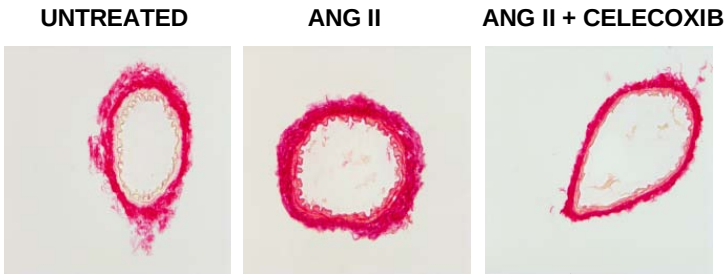
UNTREATED
ANG II
ANG II + CELECOXIB

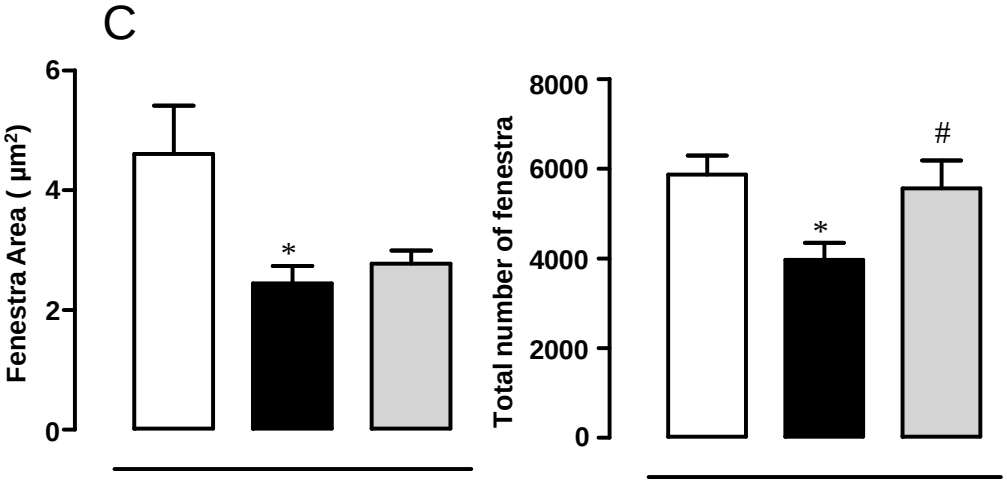
C
Fenestra Area (µm²)
6
4
2
0
*
Total number of fenestra
8000
6000
4000
2000
0
*
#

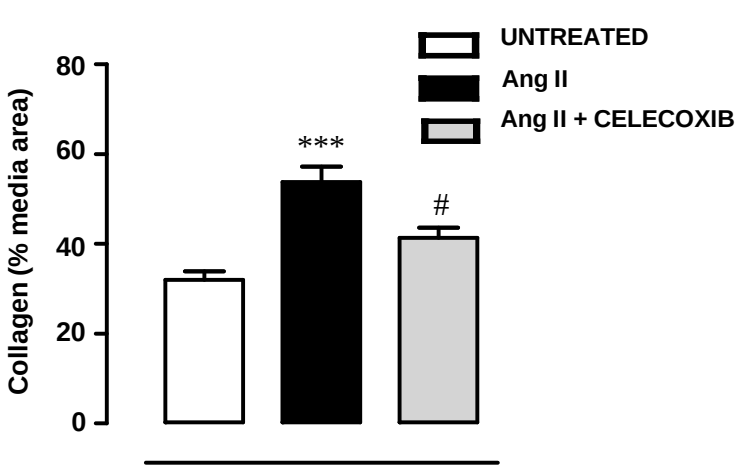
D
Collagen (% media area)
80
60
40
20
0
***
#
UNTREATED
Ang II
Ang II + CELECOXIB

Figure 3

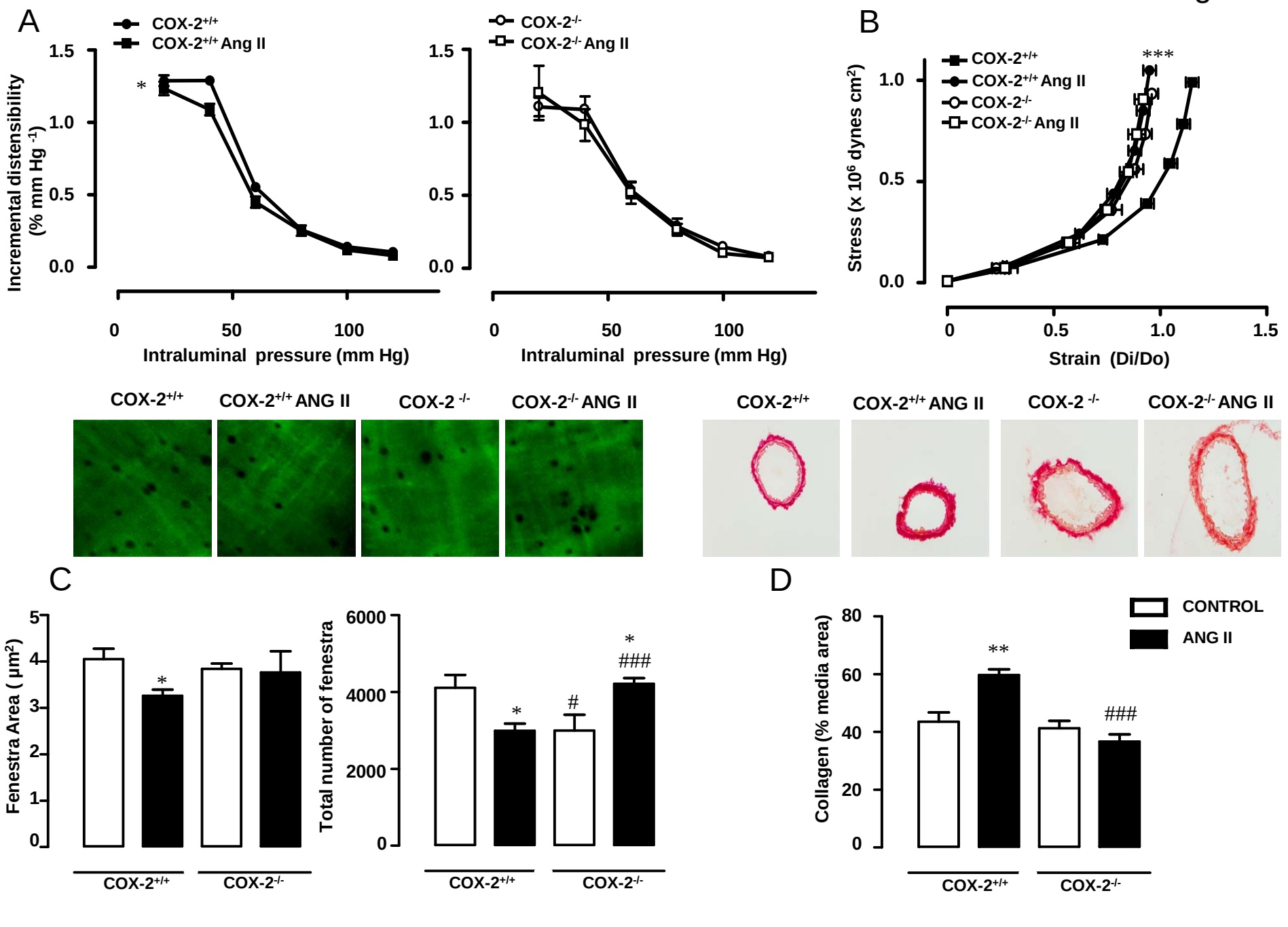
A
COX-2+/+
COX-2+/+ Ang II
COX-2-/-
COX-2-/- Ang II
Incremental distensibility (% mm Hg -1)
1.5
1.0
0.5
0.0
*
0
50
100
Intraluminal pressure (mm Hg)
B
COX-2+/+
COX-2+/+ Ang II
COX-2-/-
COX-2-/- Ang II
***
Stress (x 10^6 dynes cm^2)
1.0
0.5
0.0
0
0.5
1.0
1.5
Strain (Di/Do)
COX-2+/+
COX-2+/+ ANG II
COX-2 -/-
COX-2-/- ANG II
C
Fenestra Area (µm2)
5
4
3
2
1
0
*
COX-2+/+
COX-2-/-
Total number of fenestra
6000
4000
2000
0
*
#
*
###
D
CONTROL
ANG II
Collagen (% media area)
80
60
40
20
0
**
###

Figure 4

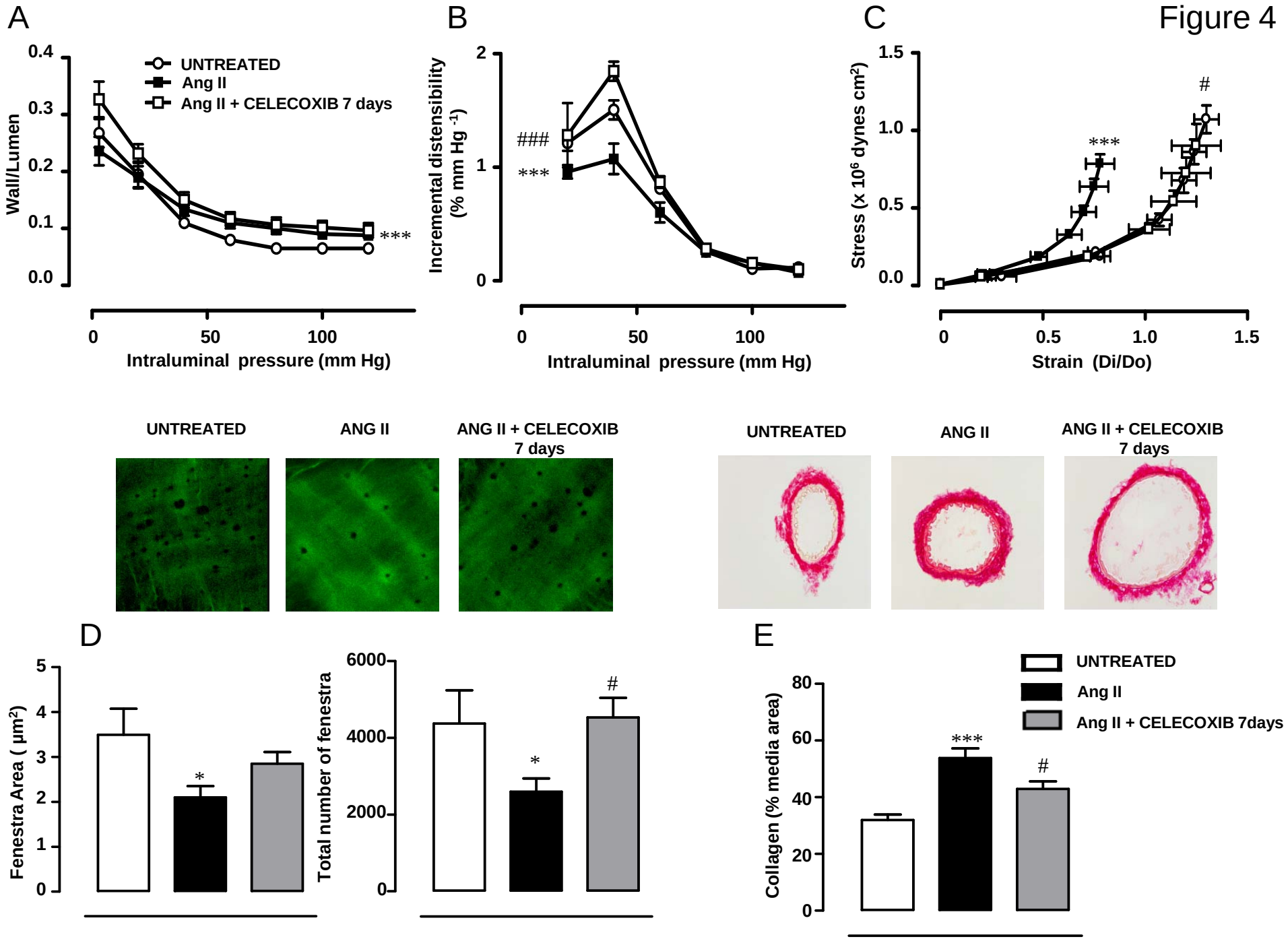
A
B
C
UNTREATED
Ang II
Ang II + CELECOXIB 7 days
Wall/Lumen
Intraluminal pressure (mm Hg)
Incremental distensibility (% mm Hg -1)
###
***
Stress (x 10⁶ dynes cm²)
Strain (Di/Do)
#
UNTREATED
ANG II
ANG II + CELECOXIB 7 days
D
E
Fenestra Area (µm²)
Total number of fenestra
Collagen (% media area)

Figure 5

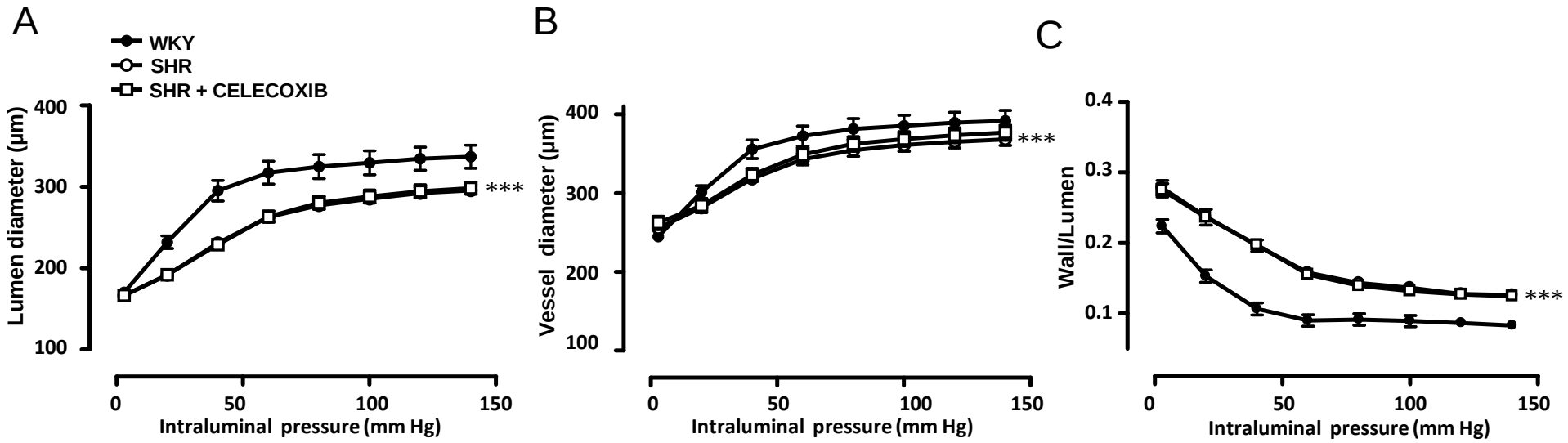
A
WKY
SHR
SHR + CELECOXIB
Lumen diameter (µm)
400
300
200
100
***
0
50
100
150
Intraluminal pressure (mm Hg)
B
Vessel diameter (µm)
400
300
200
100
***
0
50
100
150
Intraluminal pressure (mm Hg)
C
Wall/Lumen
0.4
0.3
0.2
0.1
***
0
50
100
150
Intraluminal pressure (mm Hg)

Figure 6

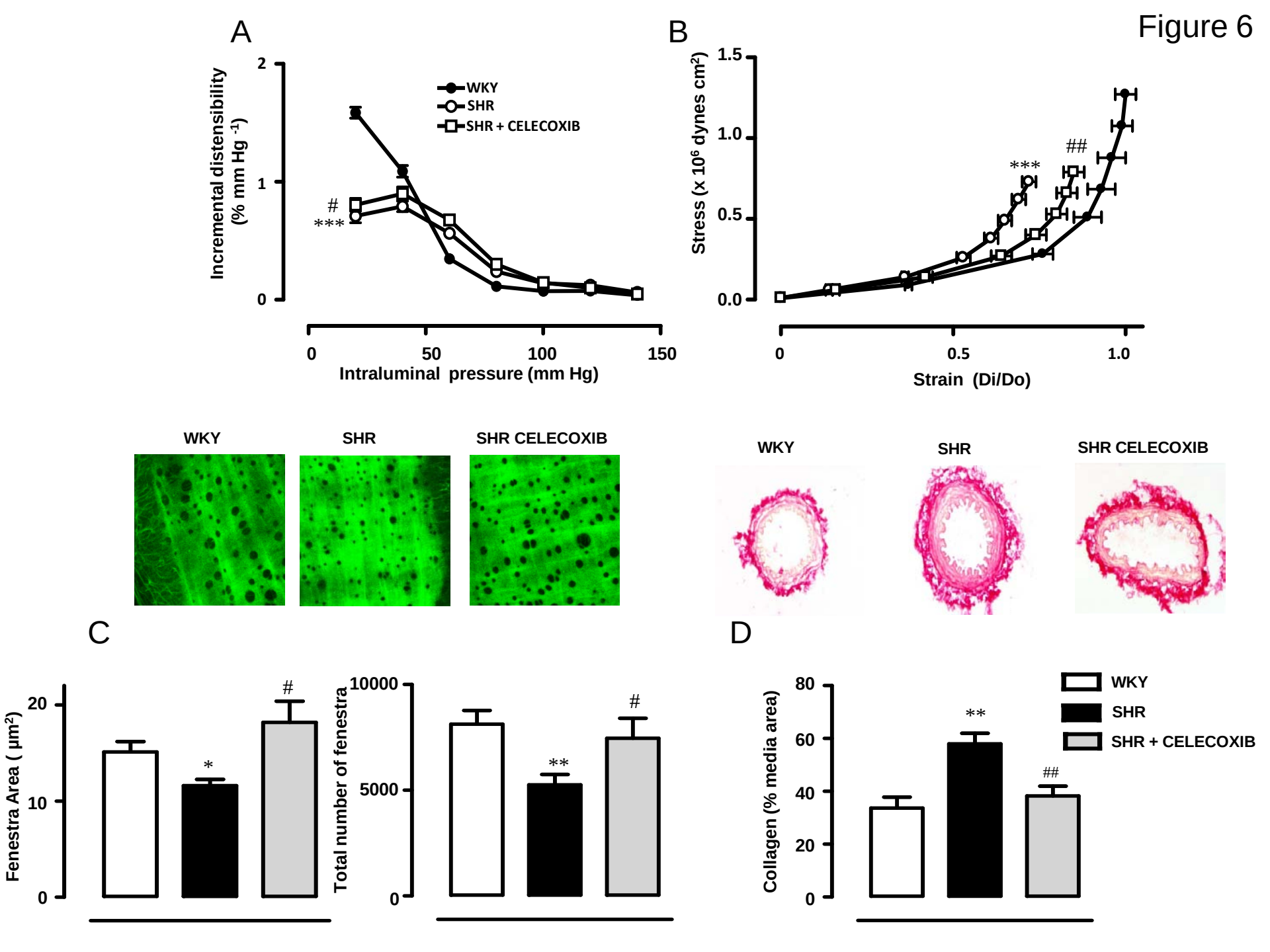
A
Incremental distensibility (% mm Hg -1)
WKY
SHR
SHR + CELECOXIB
#
***
Intraluminal pressure (mm Hg)
B
Stress (x 10⁶ dynes cm²)
***
##
Strain (Di/Do)
WKY
SHR
SHR CELECOXIB
WKY
SHR
SHR CELECOXIB
C
Fenestra Area (µm²)
*
#
Total number of fenestra
**
#
D
Collagen (% media area)
**
##
WKY
SHR
SHR + CELECOXIB

Figure 7

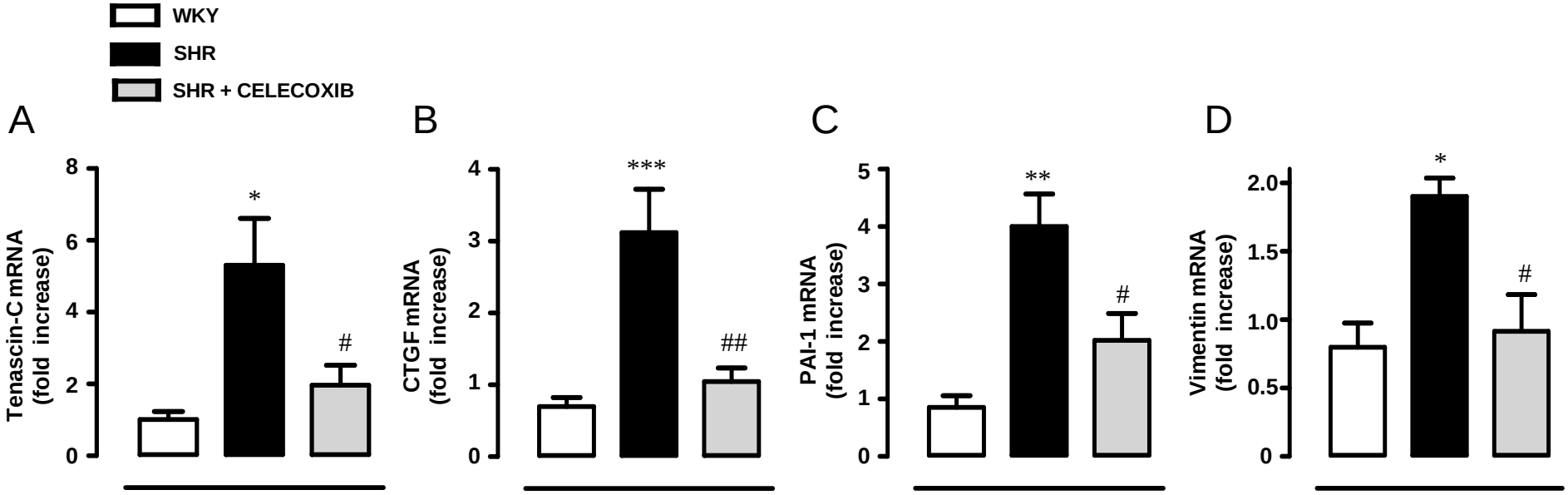
WKY
SHR
SHR + CELECOXIB
A
Tenascin-C mRNA (fold increase)
0
2
4
6
8
*
#
B
CTGF mRNA (fold increase)
0
1
2
3
4
***
##
C
PAI-1 mRNA (fold increase)
0
1
2
3
4
5
**
#
D
Vimentin mRNA (fold increase)
0
0.5
1.0
1.5
2.0
*
#

Figure 8

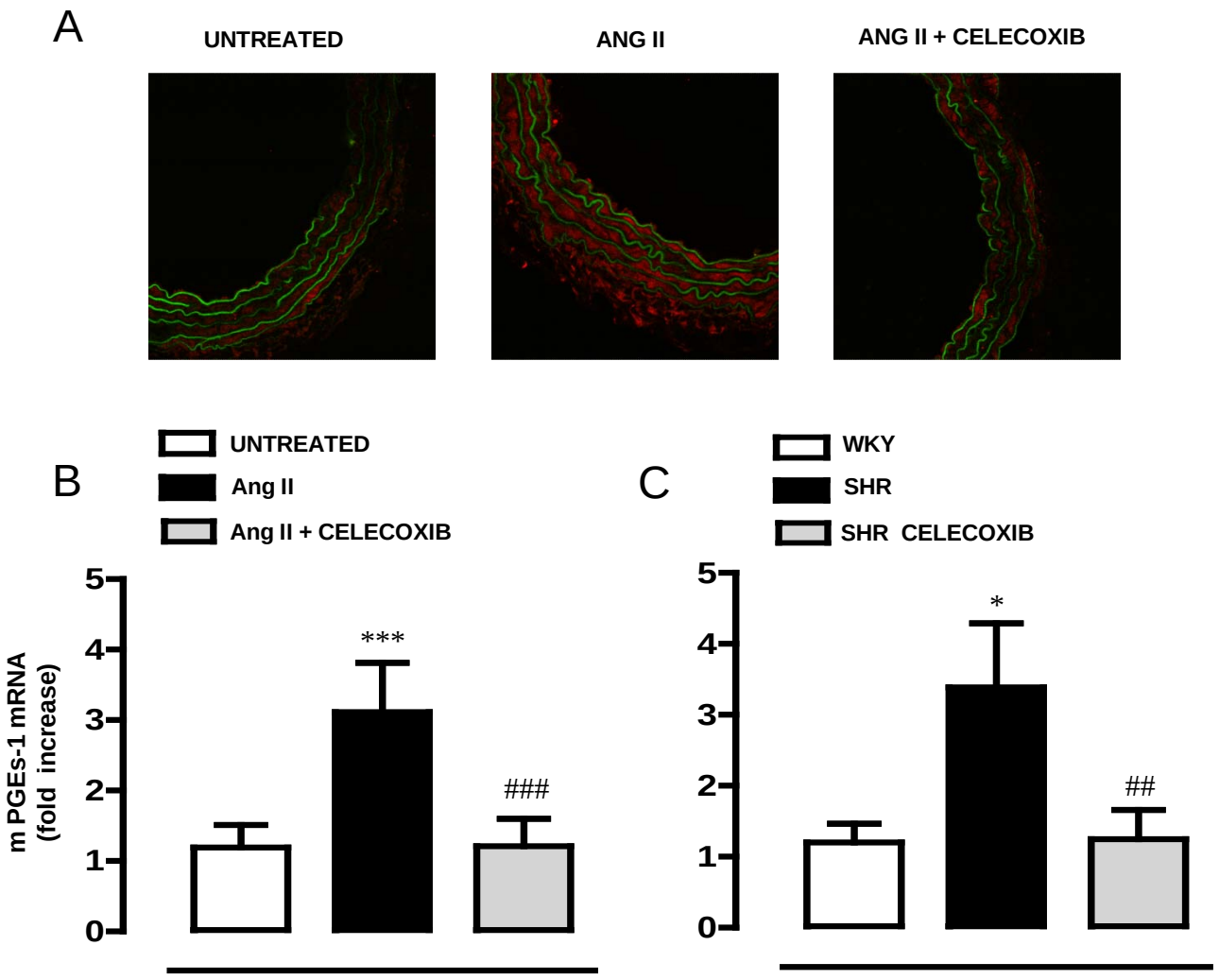
A
UNTREATED
ANG II
ANG II + CELECOXIB
B
UNTREATED
Ang II
Ang II + CELECOXIB
m PGEs-1 mRNA
(fold increase)
0
1
2
3
4
5
***
###
C
WKY
SHR
SHR CELECOXIB
0
1
2
3
4
5
*
##

Figure 9

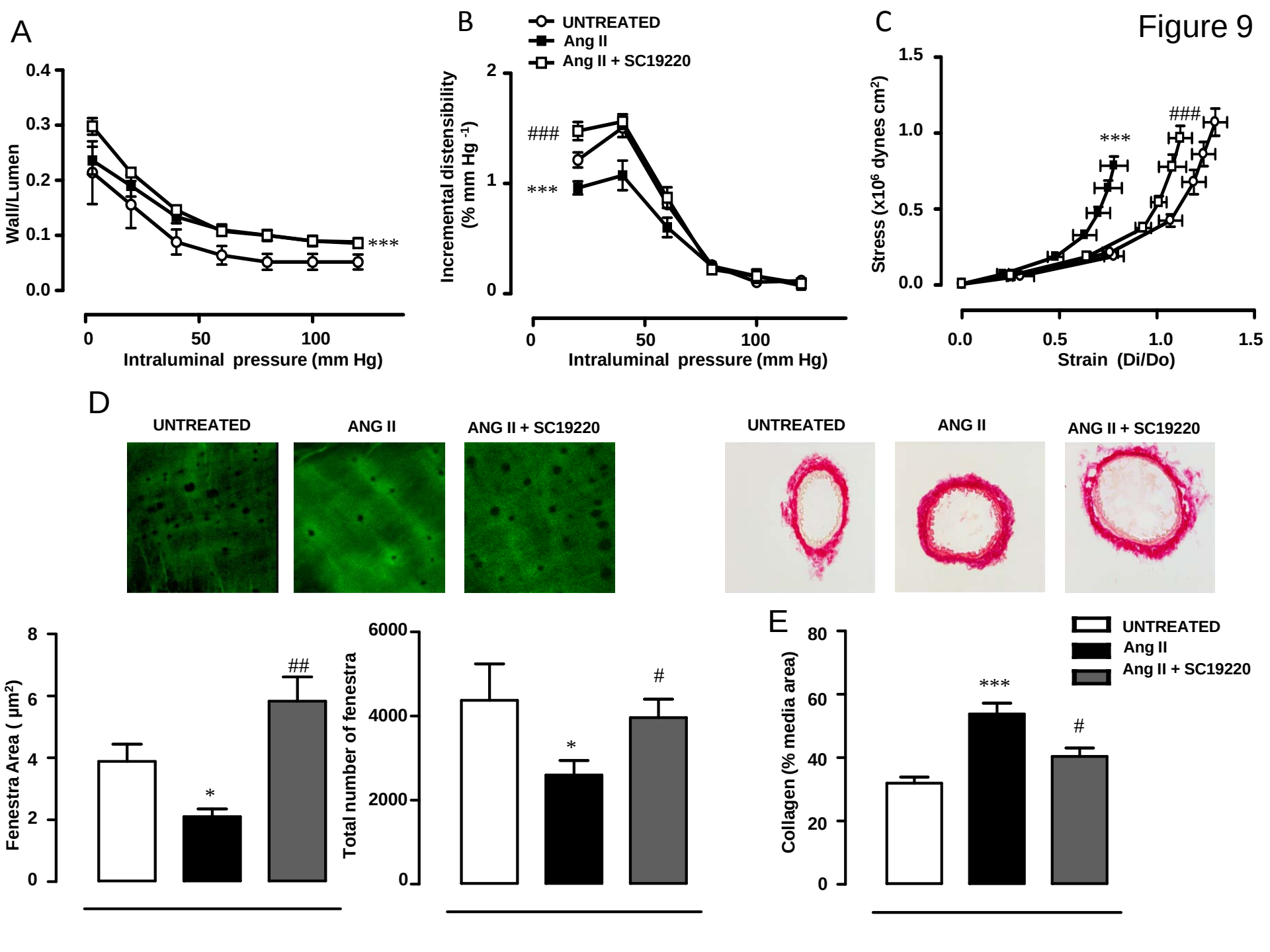
A
Wall/Lumen
0.4
0.3
0.2
0.1
0.0
***
0
50
100
Intraluminal pressure (mm Hg)
B
UNTREATED
Ang II
Ang II + SC19220
Incremental distensibility (% mm Hg -1)
2
1
0
###
***
0
50
100
Intraluminal pressure (mm Hg)
C
Stress (x10^6 dynes cm^2)
1.5
1.0
0.5
0.0
***
###
0.0
0.5
1.0
1.5
Strain (Di/Do)
D
UNTREATED
ANG II
ANG II + SC19220
UNTREATED
ANG II
ANG II + SC19220
Fenestra Area (µm^2)
8
6
4
2
0
*
##
Total number of fenestra
6000
4000
2000
0
*
#
E
Collagen (% media area)
80
60
40
20
0
***
#
UNTREATED
Ang II
Ang II + SC19220

Figure S1

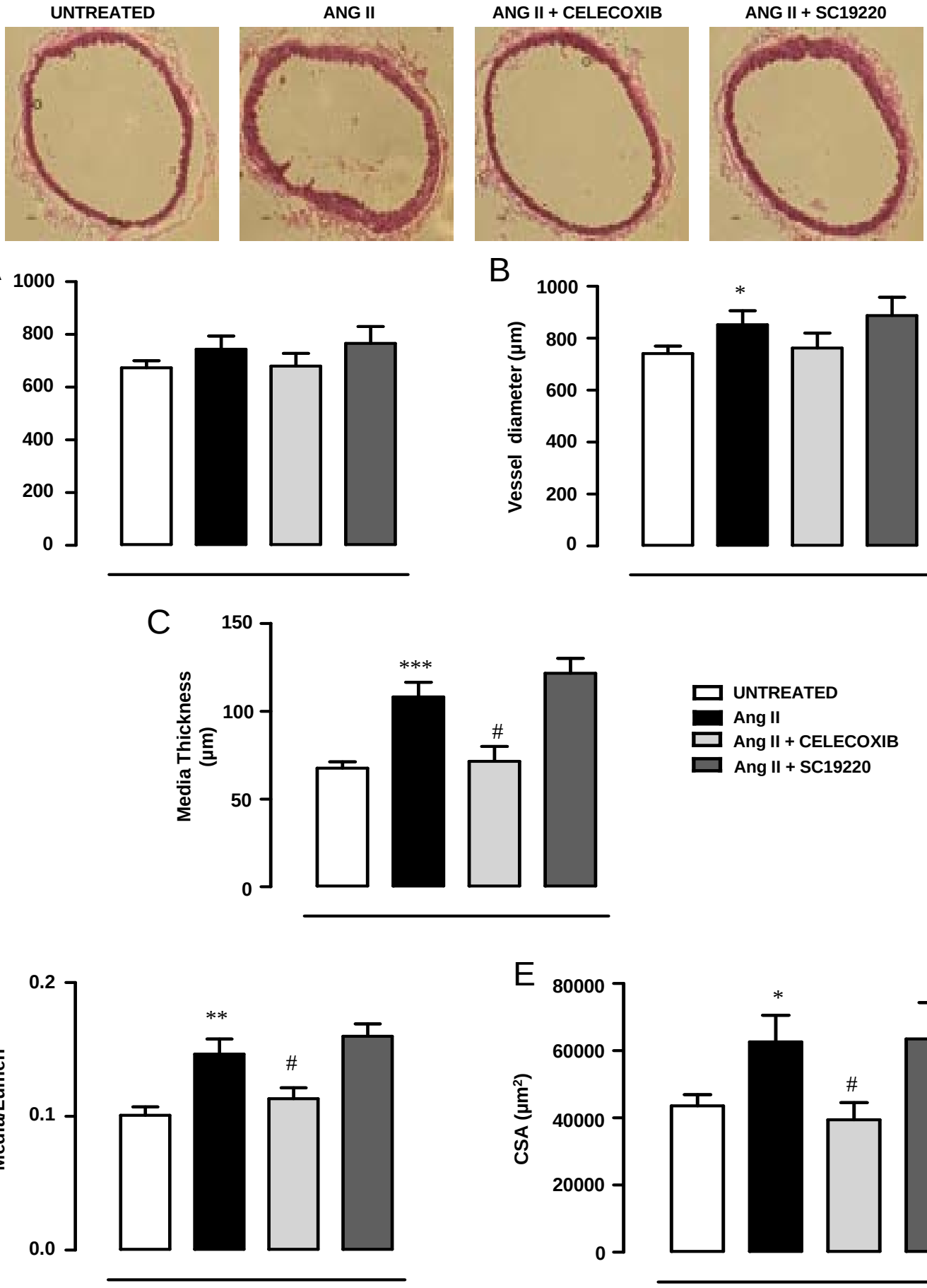
UNTREATED
ANG II
ANG II + CELECOXIB
ANG II + SC19220
A
Lumen diameter (µm)
1000
800
600
400
200
0
B
Vessel diameter (µm)
1000
800
600
400
200
0
*
C
Media Thickness (µm)
150
100
50
0
***
#
UNTREATED
Ang II
Ang II + CELECOXIB
Ang II + SC19220
D
Media/Lumen
0.2
0.1
0.0
**
#
E
CSA (µm²)
80000
60000
40000
20000
0
*
#

Figure S2

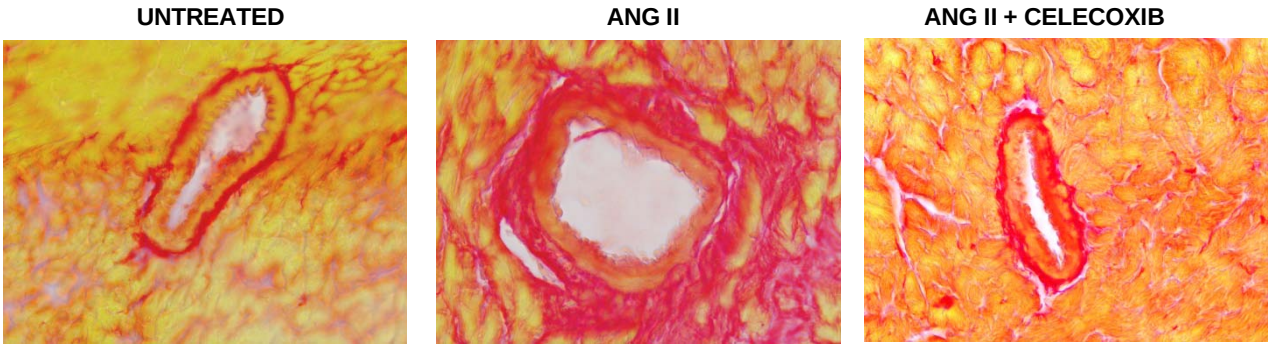
UNTREATED
ANG II
ANG II + CELECOXIB

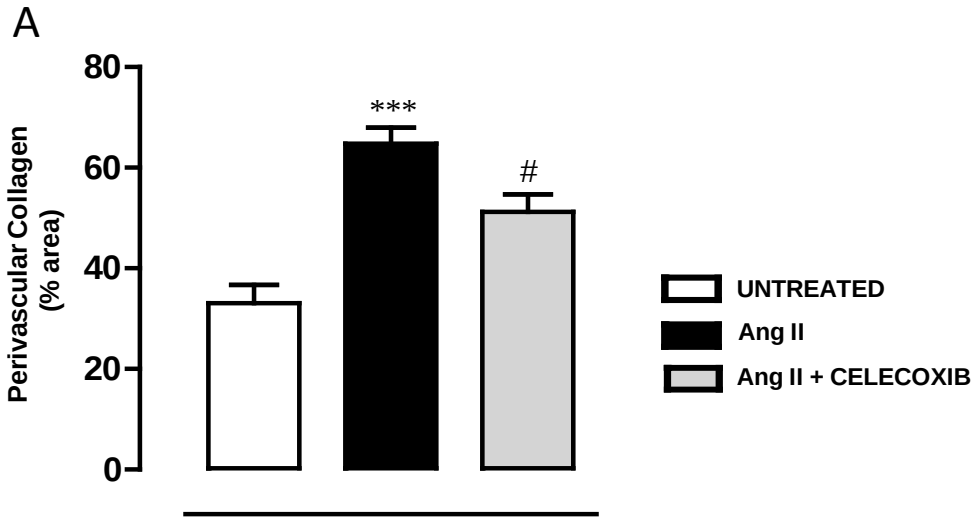
A
Perivascular Collagen (% area)
80
60
40
20
0
***
#
UNTREATED
Ang II
Ang II + CELECOXIB

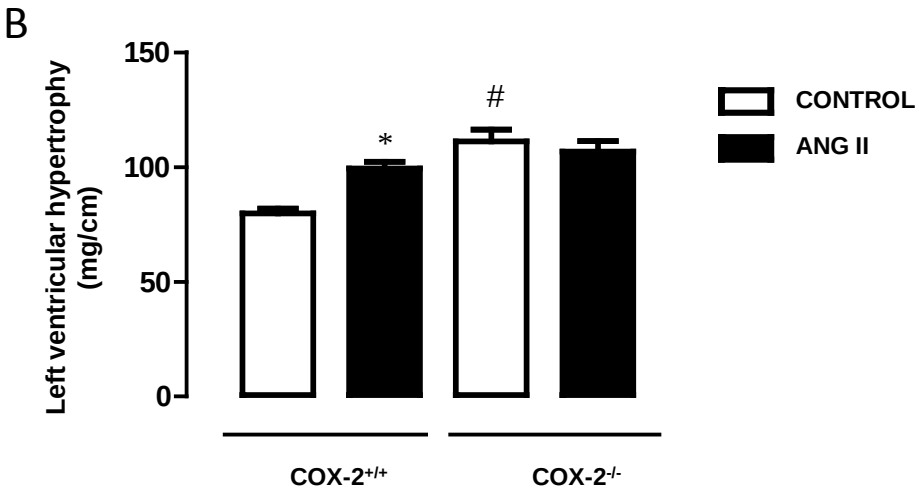
B
Left ventricular hypertrophy (mg/cm)
150
100
50
0
*
#
CONTROL
ANG II
COX-2+/+
COX-2-/-

Figure S3

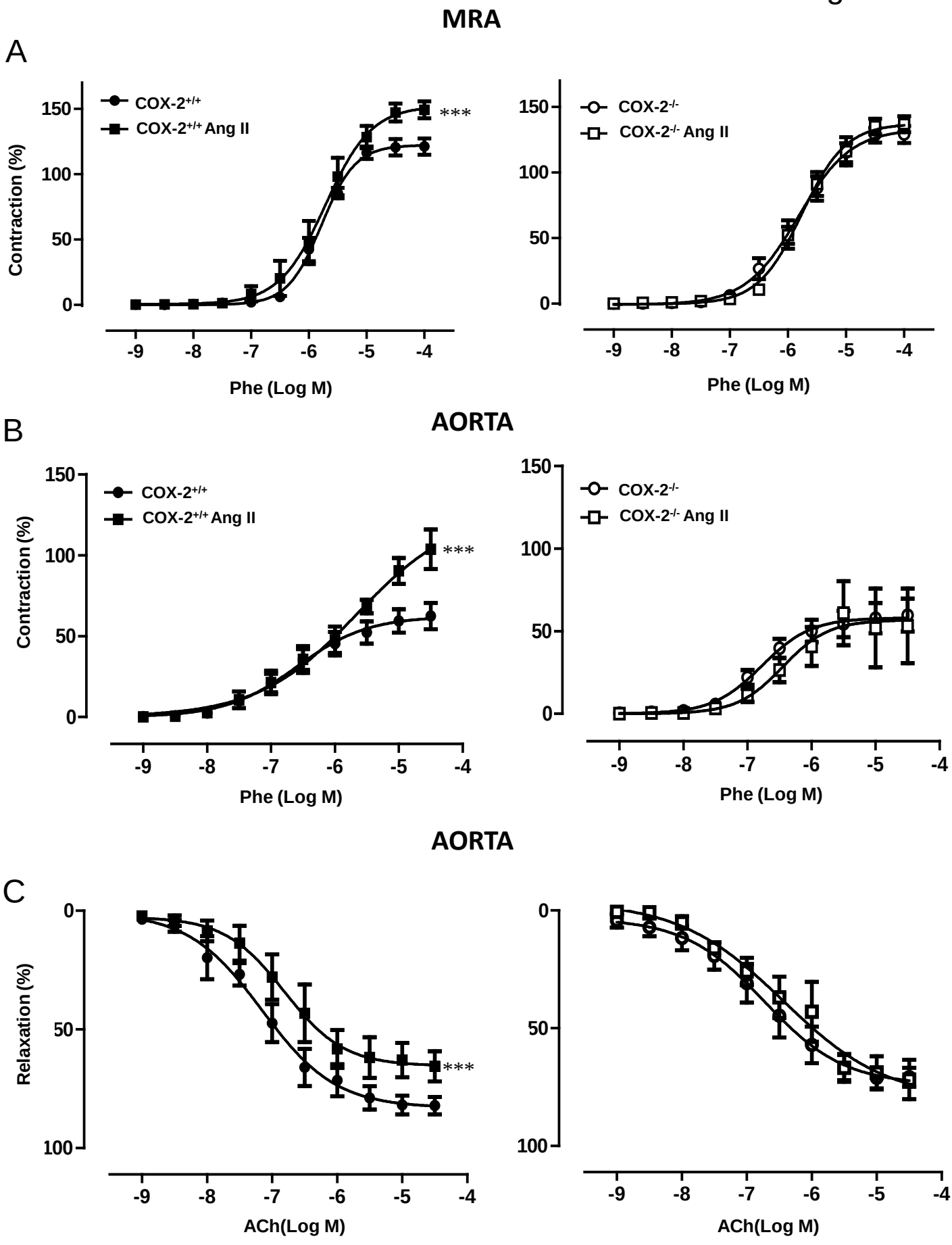
MRA
A
COX-2+/+
COX-2+/+ Ang II
***
Contraction (%)
150
100
50
0
-9
-8
-7
-6
-5
-4
Phe (Log M)
COX-2-/-
COX-2-/- Ang II
Phe (Log M)
AORTA
B
COX-2+/+
COX-2+/+ Ang II
***
Contraction (%)
Phe (Log M)
COX-2-/-
COX-2-/- Ang II
Phe (Log M)
AORTA
C
Relaxation (%)
***
ACh(Log M)
ACh(Log M)

Figure S4

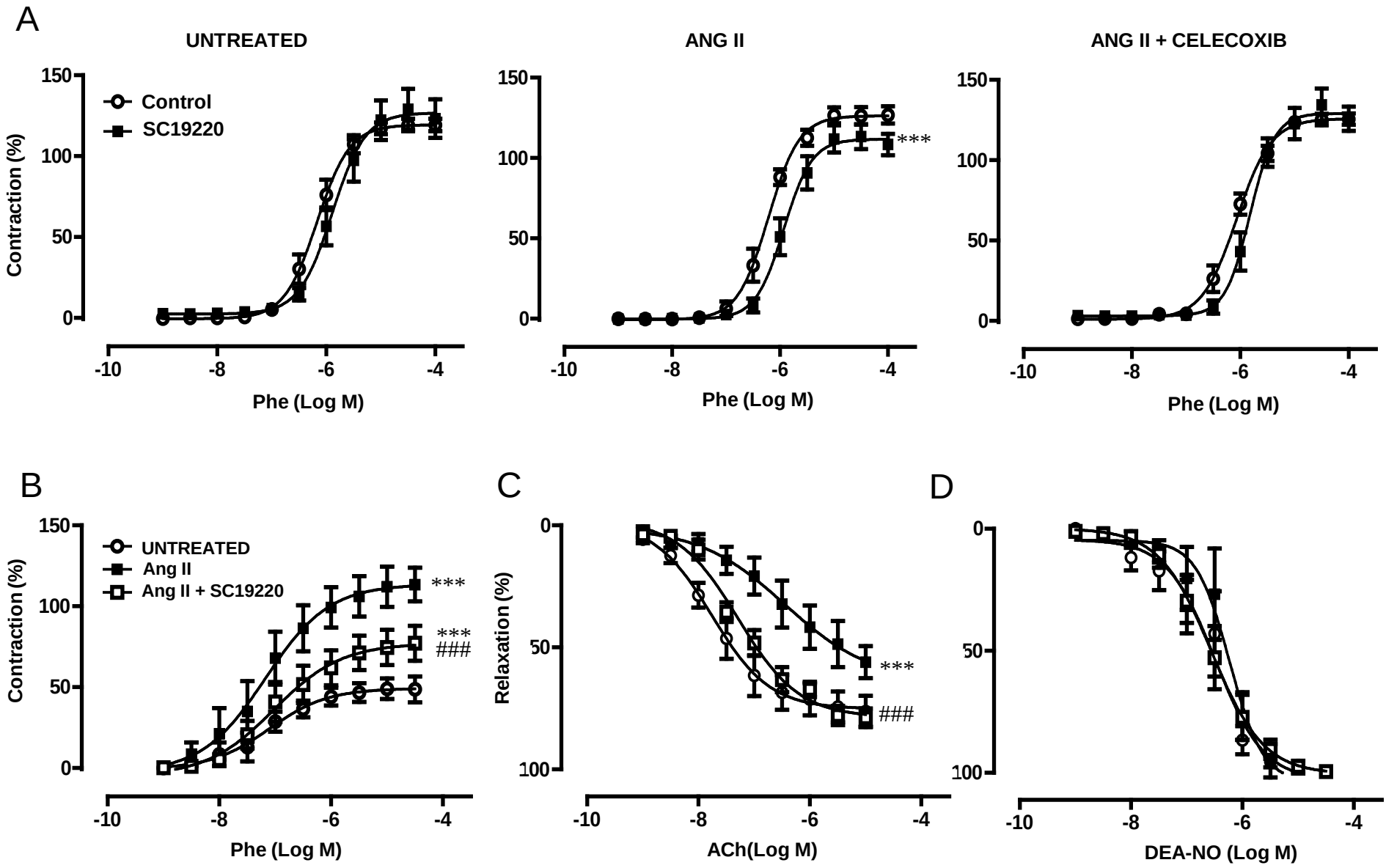
A
UNTREATED
ANG II
ANG II + CELECOXIB
Control
SC19220
Contraction (%)
Phe (Log M)
***
B
UNTREATED
Ang II
Ang II + SC19220
***
###
C
Relaxation (%)
ACh(Log M)
D
DEA-NO (Log M)

Article 4: Increased Nitric Oxide Bioavailability in Adult GRK2 Hemizygous Mice Protects Against Angiotensin II–Induced Hypertension

Avendaño MS*, Lucas E*, Jurado-Pueyo M, Martínez-Revelles S, Vila-Bedmar R, Mayor FJr, Salaices M, Briones AM, Murga C.

Hypertension. 63:00-00. 2014.

Original Article

Increased Nitric Oxide Bioavailability in Adult GRK2 Hemizygous Mice Protects Against Angiotensin II–Induced Hypertension

María S. Avendaño,* Elisa Lucas,* María Jurado-Pueyo, Sonia Martínez-Revelles, Rocío Vila-Bedmar, Federico Mayor Jr, Mercedes Salaices, Ana M. Briones, Cristina Murga

Abstract—G protein–coupled receptor kinase 2 (GRK2) is a ubiquitous serine/threonine protein kinase able to phosphorylate and desensitize the active form of several G protein–coupled receptors. Given the lack of selective inhibitors for GRK2, we investigated the effects elicited by GRK2 inhibition in vascular responses using global adult hemizygous mice ($GRK2^{+/-}$). The vasodilator responses to acetylcholine or isoproterenol were increased in aortas and mesenteric resistance arteries from $GRK2^{+/-}$ mice compared with wild-type (WT) littermates. After angiotensin II (AngII) infusion, $GRK2^{+/-}$ mice were partially protected against hypertension, vascular remodeling, and mechanical alterations, even when resting basal blood pressures were not significantly different. AngII infusion also (1) increased GRK2 levels in WT but not in $GRK2^{+/-}$ vessels; (2) increased vasoconstrictor responses to phenylephrine in WT but not in $GRK2^{+/-}$ mice; and (3) decreased vasodilator responses to acetylcholine and vascular pAkt and eNOS levels more in WT than in $GRK2^{+/-}$ animals. Vascular NO production and the modulation of vasoconstrictor responses by endothelial-derived NO remained enhanced in $GRK2^{+/-}$ mice infused with AngII. Thus, $GRK2^{+/-}$ mice are resistant to the development of vascular remodeling and mechanical alterations, endothelial dysfunction, increased vasoconstrictor responses, and hypertension induced by AngII at least partially through the preservation of NO bioavailability. In conclusion, our results describe an important role for GRK2 in systemic hypertension and further establish that an inhibition of GRK2 could be a beneficial treatment for this condition. **(*Hypertension*. 2014;63:00-00.)** ● **Online Data Supplement**

Key Words: arteries ■ GRK2 ■ hypertension ■ nitric oxide

Different receptors and signaling molecules are involved in the development of hypertension by hyper-contracting or hypo-dilating blood vessels in a deleterious manner and by affecting the structure and mechanical properties of vessels. Among them, the G protein–coupled receptor (GPCR) family is of outmost importance. Adrenergic receptors and other GPCRs, such as angiotensin II (AngII), endothelin-1 (ET-1), dopamine, and vasopressin receptors, are key for vascular physiopathology.[1] AngII is a master regulator of vascular tone, and many animal models of hypertension are based on the chronic elevation of AngII levels.

GPCRs become inactivated to different extents when agonist signals are persistent in time, a process termed desensitization. This process is regulated by G protein–coupled receptor kinases (GRKs), a family of serine/threonine kinases able to phosphorylate intracellular domains of the receptors and initiate their uncoupling from the G protein, and thus signal termination.[2] Among the 7 GRK isoforms, GRK2 is the most abundant in vessels together with GRK5 and plays a determinant role in the control of systemic vascular responses.[3,4] The levels and activity of the GRK2 isoform are increased in animal models of hypertension and in lymphocytes from young patients with hypertension.[5] In addition, GRK2 mRNA levels, but not those of GRK3 or GRK5, increase in correlation with systolic blood pressure in humans.[6] GRK2 downregulates the in vivo effects of key vasoconstrictor receptors, such as ET[7] and AngII[8] receptors and $\alpha 1_D$ adrenoceptors.[9] Therefore, the increase in vascular GRK2 could have represented a protective mechanism for adaptation against a hypertensive phenotype. However, transgenic mice overexpressing GRK2 in the vascular smooth muscle cells (VSMC) show increased resting blood pressure.[8] Moreover, elevated GRK2 levels impair vasodilator β adrenoceptors responses in different tissues and animal

Received July 5, 2013; first decision July 21, 2013; revision accepted October 8, 2013.

From the Departamento de Farmacología, Facultad de Medicina, Universidad Autónoma de Madrid (UAM) (M.S.A., S.M.-R., M.S., A.M.B.), and Departamento de Biología Molecular and Centro de Biología Molecular "Severo Ochoa", UAM-CSIC (E.L., M.J.-P., R.V.-B., F.M., C.M.), Madrid, Spain; Instituto de Investigación Sanitaria La Paz, Madrid, Spain (M.S.A., S.M.-R., M.S., A.M.B.); and Instituto de Investigación Sanitaria La Princesa, Madrid, Spain (E.L., M.J.-P., R.V.-B., F.M., C.M.).

*These authors contributed equally to this work.

The online-only Data Supplement is available with this article at http://hyper.ahajournals.org/lookup/suppl/doi:10.1161/HYPERTENSIONAHA.113.01991/-/DC1.

Correspondence to Cristina Murga, Departamento de Biología Molecular, Centro de Biología Molecular "Severo Ochoa", Facultad de Ciencias, Universidad Autónoma de Madrid, Nicolás Cabrera 1, 28049 Madrid, Spain. E-mail cristina.murga@uam.es; or Ana M. Briones, Departamento de Farmacología, Facultad de Medicina, Universidad Autónoma de Madrid, Arzobispo Morcillo, 28029 Madrid, Spain. E-mail ana.briones@uam.es

models and, interestingly, in human patients treated with β-blockers GRK2 levels return to baseline.[4,10]

Classically, the preferential desensitization by GRK2 of vasodilator receptor subtypes versus vasoconstrictor ones has been invoked to explain the effect of upregulated GRK2 levels in human and in murine hypertension.[8] However, novel results implicating GRK2 in non–GPCR-dependent pathways prompt to redefine the role of GRK2 in the regulation of vascular tone. One such example is the described interaction of GRK2 with Akt that inhibits Akt-dependent activation of NO synthase, thus impairing NO production.[11] Another important emerging question is the relative importance of endothelial GRK2 as compared with VSMC-GRK2 because depletion of GRK2 in VSMC is unable to prevent portal hypertension.[9] Our work tries to shed some light on these issues describing for the first time that a global reduction in GRK2 causes resistance to the development of systemic hypertension in adult mice. This antihypertensive effect of GRK2 downregulation prevails even when responses to both vasodilator and vasoconstrictor receptors are enhanced and this is because of the increased NO bioavailability detected in GRK2$^{+/-}$ mice. Although extensive research has been performed on the effects of GRK2 overexpression or deletion in cardiac phenotypes, few studies have addressed how systemic changes in GRK2 levels can affect vascular function and to our knowledge, this is the first report to address the effect of GRK2 in vascular structure and biomechanics.

Methods

The Materials and Methods are described in the online-only Data Supplement.

Results

GRK2 Deficiency Increases Vasoconstrictor Responses Without Influencing Receptor Levels

Partial deficiency of GRK2 increased vasoconstrictor responses to phenylephrine in aortas from male (Figure 1A; Table S1 in the online-only Data Supplement) and female (Figure S1A; Table S1) mice. ET-1 (0.1 μmol/L)–mediated vasoconstrictor responses were also increased in aorta from male GRK2$^{+/-}$ mice compared with WT littermates (Figure S2A; Table S1). After repeated exposure to ET-1, vasoconstrictor responses were reduced in WT and GRK2$^{+/-}$ mice (Figure S2A). However, contractile responses to the second and third ET-1 administration remained larger in GRK2$^{+/-}$ compared with WT mice (Figure S2A), suggesting that partial deficiency in GRK2 prevents, in part, ET-1–induced desensitization. GRK2 deficiency did not modify AngII (1 μmol/L)–induced vasoconstrictor responses (Figure S2B; Table S1) or changed the reduced vascular responses after repeated exposure to AngII (Figure S2B).

GRK2$^{+/-}$ mice displayed decreased vascular GRK2 gene and protein expression (Figures S2C and S3), but no differences in protein or gene expression of AT1, AT2, ETA, ETB, or $\alpha 1_D$ receptors were observed between WT and GRK2$^{+/-}$ mice in aortas, and a reduction of only AT2 receptor protein was observed in mesenteric resistance arteries (MRA) from GRK2$^{+/-}$ mice (Figures S2C and S3).

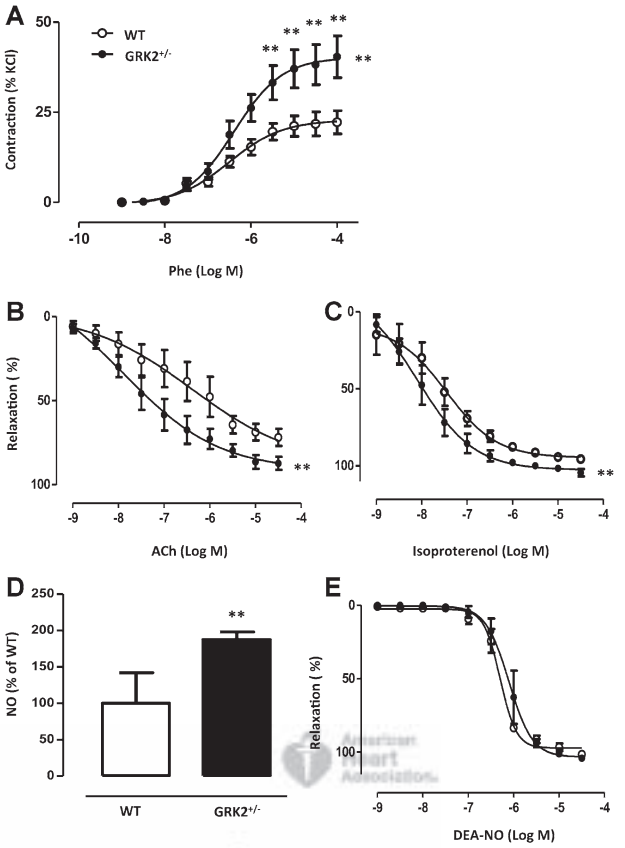

Figure 1. Effects of partial G protein–coupled receptor kinase 2 (GRK2) deficiency on vasoconstrictor and vasodilator responses and in NO production in aorta from male adult mice. Concentration–response curve to phenylephrine (Phe; **A**), acetylcholine (ACh; **B**), isoproterenol (**C**), and diethylamine NONOate (DEA-NO; **E**) and quantification of ACh-induced NO release (**D**) in aorta from male wild-type (WT) and GRK2$^{+/-}$ mice. n=5 to 10. $^{**}P<0.01$.

GRK2 Deficiency in Adult Mice Increases Endothelium-Dependent Vasodilator Responses and NO Release

The endothelium-dependent vasodilator responses induced by acetylcholine (ACh) or isoproterenol were increased in aorta from male and female GRK2$^{+/-}$ mice compared with WT mice (Figures 1B and 1C; Figure S1B and S1C). Accordingly, ACh-induced NO production was increased in aortas from GRK2$^{+/-}$ animals (Figures 1D; Figure S1D). In contrast, the endothelium-independent vasodilator responses induced by the NO donor diethylamine (DEA)-NO were similar in GRK2$^{+/-}$ and WT mice (Figures 1E; Figure S1E), suggesting that the observed differences are probably due to altered endothelium-mediated NO production. Similar results were observed in MRA from male and female mice (Figure S4A–S4F). ACh-induced NO production was also larger in MRA from male GRK2$^{+/-}$ mice (Figure S4G).

GRK2 Deficiency Reduces the Development of Hypertension and Prevents Vascular Remodeling After AngII Infusion

AngII infusion increased GRK2 levels in WT but not in GRK2$^{+/-}$ aortas (Figure 2A). Basal systolic blood pressure

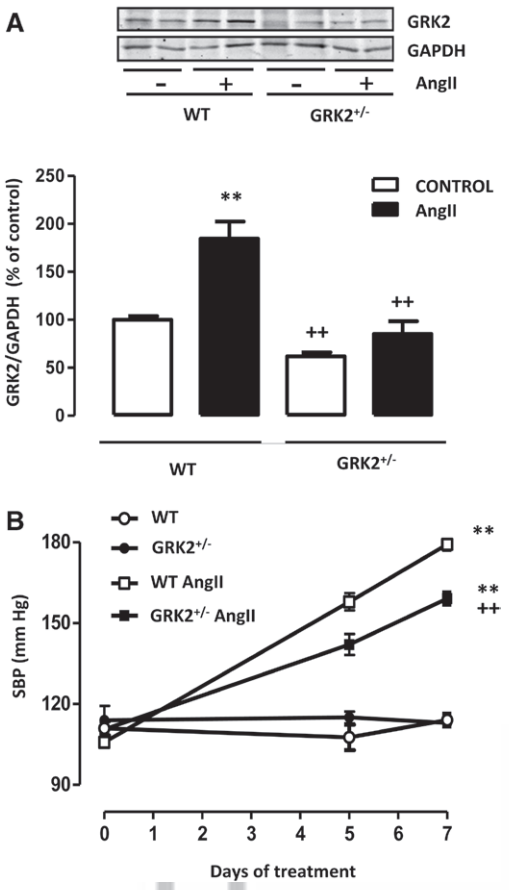

Figure 2. Partial G protein–coupled receptor kinase 2 (GRK2) deficiency reduces angiotensin II (AngII)–induced GRK2 expression and hypertension. **A**, Densitometric analysis and representative blot of GRK2 protein expression in aortic segments from wild-type (WT) and GRK2$^{+/-}$ mice treated or not with AngII. Data were normalized to the values of control WT littermates. **B**, Effect of AngII infusion on systolic blood pressure (SBP) in WT and GRK2$^{+/-}$ mice. Data represent mean±SEM. n=5 to 9. **P<0.01 vs untreated animals. ++P<0.01 vs WT either untreated (CONTROL) or treated with AngII.

(Figure 2B) and heart rate (Figure S5) were similar in untreated WT and GRK2$^{+/-}$ mice. Systemic infusion of AngII increased systolic blood pressure more in WT than in GRK2$^{+/-}$ mice (Figure 2B), but heart rate increase was indistinguishable between both groups (Figure S5).

Lumen and vessel diameter, wall thickness, and wall/lumen ratio of MRA were similar in untreated WT and GRK2$^{+/-}$ mice (Figure S6A–S6D), and vascular stiffness was also similar, as shown by the stress–strain relationship (Figure 3C), β parameter (WT, 4.87±0.3; GRK2$^{+/-}$, 4.98±0.37; n=5–6; P>0.05), and incremental distensibility (Figure S6E). After AngII infusion, lumen and vessel diameter were smaller in WT and similar or slightly larger, respectively, in GRK2$^{+/-}$ mice (Figure S7A–S7D). Wall thickness increased in both groups after AngII infusion (Figure S7E and S7F), and wall/lumen ratio was larger after AngII infusion in WT mice (Figure 3A) but not in GRK2$^{+/-}$ mice (Figure 3B). As expected, AngII increased vessel stiffness (Figure 3C, β parameter: WT, 8.31±0.51; GRK2$^{+/-}$, 6.34±0.35; n=5–7; P<0.05 versus control mice) and decreased distensibility (Figure S8) in MRA from both strains. However, these effects were less pronounced in GRK2$^{+/-}$ than in WT mice (Figure 3C; Figure S8; β parameter, P<0.05 GRK2$^{+/-}$ versus WT mice).

In aorta, lumen and vessel diameters were similar in WT and GRK2$^{+/-}$ mice irrespective of AngII infusion (data not shown). However, media thickness (Figure 3D) and media/lumen ratio (Figure 3E) increased after AngII only in WT and not in GRK2$^{+/-}$ mice, suggesting that partial deletion of GRK2 protects against AngII-induced vascular remodeling.

GRK2 Deficiency Improves Vascular Function and NO Signaling After AngII Infusion

AngII treatment increased vasoconstrictor responses to phenylephrine in WT mice, as described,[12] but not in GRK2$^{+/-}$ mice (Figure 4A and 4B). Because AngII infusion decreases NO availability in aorta,[12] the lack of effect of AngII on phenylephrine responses in GRK2$^{+/-}$ arteries might be related to a lesser decrease in NO. As shown in Figure 4C and 4D, the NOS inhibitor *N*-nitro-L-arginine methyl ester (L-NAME; 100 µmol/L) enhanced phenylephrine contraction in GRK2$^{+/-}$ aortas more than in WT vessels after AngII (dAUC WT, 59±7; GRK2$^{+/-}$, 237±31; P<0.05), suggesting that NO bioavailability after AngII was better preserved in GRK2$^{+/-}$ aortas. Interestingly, endothelium removal also increased phenylephrine contraction more in aorta from AngII-infused GRK2$^{+/-}$ than WT mice (Figure S9; dAUC WT, 149±17; GRK2$^{+/-}$, 242±29; P<0.05), suggesting that in GRK2$^{+/-}$ mice there is an important contribution of the endothelium-derived vasodilator mediators, probably NO, on vascular contractile responses.

The endothelium-dependent vasodilator responses induced by ACh (Figure S10A and S10B) but not those triggered by the endothelium-independent vasodilator DEA-NO (Figure S10C and S10D) were reduced after AngII infusion. However, this deleterious effect of AngII infusion on endothelial function was less pronounced in GRK2$^{+/-}$ mice (% inhibition of maximal response induced by AngII; WT, 41.8±10; GRK2$^{+/-}$, 8.15±3; P<0.05). In agreement, aortic NO production induced by ACh (10 µmol/L) was greater in GRK2$^{+/-}$ than in WT mice infused with AngII (Figure 4E).

To determine whether the increase in NO bioavailability observed in aorta from GRK2$^{+/-}$ mice is a result of alterations of the eNOS-Akt pathway, we measured the activation of Akt (one of the most important upstream activators of eNOS) and eNOS levels. AngII infusion decreased Akt phosphorylation and eNOS protein expression in aortic homogenates from WT mice (Figure 4F and 4G). In contrast, we did not detect any statistically significant decrease in pAkt levels after AngII infusion in GRK2$^{+/-}$ mice and the reduction on eNOS expression was lower than that observed in WT mice (Figure 4F and 4G).

Discussion

Vascular responses of adult GRK2$^{+/-}$ mice were characterized as a surrogate model of the effects exerted by a long-awaited pharmacological GRK2 inhibitor. GRK2$^{+/-}$ mice show enhanced vasodilator and vasoconstrictor responses, with only particular differences toward certain contractile agonists. However, these mice are resistant to AngII-induced systemic hypertension, vascular remodeling, and

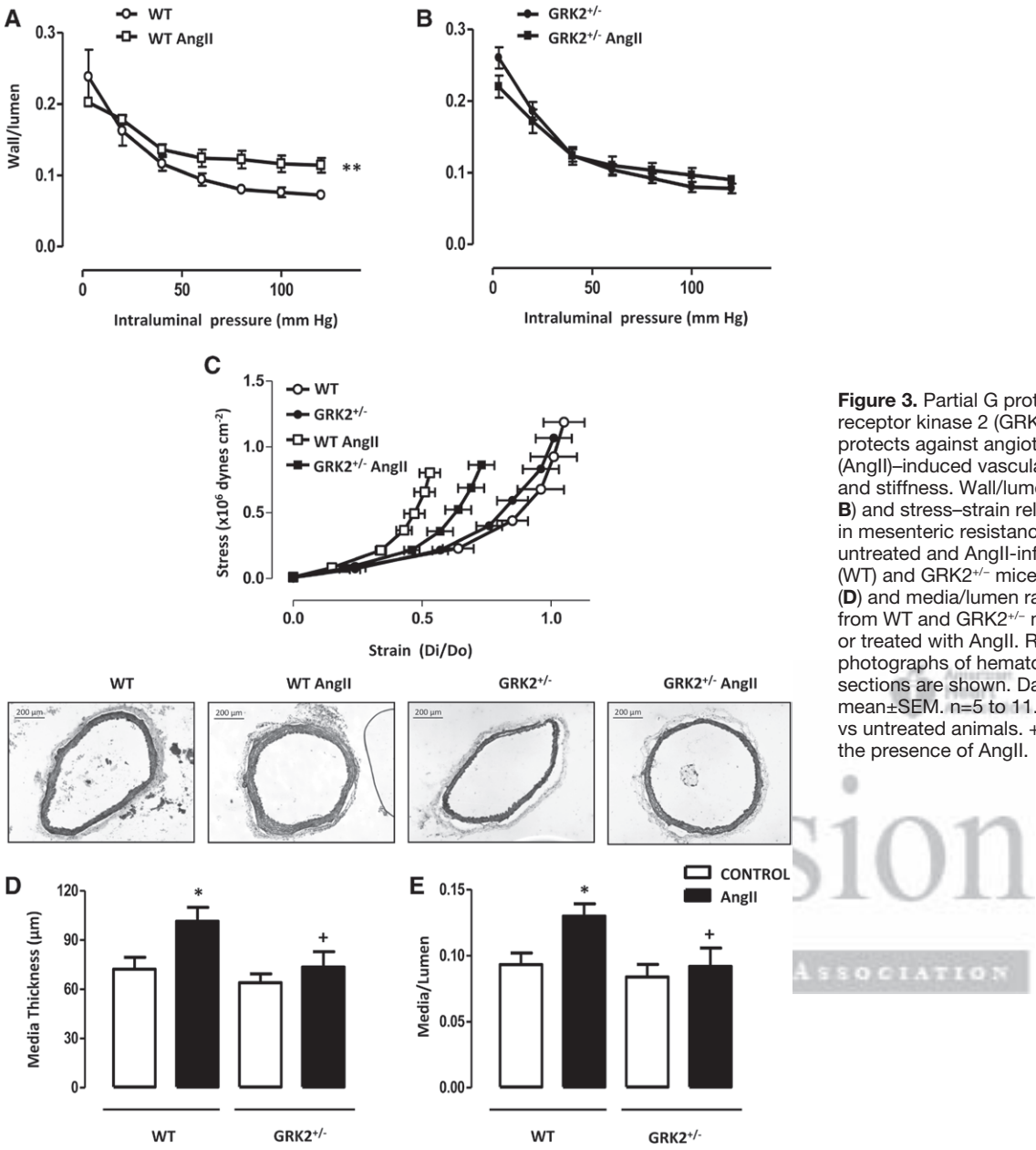

Figure 3. Partial G protein–coupled receptor kinase 2 (GRK2) deficiency protects against angiotensin II (AngII)–induced vascular remodeling and stiffness. Wall/lumen ratio (**A** and **B**) and stress–strain relationship (**C**) in mesenteric resistance arteries from untreated and AngII-infused wild-type (WT) and GRK2$^{+/-}$ mice. Media thickness (**D**) and media/lumen ratio (**E**) in aorta from WT and GRK2$^{+/-}$ mice untreated or treated with AngII. Representative photographs of hematoxylin-eosin aortic sections are shown. Data represent mean±SEM. n=5 to 11. **P*<0.05, ***P*<0.01 vs untreated animals. +*P*<0.05 vs WT in the presence of AngII.

mechanical alterations. They better maintain endothelial function and display an attenuated AngII-induced decline in the Akt-eNOS route and in eNOS levels. These data further build on previous results describing a role for GRK2 in the control of portal hypertension[9,11] and in diabetes mellitus/obesity-triggered mild hypertensive conditions.[13] This report is the first to characterize the role of an overall selective inhibition of GRK2 function in the development of systemic hypertension and in the structure and biomechanics of the vessels.

Partial GRK2 deficiency is not enough to overcome the overt hypertensive phenotype completely achieved by chronic AngII infusion. However, results in diabetic and ob/ob mice[13] showed a full reversal of these types of mild hypertension by the use of a nonselective GRK2 inhibitor. This discrepancy might be explained by differences in the hypertensive models, the use of a wide spectrum GRK2 inhibitor as opposed to a reduction in of GRK2 levels in GRK2$^{+/-}$ mice, and by the lower blood pressure implicit to the diabetes mellitus/obesity study.[13] Also, our mice have been aged until an adult stage (9 months), a period more related to the human clinical setting of hypertension occurrence.

An apparent discrepancy exists between the fact that upregulation of GRK2 in mice models or hypertensive subjects causes elevated blood pressure and results establishing that increased GRK2 protein impairs vasoconstrictor signals.[8] In fact, when GRK2 levels are decreased, desensitization of certain GPCRs is impaired in vascular beds, but, in turn, GRK2 could be regulating vasodilator preferentially over vasoconstrictor receptors.[3] We observed that changes in vasoconstrictor responses induced by GRK2 deficiency depend on the agonist studied, whereas vasodilator ones are always increased in both sexes and in both conductance and resistance arteries. So, pathways alternative to

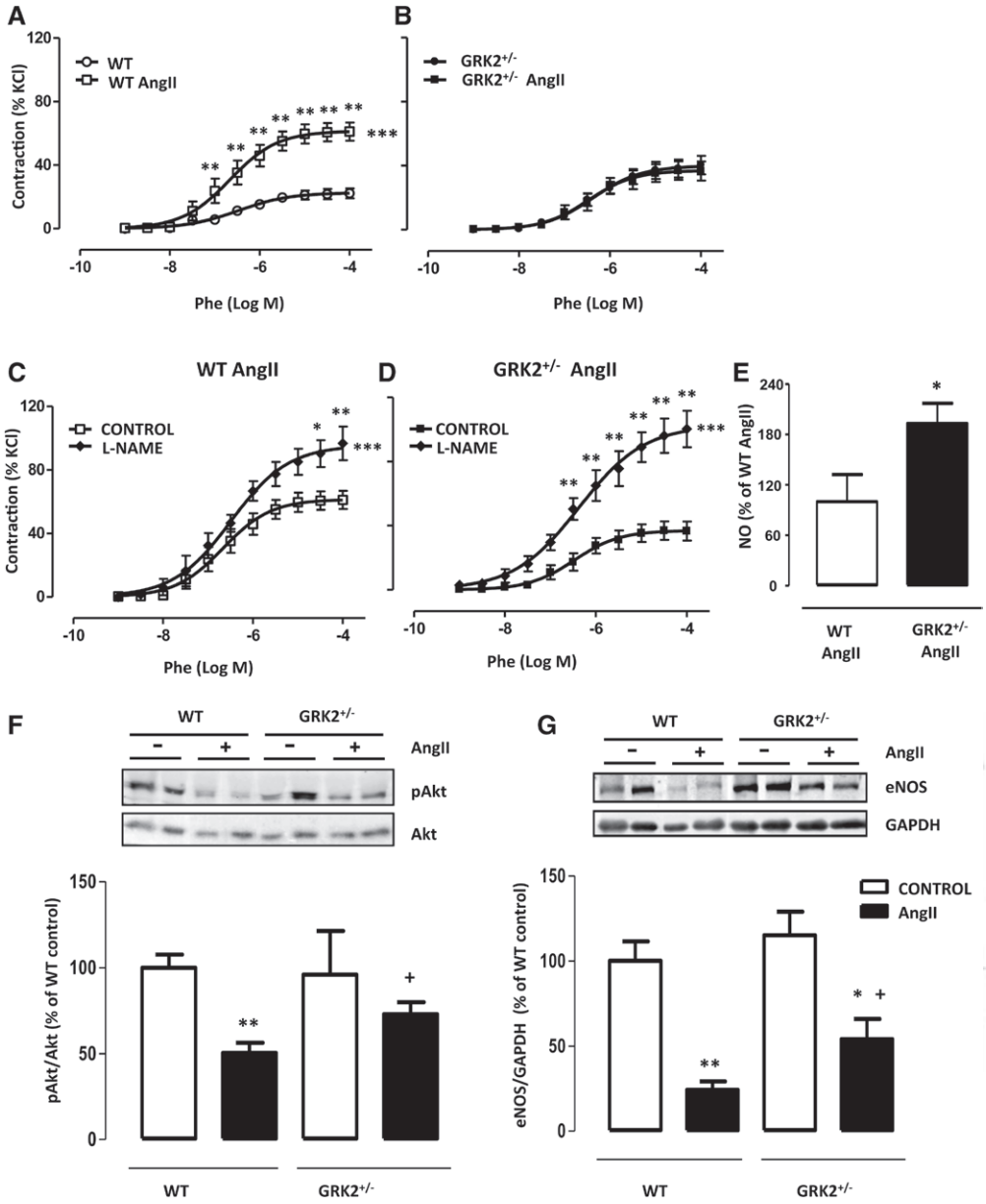

Figure 4. Partial G protein–coupled receptor kinase 2 (GRK2) deficiency protects against angiotensin II (AngII)–induced increased vasoconstriction by increasing endothelial-derived NO production. Effect of AngII infusion on the concentration–response curve to phenylephrine (Phe) in wild-type (WT) and GRK2$^{+/-}$ aortic segments (**A** and **B**). Effect of L-NAME (**C** and **D**) on the concentration–response curve to Phe in aortic segments from WT and GRK2$^{+/-}$ treated with AngII. **E**, Quantification of acetylcholine (ACh)-induced NO release in aortic segments from AngII-treated mice. Densitometric analysis and representative blots of phosphoAkt (pAKt) and Akt (**F**) and eNOS and GAPDH (**G**) in WT and GRK2$^{+/-}$ aortas from mice untreated or treated with AngII. Results are expressed as ratio of phosphoAkt to total Akt or between eNOS to GAPDH and normalized to values obtained for untreated WT mice. Data represent mean±SEM. n=4 to 13. **P*<0.05, ***P*<0.01, ****P*<0.001 vs the corresponding control. +*P*<0.05 vs WT infused with AngII.

GPCR-derived routes could be playing a role. For instance, GRK2 was described to interact with Akt, to impair eNOS activation, and to decrease NO bioavailability and GRK2 silencing reducing renal portal hypertension by increasing the Akt-NOS route,[11] and also a role for GRK2-mediated regulation of NOS in maintaining vascular responses,[14] and during diabetic- or obesity-triggered changes in blood pressure has been reported.[13] Our results represent the first demonstration that NO bioavailability is key to explain the antihypertensive phenotype derived from GRK2 down-regulation because NO production is increased basally in GRK2$^{+/-}$ aortas and mesenteric arteries, and adult GRK2$^{+/-}$ mice are capable of attenuating the AngII-induced drop in NO production much more efficiently than WT littermates. Accordingly, endothelium removal or L-NAME incubation enhanced phenylephrine contraction more in AngII-infused GRK2$^{+/-}$ than in WT aortas. Also, GRK2$^{+/-}$ mice are partially protected from AngII-induced vascular stiffness and remodeling, important determinants of high blood pressure,[15] both in the resistance and in the conductance vasculature. Of note, an increase in GRK2 protein levels in hypertensive WT but not GRK2$^{+/-}$ vessels is observed. This could be ascribed to

the lower hypertension detected in GRK2$^{+/-}$ animals and supports a pathological role of elevated vascular GRK2 levels in the hypertensive phenotype.

An increased basal blood pressure is found in mice overexpressing GRK2 in VSMC,[8] whereas mice deficient in muscular GRK2 show a lack of resistance to renal-induced hypertension.[9] Thus, the restoration of vasodilation achieved by VSMC-GRK2 targeting may not be sufficient to overcome the blunted relaxation responses elicited by endothelial cells. Moreover, Cohn et al[9] described no changes in vasoconstrictor AngII-induced vascular responses in endothelial-deprived vessels or in AngII-induced acute increases in blood pressure in VSMC-GRK2–deficient mice. In contrast, our results using global GRK2$^{+/-}$ mice demonstrate that these animals are partially resistant to AngII-induced hypertension. Comparison of these results clearly establishes that to achieve a therapeutic effect, endothelial GRK2 should be targeted, and that the control of NO bioavailability by GRK2 is crucial. GRK2 directly binds and inhibits Akt,[11] and we detect a maintenance of Akt activation after AngII treatment only in GRK2$^{+/-}$ mice, whereas WT animals efficiently inhibit this route. This preserved activation of Akt is also detected in other tissues in GRK2 hemizygous mice during aging-induced, high fat diet–induced, or tumor necrosis factor α–induced insulin resistance.[16] These changes cannot be tampered by changes in total Akt protein because, as opposed to other systems,[13] we do not detect significant changes in total Akt levels but rather an attenuation of the AngII-induced decline in total eNOS levels. Recently published studies have identified a novel role for GRK2 in mitochondria function and biogenesis. GRK2 removal from skeletal muscle cells reduces ATP production and impairs tolerance to ischemia.[17] However, elevated mitochondrial GRK2 in cardiomyocytes increases cellular injury, thus identifying GRK2 as a prodeath kinase.[18]

In conclusion, a partial deficiency of GRK2 differentially alters vasoconstrictor responses to different agonists. Nevertheless, vasodilator responses seem to be homogeneously increased in GRK2$^{+/-}$ arteries what probably explains the lack of changes in basal blood pressure observed in GRK2$^{+/-}$ mice. In addition, vascular structure and mechanics are similar in both genotypes. However, after an AngII challenge, lower GRK2 levels help to maintain the activation of eNOS through the Akt pathway, thus leading to preserved NO bioavailability. In this situation, NO-dependent vasodilation overcomes constriction which, together with the lesser deterioration of vascular structure and mechanics, explains why GRK2$^{+/-}$ mice are resistant to hypertension (Figure S11) and further highlights GRK2 as a therapeutic target for hypertension.

Perspectives

Our results provide novel evidences suggesting that a global GRK2 decrease could become an efficient treatment for hypertension and further highlight the importance of targeting endothelial GRK2 for an effective control of this condition, thus establishing that GRK2 targeting needs to include the endothelial compartment if reversal of hypertension is to be achieved.

Acknowledgments

We thank Raquel Lopez and Dr Begoña Aguado their help in gene studies.

Sources of Funding

This study was supported by Ministerio de Economía y Competitividad (SAF2009-07201, SAF2011-23800, and SAF 2012-36400), Instituto de Salud Carlos III (RD06/0014/0011, RD06/0014/0037, RD12/0042/0024, RD12/0042/0012, and PS09/01208), Comunidad de Madrid (S2011/BMD-2332), UAM-Grupo Santander, Fundación Mutua Madrileña, Fundación Ramón Areces, and the Ramón y Cajal program (AMB, RYC-2010–06473).

Disclosures

None.

References

1. Rockman HA, Koch WJ, Lefkowitz RJ. Seven-transmembrane-spanning receptors and heart function. *Nature*. 2002;415:206–212.
2. Ribas C, Penela P, Murga C, Salcedo A, García-Hoz C, Jurado-Pueyo M, Aymerich I, Mayor F Jr. The G protein-coupled receptor kinase (GRK) interactome: role of GRKs in GPCR regulation and signaling. *Biochim Biophys Acta*. 2007;1768:913–922.
3. Brinks HL, Eckhart AD. Regulation of GPCR signaling in hypertension. *Biochim Biophys Acta*. 2010;1802:1268–1275.
4. Penela P, Murga C, Ribas C, Tutor AS, Peregrín S, Mayor F Jr. Mechanisms of regulation of G protein-coupled receptor kinases (GRKs) and cardiovascular disease. *Cardiovasc Res*. 2006;69:46–56.
5. Gros R, Chorazyczewski J, Meek MD, Benovic JL, Ferguson SS, Feldman RD. G-Protein-coupled receptor kinase activity in hypertension: increased vascular and lymphocyte G-protein receptor kinase-2 protein expression. *Hypertension*. 2000;35(1 Pt 1):38–42.
6. Cohn HI, Xi Y, Pesant S, Harris DM, Hyslop T, Falkner B, Eckhart AD. G protein-coupled receptor kinase 2 expression and activity are associated with blood pressure in black Americans. *Hypertension*. 2009;54:71–76.
7. Morris GE, Nelson CP, Standen NB, Challiss RA, Willets JM. Endothelin signalling in arterial smooth muscle is tightly regulated by G protein-coupled receptor kinase 2. *Cardiovasc Res*. 2010;85:424–433.
8. Eckhart AD, Ozaki T, Tevaearai H, Rockman HA, Koch WJ. Vascular-targeted overexpression of G protein-coupled receptor kinase-2 in transgenic mice attenuates beta-adrenergic receptor signaling and increases resting blood pressure. *Mol Pharmacol*. 2002;61:749–758.
9. Cohn HI, Harris DM, Pesant S, Pfeiffer M, Zhou RH, Koch WJ, Dorn GW II, Eckhart AD. Inhibition of vascular smooth muscle G protein-coupled receptor kinase 2 enhances alpha1D-adrenergic receptor constriction. *Am J Physiol Heart Circ Physiol*. 2008;295:H1695–H1704.
10. Belmonte SL, Blaxall BC. G protein coupled receptor kinases as therapeutic targets in cardiovascular disease. *Circ Res*. 2011;109:309–319.
11. Liu S, Premont RT, Kontos CD, Zhu S, Rockey DC. A crucial role for GRK2 in regulation of endothelial cell nitric oxide synthase function in portal hypertension. *Nat Med*. 2005;11:952–958.
12. Martínez-Revelles S, Avendaño MS, García-Redondo AB, Alvarez Y, Aguado A, Pérez-Girón JV, García-Redondo L, Esteban V, Redondo JM, Alonso MJ, Briones AM, Salaices M. Reciprocal relationship between reactive oxygen species and cyclooxygenase-2 and vascular dysfunction in hypertension. *Antioxid Redox Signal*. 2013;18:51–65.
13. Taguchi K, Matsumoto T, Kamata K, Kobayashi T. Inhibitor of G protein-coupled receptor kinase 2 normalizes vascular endothelial function in type 2 diabetic mice by improving β-arrestin 2 translocation and ameliorating Akt/eNOS signal dysfunction. *Endocrinology*. 2012;153:2985–2996.
14. Taguchi K, Kobayashi T, Takenouchi Y, Matsumoto T, Kamata K. Angiotensin II causes endothelial dysfunction via the GRK2/Akt/eNOS pathway in aortas from a murine type 2 diabetic model. *Pharmacol Res*. 2011;64:535–546.
15. Briones AM, Arribas SM, Salaices M. Role of extracellular matrix in vascular remodeling of hypertension. *Curr Opin Nephrol Hypertens*. 2010;19:187–194.
16. Garcia-Guerra L, Nieto-Vazquez I, Vila-Bedmar R, Jurado-Pueyo M, Zalba G, Díez J, Murga C, Fernández-Veledo S, Mayor F Jr, Lorenzo M.

G protein-coupled receptor kinase 2 plays a relevant role in insulin resistance and obesity. *Diabetes*. 2010;59:2407–2417.
17. Fusco A, Santulli G, Sorriento D, Cipolletta E, Garbi C, Dorn GW II, Trimarco B, Feliciello A, Iaccarino G. Mitochondrial localization unveils a novel role for GRK2 in organelle biogenesis. *Cell Signal*. 2012;24:468–475.
18. Chen M, Sato PY, Chuprun JK, Peroutka RJ, Otis NJ, Ibetti J, Pan S, Sheu SS, Gao E, Koch WJ. Prodeath signaling of G protein-coupled receptor kinase 2 in cardiac myocytes after ischemic stress occurs via extracellular signal-regulated kinase-dependent heat shock protein 90-mediated mitochondrial targeting. *Circ Res*. 2013;112:1121–1134.

Novelty and Significance

What Is New?

- Partial deficiency in G protein–coupled receptor kinase 2 (GRK2) affects vasoconstrictor responses and desensitization in a differential manner depending on the agonist studied without apparent changes in receptor levels. However, endothelium-dependent vasodilator responses are homogeneously increased in adult GRK2$^{+/-}$ conductance and resistance arteries via an increased NO availability.
- After AngII challenge, the lower GRK2 levels in adult GRK2$^{+/-}$ mice maintain the activation of eNOS by preserving phosphorylation of Akt. This better maintains NO bioavailability and protects vascular function in GRK2$^{+/-}$ mice. These facts, together with a less deteriorated vascular structure and mechanics after AngII challenge in GRK2$^{+/-}$ mice, might explain their resistance to the development of hypertension.
- This is the first report to characterize the effect of a systemic reduction in GRK2 levels on vascular structure and biomechanics, both in basal and in AngII-treated adult mice.

What Is Relevant?

- Our results provide new evidences for a novel therapeutic effect of lowering GRK2 levels/activity through the modulation of vascular function and NO bioavailability.

Summary

Partial deficiency of GRK2 differentially alters vasoconstrictor responses to different agonists, whereas vasodilator responses are homogeneously increased. After an AngII challenge, GRK2$^{+/-}$ mice maintain endothelial function, exhibit diminished vasoconstrictor responses, and display improved vascular structure and vessel stiffness compared with age-matched wild-type littermates. Moreover, GRK2$^{+/-}$ mice display an impaired AngII-induced decline in both the activation of the Akt-eNOS route and in total levels of the eNOS protein, thus leading to a preserved NO availability and a resistance to the development of hypertension.

ONLINE SUPPLEMENT

INCREASED NITRIC OXIDE BIOAVALIABILITY IN ADULT GRK2- HEMIZYGOUS MICE PROTECTS AGAINST ANGIOTENSIN II-INDUCED HYPERTENSION

María S. Avendaño*[,1,2], Elisa Lucas*[,3,4], María Jurado-Pueyo[3,4], Sonia Martínez-Revelles[1,2], Rocío Vila-Bedmar[3,4], Federico Mayor Jr.[3,4], Mercedes Salaices[1,2], Ana M. Briones[&,1,2], Cristina Murga[&,3,4]

*Equal contribution

[&]Corresponding authors

[1]Departamento de Farmacología, Facultad de Medicina, Universidad Autónoma de Madrid, Spain

[2]Instituto de Investigación Sanitaria La Paz, Madrid, Spain.

[3]Departamento de Biología Molecular and Centro de Biología Molecular "Severo Ochoa", Universidad Autónoma de Madrid and CSIC, Spain

[4]Instituto de Investigación Sanitaria La Princesa, Madrid, Spain

Short title: GRK2 deficiency prevents hypertension development

Corresponding authors:

Dr. Cristina Murga
Dpto. Biología Molecular, Centro de Biología Molecular "Severo Ochoa"
Facultad de Ciencias. Universidad Autónoma de Madrid
Nicolás Cabrera 1, 28049-Madrid, Spain
Phone: 34911964641
Fax: 3491196 44 20
cristina.murga@uam.es

Dr. Ana M. Briones
Dpto. Farmacología
Facultad de Medicina. Universidad Autónoma de Madrid
Arzobispo Morcillo 2, 28029-Madrid, Spain
Phone: 34914975399
Fax: 3491497 53 80
ana.briones@uam.es

METHODS

Animal models

Male and female mice either wild type (WT) or GRK2 hemizygous ($GRK2^{+/-}$) were generated on the C57BL/6 genetic background as described.[1] Four groups of 9 month-old mice were used: 1) WT; 2) $GRK2^{+/-}$; 3) WT infused with AngII (1.44 mg/Kg/day, 1 week, subcutaneously by osmotic minipumps, Alza Corp., CA, USA); 4) $GRK2^{+/-}$ infused with AngII. In a pilot study, we observed that minipump surgery followed by infusion with saline did not alter systolic blood pressure or vascular contractile responses in WT or $GRK2^{+/-}$ mice (data not shown).

Blood pressure and heart rate were measured by tail-cuff plethysmography. The Animal Care and Use Committee of our Institution, according to the guidelines for ethical care of experimental animals of the European Community, approved all experimental procedures. The study was conducted in accordance with the National Institutes of Health (NIH) Guide for the Care and Use of Laboratory Animals (NIH Publication No. 85-23, revised 1996) and the current Spanish and European laws (RD 223/88 MAPA and 609/86).

Reactivity Experiments

Reactivity of mouse aorta and first-order branches of the mesenteric artery (MRA) was studied in a wire myograph, as previously described.[2] After a 30-min equilibration period in oxygenated Krebs Henseleit solution (KHS), arterial segments were stretched to their optimal lumen diameter for active tension development. Contractility of segments was then tested by an initial exposure to KCl (120 mM). The presence of endothelium was determined by the ability of 10 µmol/L acetylcholine (ACh) to relax arteries precontracted with phenylephrine at approximately 50% K^+-KHS contraction. Concentration-response curves to ACh, isoproterenol or diethylamine NONOate (DEA-NO) were performed in segments precontracted with phenylephrine. In other segments, concentrations response curves to phenylephrine in the presence or the absence of L-N^G-Nitroarginine Methyl Ester (L-NAME, 100 µmol/L) were performed. L-NAME was added 30 min before phenylephrine. A single concentration-dependent curve was performed in each segment. In other set of experiments, three consecutive administration of Angiotensin II (1 µmol/L) or Endothelin-1 (0.1 µmol/L) were given, at intervals of 30 min, with removal always after each dose of the drug present in the medium. In a separate group of arteries, endothelial layer was mechanically removed by rubbing the intimal surface.

Vasoconstrictor responses were expressed as a percentage of the tone generated by KCl. KCl-induced responses were similar in aorta from WT and $GRK2^{+/-}$ male and female mice (Table S1). Vasodilator responses were expressed as a percentage of the previous tone generated by phenylephrine. To compare the effect of L-NAME or endothelial removal on phenylephrine responses in segments from the different experimental groups, some results were expressed as 'differences of area under the concentration-response curves' (dAUC) in the absence and the presence of L-NAME or in the presence and in the absence of endothelial layer. AUCs were calculated from the individual concentration-response curve plots; the differences were expressed as a percentage of the AUC of the corresponding control situation.

NO Release

After an equilibration period of 60 min in HEPES buffer (in mmol/L: NaCl 119; HEPES 20; $CaCl_2$ 1.2; KCl 4.6; $MgSO_4$ 1; KH_2PO_4 0.4; $NaHCO_3$ 5; glucose 5.5; Na_2HPO_4 0.15; pH 7.4) at 37°C, aortic and mesenteric arteries segments of all the experimental conditions were incubated with the fluorescent probe 4,5-diaminofluorescein (DAF-2; 2 µmol/L) for 45 min. Then, the medium was collected to measure basal NO release. Afterwards these segments were incubated with phenylephrine 1 µmol/L and relaxed with ACh 10 µ µmol/L. At the end of this stimulation, the medium was collected to measure induced NO release. The fluorescence of the medium was measured at room temperature using a spectrofluorimeter (FLUOstar OPTIMA BMG LABTECH) with excitation wavelength set at 492 nm and emission wavelength at 515 nm.

The induced NO release was calculated by subtracting basal NO release from that evoked by ACh. Also, blank samples were collected in the same way as from segment-free medium in order to correct for background emission. The amount of NO released was expressed as arbitrary units/mg tissue. Data were expressed as % of results obtained for WT mice.

Pressure myography

The structural and mechanical properties of MRA were studied with a pressure myograph (Danish Myo Tech, Model P100, J.P. Trading I/S, Aarhus, Denmark), as previously described.[3] Briefly, the vessel was placed on two glass microcannulae and secured with surgical nylon suture. After any small branches were tied off, vessel length was adjusted so that the vessel walls were parallel without stretch. Intraluminal pressure was then raised to 120 mm Hg and the artery was unbuckled by adjusting the cannulae. The segment was then set to a pressure of 45 mm Hg and allowed to equilibrate for 60 min at 37ºC in calcium-free Krebs Henseleit Solution ($0Ca^{2+}$ KHS; omitting calcium and adding 1 mmol/L EGTA) intra and extra-vascular perfused gassed with a mixture of 95% O_2 and 5% CO_2. Intraluminal pressure was reduced to 3 mm Hg. A pressure-diameter curve was obtained by increasing intraluminal pressure in 20 mm Hg steps between 3 and 120 mm Hg. Internal and external diameters were continuously measured under passive conditions (Di0Ca, De0Ca) for 3 min at each intraluminal pressure. The final value used was the mean of the measurements taken during the last 30 seconds when the measurements reached a steady state.

Calculation of passive structural and mechanical parameters

From internal and external diameter measurements in passive conditions the following structural and mechanical parameters were calculated:

Wall:lumen =(De0Ca-Di0Ca)/ 2Di0Ca

Circumferential wall strain (ε)= (Di0Ca -D00Ca)/D00Ca, where D00Ca is the internal diameter at 3 mm Hg and Di0Ca is the observed internal diameter for a given intravascular pressure both measured in $0Ca^{2+}$ medium.

Circumferential wall stress (σ)= (P x Di0Ca)/(2WT), where P is the intraluminar pressure (1 mm Hg = 1.334×10^3 dynes/cm^2) and WT is wall thickness at each intraluminar pressure in $0Ca^{2+}$-KHS.

Arterial stiffness independent of geometry is determined by the Young's elastic modulus (E=stress/strain). The stress-strain relationship is non-linear; therefore, it is more appropriate to

obtain a tangential or incremental elastic modulus (Einc) by determining the slope of the stress-strain curve (Einc=δσ/δε). Einc was obtained by fitting the stress-strain data from each animal to an exponential curve using the equation:

$\sigma = \sigma_{orig} e^{\beta\varepsilon}$ where σorig is the stress at the original diameter (diameter at 3 mmHg). Taking derivatives on the above equation we see that Einc=βσ. For a given σ value, Einc is directly proportional to β. An increase in β implies an increase in Einc which means an increase in stiffness.

Histological analysis and vessel morphometry

Aortas were fixed with 4% paraformaldehyde and embedded in Tissue Tek OCT medium. 10-μm cross sections from fixed aortas were stained with hematoxylin-eosin. All images were acquired at room temperature using a microscope (DM2000; Leica) with 10× objective. Morphometric determinations of the lumen and vessel areas were performed by using Metamorph image analysis software (Universal Imaging, Molecular Devices Corp. Downingtown, PA, USA). All microscopic images of the sections were traced for the calculations of the areas. To determine the luminal area, the cross-sectional area enclosed by the internal elastic lamina was corrected to a circle by applying the form factor $l^2/4\pi$ to the measurement of the internal elastic lamina, where l is the length of the lamina. Vessel area was determined by the cross-sectional area enclosed by the external elastic lamina corrected to a circle, applying the same form factor ($l^2/4\pi$) to the measurement of the external elastic lamina. The media area was calculated as the difference between the corrected vessel and luminal areas. Internal and external diameters were calculated from luminal and vessel areas, respectively. This method avoids miscalculations of areas caused by eventual collapse of the immersion-fixed arteries.[4]

Western Blot

Frozen aortas and mesenteric arteries were pulverized using liquid nitrogen and a smasher and homogenized in RIPA buffer (100 mmol/L Tris-HCl pH 7.4, 0.6 mol/L NaCl, 2% Triton x-100 (v/v), 0.2% SDS, 1% DOC) completed with protease and phosphatase inhibitors (100 μmol/L PMSF, 1 μmol/L Benzamidine, 10 μg/mL STI, 16 μU Aprotinine, 10 μg/mL Bacitracine and Phosphatase Inhibitor Cocktail (PhosSTOP, Roche) following the manufacturer´s protocol for 1 h. at 4ºC. Next, samples were centrifuged at maximum speed and supernatants were quantified. To determine protein expression, 30-40 μg of protein were resolved on a 7.5% SDS-PAGE gel and transferred to nitrocellulose. The membrane was immunoblotted using primary antibodies against eNOS (BD Transduction Laboratories) (1:1000), phospho-Akt (Ser473) (Cell Signaling) (1:1000), Akt (Cell Signaling) (1:1000), GRK2 (Santa Cruz) (1:1000), AT1 (Santa Cruz) (1:200), AT2 (Santa Cruz) (1:200) and GAPDH (Abcam) (1:5000). Blots were developed using fluorescently labelled secondary antibodies and measured the signal on a LiCOR Odyssey scanner. Data were normalized to GAPDH or total protein values, and expressed as % over results obtained for untreated or WT mice.

qRT-PCR

mRNA from frozen aortas were extracted using metal beads (2 min, 30 Hz) in a Tissue Lyser and Fibrous Tissue RNeasy Mini Kit, both from QIAGEN. For quantitative PCR, total RNA was reverse transcribed using SuperScript® III First-Strand Synthesis System (Invitrogen) according manufacturer´s protocol. cDNAs were quantified by real-time PCR on an Applied Biosystems 7900HT Fast Real-Time PCR System, using specific primers for mouse *Adra1d*: 5′-GTC TTC GTC CTG TGC TGG TT-3′ and 5′-CTT GAA GAC GCC CTC TGA TG-3′, *Agtr1a*: 5′-TCT GCT GCT CTC CCG GAC T-3′ and 5′-TGC TGT GAG TTA TCC CAG ACA AAA TG-3′, *Agtr1b*: 5′-GTG ACA TGA TCC CCT GAC AGT-3′ and 5′-AGT GAG TGA ACT GTC TAG CTA AAT GC-3′, *Agtr2*: 5′-GGG AGC TGA GTA AGC TGA TTT ATG A-3′ and 5′-AGC AAC TCC AAA TTC TTA CAC CTT TTT A-3′, *Ednr*a: 5′-ACC CTC GTT CTC CAG CTC A-3′ and 5′-TTG GTC TCA CGC CTT TCT TT-3′, *Ednrb*: 5′-AAT GGT CCC AAT ATC TTG ATC G-3′ and 5′-TCC AAA TGG CCA GTC CTC T-3′, *Adrbk1:* 5′-GCA GTT TGT CCT GCA GTG TG -3′ and 5′-TTC ATC TTG GGT ACT CGC TGT-3′, *Hprt*: 5′-CCT GGT TCA TCA TCG CTA ATC-3′ and 5′-TCC TCC TCA GAC CGC TTT T-3′, *Rps29*: 5′-CTG AAC ATG TGC CGC CAG T-3′ and 5′-TCA AGG TCG CTT AGT CCA ACT TAA T-3′, *Gapdh:* 5′-CTC CCA CTC TTC CAC CTT CG-3′ and 5′-CAT ACC AGG AAA TGA GCT TGA CAA-3′, *β-actin*: 5′-CTA AGG CCA ACC GTG AAA AG-3′ and 5′-ACC AGA GGC ATA CAG GGA CA-3′ and *18S*: 5′-CTC AAC ACG GGA AAC CTC AC-3′ and 5′-CGC TCC ACC AAC TAA GAA CG-3′. PCR amplification was performed in a volume of 10 µl containing 2.5 µmol/L of each primer and 5 µl Power Sybr Green PCR Master Mix (Applied Biosystems). The conditions were 95 °C for 10 min, followed by 40 cycles of 15 s at 95 °C, 60 s at 60 °C, followed by 15 s at 95 ºC, 15 s at 60 ºC and 15 s at 95 ºC. *Adra1d, Agtr1a, Agtr1b, Agtr2, Ednra* and *Ednrb* mRNA levels were subsequently normalized to *Hprt, Rps29* and *Gapdh* mRNA which were the better for normalization according NormFinder software because of their stability through the different groups under study. The results obtained were analysed by GenEx 5.3.7 software.

Data Analysis and Statistics

All data are expressed as mean values±SEM and *n* represents the number of animals. Results were analyzed by two-way ANOVA for repeated measures followed by Bonferroni's *post hoc* test for the concentration response curves data, and by unpaired Student's *t*-test, Mann-Whitney or one-way ANOVA for the other measurements. Statistical symbols in the concentration response curves indicate differences in the two way ANOVA when placed close to the curve and differences in the *post hoc* test when placed above or below individual doses. A $p<0.05$ was considered significant.

REFERENCES

1. Jaber M, Koch WJ, Rockman H, Smith B, Bond RA, Sulik KK, Ross J Jr, Lefkowitz RJ, Caron MG, Giros B. Essential role of beta-adrenergic receptor kinase 1 in cardiac development and function. *Proc Natl Acad Sci U S A*. 1996; 93: 12974-12979.

2. Martínez-Revelles S, Avendaño MS, García-Redondo AB, Alvarez Y, Aguado A, Pérez-Girón JV, García-Redondo L, Esteban V, Redondo JM, Alonso MJ, Briones AM, Salaices M. Reciprocal Relationship Between Reactive Oxygen Species and Cyclooxygenase-2 and Vascular Dysfunction in Hypertension. *Antioxid Redox Signal*. 2013;18:51-65.

3. Briones AM, Rodríguez-Criado N, Hernanz R, García-Redondo AB, Rodrigues-Díez RR, Alonso MJ, Egido J, Ruiz-Ortega M, Salaices M. Atorvastatin prevents angiotensin II-induced vascular remodeling and oxidative stress. *Hypertension*. 2009;54:142-149.

4. Bonthu S, Heistad DD, Chappell DA, Lamping KG, Faraci FM. Atherosclerosis, vascular remodeling, and impairment of endothelium dependent relaxation in genetically altered hyperlipidemic mice. *Arterioscler Thromb Vasc Biol*. 1997; 17:2333–2340.

Table S1. Effect of partial GRK2 deletion ($GRK2^{+/-}$) on vasoconstrictor responses in aortic rings from male and female mice.

	Male		**Female**	
Vasoconstrictor drug	**WT**	**$GRK2^{+/-}$**	**WT**	**$GRK2^{+/-}$**
KCl (mN/mm)	2.50±0.31	2.82±0.45	2.59±0.12	2.61±0.19
Phe (Emax) (mN/mm)	0.69±0.12	1.14±0.17*	1.25±0.18	1.83±0.16*
ET-1 (Emax) (mN/mm)	0.08±0.05	0.26±0.05*	-	-
Ang II (Emax) (mN/mm)	0.07±0.02	0.08±0.06	-	-

Data are expressed as mean±SEM. n=4-12. *P<0.05 vs WT.

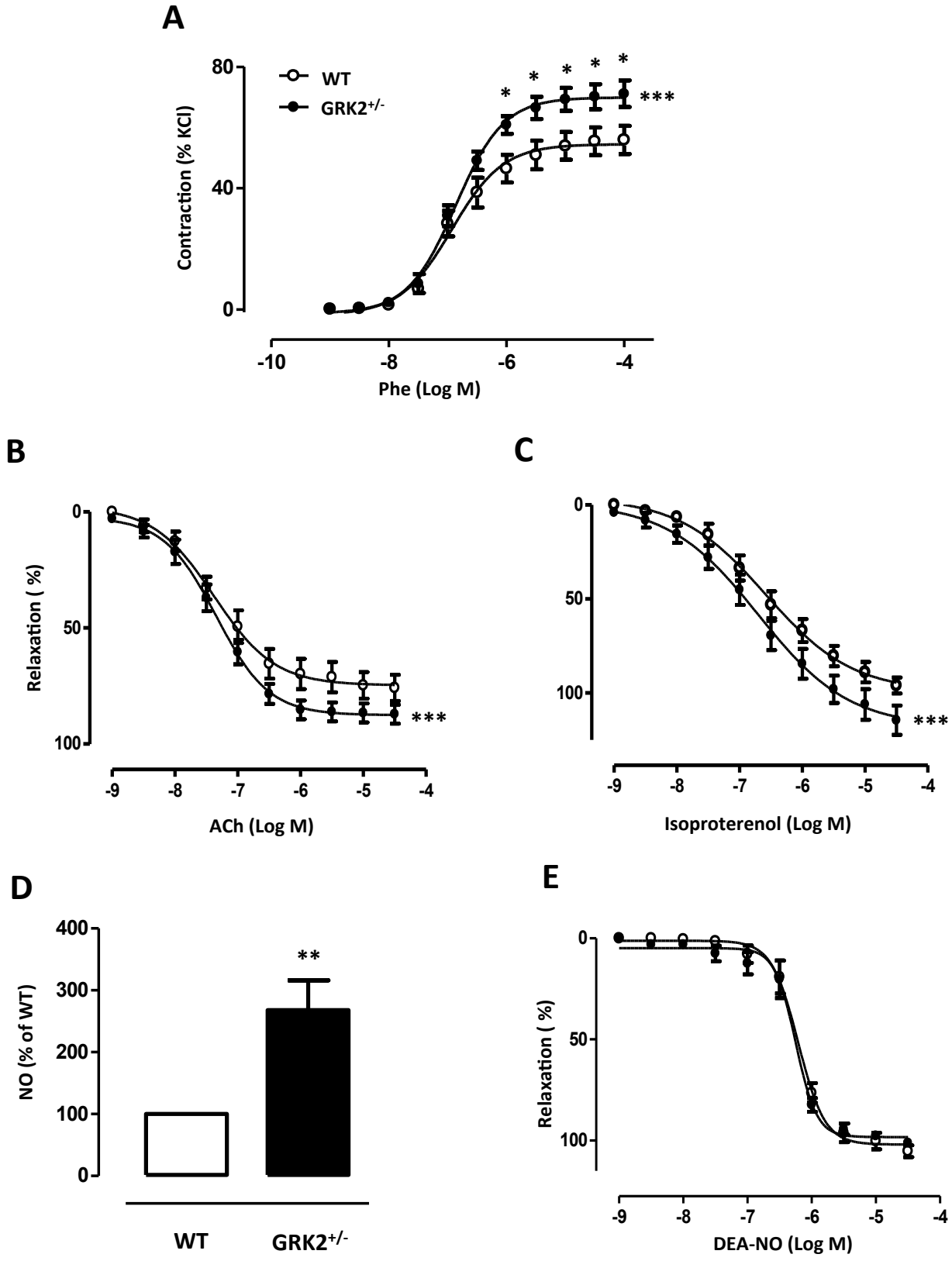

Figure S1. Effects of partial GRK2 deficiency on vasoconstrictor and vasodilator responses and in NO production in aorta from female adult mice. Concentration-response curve to phenylephrine (Phe) (A), acetylcholine (ACh) (B), isoproterenol (C), and diethylamine NONOate (DEA-NO) (E) and quantification of ACh-induced NO release (D) in aorta from female wild type (WT) and GRK2$^{+/-}$ mice. n=7-10. *P<0.05, **P<0.01, ***P<0.001.

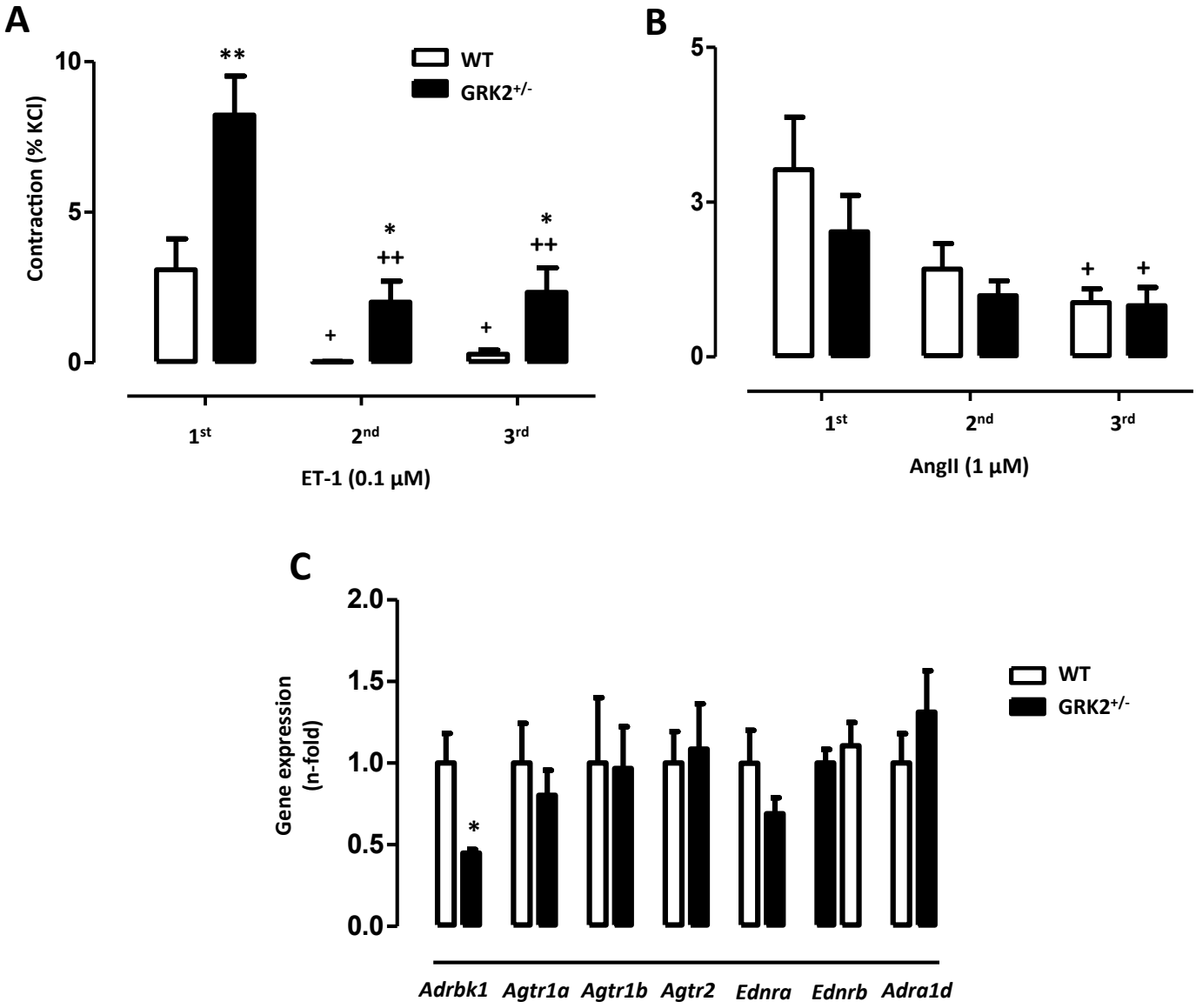

Figure S2. Vasoconstrictor responses to endothelin-1 (ET-1) (A) and Angiotensin II (AngII) (B) administered three consecutive times at intervals of 30 min in aortas from WT and GRK2 $^{+/-}$ mice. (C) Gene expression of GRK2 (*Adrbk1*), Angiotensin receptors type 1a and b and 2 (*Agtr1a, Agtr1b, Agtr2*), endothelin-1 A and B receptors (*Ednra, Ednrb*) and $\alpha 1_D$ receptor (*Adra1d*) in aorta from WT and GRK2$^{+/-}$ adult mice. Data were normalized to values of WT mice. Data represent mean±SEM. n=5-9. *P<0.05; **P<0.01 vs WT. +p<0.05, ++p<0.01 vs first administration.

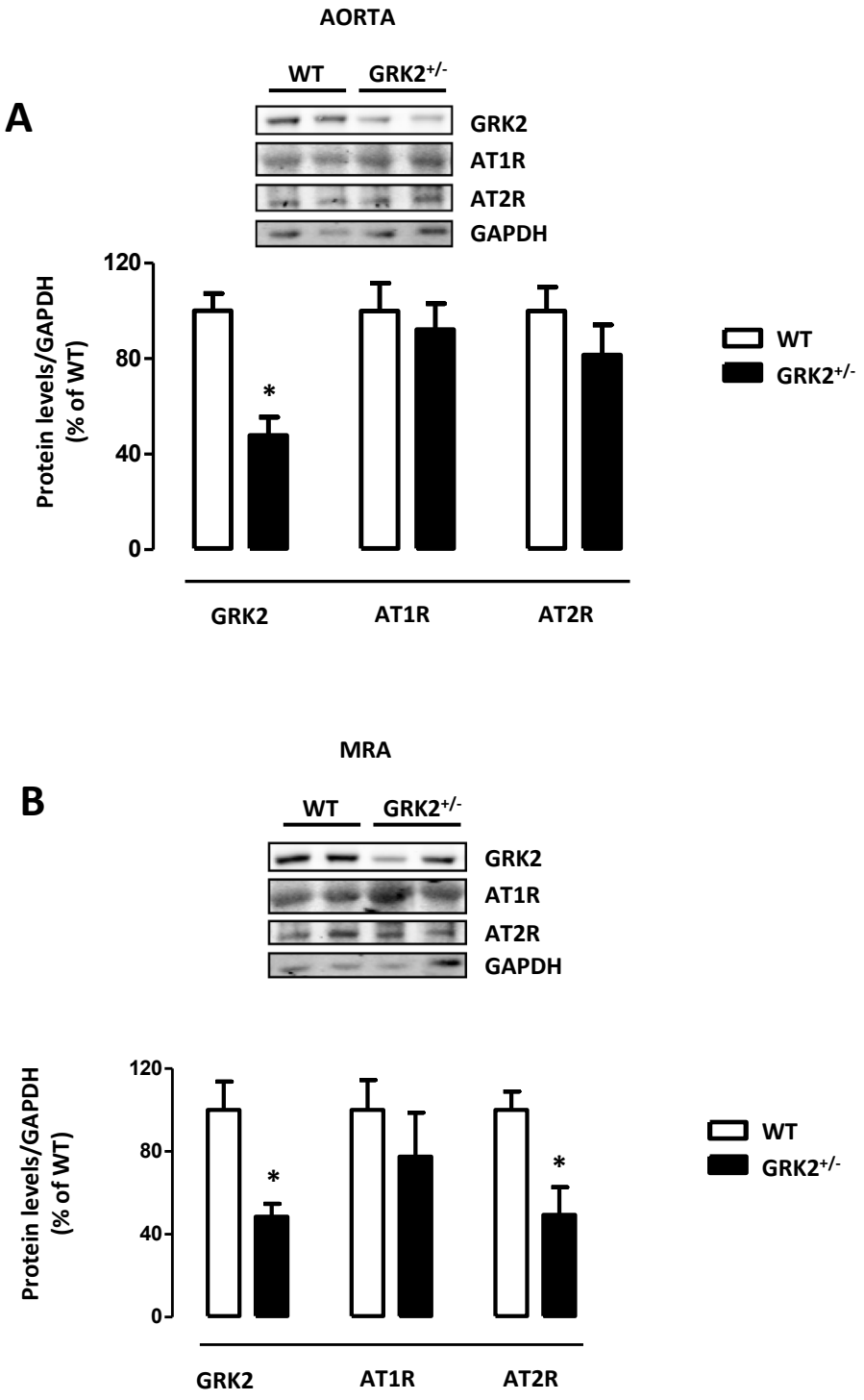

Figure S3. Effects of partial GRK2 deficiency on protein expression of GRK2 and AT1 and AT2 receptors. Representative Western Blot and quantification of the protein expression of GRK2 and AT1 and AT2 receptors (AT1R, AT2R) in aorta (A) and mesenteric resistance arteries (MRA) (B) from WT and GRK2$^{+/-}$ mice. Data were normalized to GAPDH and to values of WT mice that were considered as 100%. n=4-7. *P<0.05 vs WT.

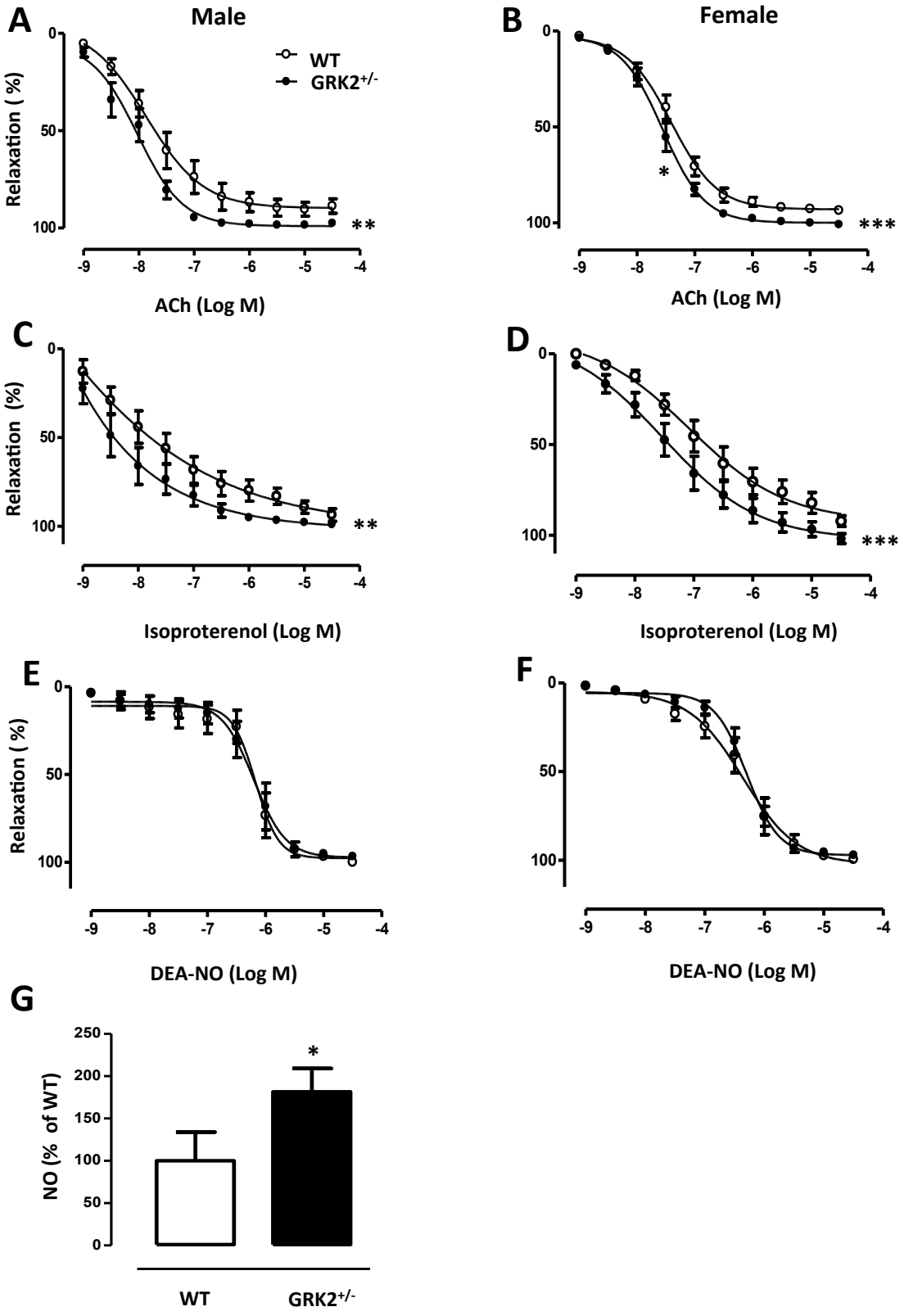

Figure S4. Partial GRK2 deficiency increases vasodilator responses and nitric oxide (NO) production in mesenteric resistance arteries (MRA). Concentration-response curve to acetylcholine (ACh) (A,B), isoproterenol (C,D) and diethylamine NONOate (DEA-NO) (E,F) in MRA from adult male and female wild type (WT) and GRK2$^{+/-}$ mice. (G) Quantification of ACh-induced NO release in MRA from male WT and GRK2$^{+/-}$ mice. n=5-10. *P<0.05, **P<0.01, ***P<0.001.

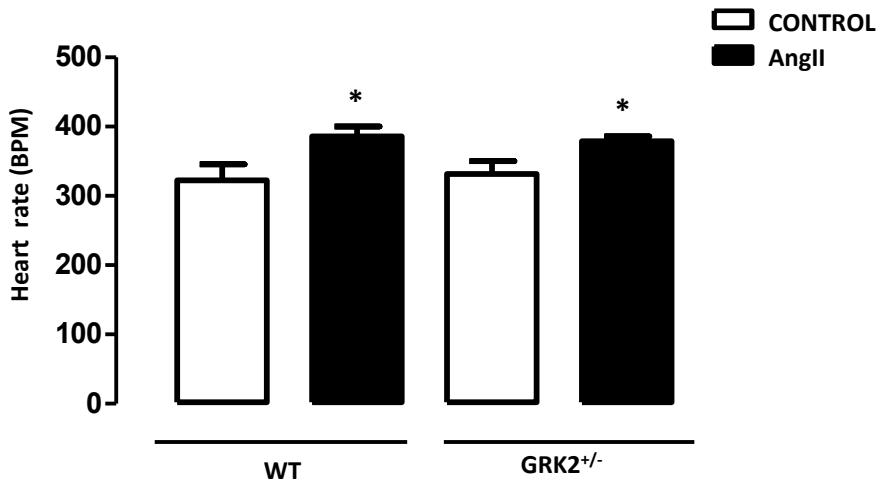

Figure S5. Partial GRK2 deficiency does not modify the effect of Angiotensin II (AngII) infusion on heart rate. Heart rate is expressed as beats per minute (BPM) and was determined in male wild type (WT) and GRK2$^{+/-}$ mice untreated (CONTROL) or treated with AngII. n=5-7. *P<0.05 vs control.

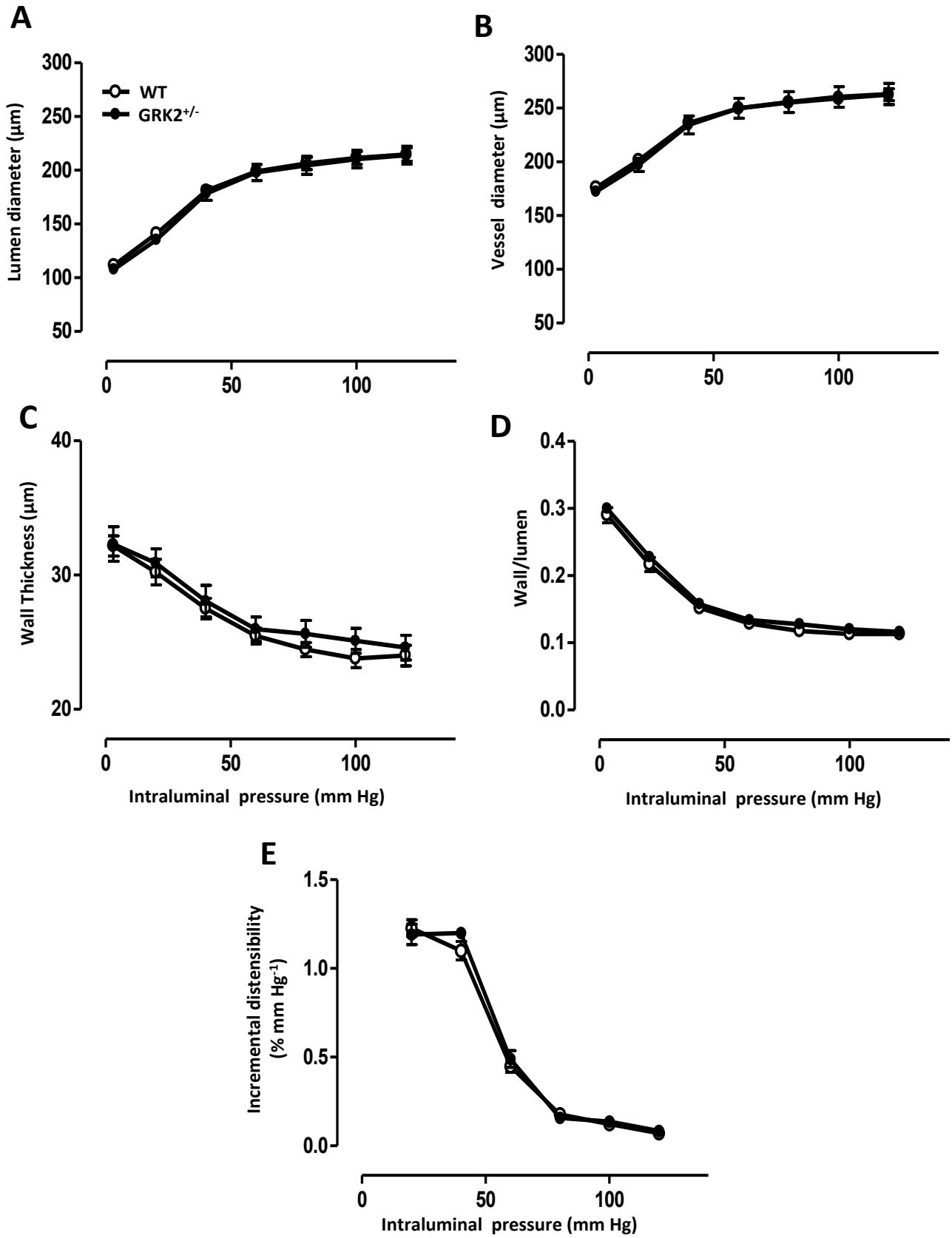

Figure S6. Effects of partial GRK2 deficiency on vascular structural and mechanical parameters. Lumen and vessel diameter-intraluminal pressure (A,B), wall thickness-intraluminal pressure (C), wall/lumen-intraluminal pressure (D), and incremental distensibility-intraluminal pressure (E) in mesenteric resistance arteries incubated in $0Ca^{2+}$Krebs Henseleit solution from wild type (WT) and $GRK2^{+/-}$ mice. n=8-9.

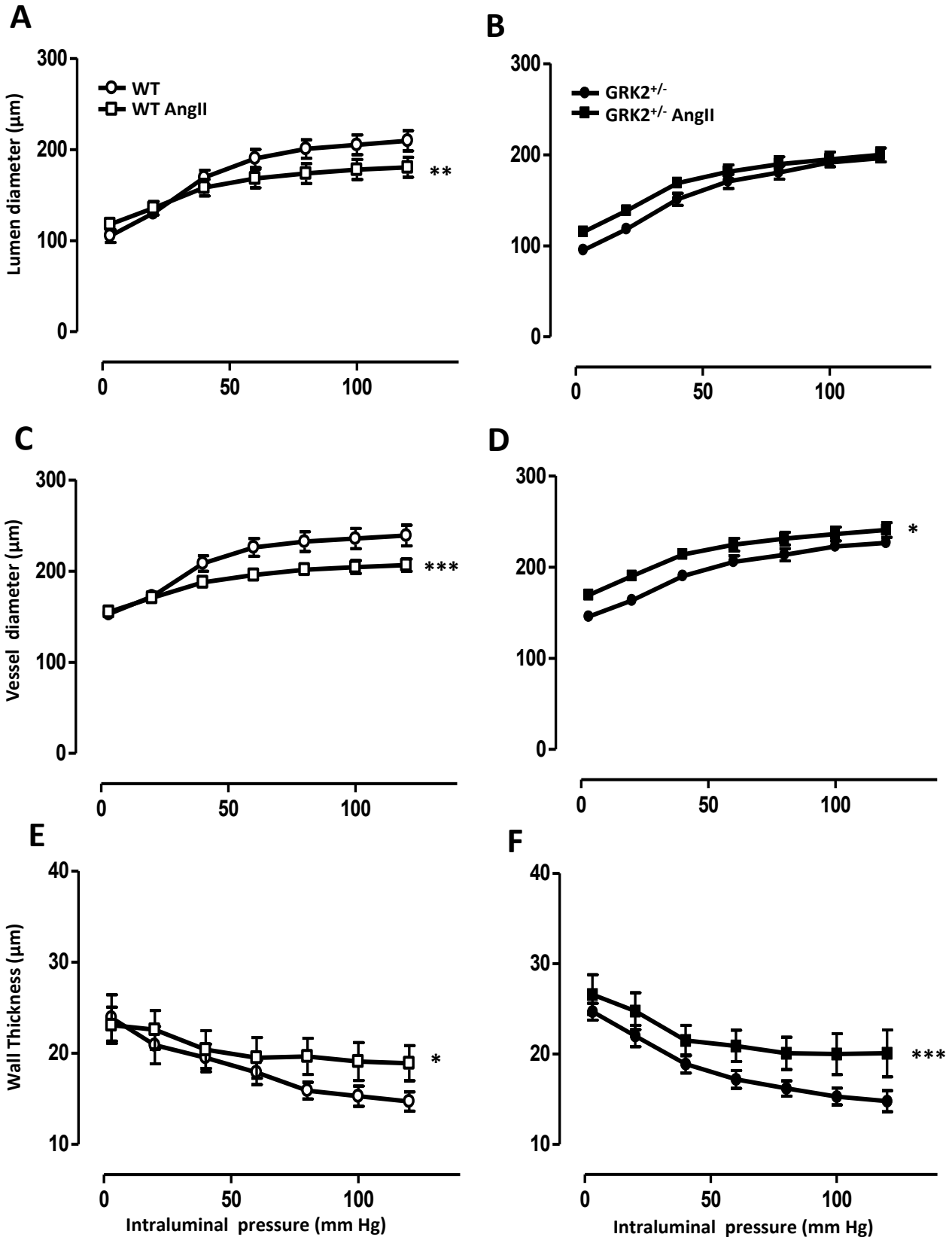

Figure S7. Effects of partial GRK2 deficiency on vascular structural parameters in Angiotensin II (AngII) infused mice. Lumen (A,B) and vessel diameter-intraluminal pressure (C,D) and wall thickness-intraluminal pressure (E,F) in mesenteric resistance arteries incubated in $0Ca^{2+}$Krebs Henseleit solution from wild type (WT) and $GRK2^{+/-}$ mice untreated and treated with AngII. n=5-7. *P<0.05, **P<0.01 , ***P<0.001 vs untreated.

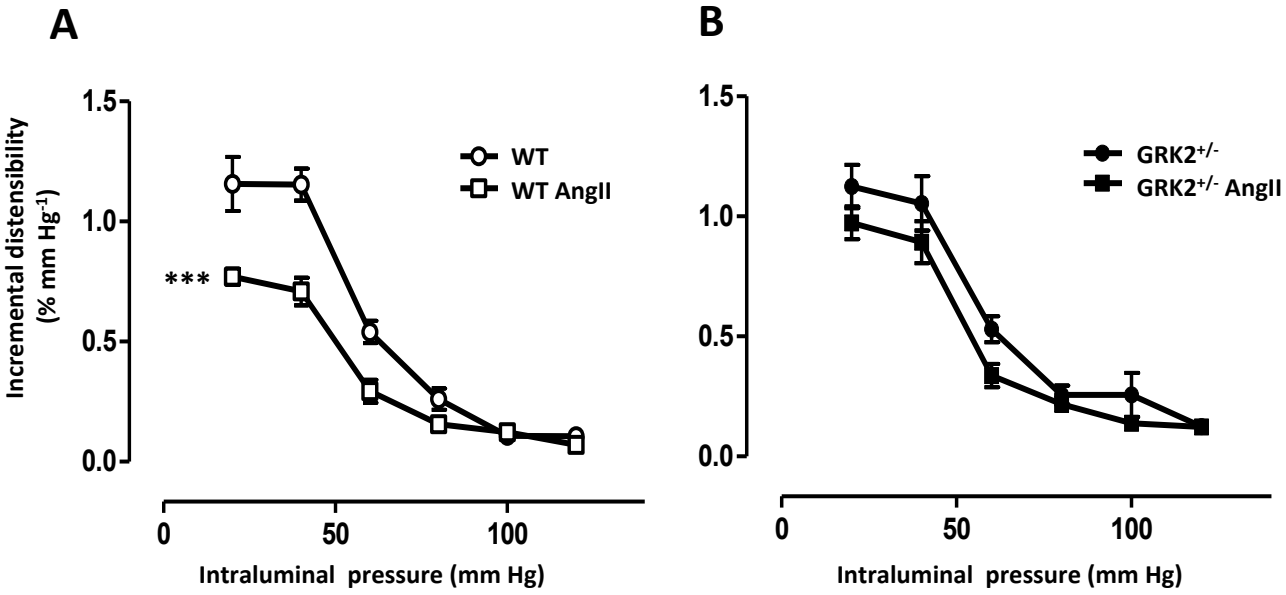

Figure S8. Effects of partial GRK2 deficiency on vascular mechanical parameters in Angiotensin II (AngII)-infused mice. Incremental distensibility-intraluminal pressure in mesenteric resistance arteries incubated in $0Ca^{2+}$Krebs Henseleit solution from wild type (WT) (A) and $GRK2^{+/-}$ (B) mice untreated and treated with AngII. n=5-7. ***P<0.001 vs untreated.

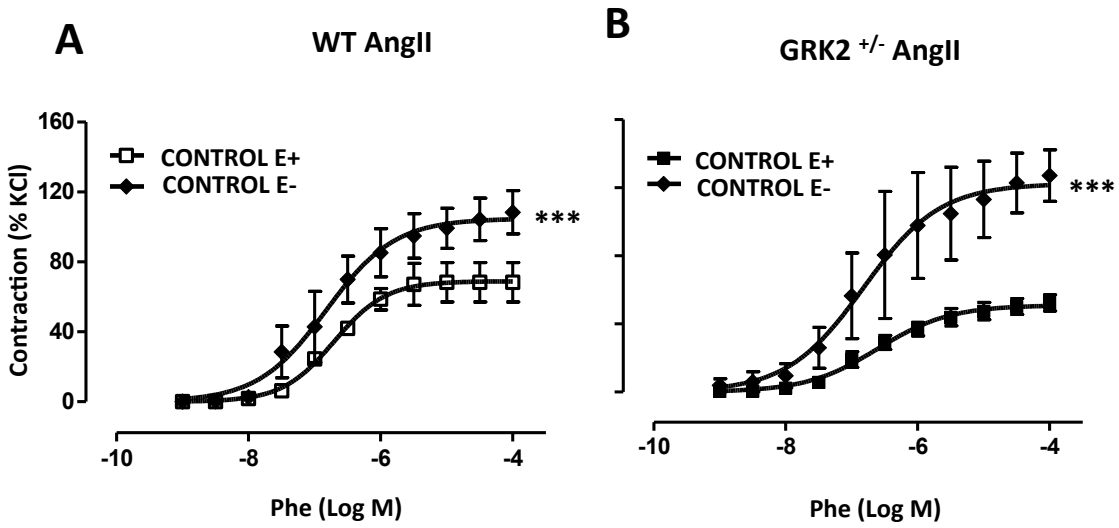

Figure S9. Partial GRK2 deficiency increases endothelial modulation of vasoconstrictor responses. Effect of endothelium removal (E-) on the concentration-response curve to phenylephrine (Phe) in aortic segments from wild type (WT) (A) and GRK2$^{+/-}$ (B) mice treated with Angiotensin II (AngII). Data represent mean±SEM. n=4. *P<0.05, ***P<0.001.

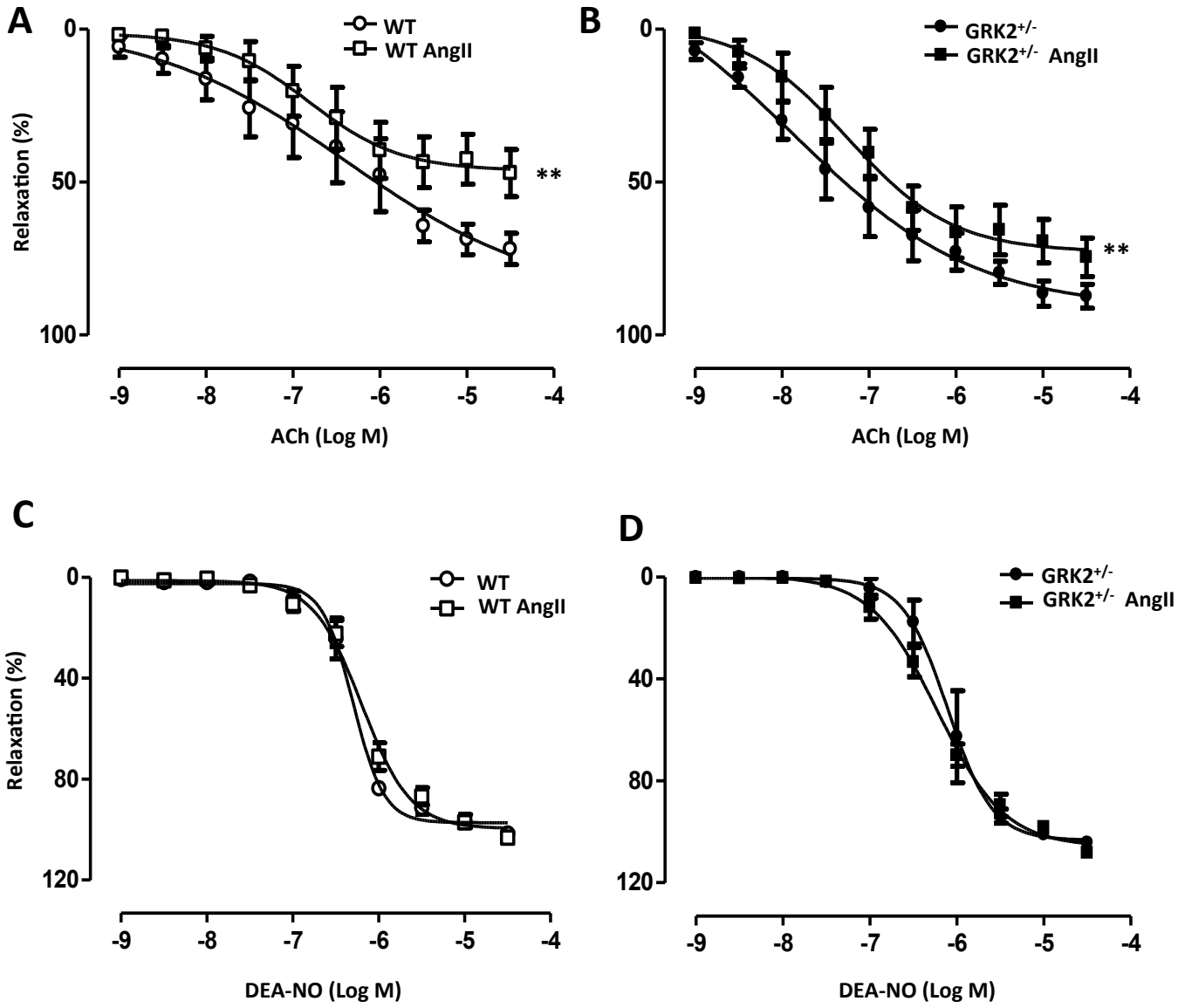

Figure S10. Partial GRK2 deficiency partially prevents Angiotensin II (AngII)-induced endothelial dysfunction but does not affect endothelium independent NO responses. Effect of AngII infusion on the concentration-response curve to acetylcholine (ACh) (A, B) or diethylamine NONOate (DEA-NO) (C, D) in aortic segments from wild type (WT) and GRK2$^{+/-}$ mice. Data represent mean±SEM. n=6-11, **P<0.01.

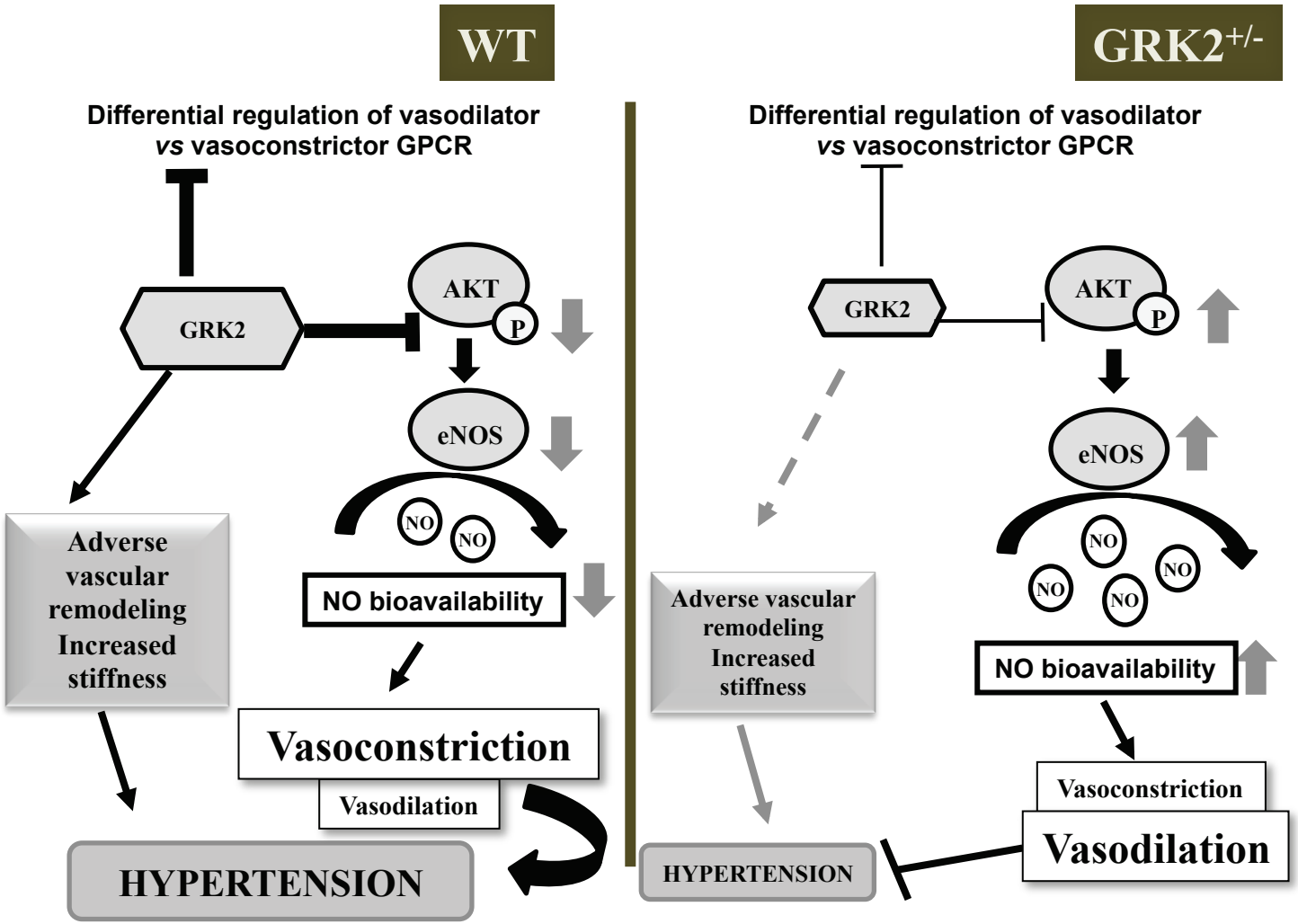

Figure S11. Role of GRK2 in hypertension and vascular responses. GRK2 participates in the regulation of vasoconstrictor and vasodilator G protein-coupled receptors (GPCR). However, GRK2 is also involved in non GPCR-dependent pathways such as the interaction with Akt that inhibits Akt-dependent activation of nitric oxide synthase (NOS) thus impairing nitric oxide (NO) production. Upon Angiotensin II (AngII) challenge, adult GRK2$^{+/-}$ mice show improved vascular remodeling, decreased vascular stiffness, increased Akt activation, less reduced eNOS expression and increased NO production. This provokes decreased vasoconstrictor and increased vasodilator responses what, together with improved vascular structure and mechanics, leads to resistance to severe AngII-induced hypertension.

Conclusions

The results obtained in this Thesis demonstrate that COX-2-derived prostanoids, ROS and GRK2 are key components involved in the functional, structural and mechanical alterations observed in hypertension, both in conductance and resistance arteries. This general conclusion emerges from the following partial conclusions obtained from the four articles presented in this Thesis:

- Long-term treatment of rats with aldosterone despite of not affecting noradrenaline contraction, alters the role of endothelium on these responses being this effect more pronounced in SHR than in WKY. Aldosterone treatment alters the release of COX-2-derived prostanoids, NO and ROS that might participate on the above mentioned endothelial modulation.

- The excess of ROS from NADPH Oxidase and/or mitochondria and the increased vascular COX-2/TP receptor axis act in reciprocal relationship to induce vascular dysfunction and hypertension, in part due to decreased NO availability.

- The COX-2/mPGES-1/EP_1 axis is involved in the development of vascular remodelling and vascular dysfunction in hypertension. More specifically, this pathway seems to be responsible of the endothelial dysfunction and the altered extracellular matrix deposition which in turn determines increased vessel stiffness in this pathology.

- GRK2 is a key determinant of Ang II-induced hypertension and vascular functional, structural and mechanical alterations. The underlying mechanism is partially dependent on decreased NO bioavailability from the AKt-eNOS pathway. Our results establish that an inhibition of GRK2 could be a beneficial treatment for hypertension.

We have provided evidences demonstrating that the previously known sources of vascular damage in hypertension, NADPH Oxidase, mitochondria and cyclooxygenase, are interrelated to create a self-perpetuating vicious circle responsible of vascular damage in this pathology. In addition, we have demonstrated that decreasing GRK2 levels/activity might constitute a promising strategy in the treatment of hypertension and associated vascular alterations. Although current pharmacological tools are effective to decrease blood pressure and alleviate, at least in part, these vascular alterations, identifying novel targets responsible of vascular damage will help in the development of more effective therapies.

References

1. Adeagbo AS, Zhang X, Patel D, Joshua IG, Wang Y, Sun X, Igbo IN, Oriowo MA. Cyclo-oxygenase-2, endothelium and aortic reactivity during deoxycorticosterone acetate salt-induced hypertension. *J Hypertens.* 23:1025-1036. 2005.

2. Agüero J, Almenar L, Montó F, Oliver E, Sánchez-Lázaro I, Vicente D, Martínez-Dolz L, D'Ocon P, Rueda J, Salvador A. Myocardial G protein receptor-coupled kinase expression correlates with functional parameters and clinical severity in advanced heart failure. *J Card Fail.* 18:53-61. 2012.

3. Akhter SA, Luttrell LM, Rockman HA, Iaccarino G, Lefkowitz RJ, Koch WJ. Targeting the receptor-Gq interface to inhibit in vivo pressure overload myocardial hypertrophy. *Science*. 280:574–577.1998.

4. Al Ghouleh I, Frazziano G, Rodriguez AI, Csányi G, Maniar S, St Croix CM, Kelley EE, Egaña LA, Song GJ, Bisello A, Lee YJ, Pagano PJ. Aquaporin 1, Nox1, and Ask1 mediate oxidant-induced smooth muscle cell hypertrophy. *Cardiovasc Res.* 97:134-142. 2013.

5. Álvarez Y, Briones AM, Balfagón G, Alonso MJ, Salaices M. Hypertension increases the participation of vasoconstrictor prostanoids from cyclooxygenase-2 in phenylephrine responses. *J Hypertens.* 23:767-777. 2005.

6. Álvarez Y, Pérez-Girón JV, Hernanz R, Briones AM, García-Redondo A, Beltrán A, Alonso MJ, Salaices M. Losartan reduces the increased participation of cyclooxygenase-2-derived products in vascular responses of hypertensive rats. *J Pharmacol Exp Ther.* 321:381-388. 2007.

7. Álvarez Y, Briones AM, Hernanz R, Pérez-Girón JV, Alonso MJ, Salaices M. Role of NADPH oxidase and iNOS in vasoconstrictor responses of vessels from hypertensive and normotensive rats. *Br J Pharmacol.* 153:926-935. 2008.

8. Amer M, Bead VR, Bathon J, Blumenthal RS, Edwards DN. Use of nonsteroidal anti-inflammatory drugs in patients with cardiovascular disease: a cautionary tale. *Cardiol Rev.* 18:204-212. 2010.

9. Amiri F, Virdis A, Neves MF, Iglarz M, Seidah NG, Touyz RM, Reudelhuber TL, Schiffrin EL. Endothelium-restricted overexpression of human endothelin-1 causes vascular remodeling and endothelial dysfunction. *Circulation.* 110:2233–2240. 2004.

10. Amiri F, Paradis P, Reudelhuber TL, Schiffrin EL. Vascular inflammation in absence of blood pressure elevation in transgenic murine model overexpressing endothelin-1 in endothelial cells. *J Hypertens.* 26:1102–1109. 2008.

11. Andrew PJ, Mayer B. Enzymatic function of nitric oxide synthases. *Cardiovasc Res.* 43:521-531. 1999.

12. Antman EM, DeMets D, Loscalzo J. Cyclooxygenase inhibition and cardiovascular risk. *Circulation.* 112:759-770. 2005.

13. Aoki T, Nishimura M, Matsuoka T, Yamamoto K, Furuyashiki T, Kataoka H, Kitaoka S, Ishibashi R, Ishibazawa A, Miyamoto S, Morishita R, Ando J, Hashimoto N, Nozaki K, Narumiya S. PGE(2) -EP(2) signalling in endothelium is activated by haemodynamic stress and induces cerebral aneurysm through an amplifying loop via NF-κB. *Br J Pharmacol.* 163:1237-1249. 2011.

14. Arribas SM, Hinek A, González MC. Elastic fibres and vascular structure in hypertension. *Pharmacol Ther*. 111:771-791. 2006.

15. Arribas SM, Briones AM, Bellingham C, González MC, Salaices M, Liu K, Wang Y, Hinek A. Heightened aberrant deposition of hard-wearing elastin in conduit arteries of prehypertensive SHR is associated with increased stiffness and inward remodeling. *Am J Physiol Heart Circ Physiol.* 295:H2299-H2307. 2008.

16. Bakker EN, van der Meulen ET, van den Berg BM, Everts V, Spaan JA, VanBavel E. Inward remodeling follows chronic vasoconstriction in isolated resistance arteries. *J Vasc Res.* 39:12-20. 2002.

17. Bakker EN, Buus CL, VanBavel E, Mulvany MJ. Activation of resistance arteries with endothelin-1: from vasoconstriction to functional adaptation and remodeling. *J Vasc Res.* 41:174-182. 2004.

18. Bakker EN, Buus CL, Spaan JA, Perree J, Ganga A, Rolf TM, Sorop O, Bramsen LH, Mulvany MJ, Vanbavel E. Small artery remodeling depends on tissue-type transglutaminase. *Circ Res.* 96:119-126. 2005.

19. Balfagón G, Márquez-Rodas I, Álvarez Y, Alonso MJ, Cachofeiro V, Salaices M, Lahera V. Aldosterone modulates neural vasomotor response in hypertension: role of calcitonin gene-related peptide. *Regul Pept.* 120:253-260. 2004.

20. Barbieri SS, Amadio P, Gianellini S, Zacchi E, Weksler BB, Tremoli E. Tobacco smoke regulates the expression and activity of microsomal

prostaglandin E synthase-1: role of prostacyclin and NADPH-oxidase. *FASEB J.* 25:3731-3740. 2011.

21. Barnes WG, Reiter E, Violin JD, Ren XR, Milligan G, Lefkowitz RJ. beta-Arrestin 1 and Galphaq/11 coordinately activate RhoA and stress fiber formation following receptor stimulation. *J Biol Chem.* 280:8041-8050. 2005.

22. Beckman JS, Koppenol WH. Nitric oxide, superoxide, and peroxynitrite: the good, the bad, and ugly. *Am J Physiol.* 271:C1424-C1437. 1996.

23. Belmonte SL, Blaxall BC. G protein coupled receptor kinases as therapeutic targets in cardiovascular disease. *Circ Res.* 109:309-319. 2011.

24. Beltrán AE, Briones AM, García-Redondo AB, Rodríguez C, Miguel M, Álvarez Y, Alonso MJ, Martínez-González J, Salaices M. p38 MAPK contributes to angiotensin II-induced COX-2 expression in aortic fibroblasts from normotensive and hypertensive rats. *J Hypertens.* 27:142-154. 2009.

25. Benetos A, Lacolley P, Safar ME. Prevention of aortic fibrosis by spironolactone in spontaneously hypertensive rats. *Arterioscler Thromb Vasc Biol.* 17:1152-1156. 1997.

26. Beswick RA, Dorrance AM, Leite R, Webb RC. NADH/NADPH oxidase and enhanced superoxide production in the mineralocorticoid hypertensive rat. *Hypertension.* 38:1107–1111. 2001.

27. Blanco-Rivero J, Cachofeiro V, Lahera V, Aras-Lopez R, Márquez-Rodas I, Salaices M, Xavier FE, Ferrer M, Balfagón G. Participation of prostacyclin in endothelial dysfunction induced by aldosterone in normotensive and hypertensive rats. *Hypertension.* 46:107–112. 2005.

28. Bobik A, Tkachuk V. Metalloproteinases and plasminogen activators in vessel remodeling. *Curr Hypertens Rep.* 5:466–472. 2003.

29. Boumaza S, Arribas SM, Osborne-Pellegrin M, McGrath JC, Laurent S, Lacolley P, Challande P. Fenestrations of the carotid internal elastic lamina and structural adaptation in stroke-prone spontaneously hypertensive rats. *Hypertension.* 37:1101-1107. 2001.

30. Boutouyrie P, Lacolley P, Briet M, Regnault V, Stanton A, Laurent S, Mahmud A. Pharmacological modulation of arterial stiffness. *Drugs.* 71:1689–1701. 2011.

31. Brandes RP, Weissmann N, Schröder K. NADPH oxidases in cardiovascular disease. *Free Radic Biol Med.* 49:687-706. 2010.

32. Bregeon J, Loirand G, Pacaud P, Rolli-Derkinderen M. Angiotensin II induces RhoA activation through SHP2-dependent dephosphorylation of the RhoGAP p190A in vascular smooth muscle cells. *Am J Physiol Cell Physiol.* 297:C1062–C1070. 2009.

33. Briet M, Schiffrin EL. Vascular actions of aldosterone. *J Vasc Res.* 50:89-99. 2013a.

34. Briet M, Schiffrin EL. Treatment of arterial remodeling in essential hypertension. *Curr Hypertens Rep.* 15:3-9. 2013b.

35. Brinks HL, Eckhart AD. Regulation of GPCR signaling in hypertension. *Biochim Biophys Acta.* 1802:1268-1275. 2010.

36. Briones AM, González JM, Somoza B, Giraldo J, Daly CJ, Vila E, González MC, McGrath JC, Arribas SM. Role of elastin in spontaneously hypertensive rat small mesenteric artery remodelling. *J Physiol.* 552:185-195. 2003.

37. Briones AM, Xavier FE, Arribas SM, González MC, Rossoni LV, Alonso MJ, Salaices M. Alterations in structure and mechanics of resistance arteries from ouabain-induced hypertensive rats. *Am J Physiol Heart Circ Physiol.* 291:H193-H201. 2006.

38. Briones AM, Rodríguez-Criado N, Hernanz R, García-Redondo AB, Rodrigues-Díez RR, Alonso MJ, Egido J, Ruiz-Ortega M, Salaices M. Atorvastatin prevents angiotensin II-induced vascular remodeling and oxidative stress. *Hypertension.* 54:142-149. 2009.

39. Briones AM, Arribas SM, Salaices M. Role of extracellular matrix in vascular remodeling of hypertension. *Curr Opin Nephrol Hypertens.* 19:187-194. 2010.

40. Briones AM, Touyz RM. Oxidative stress and hypertension: current concepts. *Curr Hypertens Rep.*12:135-142. 2010.

41. Briones AM, Tabet F, Callera GE, Montezano AC, Yogi A, He Y, Quinn MT, Salaices M, Touyz RM. Differential regulation of Nox1, Nox2 and Nox4 in vascular smooth muscle cells from WKY and SHR. *J Am Soc Hypertens.* 5:137-153. 2011.

42. Brunner H, Cockcroft JR, Deanfield J, Donald A, Ferrannini E, Halcox J, Kiowski W, Lüscher TF, Mancia G, Natali A, Oliver JJ, Pessina AC, Rizzoni D, Rossi GP, Salvetti A, Spieker LE, Taddei S, Webb DJ; Working Group on Endothelins and Endothelial Factors of the European Society of Hypertension.

Endothelial function and dysfunction. Part II: association with cardiovascular risk factors and diseases. *J Hypertens.* 23:233-246. 2005.

43. Bund SJ, Lee RM. Arterial structural changes in hypertension: a consideration of methodology, terminology and functional consequence. *J Vasc Res.* 40:547-557. 2003.

44. Cachofeiro V, Miana M, de Las Heras N, Martín-Fernández B, Ballesteros S, Fernández-Tresguerres J, Lahera V. Aldosterone and the vascular system. *J Steroid Biochem Mol Biol.* 109:331-335. 2008.

45. Camacho M, Martinez-Gonzalez J, Rodriguez C, Siguero L, Seriola C, Romero JM, Vila L. Imidazolineoxyl N-oxide induces COX-2 in endothelial cells: role of free radicals. *Front Biosci (Elite Ed).* 1;4:2654-2669. 2012.

46. Camacho M, Dilme J, Sola-Villa D, Rodriguez C, Bellmunt S, Siguero L, Alcolea S, Romero JM, Escudero JR, Martinez-Gonzalez J, Vila L. Microvascular COX-2/mPGES-1/EP-4 axis in human abdominal aortic aneurysm. *J Lipid Res*. 54:3506-3515. 2013.

47. Cao X, Peterson JR, Wang G, Anrather J, Young CN, Guruju MR, Burmeister MA, Iadecola C, Davisson RL. Angiotensin II-dependent hypertension requires cyclooxygenase 1-derived prostaglandin E2 and EP1 receptor signaling in the subfornical organ of the brain. *Hypertension.* 59:869–876. 2012.

48. Capone C, Faraco G, Anrather J, Zhou P, Iadecola C. Cyclooxygenase 1-derived prostaglandin E2 and EP1 receptors are required for the cerebrovascular dysfunction induced by angiotensin II. *Hypertension.* 55:911-917. 2010.

49. Castro MM, Tanus-Santos JE. Inhibition of matrix metalloproteinases (MMPs) as a potential strategy to ameliorate hypertension-induced cardiovascular alterations. *Curr Drug Targets*. 14:335-343. 2013.

50. Chandesris MO, Azarine A, Ong KT, Taleb S, Boutouyrie P, Mousseaux E, Romain M, Bozec E, Laurent S, Boddaert N, Thumerelle C, Tillie-Leblond I, Hoarau C, Lebranchu Y, Aladjidi N, Tron F, Barlogis V, Body G, Munzer M, Jaussaud R, Suarez F, Clément O, Hermine O, Tedgui A, Lortholary O, Picard C, Mallat Z, Fischer A. Frequent and widespread vascular abnormalities in human signal transducer and activator of transcription 3 deficiency. *Circ Cardiovasc Genet.* 5:25-34. 2012.

51. Chen L, Yang G, Xu X, Grant G, Lawson JA, Bohlooly-Y M, FitzGerald GA. Cell selective cardiovascular biology of microsomal prostaglandin E synthase-1. *Circulation.* 127:233-243. 2013.

52. Cheng Y, Wang M, Yu Y, Lawson J, Funk CD, Fitzgerald GA. Cyclooxygenases, microsomal prostaglandin E synthase-1, and cardiovascular function. *J Clin Invest.* 116:1391-1399. 2006.

53. Chiang HY, Korshunov VA, Serour A, Shi F, Sottile J. Fibronectin is an important regulator of flow-induced vascular remodeling. *Arterioscler Thromb Vasc Biol.* 29:1074-1079. 2009.

54. Christ M, Douwes K, Eisen C, Bechtner G, Theisen K, Wehling M: Rapid effects of aldosterone on sodium transport in vascular smooth muscle cells. *Hypertension.* 25:117–123. 1995.

55. Christensen KL, Mulvany MJ. Location of resistance arteries. *J Vasc Res.* 38:1-12. 2001.

56. Cipollone F, Fazia M, Iezzi A, Pini B, Cuccurullo C, Zucchelli M, de Cesare D, Ucchino S, Spigonardo F, De Luca M, Muraro R, Bei R, Bucci M, Cuccurullo F, Mezzetti A. Blockade of the angiotensin II type 1 receptor stabilizes atherosclerotic plaques in humans by inhibiting prostaglandin E2-dependent matrix metalloproteinase activity. *Circulation.* 109:1482-1488. 2004.

57. Coffman TM. Under pressure: the search for the essential mechanisms of hypertension. *Nat Med.* 17:1402-1409. 2011.

58. Cohn HI, Harris DM, Pesant S, Pfeiffer M, Zhou RH, Koch WJ, Dorn GW 2nd, Eckhart AD. Inhibition of vascular smooth muscle G protein-coupled receptor kinase 2 enhances alpha1D-adrenergic receptor constriction. *Am J Physiol Heart Circ Physiol.* 295:H1695-H1704. 2008.

59. Cohn HI, Xi Y, Pesant S, Harris DM, Hyslop T, Falkner B, Eckhart AD. G protein-coupled receptor kinase 2 expression and activity are associated with blood pressure in black Americans. *Hypertension.* 54:71-76. 2009.

60. Creager MA, Roddy MA. Effect of captopril and enalapril on endothelial function in hypertensive patients. *Hypertension.* 24:499-505. 1994.

61. Cui W, Matsuno K, Iwata K, Ibi M, Katsuyama M, Kakehi T, Sasaki M, Ikami K, Zhu K, Yabe-Nishimura C. NADPH oxidase isoforms and anti-hypertensive effects of atorvastatin demonstrated in two animal models. *J Pharmacol Sci.* 111:260-268. 2009.

62. Curnow KM, Tusie-Luna MT, Pascoe L, Natarajan R, Gu JL, Nadler JL, White PC. The product of the CYP11B2 gene is required for aldosterone biosynthesis in the human adrenal cortex. *Mol Endocrinol.* 5:1513-1522. 1991.

63. Dai DF, Johnson SC, Villarin JJ, Chin MT, Nieves-Cintrón M, Chen T, Marcinek DJ, Dorn GW 2nd, Kang YJ, Prolla TA, Santana LF, Rabinovitch PS. Mitochondrial oxidative stress mediates angiotensin II-induced cardiac hypertrophy and Galphaq overexpression-induced heart failure. *Circ Res.* 108:837-846. 2011.

64. De Cavanagh EM, Ferder LF, Ferder MD, Stella IY, Toblli JE, Inserra F. Vascular structure and oxidative stress in salt-loaded spontaneously hypertensive rats: effects of losartan and atenolol. *Am J Hypertens.* 23:1318-1325. 2010.

65. De Ciuceis C, Amiri F, Brassard P, Endemann DH, Touyz RM, Schiffrin EL. Reduced vascular remodeling, endothelial dysfunction, and oxidative stress in resistance arteries of angiotensin II-infused macrophage colony-stimulating factor-deficient mice: evidence for a role in inflammation in angiotensin-induced vascular injury. *Arterioscler Thromb Vasc Biol.* 25:2106-2113. 2005.

66. De Mello WC, Frohlich ED. On the local cardiac renin–angiotensin system. Basic and clinical implications. *Peptides.* 32:1774–1779. 2011.

67. Dikalov S. Cross talk between mitochondria and NADPH oxidases. *Free Radic Biol Med.* 51:1289-1301. 2011.

68. Dikalov SI, Kirilyuk IA, Voinov M, Grigor'ev IA. EPR detection of cellular and mitochondrial superoxide using cyclic hydroxylamines. *Free Radic Res*. 45:417-430. 2011.

69. Dikalov SI, Nazarewicz RR, Bikineyeva A, Hilenski L, Lassègue B, Griendling KK, Harrison DG, Dikalova AE. Nox2-Induced Production of Mitochondrial Superoxide in Angiotensin II-Mediated Endothelial Oxidative Stress and Hypertension. *Antioxid Redox Signal*. [Epub ahead of print]. 2013.

70. Dikalov SI, Nazarewicz RR. Angiotensin II-induced production of mitochondrial reactive oxygen species: potential mechanisms and relevance for cardiovascular disease. *Antioxid Redox Signal.* 19:1085-1094. 2013.

71. Dikalova AE, Bikineyeva AT, Budzyn K, Nazarewicz RR, McCann L, Lewis W, Harrison DG, Dikalov SI. Therapeutic targeting of mitochondrial superoxide in hypertension. *Circ Res*. 107:106-116. 2010a.

72. Dikalova AE, Góngora MC, Harrison DG, Lambeth JD, Dikalov S, Griendling KK. Upregulation of Nox1 in vascular smooth muscle leads to impaired endothelium-dependent relaxation via eNOS uncoupling. *Am J Physiol Heart Circ Physiol.* 299:H673-H679. 2010b.

73. Dornas WC, Silva ME. Animal models for the study of arterial hypertension. *J Biosci.* 36:731-737. 2011.

74. Doughan AK, Harrison DG, Dikalov SI. Molecular mechanisms of angiotensin II-mediated mitochondrial dysfunction: linking mitochondrial oxidative damage and vascular endothelial dysfunction. *Circ Res.* 102:488-496. 2008.

75. Drummond GR, Selemidis S, Griendling KK, Sobey CG. Combating oxidative stress in vascular disease: NADPH oxidases as therapeutic targets. *Nat Rev Drug Discov.* 10:453-471. 2011.

76. Dzau VJ. Significance of the vascular renin–angiotensin pathway. *Hypertension*. 8:553-559. 1986.

77. Ebrahimian T, Touyz RM. Thioredoxin in vascular biology: role in hypertension. *Antioxid Redox Signal.* 10:1127-1136. 2008.

78. Eckhart AD, Ozaki T, Tevaearai H, Rockman HA, Koch WJ. Vascular-targeted overexpression of G protein-coupled receptor kinase-2 in transgenic mice attenuates beta-adrenergic receptor signaling and increases resting blood pressure. *Mol Pharmacol*. 61:749-758. 2002.

79. Eftekhari A, Rahman A, Schaebel LH, Chen H, Rasmussen CV, Aalkjaer C, Buus CL, Mulvany MJ. Chronic cystamine treatment inhibits small artery remodelling in rats. *J Vasc Res.* 44:471–482. 2007.

80. Ergul A. Hypertension in black patients: an emerging role of the endothelin system in salt-sensitive hypertension. *Hypertension.* 36:62–67. 2000.

81. Facemire CS, Griffiths R, Audoly LP, Koller BH, Coffman TM. The impact of microsomal prostaglandin e synthase 1 on blood pressure is determined by genetic background. *Hypertension.* 55:531-538. 2010.

82. Feldman RD. Deactivation of vasodilator responses by GRK2 overexpression: a mechanism or the mechanism for hypertension? *Mol Pharmacol.* 61:707-709. 2002.

83. Félétou M, Verbeuren TJ, Vanhoutte PM. Endothelium-dependent contractions in SHR: a tale of prostanoid TP and IP receptors. *Br J Pharmacol.* 156:563-574. 2009.

84. Félétou M, Köhler R, Vanhoutte PM. Endothelium-derived vasoactive factors and hypertension: possible roles in pathogenesis and as treatment targets. *Curr Hypertens Rep*. 12:267-275. 2010.

85. Félétou M, Huang Y, Vanhoutte PM. Endothelium-mediated control of vascular tone: COX-1 and COX-2 products. *Br J Pharmacol.* 164:894-912. 2011.

86. Foudi N, Gomez I, Benyahia C, Longrois D, Norel X. Prostaglandin E2 receptor subtypes in human blood and vascular cells. *Eur J Pharmacol.* 695:1-6. 2012.

87. Francois H, Facemire C, Kumar A, Audoly L, Koller B, Coffman T. Role of microsomal prostaglandin E synthase 1 in the kidney. *J Am Soc Nephrol.* 18:1466-1475. 2007.

88. Freedman NJ, Ament AS, Oppermann M, Stoffel RH, Exum ST, Lefkowitz RJ. Phosphorylation and desensitization of human endothelin A and B receptors. Evidence for G protein-coupled receptor kinase specificity. *J Biol Chem.* 272:17734-17743. 1997.

89. Furchgott RF, Zawadzki JV. The obligatory role of endothelial cells in the relaxation of arterial smooth muscle by acetylcholine. *Nature.* 288:373-376. 1980.

90. Furchgott RF, Vanhoutte PM. Endothelium-derived relaxing and contracting factors. *FASEB J*. 3:2007-2018. 1989.

91. Galán M, Miguel M, Beltrán AE, Rodríguez C, García-Redondo AB, Rodríguez-Calvo R, Alonso MJ, Martínez-González J, Salaices M. Angiotensin II differentially modulates cyclooxygenase-2, microsomal prostaglandin E2

synthase-1 and prostaglandin I2 synthase expression in adventitial fibroblasts exposed to inflammatory stimuli. *J Hypertens.* 29:529-536. 2011.

92. Garcia-Cohen EC, Marin J, Diez-Picazo LD, Baena AB, Salaices M, Rodriguez-Martinez MA. Oxidative stress induced by tert-butyl hydroperoxide causes vasoconstriction in the aorta from hypertensive and aged rats: role of cyclooxygenase-2 isoform. *J Pharmacol Exp Ther.* 293:75-81. 2000.

93. García-Redondo AB, Briones AM, Avendaño MS, Hernanz R, Alonso MJ, Salaices M. Losartan and tempol treatments normalize the increased response to hydrogen peroxide in resistance arteries from hypertensive rats. *J Hypertens.* 27:1814-1822. 2009.

94. Gavazzi G, Banfi B, Deffert C, Fiette L, Schappi M, Herrmann F, Krause KH. Decreased blood pressure in NOX1-deficient mice. *FEBS Lett.*580:497-504. 2006.

95. Geiger B, Yamada KM. Molecular architecture and function of matrix adhesions. *Cold Spring Harb Perspect Biol.* 3:005033. 2011.

96. Ghiadoni L, Virdis A, Magagna A, Taddei S, Salvetti A. Effect of the angiotensin II type 1 receptor blocker candesartan on endothelial function in patients with essential hypertension. *Hypertension.* 35:501-506. 2000.

97. Ghiadoni L, Taddei S, Virdis A. Hypertension and endothelial dysfunction: therapeutic approach. *Curr Vasc Pharmacol.* 10:42-60. 2012.

98. Gibbons GH, Dzau VJ. The emerging concept of vascular remodeling. *N Engl J Med.* 330:1431-1438. 1994.

99. Giles TD, Sander GE, Nossaman BD, Kadowitz PJ. Impaired vasodilation in the pathogenesis of hypertension: focus on nitric oxide, endothelial-derived hyperpolarizing factors, and prostaglandins. *J Clin Hypertens (Greenwich).* 14:198-205. 2012.

100. Glagov S, Weisenberg E, Zarins CK, Stankunavicius R, Kolettis GJ. Compensatory enlargement of human atherosclerotic coronary arteries. *N Engl J Med.* 316:1371-1375. 1987.

101. Gluais P, Paysant J, Badier-Commander C, Verbeuren T, Vanhoutte PM, Félétou M. In SHR aorta, calcium ionophore A-23187 releases prostacyclin and thromboxane A2 as endothelium-derived contracting factors. *Am J Physiol Heart Circ Physiol.* 291:H2255-H2264. 2006.

102. Golledge J, Clancy P, Maguire J, Lincz L, Koblar S. The role of tenascin C in cardiovascular disease. *Cardiovasc Res.* 92:19-28. 2011.

103. Gomez E, Schwendemann C, Roger S, Simonet S, Paysant J, Courchay C, Verbeuren TJ, Félétou M. Aging and prostacyclin responses in aorta and platelets from WKY and SHR rats. *Am J Physiol Heart Circ Physiol.* 295:H2198-H2211. 2008.

104. Graham D, Huynh NN, Hamilton CA, Beattie E, Smith RA, Cochemé HM, Murphy MP, Dominiczak AF. Mitochondria-targeted antioxidant MitoQ10 improves endothelial function and attenuates cardiac hypertrophy. *Hypertension.* 54:322-328. 2009.

105. Green T, Gonzalez AA, Mitchell KD, Navar LG. The complex interplay between cyclooxygenase-2 and angiotensin II in regulating kidney function. *Curr Opin Nephrol Hypertens.* 21:7-14. 2012.

106. Griffin M, Casadio R, Bergamini CM. Transglutaminases: nature's biological glues. *Biochem J.* 368:377–396. 2002.

107. Gros R, Tan CM, Chorazyczewski J, Kelvin DJ, Benovic JL, Feldman RD. G-protein-coupled receptor kinase expression in hypertension. *Clin Pharmacol Ther*. 65:545-551. 1999.

108. Gros R, Chorazyczewski J, Meek MD, Benovic JL, Ferguson SS, Feldman RD. G-Protein-coupled receptor kinase activity in hypertension : increased vascular and lymphocyte G-protein receptor kinase-2 protein expression. *Hypertension.* 35:38-42. 2000.

109. Guan Y, Zhang Y, Wu J, Qi Z, Yang G, Dou D, Gao Y, Chen L, Zhang X, Davis LS, Wei M, Fan X, Carmosino M, Hao C, Imig JD, Breyer RM, Breyer MD. Antihypertensive effects of selective prostaglandin E2 receptor subtype 1 targeting. *J Clin Invest.* 117:2496-2505. 2007.

110. Guichard C, Moreau R, Pessayre D, Epperson TK, Krause KH. OX family NADPH oxidases in liver and in pancreatic islets: a role in the metabolic syndrome and diabetes? *Biochem Soc Trans.* 36:920-929. 2008.

111. Hamilton SJ, Chew GT, Watts GF. Therapeutic regulation of endothelial dysfunction in type 2 diabetes mellitus. *Diab Vasc Dis Res.* 4:89-102. 2007.

112. Harris DM, Cohn HI, Pesant S, Zhou RH, Eckhart AD. Vascular smooth muscle G(q) signaling is involved in high blood pressure in both induced renal and

genetic vascular smooth muscle-derived models of hypertension, *Am J Physiol Heart Circ Physiol.* 293:H3072-H3079. 2007.

113. Hasan D, Hashimoto T, Kung D, Macdonald RL, Winn HR, Heistad D. Upregulation of cyclooxygenase-2 (COX-2) and microsomal prostaglandin E2 synthase-1 (mPGES-1) in wall of ruptured human cerebral aneurysms: preliminary results. *Stroke.* 43:1964-1967. 2012.

114. Haurani MJ, Pagano PJ. Adventitial fibroblast reactive oxygen species as autacrine and paracrine mediators of remodeling: bellwether for vascular disease? *Cardiovasc Res.* 75:679-689. 2007.

115. Heagerty AM, Aalkjaaer C, Bund SJ, Korsgaard N, Mulvany MJ. Small artery structure in hypertension. Dual process of remodeling and growth. *Hypertension.* 21:391–397. 1993.

116. Hernanz R, Briones AM, Alonso MJ, Vila E, Salaices M. Hypertension alters role of iNOS, COX-2, and oxidative stress in bradykinin relaxation impairment after LPS in rat cerebral arteries. *Am J Physiol Heart Circ Physiol.* 287:H225-H234. 2004.

117. Hernanz R, Martín Á, Pérez-Girón JV, Palacios R, Briones AM, Miguel M, Salaices M, Alonso MJ. Pioglitazone treatment increases COX-2-derived prostacyclin production and reduces oxidative stress in hypertensive rats: role in vascular function. *Br J Pharmacol.* 166:1303-1319. 2012.

118. Hernanz R, Briones AM, Salaices M, Alonso MJ. New roles for old pathways? A circuitous relationship between reactive oxygen species and cyclo-oxygenase in hypertension. *Clin Sci (Lond).* 126:111-21. 2014.

119. Higashi Y, Sasaki S, Nakagawa K, Fukuda Y, Matsuura H, Oshima T, Chayama K. Tetrahydrobiopterin enhances forearm vascular response to acetylcholine in both normotensive and hypertensive individuals. *Am J Hypertens.* 15:326–332. 2002.

120. Hirono Y, Yoshimoto T, Suzuki N, Sugiyama T, Sakurada M, Takai S, Kobayashi N, Shichiri M, Hirata Y. Angiotensin II receptor type 1-mediated vascular oxidative stress and proinflammatory gene expression in aldosterone-induced hypertension: the possible role of local renin-angiotensin system. *Endocrinology.* 148:1688–1696. 2007.

121. Hu L, Zhang Y, Lim PS, Miao Y, Tan C, McKenzie KU, Schyvens CG, Whitworth JA. Apocynin but not L-arginine prevents and reverses dexamethasone-induced hypertension in the rat. *Am J Hypertens.* 19:413-418. 2006.

122. Huang PL. eNOS, metabolic syndrome and cardiovascular disease. *Trends Endocrinol Metab.* 20:295–302. 2009.

123. Iglarz M, Touyz RM, Viel EC, Amiri F, Schiffrin EL. Involvement of oxidative stress in the profibrotic action of aldosterone. Interaction wtih the renin-angiotension system. *Am J Hypertens.* 17:597–603. 2004.

124. Imanaka-Yoshida K. Tenascin-C in cardiovascular tissue remodeling: from development to inflammation and repair. *Circ J.* 76:2513-2520. 2012.

125. Intengan HD, Deng LY, Li JS, Schiffrin EL. Mechanics and composition of human subcutaneous resistance arteries in essential hypertension. *Hypertension.* 33:569-574. 1999a.

126. Intengan HD, Thibault G, Li JS, Schiffrin EL. Resistance artery mechanics, structure, and extracellular components in spontaneously hypertensive rats: effects of angiotensin receptor antagonism and converting enzyme inhibition. *Circulation.* 100:2267-2275. 1999b.

127. Intengan HD, Schiffrin EL. Vascular remodeling in hypertension: Roles of apoptosis, inflammation, and fibrosis. *Hypertension.* 38:581-587. 2001.

128. Jia Z, Zhang A, Zhang H, Dong Z, Yang T. Deletion of microsomal prostaglandin E synthase-1 increases sensitivity to salt loading and angiotensin II infusion. *Circ Res.* 99:1243-1251. 2006.

129. Jia Z, Guo X, Zhang H, Wang MH, Dong Z, Yang T. Microsomal prostaglandin synthase-1-derived prostaglandin E2 protects against angiotensin II-induced hypertension via inhibition of oxidative stress. *Hypertension.* 52:952-959. 2008.

130. Jia Z, Aoyagi T, Yang T. mPGES-1 protects against DOCA-salt hypertension via inhibition of oxidative stress or stimulation of NO/cGMP. *Hypertension.* 55:539-546. 2010.

131. Jiménez-Altayó F, Martín A, Rojas S, Justicia C, Briones AM, Giraldo J, Planas AM, Vila E. Transient middle cerebral artery occlusion causes different structural, mechanical, and myogenic alterations in normotensive and hypertensive rats. *Am J Physiol Heart Circ Physiol.* 293:H628-H635. 2007.

132. Kane MO, Etienne-Selloum N, Madeira SV, Sarr M, Walter A, Dal-Ros S, Schott C, Chataigneau T, Schini-Kerth VB. Endothelium-derived contracting factors mediate the Ang II-induced endothelial dysfunction in the rat aorta: preventive effect of red wine polyphenols. *Pflugers Arch.* 459:671-679. 2010.

133. Karaa A, Kamoun WS, Xu H, Zhang J, Clemens MG. Differential effects of oxidative stress on hepatic endothelial and Kupffer cell eicosanoid release in response to endothelin-1. *Microcirculation.* 13:457-466. 2006.

134. Kasal DA, Barhoumi T, Li MW, Yamamoto N, Zdanovich E, Rehman A, Neves MF, Laurant P, Paradis P, Schiffrin EL. T regulatory lymphocytes prevent aldosterone-induced vascular injury. *Hypertension.* 59:324-330. 2012.

135. Kietadisorn R, Juni RP, Moens AL. Tackling endothelial dysfunction by modulating NOS uncoupling: new insights into its pathogenesis and therapeutic possibilities. *Am J Physiol Endocrinol Metab.* 302:E481-E495. 2012.

136. Kim J, Cha YN, Surh YJ. A protective role of nuclear factor-erythroid 2-related factor-2 (Nrf2) in inflammatory disorders. *Mutat Res.* 690:12-23. 2010.

137. Kiowski W, Linder L, Nuesch R, Martina B. Effects of cilazapril on vascular structure and function in essential hypertension. *Hypertension.* 27:371-376. 1996.

138. Koska J. Incretins and preservation of endothelial function. *Cardiovasc Hematol Agents Med Chem.* 10:295-308. 2012.

139. Kumar R, Thomas CM, Yong QC, Chen W, Baker KM. The intracrine renin-angiotensin system. *Clin Sci (Lond).* 123:273-284. 2012.

140. Lacolley P, Regnault V, Nicoletti A, Li Z, Michel JB. The vascular smooth muscle cell in arterial pathology: a cell that can take on multiple roles. *Cardiovasc Res.* 95:194-204. 2012.

141. Lacy F, Gough DA, Schmid-Schönbein GW. Role of xanthine oxidase in hydrogen peroxide production. *Free Radic. Biol. Med.* 25:720-727. 1998.

142. Lacy F, Kailasam MT, O'Connor DT, Schmid-Schönbein GW, Parmer RJ. Plasma hydrogen peroxide production in human essential hypertension: role of heredity, gender, and ethnicity. *Hypertension.* 36:878-884. 2000.

143. Lambeth JD, Kawahara T, Diebold B. Regulation of Nox and Duox enzymatic activity and expression. *Free Radic Biol Med.* 43:319-331. 2007.

144. Landmesser U, Dikalov S, Price SR, McCann L, Fukai T, Holland SM, Mitch WE, Harrison DG. Oxidation of tetrahydrobiopterin leads to uncoupling of endothelial cell nitric oxide synthase in hypertension. *J Clin Invest.* 111:1201-1209. 2003

145. Landmesser U, Spiekermann S, Preuss C, Sorrentino S, Fischer D, Manes C, Mueller M, Drexler H. Angiotensin II induces endothelial xanthine oxidase activation: role for endothelial dysfunction in patients with coronary disease. *Arterioscler Thromb Vasc Biol.* 27:943-948. 2007.

146. Lee CW, Lin CC, Lee IT, Lee HC, Yang CM. Activation and induction of cytosolic phospholipase A2 by TNF-α mediated through Nox2, MAPKs, NF-κB, and p300 in human tracheal smooth muscle cells. *J Cell Physiol.* 226:2103-14. 2011.

147. Lerman A, Zeiher AM. Endothelial function: cardiac events. *Circulation.* 111:363-368. 2005.

148. Li JS, Sharifi AM, Schiffrin EL. Effect of AT1 angiotensin-receptor blockade on structure and function of small arteries in SHR. *J Cardiovasc Pharmacol.* 30:75-83. 1997.

149. Li YB, Han JY, Jiang W, Wang J. Selenium inhibits high glucose-induced cyclooxygenase-2 and P-selectin expression in vascular endothelial cells. *Mol Biol Rep.* 38:2301-2306. 2011.

150. Lin D, Sugawara T, Strauss JF 3rd, Clark BJ, Stocco DM, Saenger P, Rogol A, Miller WL. Role of steroidogenic acute regulatory protein in adrenal and gonadal steroidogenesis. *Science.* 267:1828-1831. 1995.

151. Liu B, Luo W, Zhang Y, Li H, Zhu N, Huang D, Zhou Y. Role of cyclooxygenase-1-mediated prostacyclin synthesis in endothelium-dependent vasoconstrictor activity of porcine interlobular renal arteries. *Am J Physiol Renal Physiol.* 302:F1133-F1140. 2012.

152. Liu S, Premont RT, Kontos CD, Zhu S, Rockey DC. A crucial role for GRK2 in regulation of endothelial cell nitric oxide synthase function in portal hypertension. *Nat Med.* 11:952-958. 2005.

153. Löhn M, Dubrovska G, Lauterbach B, Luft FC, Gollasch M, Sharma AM. Periadventitial fat releases a vascular relaxing factor. *FASEB J.* 16:1057-1063. 2002.

154. Malik RA, Schofield IJ, Izzard A, Austin C, Bermann G, Heagerty AM. Effects of angiotensin type-1 receptor antagonism on small artery function in patients with type 2 diabetes mellitus. *Hypertension*. 45:264–269. 2005.

155. Mancia G, Fagard R, Narkiewicz K, Redón J, Zanchetti A, Böhm M, Christiaens T, Cifkova R, De Backer G, Dominiczak A, Galderisi M, Grobbee DE, Jaarsma T, Kirchhof P, Kjeldsen SE, Laurent S, Manolis AJ, Nilsson PM, Ruilope LM, Schmieder RE, Sirnes PA, Sleight P, Viigimaa M, Waeber B, Zannad F. 2013

ESH/ESC Guidelines for the management of arterial hypertension: The Task Force for the management of arterial hypertension of the European Society of Hypertension (ESH) and of the European Society of Cardiology (ESC). *J Hypertens.* 31:1925-1938. 2013.

156. Mancini GB, Henry GC, Macaya C, et al. Angiotensin-converting enzyme inhibition with quinapril improves endothelial vasomotor dysfunction in patients with coronary artery disease. The TREND (Trial on Reversing ENdothelial Dysfunction) Study. *Circulation.* 94:258-265. 1996.

157. Martín A, Pérez-Girón JV, Hernanz R, Palacios R, Briones AM, Fortuño A, Zalba G, Salaices M, Alonso MJ. Peroxisome proliferator-activated receptor-γ activation reduces cyclooxygenase-2 expression in vascular smooth muscle cells from hypertensive rats by interfering with oxidative stress. *J Hypertens.* 30:315-326. 2012.

158. Martínez-Lemus LA. Persistent agonist-induced vasoconstriction is not required for angiotensin II to mediate inward remodeling of isolated arterioles with myogenic tone. *J Vasc Res.* 45:211-221. 2008.

159. Martínez-Lemus LA, Galiñanes EL. Matrix metalloproteinases and small artery remodeling. *Drug Discov Today Dis Models.* 8:21-28. 2011.

160. Martini JS, Raake P, Vinge LE, DeGeorge BR Jr, Chuprun JK, Harris DM, Gao E, Eckhart AD, Pitcher JA, Koch WJ. Uncovering G protein-coupled receptor kinase-5 as a histone deacetylase kinase in the nucleus of cardiomyocytes. *Proc Natl Acad Sci USA.* 105:12457–12462. 2008.

161. Massey KJ, Hong NJ, Garvin JL. Angiotensin II stimulates superoxide production in the thick ascending limb by activating NOX4. *Am J Physiol Cell Physiol.* 303:C781-C789. 2012.

162. Mathiassen ON, Buus NH, Sihm I, Thybo NK, Mørn B, Schroeder AP, Thygesen K, Aalkjaer C, Lederballe O, Mulvany MJ, Christensen KL. Small artery structure is an independent predictor of cardiovascular events in essential hypertension. *J Hypertens*. 25:1021-1026. 2007.

163. McNally JS, Saxena A, Cai H, Dikalov S, Harrison DG. Regulation of xanthine oxidoreductase protein expression by hydrogen peroxide and calcium. *Arterioscler Thromb Vasc Biol.* 25:1623-1628. 2005.

164. McNeill E, Channon KM. The role of tetrahydrobiopterin in inflammation and cardiovascular disease. *Thromb Haemost.* 108:832-839. 2012.

165. Michiels C. Endothelial cell functions. *J Cell Physiol.* 196:430-443. 2003.

166. Mimran A, Ribstein J, DuCailar G. Contrasting effect of antihypertensive reatment on the renal response to L-arginine. *Hypertension.* 26:937-941. 1995.

167. Mollnau H, Wendt M, Szocs K, Lassegue B, Schulz E, Oelze M, Li H, Bodenschatz M, August M, Kleschyov AL, Tsilimingas N, Walter U, Forstermann U, Meinertz T, Griendling K, Munzel T. Effects of angiotensin II infusion on the expression and function of NAD(P)H oxidase and components of nitric oxide/cGMP signaling. *Circ Res*. 90:e58–e65. 2002.

168. Moncada S. The L-arginine: nitric oxide pathway, cellular transduction and immunological roles. *Adv Second Messenger Phosphoprotein Res.* 28:97-99. 1993.

169. Montezano AC, Touyz RM. Reactive Oxygen Species, Vascular Noxs, and Hypertension: Focus on Translational and Clinical Research. *Antioxid Redox Signal.* [Epub ahead of print]. 2013.

170. Morris GE, Nelson CP, Standen NB, Challiss RA, Willets JM. Endothelin signalling in arterial smooth muscle is tightly regulated by G protein-coupled receptor kinase 2. *Cardiovasc Res.* 85:424-433. 2010.

171. Morris GE, Nelson CP, Brighton PJ, Standen NB, Challiss RA, Willets JM. Arrestins 2 and 3 differentially regulate ETA and P2Y2 receptor-mediated cell signaling and migration in arterial smooth muscle. *Am J Physiol Cell Physiol.* 302:C723-C734. 2012.

172. Mulvany MJ, Aalkjaer C. Structure and function of small arteries. *Physiol Rev.* 70:921-971. 1990.

173. Mulvany MJ. Vascular remodelling of resistance vessels: Can we define this? *Cardiovasc Res.* 41:9-13. 1999.

174. Mulvany MJ. Structural abnormalities of the resistance vasculature in hypertension. *J Vasc Res.*40:558-560. 2003.

175. Mulvany MJ. Small artery remodelling in hypertension: causes, consequences and therapeutic implications. *Med Biol Eng Comput*. 46:461-467. 2008.

176. Mulvany MJ. Small artery remodelling in hypertension. *Basic Clin Pharmacol Toxicol.* 110:49-55. 2012.

177. Muzaffar S, Shukla N, Lobo C, Angelini GD, Jeremy JY. Iloprost inhibits superoxide formation and gp91phox expression induced by the thromboxane A2

analogue U46619, 8-isoprostane F2alpha, prostaglandin F2alpha, cytokines and endotoxin in the pig pulmonary artery. *Br J Pharmacol*. 141:488-496. 2004.

178. Muzaffar S, Shukla N, Massey Y, Angelini GD, Jeremy JY. NADPH oxidase 1 mediates upregulation of thromboxane A2 synthase in human vascular smooth muscle cells: inhibition with iloprost. *Eur J Pharmacol.* 658:187-192. 2011.

179. Nakahata N. Thromboxane A2: physiology/pathophysiology, cellular signal transduction and pharmacology. *Pharmacol Ther.* 118:18-35. 2008.

180. Nathan C. Is iNOS beginning to smoke? *Cell.* 147:257-258. 2011.

181. Nguyen Dinh Cat A, Touyz RM. A new look at the renin-angiotensin system--focusing on the vascular system. *Peptides.* 32:2141-2150. 2011a.

182. Nguyen Dinh Cat A, Touyz RM. Cell signaling of angiotensin II on vascular tone: novel mechanisms. *Curr Hypertens Rep.* 13:122-128. 2011b.

183. Nguyen Dinh Cat A, Jaisser F. Extrarenal effects of aldosterone. *Curr Opin Nephrol Hypertens.* 21:147-156. 2012.

184. Nishiyama A, Yao L, Nagai Y, Miyata K, Yoshizumi M, Kagami S, Kondo S, Kiyomoto H, Shokoji T, Kimura S, Kohno M, Abe Y. Possible contributions of reactive oxygen species and mitogenactivated protein kinase to renal injury in aldosterone/salt-induced hypertensive rats. *Hypertension.* 43:841-848. 2004.

185. Noma K, Oyama N, Liao JK. Physiological role of ROCKs in the cardiovascular system. *Am J Physiol Cell Physiol.* 290:C661-C668. 2006.

186. Norel X. Prostanoid receptors in the human vascular wall. *Scientific World Journal*. 7:1359-1374. 2007.

187. Nørrelund H, Christensen KL, Samani NJ, Kimber P, Mulvany MJ, Korsgaard N. Early narrowed afferent arteriole is a contributor to the development of hypertension. *Hypertension.* 24:301-308. 1994.

188. Ohnaka K, Numaguchi K, Yamakawa T, Inagami T. Induction of cyclooxygenase-2 by angiotensin II in cultured rat vascular smooth muscle cells. *Hypertension.* 35:68-75. 2000.

189. Okamura T, Miyazaki M, Inagami T, Toda N. Vascular renin–angiotensin system in two-kidney, one clip hypertensive rats. *Hypertension.* 8:560-565. 1986.

190. Ong KT, Delerme S, Pannier B, Safar ME, Benetos A, Laurent S, Boutouyrie P; investigators. Aortic stiffness is reduced beyond blood pressure lowering by short-term and long-term antihypertensive treatment: a metaanalysis of individual data in 294 patients. *J Hypertens.* 29:1034-1042. 2011.

191. Örneskog G, Kahan T, Ekholm M, Bröijersén A, Wallén NH. Altered vascular responses to circulating angiotensin II in familial combined hyperlipidemia. *J Cardiovasc Med.* 9:1037–1044. 2008.

192. Ouwens DM, Sell H, Greulich S, Eckel J. The role of epicardial and perivascular adipose tissue in the pathophysiology of cardiovascular disease. *J Cell Mol Med.* 14:2223-2234. 2010.

193. Pankov R, Yamada KM. Fibronectin at a glance. *J Cell Sci.* 115:3861-3863. 2002.

194. Park JB, Schiffrin EL. Cardiac and vascular fibrosis and hypertrophy in aldosterone-infused rats: role of endothelin-1. *Am J Hypertens.* 15:164-169. 2002.

195. Patel BM, Mehta AA. Aldosterone and angiotensin: Role in diabetes and cardiovascular diseases. *Eur J Pharmacol.* 697:1-12. 2012.

196. Pena-Silva R.A, Heistad DD. EP1c times for angiotensin: EP1 receptors facilitate angiotensin II-induced vascular dysfunction. *Hypertension.* 55:846-848. 2010.

197. Penela P, Murga C, Ribas C, Tutor AS, Peregrin S, Mayor F, Jr. Mechanisms of regulation of G protein-coupled receptor kinases (GRKs) and cardiovascular disease. *Cardiovasc Res.* 69:46-56. 2006.

198. Pitcher JA, Freedman NJ, Lefkowitz RJ. G protein-coupled receptor kinases. *Annu Rev Biochem.* 67:653-692. 1998.

199. Ramos-Ruiz R, Penela P, Penn RB, Mayor F Jr. Analysis of the human G proteincoupled receptor kinase 2 (GRK2) gene promoter: regulationby signal transduction systems in aortic smooth muscle cells. *Circulation.* 101:2083-2089. 2000.

200. Renna NF, de Las Heras N, Miatello RM. Pathophysiology of vascular remodeling in hypertension. *Int J Hypertens.* 2013:808353.2013.

201. Rey FE, Pagano PJ. The reactive adventitia: fibroblast oxidase in vascular function. *Arterioscler Thromb Vasc Biol.* 22:1962-1971. 2002.

202. Rhodin JAG. Architecture of the Vessel Wall. Comprehensive Physiology. *John Wiley & Sons Inc*. 1–31. 2011.

203. Ribas C, Penela P, Murga C, Salcedo A, García-Hoz C, Jurado-Pueyo M, Aymerich I, Mayor F Jr. The G protein-coupled receptor kinase (GRK) interactome: role of GRKs in GPCR regulation and signaling. *Biochim Biophys Acta.* 1768:913-922. 2007.

204. Ricciotti E, FitzGerald GA. Prostaglandins and inflammation. *Arterioscler Thromb Vasc Biol.* 31:986-1000. 2011.

205. Rizzoni D, Porteri E, Boari GE, De Ciuceis C, Sleiman I, Muiesan ML, Castellano M, Miclini M, Agabiti-Rosei E. Prognostic significance of small-artery structure in hypertension. *Circulation.* 108:2230-2235. 2003.

206. Rizzoni D, Porteri E, De Ciuceis C, Sleiman I, Rodella L, Rezzani R, Paiardi S, Bianchi R, Ruggeri G, Boari GE, Muiesan ML, Salvetti M, Zani F, Miclini M, Rosei EA. Effect of treatment with candesartan or enalapril on subcutaneous small artery structure in hypertensive patients with non-insulin-dependent diabetes mellitus. *Hypertension.* 45:659-665. 2005.

207. Rizzoni D, Agabiti-Rosei E. Structural abnormalities of small resistance arteries in essential hypertension. *Intern Emerg Med.* 7:205-212. 2012.

208. Rocha R, Martin-Berger CL, Yang P, Scherrer R, Delyani J, McMahon E. Selective aldosterone blockade prevents angiotensin II/salt-induced vascular inflammation in the rat heart. *Endocrinology.* 143:4828-4836. 2002.

209. Rockman HA, Koch WJ, Lefkowitz RJ. Seven-transmembrane-spanning receptors and heart function. *Nature.* 415:206-212. 2002.

210. Ross R. Atherosclerosis--an inflammatory disease. *N Engl J Med.* 340:115-126. 1999.

211. Rubanyi GM. Endothelium-derived relaxing and contracting factors. *J Cell Biochem.* 46:27-36. 1991.

212. Ryan MJ, Didion SP, Mathur S, Faraci FM, Sigmund CD. Angiotensin II-induced vascular dysfunction is mediated by the AT1A receptor in mice. *Hypertension.* 43:1074-1079. 2004.

213. Samuelsson B, Morgenstern R, Jakobsson PJ. Membrane prostaglandin E synthase-1: a novel therapeutic target. *Pharmacol Rev.* 59:207-224. 2007.

214. Sanada H, Jose PA, Hazen-Martin D, Yu PY, Xu J, Bruns DE, Phipps J, Carey RM, Felder RA. Dopamine-1 receptor coupling defect in renal proximal tubule cells in hypertension. *Hypertension.* 33:1036-1042. 1999.

215. Sancho P, Martín-Sanz P, Fabregat I. Reciprocal regulation of NADPH oxidases and the cyclooxygenase-2 pathway. *Free Radic Biol Med.* 51:1789-1798. 2011.

216. Santos CX, Nabeebaccus AA, Shah AM, Camargo LL, Filho SV, Lopes LR. ER stress and Nox-mediated ROS signaling in the peripheral vasculature: potential role in hypertension. *Antioxid Redox Signal.* [Epub ahead of print]. 2013.

217. Sanz-Rosa D, Oubiña MP, Cediel E, De las Heras N, Aragoncillo P, Balfagón G, Cachofeiro V, Lahera V. Eplerenone reduces oxidative stress and enhances eNOS in SHR: vascular functional and structural consequences. *Antioxid Redox Signal.* 7:1294-1301. 2005.

218. Savoia C, Schiffrin EL. Vascular inflammation in hypertension and diabetes: molecular mechanisms and therapeutic interventions. *Clin Sci (Lond).* 112:375-384. 2007.

219. Schiffrin EL, Park JB, Intengan HD, Touyz RM. Correction of arterial structure and endothelial dysfunction in human essential hypertension by the angiotensin receptor antagonist losartan. *Circulation.* 101:1653-1659. 2000.

220. Schiffrin EL. Vascular and cardiac benefits of angiotensin receptor blockers. *Am J Med.* 113:409-418. 2002.

221. Schiffrin EL, Touyz RM. From bedside to bench to bedside: role of renin-angiotensin-aldosterone system in remodeling of resistance arteries in hypertension. *Am J Physiol Heart Circ Physiol.* 287:H435-H446. 2004.

222. Schiffrin EL. Vascular remodeling in hypertension: mechanisms and treatment. *Hypertension.* 59:367-374. 2012.

223. Schramm A, Matusik P, Osmenda G, Guzik TJ. Targeting NADPH oxidases in vascular pharmacology. *Vascul Pharmacol.* 56:216-231. 2012.

224. Schröder K, Zhang M, Benkhoff S, Mieth A, Pliquett R, Kosowski J, Kruse C, Luedike P, Michaelis UR, Weissmann N, Dimmeler S, Shah AM, Brandes RP. Nox4 is a protective reactive oxygen species generating vascular NADPH oxidase. *Circ Res*. 110:1217-1225. 2012.

225. Schulz E, Jansen T, Wenzel P, Daiber A, Münzel T. Nitric oxide, tetrahydrobiopterin, oxidative stress, and endothelial dysfunction in hypertension. *Antioxid Redox Signal.* 10:1115-1126. 2008.

226. Schulz E, Gori T, Münzel T. Oxidative stress and endothelial dysfunction in hypertension. *Hypertens Res.* 34:665-673. 2011.

227. Schulz E, Wenzel P, Münzel T, Daiber A. Mitochondrial redox signaling: interaction of mitochondrial reactive oxygen species with other sources of oxidative stress. *Antioxid Redox Signal.* [Epub ahead of print]. 2012.

228. Sharifi AM, Li JS, Endemann D, Schiffrin EL. Effects of enalapril and amlodipine on small-artery structure and composition, and on endothelial dysfunction in spontaneously hypertensive rats. *J Hypertens.* 16:457-466. 1998.

229. Shoback DM, Williams GH, Moore TJ, Dluhy RG, Podolsky S, Hollenberg NK. Defect in the sodium-modulated tissue responsiveness to angiotensin II in essential hypertension. *J Clin Invest.* 72:2115-2124. 1983.

230. Sparks MA, Makhanova NA, Griffiths RC, Snouwaert JN, Koller BH, Coffman TM. Thromboxane receptors in smooth muscle promote hypertension, vascular remodeling, and sudden death. *Hypertension.* 61:166-173. 2013.

231. Stenmark KR, Yeager ME, El Kasmi KC, Nozik-Grayck E, Gerasimovskaya EV, Li M, Riddle SR, Frid MG. The adventitia: essential regulator of vascular wall structure and function. *Annu Rev Physiol.* 75:23-47. 2013.

232. Stichtenoth DO, Marhauer V, Tsikas D, Gutzki FM, Frölich JC. Effects of specific COX-2-inhibition on renin release and renal and systemic prostanoid synthesis in healthy volunteers. *Kidney Int.* 68:2197-2207. 2005.

233. Tabit CE, Chung WB, Hamburg NM, Vita JA. Endothelial dysfunction in diabetes mellitus: molecular mechanisms and clinical implications. *Rev Endocr Metab Disord.* 11:61-74. 2010.

234. Taddei S, Virdis A, Abdel-Haq B, Giovannetti R, Duranti P, Arena AM, Favilla S, Salvetti A. Indirect evidence for vascular uptake of circulating renin in hypertensive patients. *Hypertension.* 21:852-860. 1993.

235. Taddei S, Virdis A, Ghiadoni L, Mattei P, Salvetti A. Effects of angiotensin converting enzyme inhibition on endothelium-dependent vasodilatation in essential hypertensive patients. *J Hypertens.* 16:447-456. 1998.

236. Taddei S, Virdis A, Ghiadoni L, Sudano I, Salvetti A. Effects of antihypertensive drugs on endothelial dysfunction: clinical implications. *Drugs*. 62:265-284. 2002.

237. Taguchi K, Kobayashi T, Takenouchi Y, Matsumoto T, Kamata K. Angiotensin II causes endothelial dysfunction via the GRK2/Akt/eNOS pathway in aortas from a murine type 2 diabetic model. *Pharmacol Res.* 64:535–546. 2011.

238. Takimoto E, Champion HC, Li M, Ren S, Rodriguez ER, Tavazzi B, Lazzarino G, Paolocci N, Gabrielson KL, Wang Y, Kass DA. Oxidant stress from nitric oxide synthase-3 uncoupling stimulates cardiac pathologic remodeling from chronic pressure load. *J Clin Invest.* 115:1221-1231. 2005.

239. Tang EH, Leung FP, Huang Y, Félétou M, So KF, Man RY, Vanhoutte PM. Calcium and reactive oxygen species increase in endothelial cells in response to releasers of endothelium-derived contracting factor. *Br J Pharmacol.* 151: 15-23. 2007.

240. Tang EH, Vanhoutte PM. Prostanoids and reactive oxygen species: Team players in endothelium-dependent contractions. *Pharmacol Ther.* 122:140-149. 2009.

241. Tasatargil A, Tekcan M, Celik-Ozenci C, Ece Gungor N, Dalkiran B Aldosterone-induced endothelial dysfunction of rat aorta: role of poly(ADP-ribose) activation. *J Renin Angiotensin Aldosterone Syst*. 10:127-137. 2009.

242. Theilade J, Hansen JL, Haunsø S, Sheikh SP. MAP kinase protects G proteincoupled receptor kinase 2 from proteasomal degradation. *Biochem Biophys Res Commun.* 330:685-689. 2005.

243. Tian XY, Wong WT, Leung FP, Zhang Y, Wang YX, Lee HK, Ng CF, Chen ZY, Yao X, Au CL, Lau CW, Vanhoutte PM, Cooke JP, Huang Y. Oxidative stress-dependent cyclooxygenase-2-derived prostaglandin f(2α) impairs endothelial function in renovascular hypertensive rats. *Antioxid Redox Signal.* 16:363-373. 2012.

244. Tousoulis D, Kampoli AM, Tentolouris C, Papageorgiou N, Stefanadis C. The role of nitric oxide on endothelial function. *Curr Vasc Pharmacol.* 10:4-18. 2012.

245. Touyz RM, Schiffrin EL. Increased generation of superoxide by angiotensin II in smooth muscle cells from resistance arteries of hypertensive patients: role of phospholipase D-dependent NAD(P)H oxidase-sensitive pathways. *J Hypertens.* 19:1245-1254. 2001.

246. Touyz RM, Wu XH, He G, Park JB, Chen X, Vacher J, Rajapurohitam V, Schiffrin EL. Role of c-Src in the regulation of vascular contraction and Ca^{2+} signaling by angiotensin II in human vascular smooth muscle cells. *J Hypertens*. 19:441-449. 2001.

247. Touyz RM, Berry C. Recent advances in angiotensin II signaling. *Braz J Med Biol Res.* 35:1001-1015. 2002.

248. Touyz RM, Chen X, Tabet F, Yao G, He G, Quinn MT, Pagano PJ, Schiffrin EL. Expression of a functionally active gp91phox-containing neutrophil-type NAD(P)H oxidase in smooth muscle cells from human resistance arteries: regulation by angiotensin II. *Circ Res.* 90:1205-1213. 2002.

249. Touyz RM. Intracellular mechanisms involved in vascular remodelling of resistance arteries in hypertension: role of angiotensin II. *Exp Physiol.* 90:449-455. 2005.

250. Touyz RM, Briones AM. Reactive oxygen species and vascular biology: implications in human hypertension. *Hypertens Res.* 34:5-14. 2011.

251. Trachootham D, Alexandre J, Huang P. Targeting cancer cells by ROS-mediated mechanisms: a radical therapeutic approach? *Nat Rev Drug Discov.* 8:579-591. 2009.

252. Vanhoutte PM, Félétou M, Taddei S. Endothelium-dependent contractions in hypertension. *Br J Pharmacol.* 144:449-458. 2005.

253. Vecchione C, Fratta L, Rizzoni D, Notte A, Poulet R, Porteri E, Frati G, Guelfi D, Trimarco V, Mulvany MJ, Agabiti-Rosei E, Trimarco B, Cotecchia S, Lembo G. Cardiovascular influences of alpha1b-adrenergic receptor defect in mice. *Circulation.* 105:1700-1707. 2002.

254. Versari D, Virdis A, Ghiadoni L, Daghini E, Duranti E, Masi S, Magagna A, Taddei S. Effect of verapamil, trandolapril and their combination on vascular

function and structure in essential hypertensive patients. *Atherosclerosis.* 205:214-220. 2009.

255. Virdis A, Neves MF, Amiri F, Viel E, Touyz RM, Schiffrin EL. Spironolactone improves angiotensin-induced vascular changes and oxidative stress. *Hypertension.* 40:504-510. 2002.

256. Virdis A, Neves MF, Amiri F, Touyz RM, Schiffrin EL. Role of NAD(P)H oxidase on vascular alterations in angiotensin II-infused mice. *J Hypertens.* 22:535-542. 2004.

257. Virdis A, Colucci R, Fornai M, Duranti E, Giannarelli C, Bernardini N, Segnani C, Ippolito C, Antonioli L, Blandizzi C, Taddei S, Salvetti A, Del Tacca M. Cyclooxygenase-1 is involved in endothelial dysfunction of mesenteric small arteries from angiotensin II-infused mice. *Hypertension.* 49:679-686. 2007.

258. Virdis A, Colucci R, Versari D, Ghisu N, Fornai M, Antonioli L, Duranti E, Daghini E, Giannarelli C, Blandizzi C, Taddei S, Del Tacca M. Atorvastatin prevents endothelial dysfunction in mesenteric arteries from spontaneously hypertensive rats: role of cyclooxygenase 2-derived contracting prostanoids. *Hypertension.* 53:1008-1016. 2009.

259. Virdis A, Colucci R, Neves MF, Rugani I, Aydinoglu F, Fornai M, Ippolito C, Antonioli L, Duranti E, Solini A, Bernardini N, Blandizzi C, Taddei S. Resistance artery mechanics and composition in angiotensin II-infused mice: effects of cyclooxygenase-1 inhibition. *Eur Heart J.* 33:2225-2234. 2012.

260. Virdis A, Bacca A, Colucci R, Duranti E, Fornai M, Materazzi G, Ippolito C, Bernardini N, Blandizzi C, Bernini G, Taddei S. Endothelial dysfunction in

small arteries of essential hypertensive patients: role of cyclooxygenase-2 in oxidative stress generation. *Hypertension.* 62:337-344. 2013.

261. Wagenseil JE, Mecham RP. Vascular extracellular matrix and arterial mechanics. *Physiol Rev.* 89:957-989. 2009.

262. Wang D, Chabrashvili T, Borrego L, Aslam S, Umans JG. Angiotensin II infusion alters vascular function in mouse resistance vessels: roles of O and endothelium. *J Vasc Res.* 43:109-119. 2006.

263. Wang M, Lee E, Song W, Ricciotti E, Rader DJ, Lawson JA, Puré E, FitzGerald GA. Microsomal prostaglandin E synthase-1 deletion suppresses oxidative stress and angiotensin II-induced abdominal aortic aneurysm formation. *Circulation.* 117:1302-1309. 2008.

264. Wang M, Ihida-Stansbury K, Kothapalli D, Tamby MC, Yu Z, Chen L, Grant G, Cheng Y, Lawson JA, Assoian RK, Jones PL, Fitzgerald GA. Microsomal prostaglandin e2 synthase-1 modulates the response to vascular injury. *Circulation.* 123:631-639. 2011.

265. Wang W, McClain JM, Zucker IH. Aldosterone reduces baroreceptor discharge in the dog. *Hypertension.* 19:270-277. 1992.

266. Wassmann S, Nickenig G. Pathophysiological regulation of the AT1-receptor and implications for vascular disease. *J Hypertens*. 24:S15–S21. 2006.

267. Wehling M, Neylon CB, Fullerton M, Bobik A, Funder JW. Nongenomic effects of aldosterone on intracellular Ca^{2+} in vascular smooth muscle cells. *Circ Res.* 76:973-979. 1995.

268. Welch WJ, Patel K, Modlinger P, Mendonca M, Kawada N, Dennehy K, Aslam S, Wilcox CS. Roles of vasoconstrictor prostaglandins, COX-1 and -2, and AT1, AT2, and TP receptors in a rat model of early 2K,1C hypertension. *Am J Physiol Heart Circ Physiol.* 293:H2644-H2649. 2007.

269. Widlansky ME, Gokce N, Keaney JF Jr, Vita JA. The clinical implications of endothelial dysfunction. *J Am Coll Cardiol.* 42:1149-1160. 2003.

270. Widlansky ME, Gutterman DD. Regulation of endothelial function by mitochondrial reactive oxygen species. *Antioxid Redox Signal.* 15:1517-1530. 2011.

271. Wilkinson IB, Franklin SS, Cockcroft JR. Nitric oxide and the regulation of large artery stiffness: from physiology to pharmacology. *Hypertension.* 44:112-116. 2004.

272. Wong SL, Wong WT, Tian XY, Lau CW, Huang Y. Prostaglandins in action indispensable roles of cyclooxygenase-1 and -2 in endothelium-dependent contractions. *Adv Pharmacol.* 60:61-83. 2010.

273. Wong SL, Lau CW, Wong WT, Xu A, Au CL, Ng CF, Ng SS, Gollasch M, Yao X, Huang Y. Pivotal role of protein kinase C delta in angiotensin II-induced endothelial cyclooxygenase-2 expression: a link to vascular inflammation. *Arterioscler Thromb Vasc Biol.* 31:1169-1176. 2011.

274. Wong WT, Tian XY, Huang Y. Endothelial dysfunction in diabetes and hypertension: cross talk in RAS, BMP4, and ROS-dependent COX-2-derived prostanoids. *J Cardiovasc Pharmacol.* 61:204-214. 2013.

275. Wosniak J Jr, Santos CX, Kowaltowski AJ, Laurindo FR. Cross-talk between mitochondria and NADPH oxidase: effects of mild mitochondrial dysfunction on angiotensin II-mediated increase in Nox isoform expression and activity in vascular smooth muscle cells. *Antioxid Redox Signal.* 11:1265-1278. 2009.

276. Wu R, Laplante MA, De Champlain J. Cyclooxygenase-2 inhibitors attenuate angiotensin II-induced oxidative stress, hypertension, and cardiac hypertrophy in rats. *Hypertension.* 45:1139-1144. 2005.

277. Wu R, Duchemin S, Laplante MA, De Champlain J, Girouard H. Cyclo-oxygenase-2 knockout genotype in mice is associated with blunted angiotensin II-induced oxidative stress and hypertension. *Am J Hypertens.* 24:1239-1244. 2011.

278. Wu TC, Chao CY, Lin SJ, Chen JW. Low-dose dextromethorphan, a NADPH oxidase inhibitor, reduces blood pressure and enhances vascular protection in experimental hypertension. *PLoS One.* 7:e46067. 2012.

279. Xanthakis V, Vasan RS. Aldosterone and the risk of hypertension. *Curr Hypertens Rep.* 15:102-107. 2013.

280. Xavier FE, Aras-López R, Arroyo-Villa I, Campo LD, Salaices M, Rossoni LV, Ferrer M, Balfagón G. Aldosterone induces endothelial dysfunction in resistance arteries from normotensive and hypertensive rats by increasing thromboxane A2 and prostacyclin. *Br J Pharmacol.* 154:1225-1235. 2008.

281. Xing W, Li Y, Zhang H, Mi C, Hou Z, Quon MJ, Gao F. Improvement of vascular insulin sensitivity by downregulation of GRK2 mediates exercise-

induced alleviation of hypertension in spontaneously hypertensive rats. *Am J Physiol Heart Circ Physiol.* 305:H1111-H1119. 2013.

282. Yang D, Félétou M, Boulanger CM, Wu HF, Levens N, Zhang JN, Vanhoutte PM. Oxygen-derived free radicals mediate endothelium-dependent contractions to acetylcholine in aortas from spontaneously hypertensive rats. *Br J Pharmacol.* 136:104-110. 2002.

283. Yang HM, Kim HS, Park KW, You HJ, Jeon SI, Youn SW, Kim SH, Oh BH, Lee MM, Park YB, Walsh K. Celecoxib, a cyclooxygenase-2 inhibitor, reduces neointimal hyperplasia through inhibition of Akt signaling. *Circulation.* 110:301-308. 2004.

284. Yuhki K, Kojima F, Kashiwagi H, Kawabe J, Fujino T, Narumiya S, Ushikubi F. Roles of prostanoids in the pathogenesis of cardiovascular diseases: Novel insights from knockout mouse studies. *Pharmacol Ther*. 129:195-205. 2011.

285. Zhang J, Zou F, Tang J, Zhang Q, Gong Y, Wang Q, Shen Y, Xiong L, Breyer RM, Lazarus M, Funk CD, Yu Y. Cyclooxygenase-2-derived prostaglandin E_2 promotes injury-induced vascular neointimal hyperplasia through the E-prostanoid 3 receptor. *Circ Res.* 113:104-114. 2013.

286. Zou MH, Shi C, Cohen RA. High glucose via peroxynitrite causes tyrosine nitration and inactivation of prostacyclin synthase that is associated with thromboxane/prostaglandin h(2) receptor-mediated apoptosis and adhesion molecule expression in cultured human aortic endothelial cells. *Diabetes.* 51:198-203. 2002.